DISSERTATION ZUR ERLANGUNG DES DOKTORGRADES

DER FAKULTÄT FÜR CHEMIE UND PHARMAZIE

DER LUDWIG-MAXIMILIANS-UNIVERSITÄT MÜNCHEN

Synthesis and Characterization of New Environmentally Benign Secondary Explosives Based on Azoles

– and –

Further Characterization of TKX-50 and K_2DNABT toward Industrial Scale-Up

Marc Florian Bölter

aus

Frankfurt am Main

2018

Erklärung:

Diese Dissertation wurde im Sinne von § 7 der Promotionsordnung vom 28. November 2011 von Herrn Professor Dr. Thomas M. Klapötke betreut.

Eidesstattliche Versicherung:

Diese Dissertation wurde eigenständig und ohne unerlaubte Hilfe erarbeitet.

München, 16.10.2018… ……

Marc Florian Bölter

Dissertation eingereicht am:	16.10.2018
1. Gutachter:	Prof. Dr. Thomas M. Klapötke
2. Gutachter:	Prof. Dr. Konstantin Karaghiosoff
Mündliche Prüfung am:	29.11.2018

„Ein guter Explosivstoff basiert immer auf Glyoxal“

–Dr. Dennis Fischer (2015)–

Danksagung

Mein Dank gilt an erster Stelle meinem Doktorvater Herrn Professor Dr. Thomas M. Klapötke für die Aufnahme in den Arbeitskreis und die interessante Aufgabenstellung der Sekundären Explosivstoffe. Neben der pekuniären Unterstützung möchte ich mich ebenfalls für die kontinuierliche Begleitung, Unterstützung, Freiheit der Forschungsarbeit sowie für die Teilnahme an internationalen Konferenzen bedanken.

Als nächstes möchte ich mich bei Herrn Prof. Dr. Konstantin Karaghiosoff für die Übernahme des Zweitgutachtens dieser Doktorarbeit bedanken. Außerdem möchte ich mich für das stets offene Ohr, die vielen fachlichen Diskussionen und Anregungen, sowie für das Messen zahlreicher Kristallstrukturen und für Hilfe bei der Auswertung von NMR Spektren bedanken.

Ebenso Dank gilt den weiteren Teilnehmern der Prüfungskommission bestehend aus Prof. Wolfgang Beck, Prof. Lena Daumann, Prof. Ingo Lorenz und Prof. Robert Schmucker.

Bei Herrn Dr. Jörg Stierstorfer möchte ich mich für mehrere Dinge bedanken. Unter anderem für die Hilfe (bzw. komplette Lösung) zahlreicher Kristallstrukturen, guter chemischer Ideen, Mitbetreuung und Hilfe beim Verfassen von Manuskripten. Für seine Habilitation (und die nebenberufliche Karriere als Erfolgscoach des Dynamo Drophammer Teams) wünsche ich ihm weiterhin alles Gute und viel Erfolg.

Als nächstes möchte ich mich bei Frau Irene Scheckenbach für ihr organisatorisches Talent und die exzellente Begleitung durch den Bürokratiedschungel der LMU bedanken.

Ebenfalls möchte ich mich bei Herrn Dr. Burkhard Krumm für das Messen und Auswerten von NMR Spektren bedanken, sowie für die zahlreichen (teilweise) einseitigen Fußballdisskusionen über den FC Bayern und Borussia Dortmund (meist hinter dem FC Bayern in der Tabelle). Außerdem wünsche ich Ihnen viel Glück beim nächsten Arbeitskreis internen Tipp-Spiel.

Ebenfalls möchte ich mich bei Herrn Stefan Huber für seine lustige Art und die Messung zahlreicher Sensitivitäten bedanken.

Allen Mitgliedern des Arbeitskreises danke ich für die gute Zusammenarbeit und ich wünsche euch allen viel Erfolg in der Zukunft. Besonders werden mir der Gewinn des Campus Turnieres (2017), Grillmittage, Tastings von Getränken jeglicher Art, Wiesn und Starkbierfest-Trips und die Skiausflüge in Erinnerung bleiben. Greta Bikelyte danke ich für die HPLC Messungen.

Den Mitkollegen aus Labor D 3.110 im einzelnen Max Born, Dr. Dennis Fischer, Maj. Mohamed Hussien, Jelena Reinhardt, Dr. Philipp Schmid, Maurus Völkl, und Dr. Tomasz Witkowski danke ich für die stets angenehme Arbeitsatmosphäre. Besonders hervorheben möchte ich hierbei Dr. Dennis Fischer, für sein enormes theoretisches und praktisches chemisches Wissen und seiner Hilfe bei Problemen jeglicher Art.

Ein besonderer Dank geht auch meinen Bacheloranden und F-Praktikanten Maximilian Benz, Alexander Harter, Jan Heinemann, Maximilian Mader, Stefan Krombholz, Tessa Kustermann, Tobias Lenz, Igor Martin und Maximilian Schuster die ebenfalls einen großen Teil zu dieser Arbeit beigetragen haben. Besonderer Dank gilt hierbei Tessa Kustermann für ihre tatkräftige Unterstützung, welche zum gelungenen Abschluss eines Projekts geführt hat. Weiterer Dank gilt auch Michael Gruhne für die Unterstützung im zweiten Projekt.

Außerdem möchte ich mich bei meinen AK-Freunden Anne Friedrichs, Dr. Johann Glück, Ivan Gospodinov (Brudi und Organisationstalent), Marcel Holler, Teresa Küblböck und Dr. Thomas Reith (Bierzilla und Zimmerpartner) für die niveauvollen Gespräche während des Mittagessens, jegliche Ausflüge und unseren legendären Trip nach Prag (Elsa…) bedanken. Hervorheben möchte ich hierbei noch Ivan Gopodinov für seine Hilfsbereitschaft in chemischer Fragestellung und das Korrektulesen dieser Arbeit. Ebenfalls möchte ich mich bei Teresa Küblböck für das Korrekturlesen dieser Arbeit, sowie für ihre phänomenalen Illustrator Kenntnisse bedanken.

Bei meinen Erstsemesterfreunden Bernhard Böller, Niklas Cordes, Laura Jochem, Dr. Marthe Ketels, Dr. Angela Metz, Hendrik Schlomberg und Dorothee Ziegler möchte ich mich ebenfalls für die schöne Zeit während des kompletten Studiums und der Promotion bedanken. Ein weiterer Dank geht an Dr. Ramona Ludolph für die langjährige Unterstützung und Motivation während dieser Dissertation.

Zuletzt geht mein Dank an meine Familie, insbesondere an meine Eltern Martina und Hendrick und meinen zwei Geschwistern Natalie und Nico. Als letztes möchte ich mich noch bei meinen Großeltern Helene und Hendrick Bölter, sowie Anne-Marie und Rolf Steinebronn bedanken.

Table of Contents

1 Introduction

1.1 Definition and Classification of Energetic Materials

The research on explosives or energetic compositions is a very interesting and diversified field in chemistry. According to the German law Sprengstoffgesetz (SprengG) potentially explosive materials are described as solid or liquid compounds and formulations, *"which could detonate due to a not extraordinary thermal, mechanical or other stress*" and "*show explosive behavior during test methods such as thermal sensitivity and mechanical sensitivity with respect to either shock or friction*".[1] The American Society for Testing and Material (ASTM) defines energetic materials as *"chemical compounds or compositions that contain both the fuel and the oxidizer and rapidly react to release energy and gas"*.[2] Davin Piercey characterizes explosives in his PhD thesis as *"a metastable compound or mixture capable of the rapid release of stored potential energy."*[3]

Energetic materials can be distinguished into three main classes according to their different energetic performance and usage: propellants, pyrotechnics and explosives (Figure 1.1).[4] This thesis focuses on explosives, which can further be subdivided into primary and secondary explosives due to their sensitivity and energetic properties.[4]

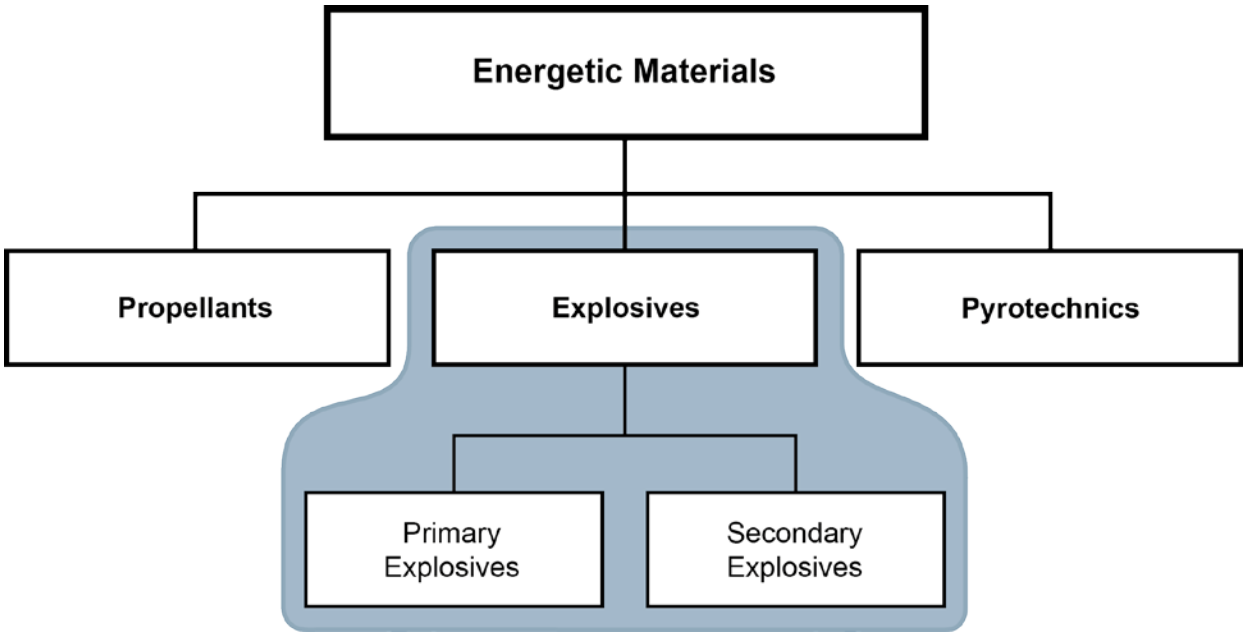

Figure 1.1. Classification of energetic materials.[4]

Primary explosives are substances marked by their highly sensitivity as well as their fast transition from deflagration to detonation.[5] Generally, these compounds are more sensitive towards thermal, mechanical or electrostatic stimuli than secondary explosives with typical values of ≤ 4 J for impact, ≤ 10 N for friction and ≤ 20 mJ for electrostatic discharge.[4-6] Likewise, primary explosives show lower energetic performances regarding detonation velocity, detonation pressure or heat of explosion.[5] After ignition, they generate either a large quantity of heat or a shockwave, which could ignite a less sensitive secondary explosive such as RDX.[5] Based on this property, primary explosives are used as initiators (*e.g.* detonators, blasting caps or primers) or as ignitor for secondary booster charges, main charges or propellants.[7] Commonly used primary explosives are lead azide (LA)[8] and lead styphnate (LS)[9] as well in former times also mercury fulminate (MF)[10] (Figure 1.2). The main disadvantage using the mentioned primary explosives is the attendance of heavy metals like lead and mercury, which causes environmental and human impact.[7] Due to the toxicity of lead or mercury, different primary explosives with absence of heavy metals are preferred such as diazadinitrophenole (DDNP), cyanuric triazide (CTA), tetrazene (GNGT), copper(I) 5-nitrotetrazolate (DBX-1) or dipotassium 1,1'-dinitramino-5,5'-bistetrazolate (K_2DNABT).[4-5, 11]

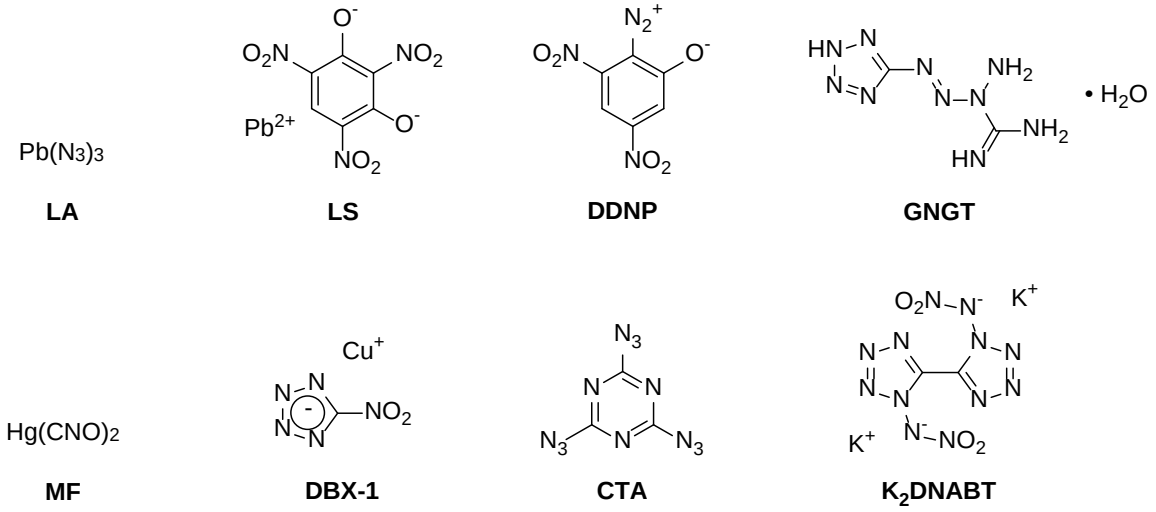

Figure 1.2. Overview of selected primary explosives: lead azide (LA), lead styphnate (LS), mercury fulminate (MF); diazadinitrophenole (DDNP), tetrazene (GNGT), copper(I) 5-nitrotetrazolate (DBX-1), cyanuric triazide (CTA) and dipotassium 1,1'-dinitramino-5,5'-bistetrazolate (K_2DNABT).

Secondary explosives are less sensitive towards external stimuli compared to primary explosives with values of ≥ 4 J for impact and ≥ 80 N for friction.[4] Due to their higher structural stability; secondary explosives cannot be ignited as easy as primary explosives. The ignition of a secondary explosive can be carried out by using sufficient thermal stimuli or a shockwave of a primary explosive. Usually, the detonation parameters (heat of explosion Q, detonation velocity V_D and

detonation pressure p_{CJ}) are higher than a primary explosive.[4] Most commonly used secondary explosives are trinitrotoluol (TNT), hexogen (RDX), octogen (HMX) and pentaerythriol tetranitrate (PETN) (Figure 3).[12] However, some of the up to date known explosives suffer from high sensitivity, low decomposition temperature, high toxicity or/and low energetic performance making further investigation mandatory.[4, 13] Especially the toxicity leads to an intensive research in the attempted replacements of RDX.[14-16] More recently developed compounds are 1,1-diamino-2,2-dinitro ethene (FOX-7), hexanitro hexaazaisowurtzitane (CL-20), octanitrocubane (ONC), 5,5´-bis(2,4,6-trinitrophenyl)-2,2´-bi(1,3,4-oxadiazole) (TKX-55), bis(3,4,5-trinitropyrazol-1-yl) methane (BTNPM), 2,6-diamino-3,5-dinitro-pyrazine-1-oxide (LLM-105) and dihydroxylammonium 5,5´-bitetrazole-1,1´-dioxide (TKX-50) (Figure 1.3).[4, 17-19]

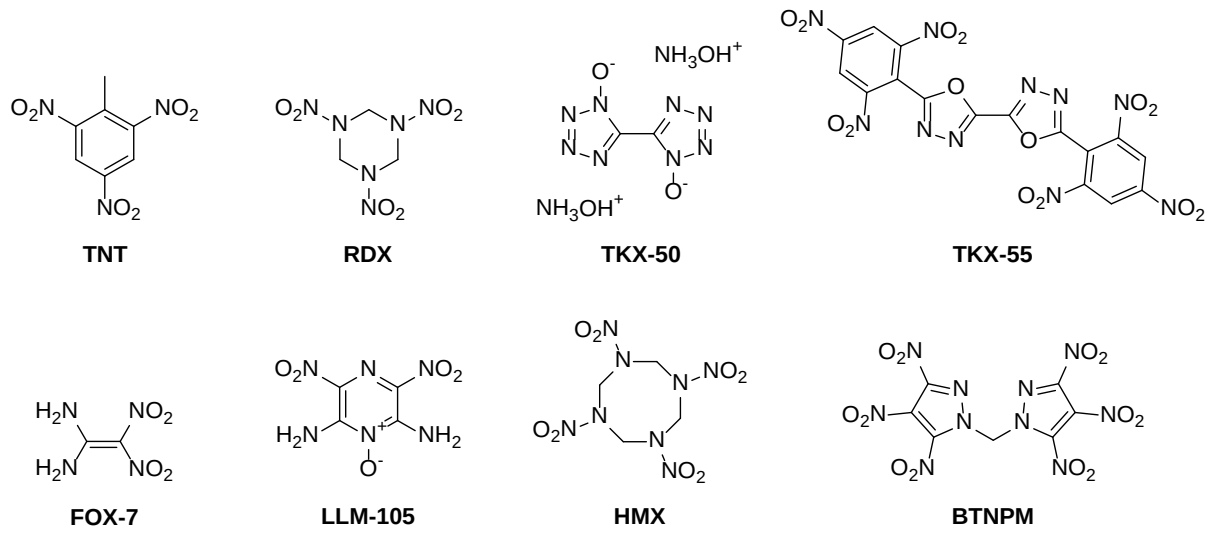

Figure 1.3. Overview of selected secondary explosives: 2,4,6-trinitro-toluene (TNT), hexogen (RDX), octogen (HMX), 1,1-diamino-2,2-dinitro ethene (FOX-7), 5,5´-bis(2,4,6-trinitrophenyl)-2,2´-bi(1,3,4-oxadiazole) (TKX-55), bis(3,4,5-trinitropyrazol-1-yl) methane (BTNPM), 2,6-diamino-3,5-dinitro-pyrazine-1-oxide (LLM-105) and dihydroxylammonium 5,5´-bitetrazole-1,1´-dioxide (TKX-50).

Propellants commonly consist of a fuel and an oxidizer in various ratios according to their respective application.[4] They can further be subclassified into rocket propellants and propellant charges for guns. The main requirement for propellants is the generation of hot gases by combustion to accelerate projectiles, missiles or rockets due to the resulting propulsive force.[20] Another property is the almost balanced oxygen content, whereby the substances or mixtures can completely combust with itself.[21] Commonly used gun propellants are *e.g.* nitrocellulose (NC), nitroguanidine (NQ) or nitroglycerine (NG) (Figure 1.4). Depending on the usage there are three different types of compositions: single, double or triple base compositions. Smokeless single base propellants consist of NC, whereas the addition of NG leads to double base propellants. The addition

of NQ to the double base composition results in tripe base propellants. Rocket propellants can be categorized into either solid (*e.g.* NH_4ClO_4) or liquid (*e.g.* monomethylhydrazine) propellants. Solid rocket propellants can be subdivide into homogenous (double-base, *e.g.* NC/NG) or heterogeneous (NH_4ClO_4, aluminum and binder) propellants. Liquid propellants can be distinguished into monopropellants (*e.g.* hydrazine) and bipropellants. The latter consists of a fuel (*e.g.* hydrazine, monomethylhydrazine) and an oxidizer (*e.g.* HNO_3 or dinitrogen tetroxide), which reacts hypergolic after contact of both liquids.[4, 22] According to the environmental impact of the widely used ammonium perchlorate, intensive research is carried out to replace that compound in propellants.[23-24]

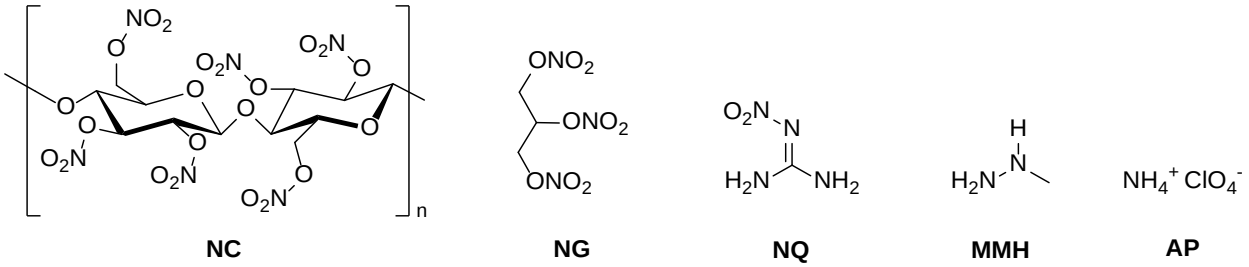

Figure 1.4. Chemical structures of selected gun propellants and rocket fuels: nitrocellulose (NC), nitroglycerine (NG), nitroguanidine (NQ), monomethylhydrazine (MMH) and ammonium perchlorate (AP).

Pyrotechnics. The expression *„pyrotechnic"* can be derived from the greek words *pyros* and *techne*, which can be translated as the art of fire.[25] Usually, pyrotechnical formulations are designed to display a special effect such as heat, light, sound, smoke or to produce specific reaction products. In contrast to other energetic materials, pyrotechnics undergo a slower, non-detonative and self-sustaining exothermic reaction forming in general solid residues. [4, 25-26] The exact content of each pyrotechnical mixture depends on the intended application; however, the main ingredients oxidizer, reducing agent and fuel remain the same. [27] The common knowledge use of pyrotechnics in the civil sector are fireworks, while research is primarily of military interest for the application as for example signal flares or obscurants. [26, 28-29] It is a well-known fact that historical pyrotechnic formulations containing perchlorates, halogens, heavy metals or potassium dichromate come with risks for environment and health. Nowadays, these former mixtures should be replaced by more harmless ones reducing the environmental impact with consistent or even higher performance. [30-31] Regarding the research of Sabatini *et al.* it was already possible to remove the chlorine source in red-burning illuminants by using fuels such as 5-amino-1*H*-tetrazole or hexamethylentetramine.

1.2 Primary Explosives with focus on K_2DNABT

As mentioned above, the commonly used primary explosives are still lead azide and lead styphnate. These historically applied compounds contain heavy metals making much *"greener"* alternatives necessary due to their environmental impact. Moreover, lead azide and lead styphnate are listed on the REACH (Registration, Evaluation, Authorization and Restriction of Chemicals) candidate list as "*substances of very high concern*" and will be prohibited for future use.[32] In the USA, lead is classified as a toxic pollutant and therefore, it should be removed from facilities like the areas of the US Department of Defense.[33] Lead is a chronic and acute toxin, which is not easy to remove from human bodies after it has been absorbed or dissolved in the blood.[6] In addition to its environmental impact, lead azide decomposes under ambient conditions by reacting with carbon dioxide and water to basic lead carbonate and greatly toxic hydrazoic acid (HN_3). Besides these difficulties, lead azide also shows an insufficient chemical stability, since it reacts with oxidizing reagents and ammonia.[34]

More recent developed heavy metal-free primary explosives as replacement for lead azide are copper(I) 5-nitrotetrazolate (DBX-1) and diazadinitrophenole (DDNP). However, both compounds suffer either from a relatively low decomposition temperature (DDNP: 142 °C)[35] or decomposition reactions with periodates in the case of DBX-1.[36] Therefore, there is still a claim for the development of a new *"green"* primary explosive. The main requirements for the development of new primary explosive are insensitivity to light and moisture, appropriate sensitivity values, high decomposition temperature, fast DDT, high initiation capability, long-term stability, heavy-metal-free, cheap reagents as well as an easy and especially safe synthesis.[4]

K_2DNABT is the abbreviation of the dipotassium salt of 1,1'-dinitramino-5,5'-bistetrazolate, which was firstly synthesized by Fischer *et al.* in 2014. This compound fulfills the majority of all mentioned requirements for a more environmentally benign primary explosive.[37] The energetic properties and calculated performance data of lead azide, DDNP, DBX-1 and **K_2DNABT** are summarized in Table 1. The sensitivity values towards external stimuli of these four primary explosives are in a similar range. The impact sensitivity values according to BAM standards[2] are in between 0.036 J and 4 J and the friction sensitivity is in between 0.098 N and 5 N. All evaluated compounds are classified as very sensitive towards electrostatic discharge ranging from 3–12 mJ. Further, **K_2DNABT** shows the highest nitrogen content with 50% and the highest oxygen balance (−4.8%). DDNP has the lowest decomposition temperature (157 °C), whereas all others are higher than 200 °C. The densities are with exception of DDNP (1.719 g cm^{-3}) higher than 2.0 g cm^{-3}.

The heats of formation are all positive with lead azide as the highest (450 kJ mol^{-1}). The detonation parameters for all compounds were recalculated with EXPLO5 V6.03 using recalculated X-ray densities for a precise comparison. As shown in Table 1.1, the calculated detonation velocities and the detonation pressures lie in the range of 6121–8751 m s^{-1} and 183–484 kbar. **K_2DNABT** has the highest detonation properties of the four presented primary explosives. To further determine the toxicity to aquatic life, the luminescent marine bacterium *Vibrio fischeri* was used.[38-39] Due to the fact of an insufficient water solubility of DBX-1 and lead azide[40], the values could only be determined for DDNP and **K_2DNABT**. With an EC_{50} (15 min) value lower than 5.93 g L^{-1}, it can be classified as nontoxic for aquatic life, whereas DDNP (0.001 g L^{-1}) is classified as very toxic.[38]

The synthetic route toward **K_2DNABT** starting from commercially available dimethyl carbonate within a six-step synthesis is shown in Scheme 1.1.[37]

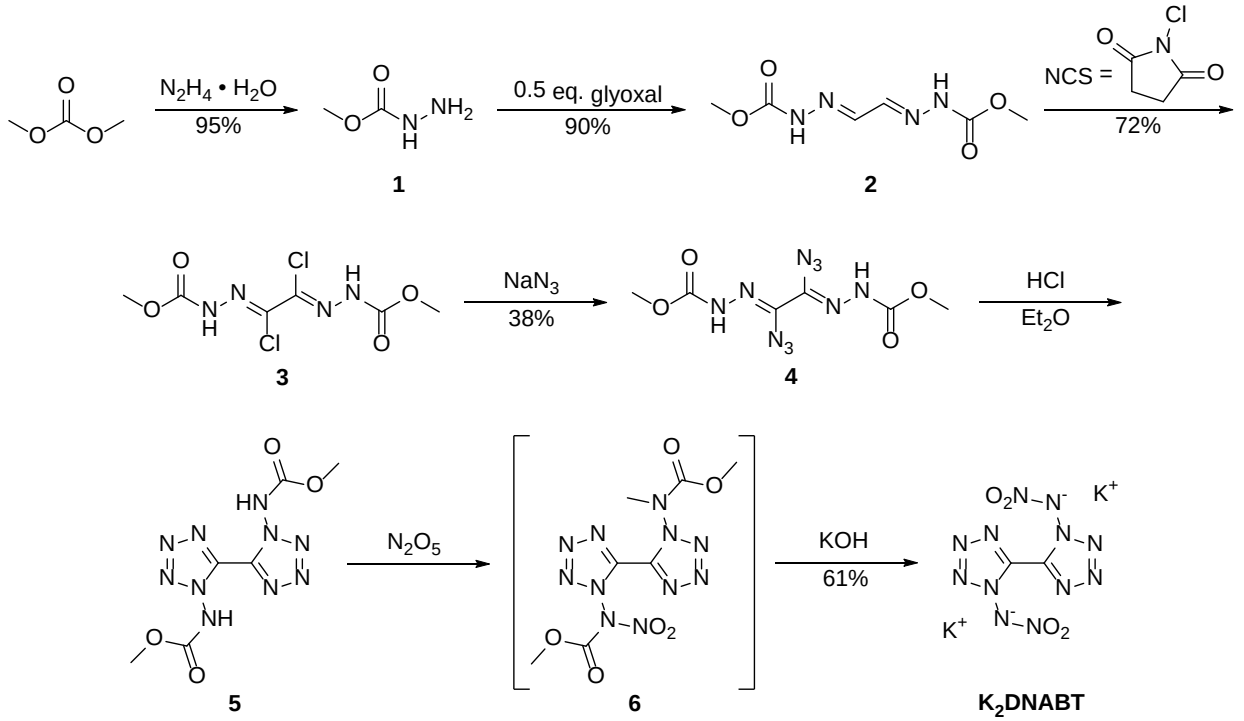

Scheme 1.1. Synthesis of **K_2DNABT** according to Fischer *et al.*[37]

The synthesis starts with the condensation of dimethyl carbonate with hydrazine hydrate to receive methyl carbazate (**1**) followed by a further condensation reaction using 0.5 eq. aqueous glyoxal solution to give (**2**).[41-42] Compound (**2**) is chlorinated using *N*-chlorosuccinimide (NCS) in DMF to get the dichloride (**3**). The nucleophilic chloro/azido-substitution is carried out using sodium azide in DMF to obtain (**4**), which is further ring-closed (**5**) by the aid of gaseous HCl in ether suspension.

Finally, compound (**5**) is nitrated with dinitrogen pentoxide in acetonitrile followed by an alkaline work-up with potassium hydroxide to yield **K_2DNABT** as a colorless powder.

Table 1.1. Energetic properties and detonation parameters of DDNP, DBX-1, $Pb(N_3)_2$ and **K_2DNABT**.

	DDNP[18]	**DBX-1**[11, 43]	**$Pb(N_3)_2$**[5]	**K_2DNABT**[37]
Formula	$C_6H_2N_4O_5$	$CuCN_5O_2$	PbN_6	$C_2K_2N_{12}O_4$
FW [g mol^{-1}]	210.1	177.6	291.3	334.3
IS [J] [a]	1.0	0.036	2.5–4.0	<1.0
FS [N] [b]	5.0	0.098	0.1–1.0	<1.0
ESD [J] [c]	0.012	0.0031	<0.005	0.003
N [%] [d]	26.7	39.4	28.9	50.3
Ω [%] [e]	−60.9	−9.0	−11.0	−4.8
$T_{dec.}$ [°C] [f]	157	337	315	200
ρ [g cm^{-3}] [g]	1.719	2.51	4.8	2.11
$\Delta_f H_m°$ [kJ mol^{-1}] [h]	139.0	49.9	450.1	326.4
$\Delta_f U°$ [kJ kg^{-1}] [i]	350.5	329.8	1574.9	1036.1
EXPLO5 V6.03				
$-\Delta_{Ex}U°$ [kJ kg^{-1}] [j]	4174	2464	1575	4962
T_{det} [K] [k]	3375	2899	3264	3408
p_{CJ} [kbar] [l]	183	236	350	328
V_D [m s^{-1}] [m]	6861	6739	6121	8751
V_0 [L kg^{-1}] [n]	467	482	252	484
Toxicity				
EC_{50} (15 min) [g L^{-1}] [o]	0.001[38]	–	–	>5.93[38]
EC_{50} (30 min) [g L^{-1}] [o]	0.001[38]	–	–	11.63[38]

[a] Impact sensitivity according to BAM drophammer (method 1 of 6); [b] Friction sensitivity according to BAM friction tester (method 1 of 6); [c] Electrostatic discharge sensitivity (OZM ESD tester); [d] Nitrogen content; [e] Oxygen balance; [f] Onset temperature of decomposition according to DSC (heating rate of 5 C min^{-1}); [g] Density at room temperature; [h] Heat of formation; [i] Energy of formation. [j] Heat of detonation; [k] Temperature of detonation; [l] Detonation pressure; [m] Detonation velocity; volume of gases after detonation; [n] Gas volume after detonation; [o] Toxicity measurements to aquatic life using luminescent marine bacterium *Vibrio fischeri*

1.3 Secondary Explosives with focus on TKX-50

RDX and TNT are mainly applied in charges due to their facile synthesis, cheap reagents and sufficient energetic performance. However, these compounds have a huge bearing on its surroundings due to their toxicity and carcinogenicity.[44] During WWI, the United Kingdom's female shell makers got the nickname *"canary girls"*, since the exposure of TNT caused skin eruption and turned their skin into orange-yellow.[45] Furthermore, studies on TNT-treated rats showed a possible carcinogenic hazard.[46] TNT and RDX are both nerve poisons and were found to cause liver injury.[47-48] Drinking water supplies close to the US Army ammunition plants were intensively contaminated with RDX. Due to the toxicity, the American Environmental Protection Agency (EPA) recommended a limit concentration of 2 μg L^{-1} for RDX in tap water. The National Institute for Occupational Safety and Health (NIOSH) had set the recommended exposure limit of TNT[49] as 0.5 mg m^{-3} and as 1.5 mg m^{-3} for RDX[50]. Further, even the decomposition products are toxic for plants, microorganisms or microbes.[47] Recent studies discussed that plants die with an RDX concentrations above 580 mg kg^{-1}.[51] The exposure to RDX can cause hyperirritability, nausea, seizures, amnesia, and vomiting as well as prolonged postictal confusion.[14-15, 47]

According to the bad environmental compatibility of RDX, there is a demand for the research of new *"greener"* secondary explosives. The main requirements for the new capable secondary explosive are high performance, low sensitivity toward external stimuli, low/no solubility in water, simple and safe synthesis with high yields, low toxicity of itself and its detonation products, high density, acceptable oxygen balance, cheap starting reagents, high thermal stability and compatibility with binder or plasticizer (Figure 1.5).

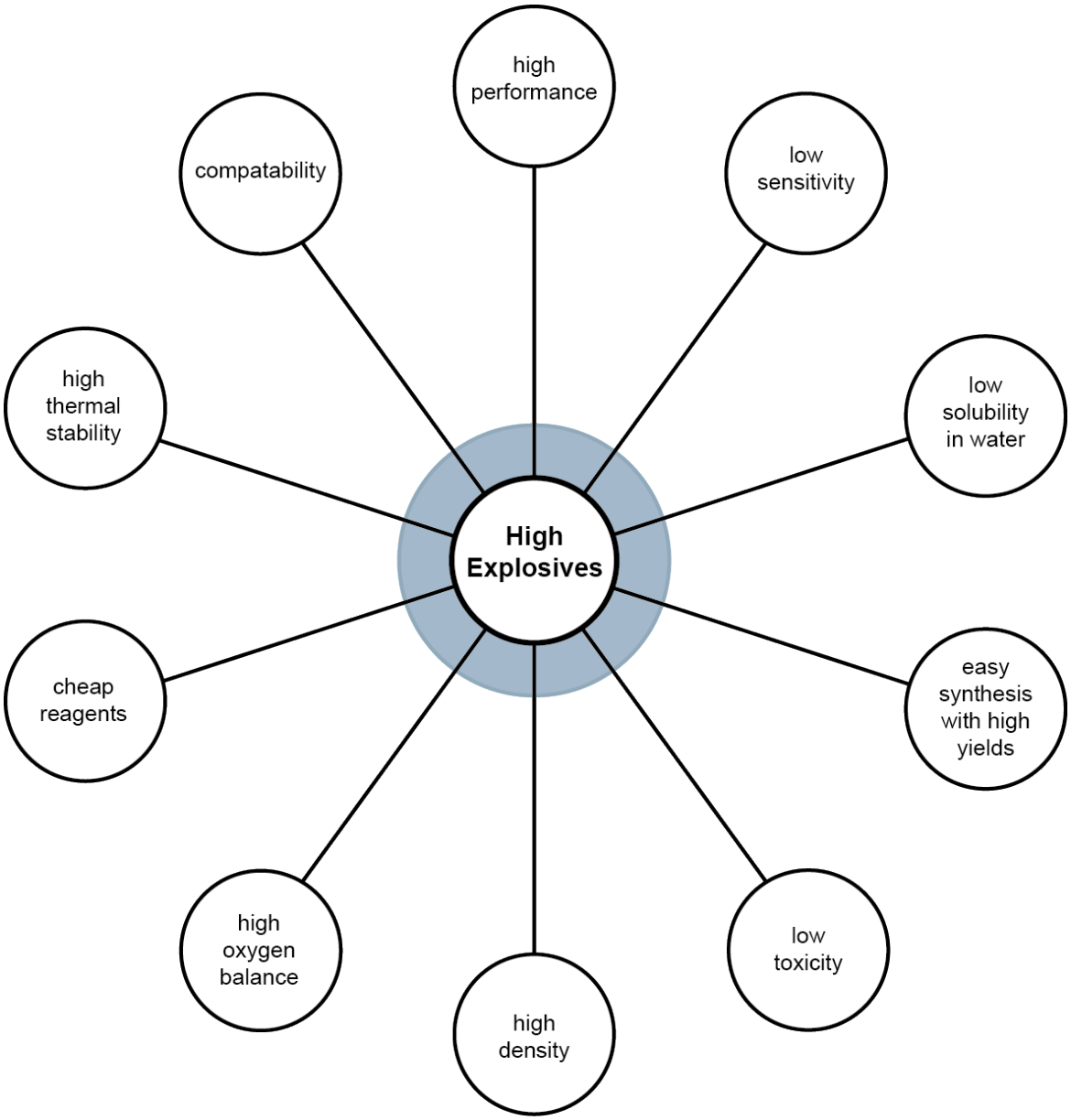

Figure 1.5. Requirements for new secondary explosives.

During the last half century, a lot of different secondary explosives were synthesized in order to substitute RDX and fulfill the requirements mentioned above. The most relevant compounds with respect to their performance, sensitivity, thermal stability and synthetic practicability are FOX-7[52], Cl-20[53], BTNPM, LLM-105[54], dihydroxylammonium-3,3′-dinitro-5,5′-bi(1,2,4-triazole)-1,1′-dioxide (MAD-X1)[55], 3-nitro-1,2,4-triazole-5-one (NTO)[56] and dihydroxylammonium 5,5´-bitetrazole-1,1´-dioxide (**TKX-50**)[17] (Figure 1.6).

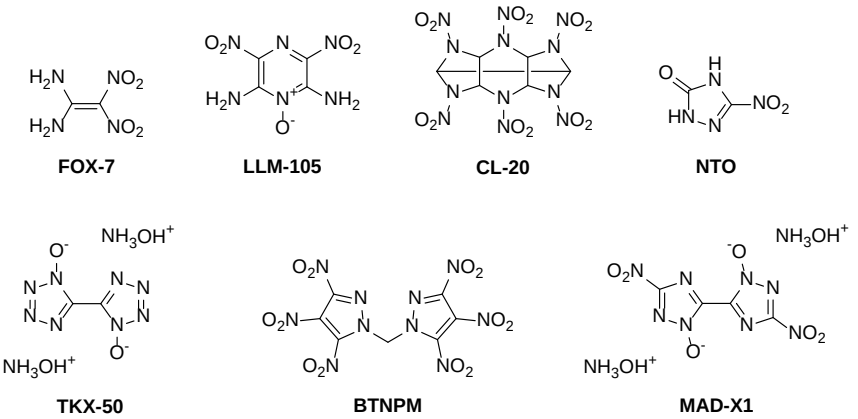

Figure 1.6. Overview of possible RDX replacements: FOX-7, Cl-20, BTNPM, LLM-105, dihydroxylammonium-3,3′-dinitro-5,5′-bi(1,2,4-triazole)-1,1′-dioxide (MAD-X1), 3-nitro-1,2,4-triazole-5-one (NTO) and dihydroxylammonium 5,5´-bitetrazole-1,1´-dioxide (**TKX-50**).

NTO – as the oldest possible RDX replacement – was first prepared in 1905 by Manchot *et al.*, however, major interest in its explosive characteristics was aroused first in the 1980s.[56-57] The synthesis is performed starting from formic acid and semicarbazide hydrochloride in a two-step synthesis. Australian scientists performed the reaction without isolation of the intermediate triazolone in an one-pot reaction.[58] NTO shows a high density (1.91 g cm^{-3}), detonation velocity (8590 m s^{-1}) and low sensitivity values (IS: 22 J, FS: 353 N).[58-59] Due to its characteristics, it has already found application in gas generators and is investigated to be part in low vulnerable warheads.[4, 60]

CL-20 was firstly synthesized by Nilsen *et al.* at the Naval Air Warefare Center Wepaons Division in China Lake in 1987.[53] The caged compound possesses a high density, excellent energetic performance (V_D = 9455 m s^{-1}) and acceptable sensitivities (IS: 4 J, FS: 48 N).[61] It exists in different polymorphs, but only the ε-polymorph was already investigated in formulations due to the highest density (2.04 g cm^{-3}).[62] However, the explosive has three main disadvantages, which are the prize (800 $ kg^{-1}), the existence of different polymorphs and the extensive synthesis involving expensive palladium catalysis.[11, 61]

LLM-105 was synthesized in 1994 at the Lawrence Livermore National Laboratories by Pagoria *et al.* and shows insensitivity to external stimuli (IS: > 40 J, FS: 360 N)[63-64], high thermal decomposition temperate of 354 °C and a detonation velocity of 8730 m s^{-1}, which is in the range of RDX.[4, 11] There are two different synthetic routes starting either with commercially available 2,6-dichloropyrazine within four steps or with *N*-chloro bis(cyanomethyl) amine (2 steps) in a two-step synthesis.[54] A further synthesis route was carried out by Zuckerman *et al.* using a micro reactor starting either with 2,6-diaminopyrazine-1-oxide or 2,6-dimethoxypyrazine.[65]

In 1998, the insensitive and thermally stable FOX-7 was synthesized by the Swedish FOI.[52] It is stable up to 238 °C, exhibits a detonation velocity of 8870 m s^{-1} and is less sensitive than RDX toward external stimuli.[4] There are different ways for the synthesis mentioned in the literature starting with either 4,6-dihydroxy-2-methylpyrimidine in a two-step synthesis, 2-methyl-imidazole in a three-step synthesis or with a mixture of acetamidine hydrochloride and diethyl oxalate in a three-step synthesis.[4, 52, 66] However, FOX-7 exists in at least three different polymorphs with different densities and thermal decomposition making its synthesis and application challenging.[66]

The main characteristics (synthesis steps, IS, detonation velocity and decomposition temperature) of the mentioned RDX replacements (NTO, CL-20, LLM-105 and FOX-7), which were synthesized in other research groups, are summarized in Figure 1.7.

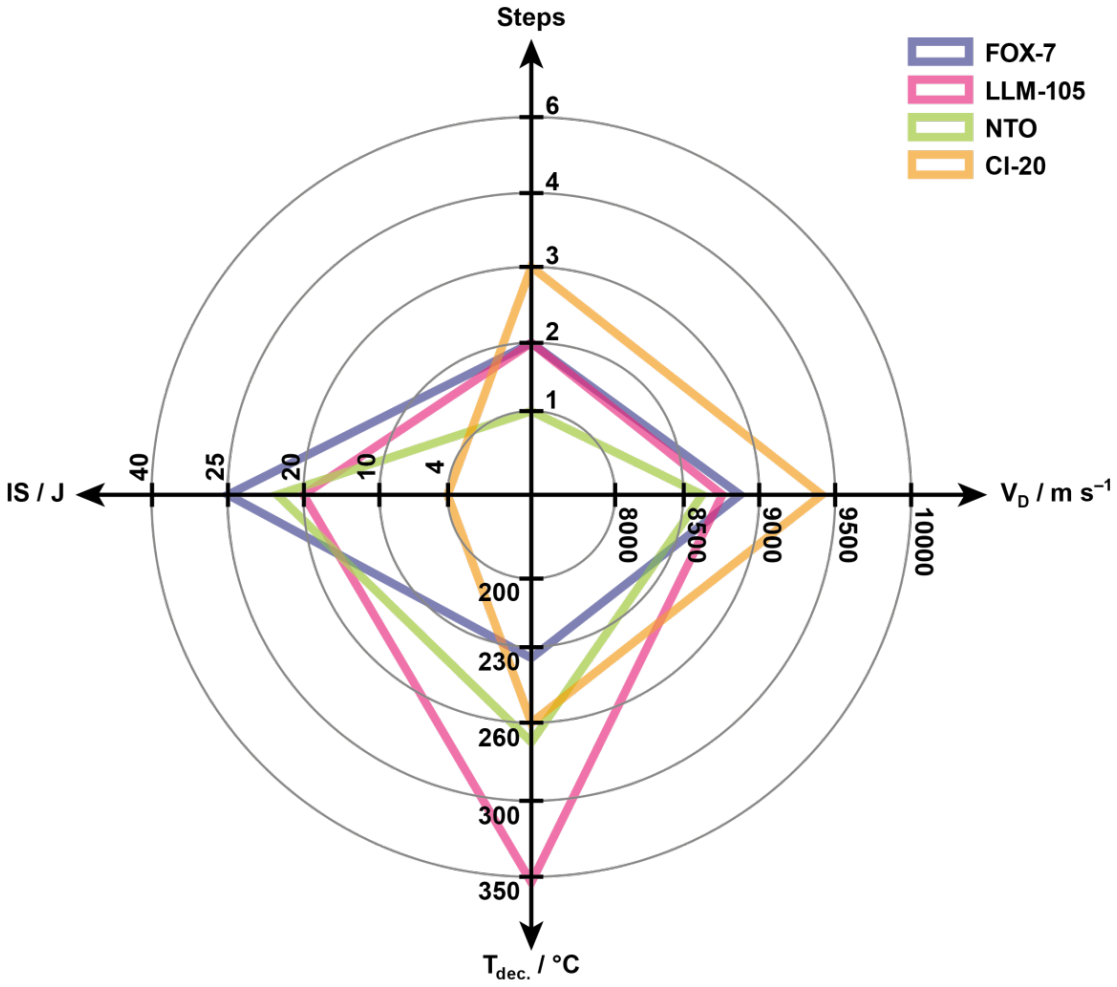

Figure 1.7. Comparison of selected main characteristics (synthesis steps, impact sensitivity, detonation velocity and decomposition temperature) of the possible RDX replacements FOX-7, LLM-105, NTO and Cl-20, which were synthesized in other working groups.

Also in the Klapötke group, three new possible RDX replacements were characterized within the last six years, named MAD-X1, BTNPM and **TKX-50**.[17-19, 55] MAD-X1 is an ionic explosive and can be synthesized starting with cheap oxalic acid. However, during the synthesis of MAD-X1 a diazotization is performed leading to an intermediate diazonium salt, which can explode spontaneously. MAD-X1 is not sensitive to external stimuli (IS: >40 J; FS: >360 N), has a high thermal stability (217 °C) and shows a high density of 1.90 g cm^{-3} (room temperature).[55] The calculated energetic parameters show a high detonation velocity of 9087 m s^{-1} which surpasses the performance of RDX (8919 m s^{-1}). BTNPM is a neutral explosive based on nitrated pyrazoles.[18-19] It decomposes at 205 °C, implicates a high density (1.934 g cm^{-3}, room temperature), acceptable sensitivity values (IS: 4 J, FS: 144 N), a very promising detonation velocity of 9304 m s^{-1} and can be synthesized from commercially available 1*H*-pyrazole in a six-step synthesis.

TKX-50, which is the common name for the dihydroxylammonium salt of 5,5-bitetrazole 1,1'-dioxide and one of the most promising replacements for RDX, is an ionic explosive developed by Fischer *et al.* in 2012.[17] This molecule fulfills all requirements for a new environmentally benign secondary explosive as outlined in Figure 5. The impact sensitivity of **TKX-50** is 20 J, which is much lower in comparison to TNT (15 J), RDX (7.5 J) and HMX (7 J). The same trend was observed for the friction sensitivity, where **TKX-50** reached a value of 120 N, which is equal or lower to RDX (120 N) and HMX (112 N). The ESD sensitivity of the selected explosives shows similar values between 0.1–0.2 J, which is lower than the maximum generated electrostatic discharge by humans (25 mJ). For military requirements, the thermal stability is an important characteristic, whereas in particular a decomposition temperature higher than 200 °C is favored. **TKX-50** has a decomposition temperature up to 221 °C. The energetic performance of the four explosives TNT, RDX, HDX and **TKX-50** was calculated with the computer code EXPLO5 V6.03 for a possible comparison (Table 2).[67] **TKX 50** obtained the highest calculated detonation velocity (V_D = 10026 m s^{-1}) as well as the highest detonation pressure (p_{CJ} = 41 GPa). To determine the toxicity to aquatic life of explosives, the luminescent marine bacterium *Vibrio fischeri* was applied.[38] The determined EC_{50} values of **TKX-50** is higher than the ones of RDX. Therefore, **TKX-50** is classified as less toxic toward aquatic life.[38] The only drawback of **TKX-50** at least is the extensive four-step synthesis involving sensitive intermediates.

The main characteristics with respect to synthesis steps, impact sensitivity, detonation velocity and decomposition temperature of the mentioned RDX replacements, which were synthesized by the Klapötke group, are summarized in Figure 1.8.

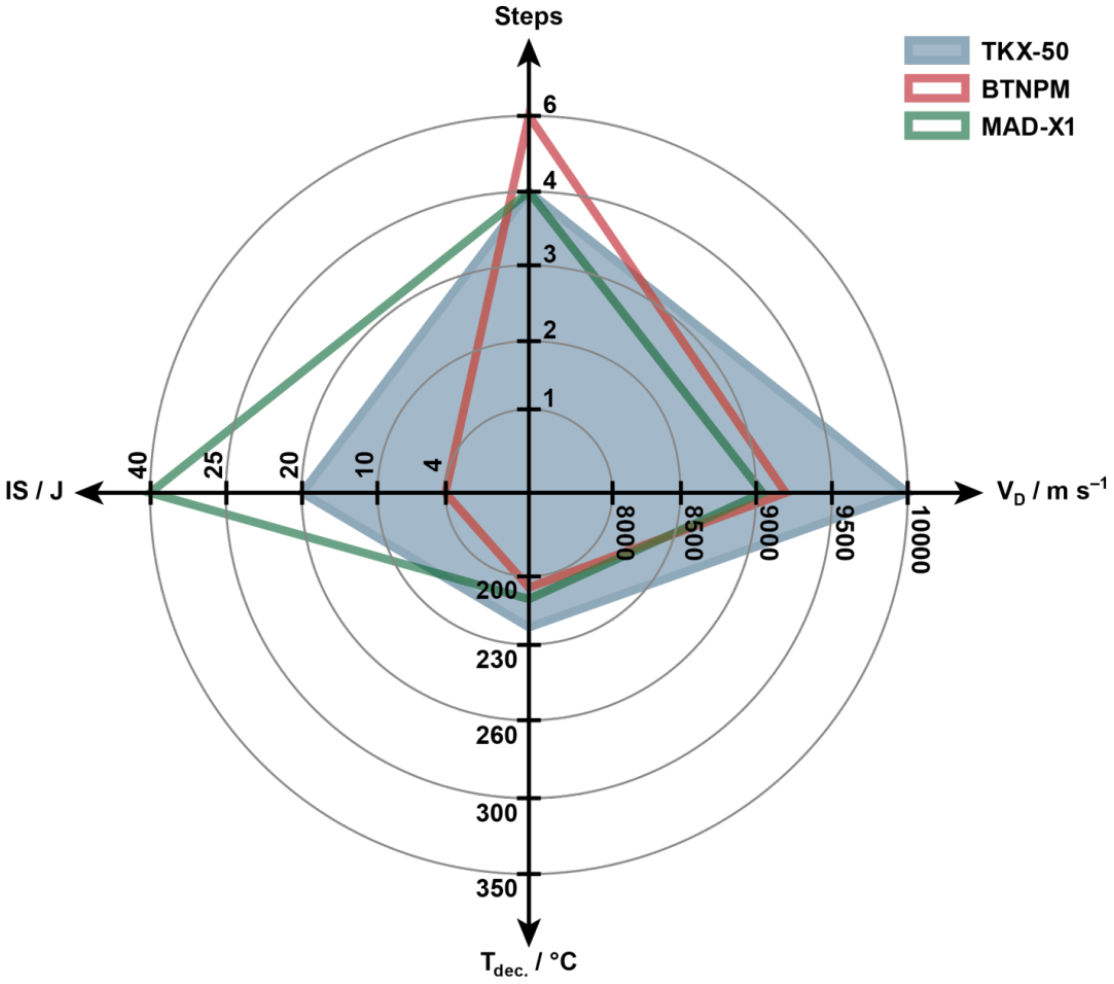

Figure 1.8. Comparison of selected main characteristics (synthesis steps, impact sensitivity, detonation velocity and decomposition temperature) of the possible RDX replacements **TKX-50**, BTNPM and MAD-X1, which were synthesized in our research group.

The extensive synthesis (five steps) of **TKX-50** including gaseous reactions and the isolation of sensitive intermediates is depicted in Scheme 1.2.

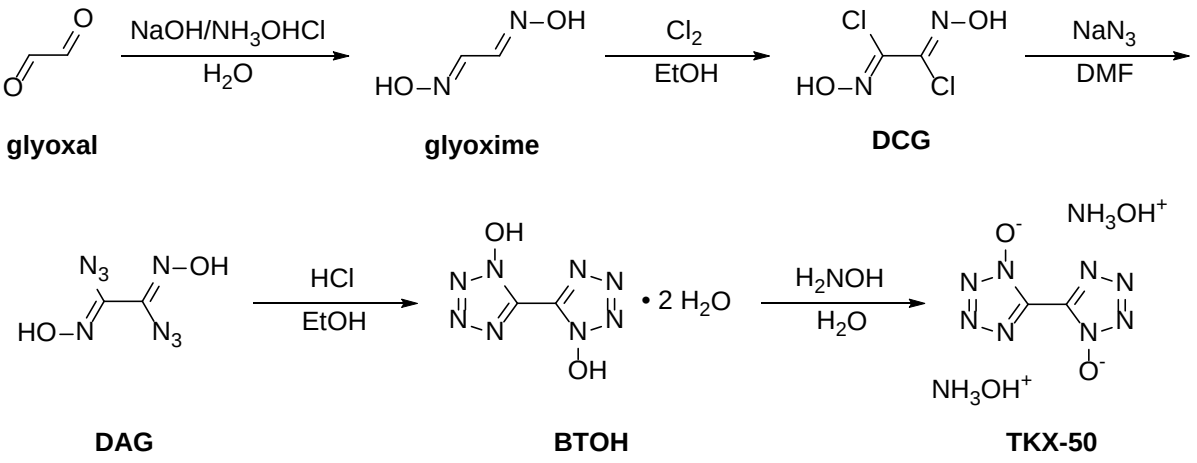

Scheme 1.2. Overview of the synthesis of TKX-50 from glyoxal with all intermediate steps: glyoxime, DCG (dichloroglyomine), DAG (diazidoglyoxime), BTOH (1,1'-dihydroxybitetrazole).[17]

The synthesis starts with conventional glyoxal solution, which is reacted with sodium hydroxide and hydroxylammonium chloride in water to form glyoxime in high yields (95 %). The chlorination of glyoxime was carried out by bubbling chlorine gas through a solution of glyoxime in ethanol at –20 °C to obtain dichloroglyoxime (DCG) as a colorless product. Next, the chloro/azido exchange was done using sodium azide at 0 °C in *N,N*-dimethylformamide (DMF) to afford the highly sensitive diazidoglyoxime (DAG). The cyclization step was carried out by suspending DAG in diethyl ether and bubbling gaseous HCl through the mixture. **TKX-50** was obtained by adding hydroxylamine solution in warm water. Due to the high sensitivity of diazidoglyoxime (DAG), a four-step route called "*One-pot way in DMF*" was invented. In this context, the mixture of the chloro/azido exchange was added to the ether solution without isolating DAG.

For a better overview, the energetic properties and recalculated performance data using the EXPLO5 V6.03 of **TKX-50** compared to TNT, RDX and HMX are shown in Table 1.2.[67]

Table 1.2. Energetic properties of TKX-50 compared to commonly used secondary explosives: TNT, RDX and HMX.[17]

	TNT[4]	**RDX[4]**	**HMX[4]**	**TKX-50**
Formula	$C_7H_5N_3O_6$	$C_3H_6N_6O_6$	$C_4H_8N_8O_8$	$C_2H_8N_{10}O_4$
FW [g mol^{-1}]	227.13	222.12	296.16	236.15
IS [J] [a]	15	7.5	7.0	20
FS [N] [b]	353	120	112	120
ESD [J] [c]	–	0.2	0.2	0.1
N [%] [d]	18.5	37.84	37.84	59.3
Ω [%] [e]	–74.0	–21.6	–21.6	–27.1
$T_{dec.}$ [°C] [f]	290	210	279	221
ρ [g cm^{-3}] [g]	1.648	1.806	1.904	1.877
$\Delta_f H_m°$ [kJ mol^{-1}] [h]	–55.5	86.3	116.1	446.6
$\Delta_f U°$ [kJ kg^{-1}] [i]	–168.0	489.0	492.5	2006.4
EXPLO5 V6.03[67]				
$-\Delta_{Ex}U°$ [kJ kg^{-1}] [j]	4999	5743	5708	5745
T_{det} [K] [k]	3192	3749	3624	3521
p_{CJ} [GPa] [l]	18.8	34.3	38.6	41.0
V_D [m s^{-1}] [m]	6878	8919	9328	10026
V_0 [L kg^{-1}] [n]	643	790	771	914
Toxicity				
EC_{50} (15 min) [g L^{-1}] [o]	–	0.33[38]	–	1.17[38]
EC_{50} (30 min) [g L^{-1}] [o]	–	0.24[38]	–	0.58[38]

[a] Impact sensitivity according to the BAM drop hammer (method 1 of 6); [b] Friction sensitivity according to the BAM friction tester (method 1 of 6); [c] Electrostatic discharge sensitivity (OZM ESD tester); [d] Nitrogen content; [e] Oxygen balance; [f] Temperature of decomposition according to DSC (onset temperatures at a heating rate of 5 C min^{-1}); [g] Density at room temperature; [h] Heat of formation; [i] Energy of formation. [j] Heat of detonation; [k] Temperature of detonation; [l] Detonation pressure; [m] Detonation velocity; volume of gases after detonation; [n] Gas volume after detonation; [o] Toxicity measurements to aquatic life using the luminescent marine bacterium *Vibrio fischeri*.

Due to the fact that **TKX-50** has the potential of being the RDX replacement in the future, it attracts great attention in the chemical community. Since 2012, over 60 journal articles or patents related to **TKX-50** were found in the literature.

The growing interest for **TKX-50** leads to a wide range of studies to get a closer understanding regarding synthesis, molecular processes, thermal behavior/decomposition, compatibility, solubility, sensitivity, polymorphism, co-crystallization, estimated detonation velocities, decomposition products and formulations using **TKX-50**.[68-80]

One main goal of research is the improvement of the extensive synthetic pathway toward **TKX-50**. In 2014 and 2015, two Chinese patents each described three-step synthesis starting from aqueous glyoxal solution with a total yields up to 72 %.[81-82] Zhang *et al.* prepared glyoxal in the first step, which is further combined with the chlorination using *N*-chlorosuccinimide (NCS) or *N*-bromosuccinimide (NBS) and azidation. In the final step, gaseous HCl was used for the ring-closing reaction followed by an extensive work-up.[82] Zhou *et al.* likewise prepared first glyoxal, which is then chlorinated using chlorine gas.[81] The third step includes the azidation, ring-closing using gaseous HCl and salt formation while isolating the sodium BTO salt.[81] However, both methods include gaseous HCl, transferring mixtures to new flasks as well as isolation of intermediates, for this reason these routes are still extensive and at least technically four-step synthesis.

In 2017, an Indian patent by Pradhan *et al.* reported about different synthesis of **TKX-50**.[83] However, the patent explains the original synthesis using different solvents (*e.g.* ethanol for chloro/azido exchange) or other reaction conditions. Also in 2017, a one-pot-synthesis by Damavarapu *et al.* was patented with a yield up to 71 %.[84] The patent explains the synthesis toward **TKX-50** starting from glyoxime in DMF adding NCS for chlorination, NaN_3 for chloro/azido exchange and a 4 M HCl dioxane solution for the ring-closing. But the synthesis shows disadvantages such as the sealing of the reaction mixture, long reaction durations and evaporation of the solvents after the ring-closing step.

Another publication reported on the optimization of the **TKX-50** synthesis established by Yolenko *et al.*.[85] They focused on the improvement of the cyclization step and further combining several reaction steps. Interestingly, the ring-closing method by Tselinskii *et al.*[86] using a different reagent was optimized and an one-pot-reaction in *N*-methyl-2-pyrrolidon (NMP) starting from glyoxime using dioxane and gaseous HCl for the ring-closing was established with a yield of 74 %. However, the mentioned one-pot reaction is more a two-pot reaction due to the isolation of an intermediate. Moreover, it is an extensive synthesis including reaction steps which are complex to transfer to industrial scale.

The most recent synthetic approach was carried out accidentally by Shreeve *et al.* in 2018.[68] They reported on the unpredictable loss of a carbon atom and the oxime moiety during the synthesis of bisoxadiazoles and bis-(1-hydroxy-1*H*-tetrazol-5-yl)-methanone oxime (Scheme 1.3). The latter leads to the not expected formation of **TKX-50** by cleaving the –C=NOH group between the tetrazoles. The new route avoids the usage of expensive and hard-to-remove solvents, however, still four synthesis steps are necessary to obtain **TKX-50**.

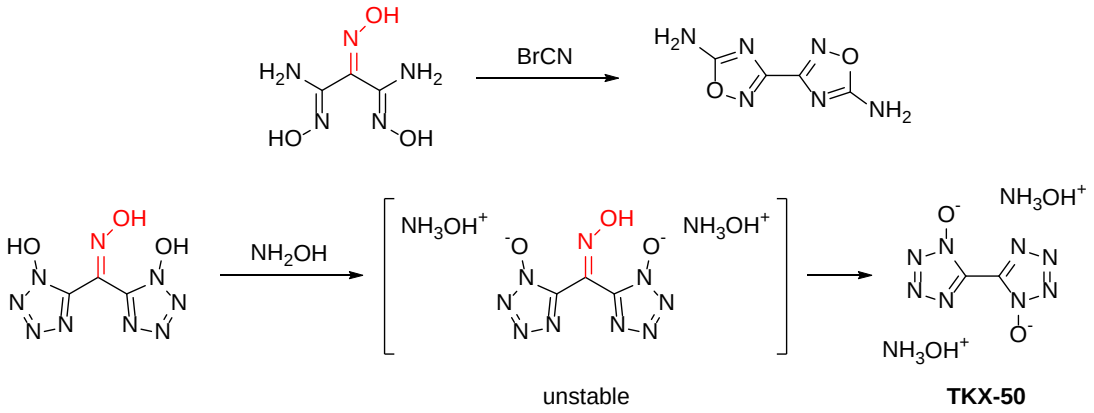

Scheme 1.3. Oxime loss during the synthesis leading toward **TKX-50** according to Shreeve *et al.*[68]

Detailed knowledge of possible phase transitions and thermal behaviour as well as decomposition were investigated by Dreger *et al.*, Lu *et al.* and Steele *et al.*[69, 87-88] First, Dreger *et al.* found a polymorphic phase transition while the ambient pressure phase of **TKX-50** is heated above 180 °C by Raman measurements. Second, he explained the high structural and chemical stability by the interionic hydrogen bonds between the molecular moieties. Under high pressure and high temperature, intermolecular hydrogen transfers were detected. This H-transfer from NH_3OH^+ to $C_2O_2N_8^-$ lead to disintegration of the N–O bond and release of gaseous products, which promotes the decomposition of **TKX-50**. Additionally, the decomposition of **TKX-50** can be characterized as a transformation into two intermediates. The first part of the decomposition is the formation of BTOH and NH_2OH. While hydroxylamine subverts into gaseous products such as N_2O, NH_3 and H_2O, bistetrazole-dioxide (BTOH) reacts with ammonia to diammonium-5,5´-bitetrazole-1,1´-dioxide, which is the dominating product of decomposition and decomposes into polymeric residues.[69] The finding of a phase transition by Dreger *et al.* was confirmed by Lu *et al.*, who reported on a new metastable phase named meta-**TKX-50** at ~180 °C.[69, 87] Further research by Steele *et al.* led to three new phases of **TKX-50**, each with different hydrogen bonding topology and crystallographic packing of the cation (NH_3OH^+) and anion ($C_2N_8O_2^{2-}$). The first phase (*P*-1) is predicted to be energetically competitive with normal phase near ambient conditions, while the other two phases are stable above either 19.9 GPa ($C2/c$) or 30.3 GPa ($P2_1/c$).[88]

Different attempts to change the mechanical properties, moldability and sensitivities were carried out by preparing formulations with **TKX-50**.[72, 74, 89-90] Wang *et al.* prepared **TKX-50**/graphene oxide composites with the result of changing the morphology to a spherical-like structure, which additionally lowers the sensitivity values.[72] As a conclusion, they promote their composite as a promising candidate for new insensitive high energetic materials.

Two other research groups dealt with studies about insensitive **TKX-50**-based melt cast high explosives.[74, 89] Both studies carried out formulations using **TKX-50** and/or RDX, HMX and/or TNT. Using a melt cast formulation consisting of **TKX-50**/TNT instead of RDX/TNT results in a higher thermal stability and lower friction sensitivity.[74] The formulations instigated by Yu *et al.* point also a higher performance and thermal stability of **TKX-50**/TNT and **TKX-50**/TNT/Wax formulations compared to HMX/TNT and HMX/TNT/Wax.[89] Both research groups emphasize the potential of **TKX-50** as replacement for RDX/HMX based melt cast formulations.[74, 89] Beside melt cast explosive formulations, **TKX-50** could also serve in polymer-bonded explosives.[90-93]

In the paper Yu *et al.*, molecular dynamics (MD) simulations are carried out to study the characteristics of **TKX-50** based polymer-bonded explosives using fluorine (F_{2311}), fluorine resin (F_{2641}), polyethylene glycol or ethylene vinyl acetate copolymer as binders.[93] They concluded that the best improvements in plasticity, moldability and binding energy were calculated for PEG. Further MD studies on polymer-bonded explosives with additional **TKX-50** were carried out by Ma *et al.* using polyvinylidene difluoride and polychlorotrifluoroethylene as polymer.[92] Using these binders lead to an improvement of the ductility and decreasing the sensitivities. Besides these promising calculations, Niu *et al.* performed practical polymer-bonded explosives formulations using 10 % of a $(C_3H_4O_5N)_n$ binder, which were analyzed by X-ray diffraction and thermal analysis.[90] The results revealed that the binder has only a weak effect on the thermal decomposition of that polymer bonded explosive.

Despite the promising characteristics of **TKX-50**, Xiong *et al.* were interested in new compositions by combining different explosives like RDX, HMX or CL-20 with **TKX-50** to obtain co-crystals.[75, 91, 94] The co-crystals of **TKX-50**/RDX, **TKX-50**/HMX and **TKX-50**/ CL-20 were closer investigated by molecular dynamics simulations in order to expand the application range of CL-20 and minimize the disadvantages of both single compounds. According to the calculations of Xiong *et. al.*, hydrogen bonding exists between the three **TKX-50** co-crystals resulting in significant lower sensitivity values as well as an improvement of the thermodynamic stability.[75, 91, 94]

To prove the calculated detonation properties using EXPLO5 or CHEETAH of different explosives, a new technique named LASEM (laser-induced air shock from energetic materials) was carried out and published by Gottfried *et al.* in 2017.[95] This method was utilized for commonly used and recently developed secondary explosives such as RDX, TNT, BTNPM or **TKX-50**. The tests showed that **TKX-50** produced the third largest laser-induced deflagration of the measured explosives. Further, the estimated detonation velocities based on the LASEM measurements are in agreement with the calculated ones with less than 1.5 % deviation.[95]

Using an underwater initiation test, the initiating capability of detonators containing different common (RDX, HDX, PETN) and recent explosives (**TKX-50**, MAD-X1, PETNC, DAAF) was undertaken by Klapötke *et al.* in 2016.[96] In the underwater experiment, the total energy is a sum of the shock wave energy and the gas bubble energy. In detail, the total energy of **TKX-50** was the third highest behind MAD-X1 and DAAF. The obtained densities during the experiments were lower for all recent explosives than the theoretically maximum density. In summary, **TKX-50** can be used as based charge detonators at which the pressing density has to be increased to maximize the performance parameters.[96]

According to Huang *et al.*, **TKX-50** shows excellent heat-resistance ability (critical temperature of thermal explosion: 523.39 K). Moreover, the main decomposition products were determined by TG-FTIR as well as TG-DSC-MS to be N_2, H_2O, NH_3, NH_2, N_2O and NO.[77]

Further, a compatibility study of **TKX-50** with different binders, explosives as well as additives was carried out by Huang *et al.* using DSC measurements.[76] However, their testing setup and rating was performed completely different than the official STANAG 4147 agreement.[97] Anyway, as a result of their study **TKX-50**/HNE as well as **TKX-50**/DNAN possess beneficial compatibility and **TKX-50**/HMX moderate compatibility. The compatibility of **TKX-50** with TNT, RDX, Cl-20, NC, ammonium perchlorate, aluminium, GAP (glycidyl azide polymer) and HTPB (hydroxyl-terminated polybutadiene) is according to their rating poor.[76]

Another compatibility test was performed by Nicolich *et al.* using a traditional vacuum stability test in accordance to the STANAG 4556[98] agreement.[80, 98] They reported on the outstanding compatibility of **TKX-50** toward polymers, plasticizers, metals and metal oxides.

Zhang *et al.* analyzed the solubility of **TKX-50** in different solvents by gravimetric methods with the order of solubility: ethyl acetate < ethanol < toluene < water < DMF < formic acid < DMSO.[79] Further, a linear relationship between the solubility of **TKX-50** and the temperature was found.[79]

An *et al.* investigated the anisotropic impact sensitivity and shock induced plasticity using molecular dynamics simulations.[78] The focus during that work was to set on the mechanical response under shock directions from (100), (010) and (001). Due to the calculated Hugoniot Elastic Limits (HEL), they expect anisotropic sensitivity, whereas (010) is the most sensitive shock direction with the highest HEL (14.2 GPa), (100) the insensitive shock direction with the lowest HEL (6.1 GPa) and (001) is the most moderate sensitive shock direction with 9.1 GPa.[78]

More recent in 2018, two patents related to **TKX-50** were published dealing with explosive nanowires or of being a possible explosive in an electromagnetic mobile active system for fitting in a missile with a detonation-operated magnetic field compressor.[99-100]

1.4 Concept, Motivation and Objectives

Goals and motivation of this thesis consist of three main parts: the first part deals with the synthesis and characterization of new *"green"* secondary explosives based on azoles, while the second part discusses the synthetic improvement and further characterization of the primary explosive **K_2DNABT**. The last part explains the synthetic improvement and further characterization of the secondary explosive **TKX-50**.

The main features and characteristics of a new potential RDX replacement are a thermal stability over 200 °C, higher performance ($V_D \geq 8800$; $p_{CJ} \geq 340$ kbar), lower sensitivities toward external stimuli (IS ≥ 7.5 J; FS ≥ 120 N) and environmental compatibility.

The first goal regarding the synthesis, intensive characterization and investigation of new secondary explosives should be solved by utilization of nitrogen-rich heterocycles such as pyrazoles or by combining 1,2,4-triazoles and 1,2,4,-oxadiazoles (Figure 1.9). These azoles as building blocks are suitable to synthesize new energetic materials inclosing the main characteristics mentioned above.[13, 101-102]

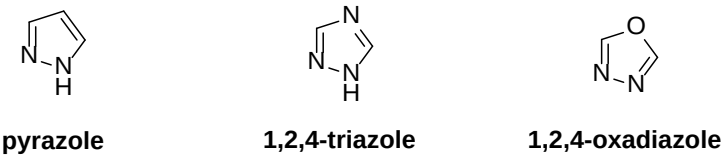

Figure 1.9. Chemical structures of selected nitrogen-rich heterocycles used as backbone for the synthesis of new secondary explosives.

Pyrazoles – especially nitrated pyrazoles – arouse interest in the past due to their different characteristics and cheap price for the investigation of new environmentally friendly energetic materials.[103-107] The design of new functionalized pyrazole derivatives is an ongoing progress and many remarkable compounds were synthesized.[18, 23, 108-109]

The main concept to enhance the energetic properties is to get rid of the acidic proton of the pyrazole ring which could cause compatibility problems.[23] Therefore, different strategies are known such as salt formation[110], methylation[111], *N*-functionalization[104, 109], azo-bridging[103], amination[108, 112], *N*-oxidation[113-114], ethylene[115] or methylene bridging[18] as well as combination with other heterocycles (Figure 1.10).

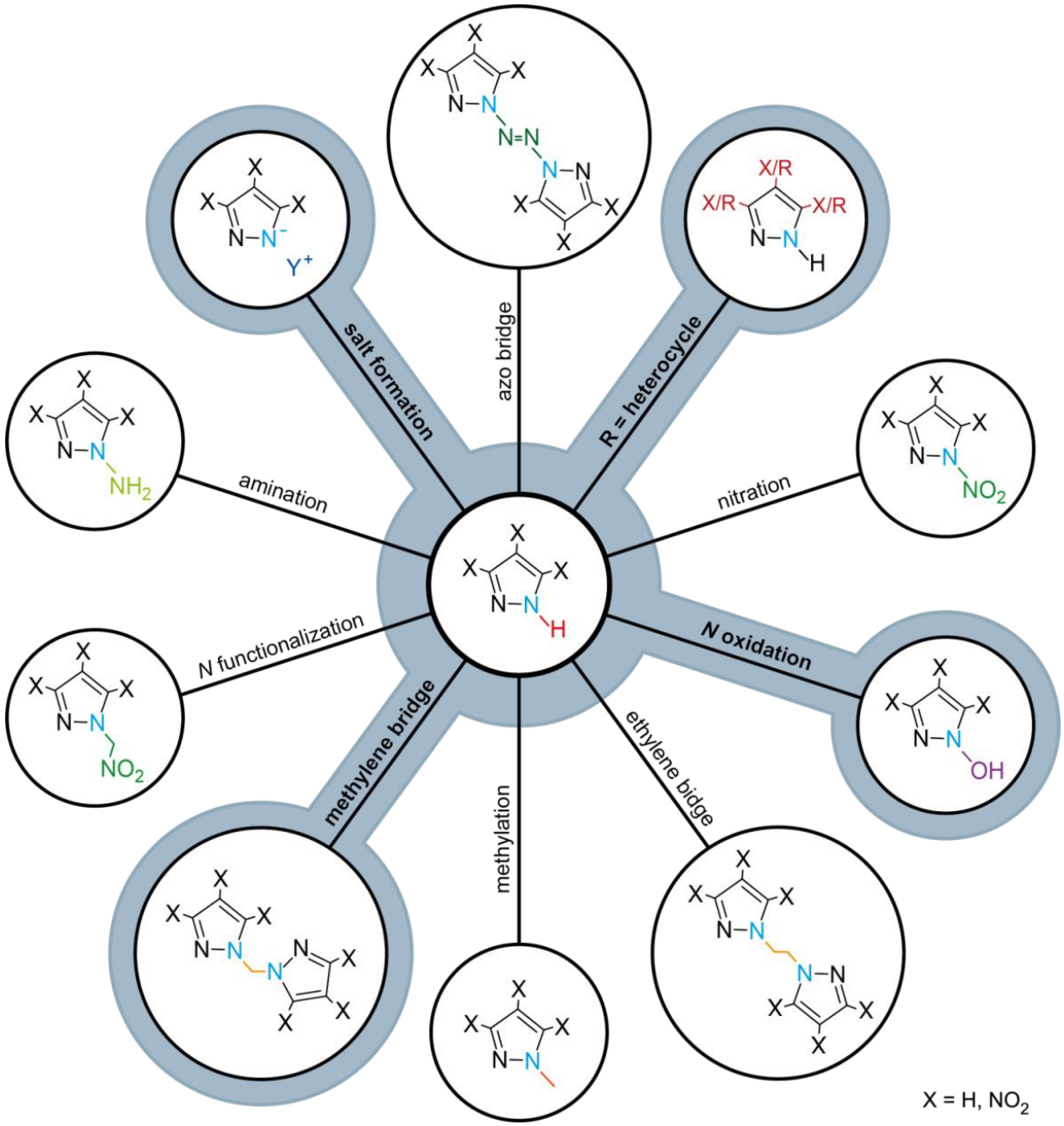

Figure 1.10. Functionalization possibilities of nitrated pyrazoles by either detaching the acid proton or connecting with other heterocycles. The blueish highlighted bubbles are discussed in this thesis.

Salt formation using nitrogen-rich cations generally improve the thermal stability and – in some cases – also the stability toward external stimuli caused by hydrogen bonding interactions.[116] *N*-Functionalization such as the introduction of a trinitromethyl group to the nitrogen atom of 3,4-dinitropyrazole and 3,5-dinitropyrazole (T_{dec} = 141–143 °C; V_D = 8668–8733 m s^{-1}) or reacting bromonitromethane with trinitropyrazole (TNP) mainly increase the oxygen balance and the density, whereas these compounds can be classified as a high energetic density oxidizer due to their high oxygen content.[23, 109]

New pyrazole derivatives could further be synthesized by linking azoles via *N,N´*-alkyl-bridging.[117-118] Examples are linked nitramino or azido substituted nitropyrazoles with nitroimino-tetrazoles via an *N,N'*-ethylene-bridge to get either thermal sensitive but powerful explosives (T_{dec} = 89–137 °C; V_D = 8659–8804 m s^{-1}).[118] Decreasing the carbon amount leads to *N,N'*-methylene-bridged compounds such as bispyrazolylmethanes, which were firstly described by Fischer *et al.*. The hexanitro-bridged pyrazole shows the highest detonation velocity (V_D = 9304 m s^{-1}) and a sufficient thermal stability (T_{dec} = 205 °C) and can therefore be compared to hexanitro-hexaazaisowurtzitane (CL-20).[119-120]

Another promising concept is the introduction of *N*-oxides in tetrazoles, triazoles or pyrazoles which results in higher energetic performances due to a higher oxygen balance, as well as the density and hence the detonation parameters. [17, 55, 114, 121-123] This class of compounds can easily be synthesized by using either Oxone® or hypofluorous acid (HOF).[124-125] Therefore, the *N*-oxide of TNP and some nitrogen-rich salts thereof were obtained by using Oxone® and a corresponding base. As a result, some of the newly developed compounds showed qualified properties as energetic materials (V_D = 8175–8676 m s^{-1}) with acceptable decomposition temperatures (T_{dec} = 118–186 °C).[126] Nevertheless, TNP oxide is a liquid and a very high impact sensitivity (IS: 1 J) was observed.[126] The last possible option is the combination of pyrazoles with different nitrogen-rich heterocylces such as triazoles, oxdiazoles or tetrazoles, which further leads to biheterocyclic C–C- or C–N-bonded compounds exhibiting promising energetic performances.[127-129]

This thesis focuses on four of the mentioned concepts (*N*-oxidation, salt formation, methylene-bridging and combination with tetrazoles) carried out with (nitrated) pyrazoles (Figure 1.11).

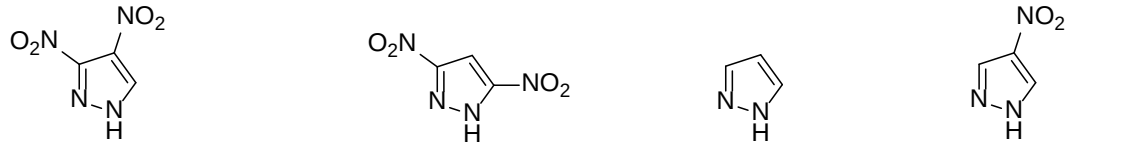

3,4-dinitro-1*H*-pyrazole **3,5-dinitro-1*H*-pyrazole** **1*H*-pyrazole** **4-nitro-1*H*-pyrazole**

Figure 1.11. Chemical structures of (nitrated) pyrazoles used and functionalized in this thesis.

1.5 References

[1] C. Papsthart, *Waffenrecht, Waffengesetz, Beschussgesetz, Sprengstoffgesetz, Gesetz über die Kontrolle von Kriegswaffen und Durchführungsvorschriften ; Textausgabe mit Sachverzeichnis und einer Einführung*, 16., überarb. Aufl., Dt. Taschenbuch-Verl., München, **2012**.

[2] http://www.astm.org; Accessed July 2018.

[3] D. Piercey, *Dissertation*, Ludwig-Maximilians-Universität München, **2013**, p. 4.

[4] T. M. Klapötke, *Chemistry of High-Energy Materials*, 4th ed., De Gruyter, Berlin, **2017**.

[5] R. Matyáš, J. Pachman, *Primary Explosives*, Springer Heidelberg, **2013**.

[6] M. Neha, O. Karl, C. Gartung, S. Akash, M. John, Y. Kin, *Z. Anorg. Allg. Chem.* **2014**, *640*, 1309–1313.

[7] T. M. Klapötke, N. Mehta, *Propellants Explos. Pyrotech.* **2014**, *39*, 7–8.

[8] N. Fischer, M. Joas, T. M. Klapötke, J. Stierstorfer, *Inorg. Chem.* **2013**, *52*, 13791–13802.

[9] D. Fischer, T. M. Klapötke, J. Stierstorfer, *Angew. Chem. Int. Ed.* **2014**, 8172–8175.

[10] W. Beck, J. Evers, M. Göbel, G. Oehlinger, T. M. Klapötke, *Z. Anorg. Allg. Chem.* **2007**, *633*, 1417–1422.

[11] J. Sabatini, K. Oyler, *Crystals* **2016**, *6*, 5.

[12] P. W. Cooper, *Explosives engineering*, Wiley-VCH, New York, Chichester, Weinheim, Brisbane, Singapore, Toronto, **1996**.

[13] T. M. Klapötke, P. C. Schmid, S. Schnell, J. Stierstorfer, *Chem. Eur. J.* **2015**, *21*, 9219–9228.

[14] H. Abadin, C. Smith, in *Toxicological Profile For RDX*, U.S. Department of Health and Human Serivces, Public Health Service, Agency for Toxic Substances and Disease Registry, **2012**.

[15] E. L. Etnier, *Regul. Toxicol. Pharm.* **1989**, *9*, 147–157.

[16] L. M. Sweeney, C. P. Gut, M. L. Gargas, G. Reddy, L. R. Williams, M. S. Johnson, *Regul. Toxicol. Pharm.* **2012**, *62*, 107-114.

[17] N. Fischer, D. Fischer, T. M. Klapötke, D. G. Piercey, J. Stierstorfer, *J. Mater. Chem.* **2012**, *22*, 20418–20422.

[18] D. Fischer, J. L. Gottfried, T. M. Klapötke, K. Karaghiosoff, J. Stierstorfer, T. G. Witkowski, *Angew. Chem. Int. Ed.* **2016**, *55*, 16132–16135.

[19] T. M. Klapötke, T. G. Witkowski, *ChemPlusChem* **2016**, *81*, 357–360.

[20] G. Steinhauser, T. M. Klapötke, *Angew. Chem. Int. Ed.* **2008**, *47*, 3330–3347.

[21] J. Stierstorfer, *Dissertation*, Ludwig-Maximilians-Universität München, **2009**.

[22] I. Frank, A. Hammerl, T. M. Klapötke, C. Nonnenberg, H. Zewen, *Propellants Explos. Pyrotech.* **2005**, *30*, 44–52.

[23] D. Kumar, G. H. Imler, D. A. Parrish, J. M. Shreeve, *J. Mater. Chem. A* **2017**, *5*, 10437–10441.

[24] T. M. Klapötke, B. Krumm, T. Reith, *Z. Anorg. Allg. Chem.* **2017**, *643*, 1474–1481.

[25] F. Keller, *Chem. unserer Zeit* **2012**, *46*, 248–265.

[26] U. S. Army Material Command, *Engineering Design Handbook: Theory and Application*, Military Pyrotechnics Series, Part One, Washington, DC, USA, **1967**.

[27] H. Ellern, *Military and civilian pyrotechnics*, Chemical Pub. Co, New York, **1968**.

[28] M. Russell, *The Chemistry of Fireworks*, The Royal Society of Chemistry, Cambridge, UK, **2009**.

[29] J. A. Conkling, C. Mocella, *Chemistry of Pyrotechnics: Basic Principles and Theory*, CRC Press, Boca Raton, **2010**.

[30] J. D. Moretti, J. J. Sabatini, J. C. Poret, *Chem. Eur. J.* **2014**, *20*, 8800–8804.

[31] Strategic Environmental Research and Development Program (SERDP), *Novel Pyrotechnics that Reduce Environmental Impact*, SON Number: WPSON-19-C4, FY 2019 Statement of Need, Alexandria, VA, USA, **2017**.

[32] https://echa.europa.eu/candidate-list-table?p_p_id=disslists_WAR_disslistsportlet&p_p_lifecycle=1&p_p_state=normal&p_p_mode=view&p_p_col_id=column-1&p_p_col_pos=2&p_p_col_count=3&_disslists_WAR_disslistsportlet_javax.portlet.action=searchDissLists, Accessed July 2018.

[33] W. J. Clinton, *Executive order 12856—Federal compliance with right-to-know laws and pollution prevention requirements*, Washington, DC, USA, **1993**.

[34] J. Akhavan, *Chemistry of Explosives*, 3rd ed., The Royal Society of Chemistry, Cambridge, UK, **2011**.

[35] M. Kaiser, U. Ticmanis, *Thermochim. Acta* **1995**, *250*, 137–149.

[36] M. Klapötke Thomas, G. Piercey Davin, N. Mehta, D. Oyler Karl, J. Sabatini Jesse, in *Zeitschrift für Naturforschung B, Vol. 69*, **2014**, p. 125.

[37] D. Fischer, T. M. Klapötke, J. Stierstorfer, *Angew. Chem. Int. Ed.* **2014**, *53*, 8172–8175.

[38] R. Scharf, Dissertation thesis, LMU München **2016**.

[39] G. I. Sunahara, S. Dodard, M. Sarrazin, L. Paquet, G. Ampleman, S. Thiboutot, J. Hawari, A. Y. Renoux, *Ecotoxicol. Environ. Saf.* **1998**, *39*, 185–194.

[40] E. Lieber, C. N. R. Rao, H. E. Dingle, J. Teetsov, *Journal of Chemical & Engineering Data* **1966**, *11*, 105–105.

[41] O. Diels, *Chem. Ber.* **1914**, *47*, 2183–2195.

[42] R. R. Gallucci, *J. Chem. Eng. Data* **1982**, *27*, 217–219.

[43] J. W. Fronabarger, M. D. Williams, W. B. Sanborn, J. G. Bragg, D. A. Parrish, M. Bichay, *Propellants Explos. Pyrotech.* **2011**, *36*, 541–550.

[44] G. A. Parker, G. Reddy, M. A. Major, *Int. J. Toxicol.* **2006**, *25*, 373–378.

[45] S. V. Rosser, *Women, Science, and Myth: Gender Beliefs from Antiquity to the Present*, ABC-CLIO, INC. , Santa Barbara, **2008**.

[46] J. Ashby, B. Burlinson, P. A. Lefevre, J. Topham, *Arch. Toxicol.* **1985**, *58*, 14–19.

[47] T. M. Klapötke, *Chemistry of High-Energy Materials*, De Gruyter, Berlin, **2011**.

[48] L. M. Sweeney, C. P. Gut Jr, M. L. Gargas, G. Reddy, L. R. Williams, M. S. Johnson, *Regul. Toxicol. Pharm.* **2012**, *62*, 107–114.

[49] T. S. S. Dikshith, *Hazardous Chemicals: Safety Management and Global Regulations*, Taylor & Francis, Boca Raton, **2013**.

[50] National Institute for Occupational Safety Health, *NIOSH Pocket Guide to Chemical Hazards*, U.S. Department of Health and Human Services, Public Health Service, Centers for Disease Control and Prevention, National Institute for Occupational Safety and Health, **2000**.

[51] J. Akhavan, *The Chemistry of Explosives*, Royal Society of Chemistry, Cambridge, **2011**.

[52] N. V. Latypov, J. Bergman, A. Langlet, U. Wellmar, U. Bemm, *Tetrahedron* **1998**, *54*, 11525–11536.

[53] A. T. Nielsen, A. P. Chafin, S. L. Christian, D. W. Moore, M. P. Nadler, R. A. Nissan, D. J. Vanderah, R. D. Gilardi, C. F. George, J. L. Flippen-Anderson, *Tetrahedron* **1998**, *54*, 11793–11812.

[54] P. F. Pagoria, M. X. Zhang, U.S. Patent 20100267955, **2010**.

[55] A. A. Dippold, T. M. Klapötke, *J. Am. Chem. Soc.* **2013**, *135*, 9931–9938.

[56] K.-Y. Lee, L. B. Chapman, M. D. Cobura, *J.Energ. Mat.* **1987**, *5*, 27–33.

[57] W. Manchot, R. Noll, *Liebigs Ann.* **1905**, *343*, 1–27.

[58] R. J. Spear, C. N. Louey, M. G. Wolfson, *A Preliminary Assessment of 3-Nitro-1,2,4-Triazol-5-One (NTO) as an Insensitive High Explosive*, Materials Research Laboratory, Melbourne, Australia, **1989**.

[59] M. W. Smith, M. D. Cliff, *NTO-Based Explosive Formulations: A Technology Review*, **1999**.

[60] A. Becuwe, A. Delclos, *Propellants Explos. Pyrotech.* **1993**, *18*, 1–10.

[61] D. S. Viswanath, T. K. Ghosh, V. M. Boddu, in *Emerging Energetic Materials: Synthesis, Physicochemical, and Detonation Properties*, Springer Netherlands, Dordrecht, **2018**, pp. 59–100.

[62] S. S. Samudre, U. R. Nair, G. M. Gore, R. Kumar Sinha, A. Kanti Sikder, S. Nandan Asthana, *Propellants Explos. Pyrotech.* **2009**, *34*, 145–150.

[63] T. D. Tran, P. F. Pagoria, D. M. Hoffman, J. L. Cutting, R. S. Lee, R. L. Simpson, in *Int. Ann. Conf. ICT (33)*, **2002**, pp. 45–41–45–16.

[64] C. M. Tarver, P. A. Urtiew, T. D. Tran, *J. Energ. Mater.* **2005**, *23*, 183–203.

[65] N. B. Zuckerman, M. Shusteff, P. F. Pagoria, A. E. Gash, *J. Flow Chem.* **2015**, *5*, 178–182.

[66] A. J. Bellamy, in *High Energy Density Materials* (Ed.: T. M. Klapötke), Springer, Berlin, Heidelberg, **2007**, pp. 1–33.

[67] M. Sućeska, *EXPLO5 V6.03 program*, Zagreb, Croatia, **2015**.

[68] G. Zhao, C. He, P. Yin, G. H. Imler, D. A. Parrish, J. M. Shreeve, *J. Am. Chem. Soc.* **2018**, *140*, 3560–3563.

[69] Z. A. Dreger, C. J. Breshike, Y. M. Gupta, *Chem. Phys. Lett.* **2017**, *679*, 212–218.

[70] X. J. Wang, Q. Su, L. J. Li, S. H. Jin, H. Niu, S. S. Chen, Q. H. Shu, *J. Heterocycl. Chem.* **2017**, *54*, 2228–2236.

[71] Y. Yu, S. Chen, T. Li, S. Jin, G. Zhang, M. Chen, L. Li, *RSC Advances* **2017**, *7*, 31485-31492.

[72] J. Wang, S. Chen, Q. Yao, S. Jin, S. Zhao, Z. Yu, J. Li, Q. Shu, *Propellants Explos. Pyrotech.* **2017**, *42*, 1104–1110.

[73] Z. Lu, Q. Zeng, X. Xue, Z. Zhang, F. Nie, C. Zhang, *PCCP* **2017**, *19*, 23309–23317.

[74] D. Badgujar, M. Talawar, *Propellants Explos. Pyrotech.* **2017**, *42*, 883–888.

[75] S. Xiong, S. Chen, S. Jin, *J. Mol. Graphics Modell.* **2017**, *74*, 171–176.

[76] H. Huang, Y. Shi, J. Yang, B. Li, *J.Energ. Mat.* **2015**, *33*, 66–72.

[77] H. Huang, Y. Shi, J. Yang, *J. Therm. Anal. Calorim.* **2015**, *121*, 705–709.

[78] Q. An, T. Cheng, W. A. Goddard, S. V. Zybin, *J. Phys. Chem. C* **2015**, *119*, 2196–2207.

[79] C. Zhang, S. Jin, S. Chen, Y. Zhang, L. Qin, X. Wei, Q. Shu, *J. Chem. Eng. Data* **2016**, *61*, 1873–1875.

[80] S. Nicolich, P. Samuels, R. Damavarapu, A. J. Paraskos, E. Cooke, V. Stepanov, P. Cook, K. Caflin, R. Duddu, in *Proceedings of the Insensitive Munitions Energetic Materials Technology Symposium (IMEMTS), Rome, Italy*, **2015**.

[81] Z. Zhou, L. Liang, L. Tang, C. Bian, M. Zhang, Beijing Institute of Technology, Peop. Rep. China, CN103524444A, **2014**.

[82] C. Zhang, S. Jin, Q. Shu, X. Wang, X. Zhang, S. Chen, X. Wei, Y. Dai, Beijing Institute of Technology, Peop. Rep. China, CN104829548A, **2015**.

[83] B. S. Pradhan, N. Vempala, S. V. Rao, Primodia Chemicals & Pharmaceuticals Pvt. Ltd., India, IN2015CH03944A, **2017**.

[84] R. S. Damavarapu, R. G. Duddu, US Secretary of Army, US9643937B1, **2017**.

[85] Y. D. Golenko, M. A. Topchiy, A. F. Asachenko, M. S. Nechaev, D. V. Pleshakov, *Chin. J. Chem .* **2017**, *35*, 98–102.

[86] I. V. Tselinskii, S. F. Mel'nikova, T. V. Romanova, *Russ. J. Org. Chem.* **2001**, *37*, 430–436.

[87] Z. Lu, X. Xue, L. Meng, Q. Zeng, Y. Chi, G. Fan, H. Li, Z. Zhang, F. Nie, C. Zhang, *J. Phys. Chem. C* **2017**, *121*, 8262–8271.

[88] B. A. Steele, I. I. Oleynik, in *AIP Conference Proceedings, Vol. 1979*, **2018**, p. 150036.

[89] Y. Yu, S. Chen, T. Li, S. Jin, G. Zhang, M. Chen, L. Li, *RSC Adv.* **2017**, *7*, 31485–31492.

[90] H. Niu, S. Chen, Q. Shu, L. Li, S. Jin, *J. Hazard. Mater.* **2017**, *338*, 208–217.

[91] S. Xiong, S. Chen, S. Jin, C. Zhang, *RSC Adv.* **2016**, *6*, 4221–4226.

[92] S. Ma, Y. Li, Y. Li, Y. Luo, *J. Mol. Model.* **2016**, *22*, 1–11.

[93] Y. Yu, S. Chen, X. Li, J. Zhu, H. Liang, X. Zhang, Q. Shu, *RSC Adv.* **2016**, *6*, 20034–20041.

[94] S. Xiong, S. Chen, S. Jin, Z. Zhang, Y. Zhang, L. Li, *RSC Advances* **2017**, *7*, 6795–6799.

[95] J. L. Gottfried, T. M. Klapötke, T. G. Witkowski, *Propellants Explos. Pyrotech.* **2017**, *42*, 353–359.

[96] T. M. Klapötke, T. G. Witkowski, Z. Wilk, J. Hadzik, *Propellants Explos. Pyrotech.* **2016**, *41*, 92–97.

[97] NATO standardization agreement (STANAG), *Chemical Compatibility Of Ammunition Components With Explosives And Propellants (non-nuclear applications)*, no. 4147, Edition 2, **2001**.

[98] NATO standardization agreement (STANAG), *Explosives: Vacuum Stability Test,* no. 4556 ED. 1, **1999**.

[99] M. Graswald, R. Gutser, TDW Gesellschaft für verteidigungstechnische Wirksysteme mbH, US2018038675A1, **2018**.

[100] Z. Yang, F. Gong, J. Liu, J. Zhang, L. Ding, Institute of Chemical Materials, China Academy of Engineering Physics, CN108164375, **2018**.

[101] T. M. Klapötke, M. Leroux, P. C. Schmid, J. Stierstorfer, *Chem. Asian J.* **2016**, *11*, 844–851.

[102] A. A. Dippold, D. Izsák, T. M. Klapötke, *Chem. Eur. J.* **2013**, *19*, 12042–12051.

[103] P. Yin, D. A. Parrish, J. M. Shreeve, *Chem. Eur. J.* **2014**, *20*, 6707–6712.

[104] I. L. Dalinger, K. Y. Suponitsky, A. N. Pivkina, A. B. Sheremetev, *Propellants Explos. Pyrotech.* **2016**, *41*, 789–792.

[105] J. W. A. M. Janssen, H. J. Koeners, C. G. Kruse, C. L. Habrakern, *J. Org. Chem.* **1973**, *38*, 1777–1782.

[106] C. Li, L. Liang, K. Wang, C. Bian, J. Zhang, Z. Zhou, *J. Mater. Chem. A* **2014**, *2*, 18097–18105.

[107] M. I. Kanishchev, N. V. Korneeva, S. A. Shevelev, A. A. Fainzil'berg, *Chem. Heterocycl. Compd.* **1988**, *24*, 353–370.

[108] P. Yin, J. Zhang, C. He, D. A. Parrish, J. M. Shreeve, *J. Mater. Chem. A* **2014**, *2*, 3200-3208.

[109] I. L. Dalinger, I. A. Vatsadze, T. K. Shkineva, A. V. Kormanov, M. I. Struchkova, K. Y. Suponitsky, A. A. Bragin, K. A. Monogarov, V. P. Sinditskii, A. B. Sheremetev, *Chem. Asian J.* **2015**, *10*, 1987–1996.

[110] Y. Zhang, Y. Guo, Y.-H. Joo, D. A. Parrish, J. M. Shreeve, *Chem. Eur. J.* **2010**, *16*, 10778-10784.

[111] M. W. Holladay, G. Liu, Plexxikon Inc., USA, WO2017019804A2, **2017**.

[112] X. Zhao, C. Qi, L. Zhang, Y. Wang, S. Li, F. Zhao, S. Pang, *Molecules* **2014**, *19*, 896.

[113] V. M. Vinogradov, I. L. Dalinger, B. I. Ugrak, S. A. Shevelev, *Mendeleev Commun.* **1996**, *6*, 139–140.

[114] P. Yin, L. A. Mitchell, D. A. Parrish, J. M. Shreeve, *Chem. Asian J.* **2017**, *12*, 378–384.

[115] D. Kumar, L. A. Mitchell, D. A. Parrish, J. M. Shreeve, *J. Mater. Chem. A* **2016**, *4*, 9931–9940.

[116] T. Fendt, N. Fischer, T. M. Klapötke, J. Stierstorfer, *Inorg. Chem.* **2011**, *50*, 1447–1458.

[117] D. Kumar, G. H. Imler, D. A. Parrish, J. M. Shreeve, *Chem. Eur. J.* **2017**, *23*, 7876–7881.

[118] D. Kumar, G. H. Imler, D. A. Parrish, J. M. Shreeve, *New J. Chem.* **2017**, *41*, 4040–4047.

[119] D. Fischer, J. L. Gottfried, T. M. Klapötke, K. Karaghiosoff, J. Stierstorfer, T. G. Witkowski, *Angew. Chem.* **2016**, *128*, 16366-16369.

[120] M. H. Kim, B. Lee, N. Kim, M. Shin, H. J. Shin, K. Kwon, J. S. Kim, S. K. Lee, Y. G. Kim, *Bull. Korean Chem. Soc.* **2017**, *38*, 751–755.

[121] P. Yin, L. A. Mitchell, D. A. Parrish, J. M. Shreeve, *Angew. Chem. Int. Ed.* **2016**, *55*, 14409–14411.

[122] M. Göbel, K. Karaghiosoff, T. M. Klapötke, D. G. Piercey, J. Stierstorfer, *J. Am. Chem. Soc.* **2010**, *132*, 17216–17226.

[123] D. Fischer, T. M. Klapötke, M. Reymann, P. C. Schmid, J. Stierstorfer, M. Sućeska, *Propellants Explos. Pyrotech.* **2014**, *39*, 550–557.

[124] T. Harel, S. Rozen, *J. Org. Chem.* **2010**, *75*, 3141–3143.

[125] T. M. Klapötke, M. Q. Kurz, P. C. Schmid, J. Stierstorfer, *J.Energ. Mater.* **2015**, *33*, 191–201.

[126] Y. Zhang, D. A. Parrish, J. M. Shreeve, *J. Mater. Chem.* **2012**, *22*, 12659–12665.

[127] Y. Tang, C. He, L. A. Mitchell, D. A. Parrish, J. M. Shreeve, *J. Mater. Chem. A* **2016**, *4*, 3879-3885.

[128] I. L. Dalinger, T. I. Cherkasova, G. P. Popova, T. K. Shkineva, I. A. Vatsadze, S. A. Shevelev, M. I. Kanishchev, *Russ. Chem. Bull.* **2009**, *58*, 410–413.

[129] I. L. Dalinger, I. A. Vatsadze, T. K. Shkineva, A. V. Kormanov, A. M. Kozeev, B. B. Averkiev, A. I. Dalinger, M. K. Beklemishev, A. B. Sheremetev, *Chem. Heterocycl. Compd.* **2015**, *51*, 545–552.

2 Summary and Conclusion

Chapters 3–7 deal with the synthesis and characterization of new environmentally benign energetic materials with focus on secondary explosives. Chapters 3–4 and 7 have been published in peer-reviewed scientific journals. The content of the articles is consistent with the particular publication; however, the layout has been modified to fit in this thesis.

2.1 Isomers of Dinitropyrazoles: Synthesis, Comparison and Tuning of Their Physicochemical Properties

The improved synthesis and intensive characterization of three isomeric dinitro-1*H*-pyrazoles (3,4-DNP, 1,3-DNP and 3,5-DNP) is presented (Figure 2.1). The nitrated pyrazoles can be prepared starting from readily available 1*H*-pyrazole by nitration and rearrangement reactions. These three isomers implicate high densities, high detonation velocities, low sensitivity values and an interesting thermal behavior for using as melt-cast materials (1,3-DNP and 3,5-DNP).

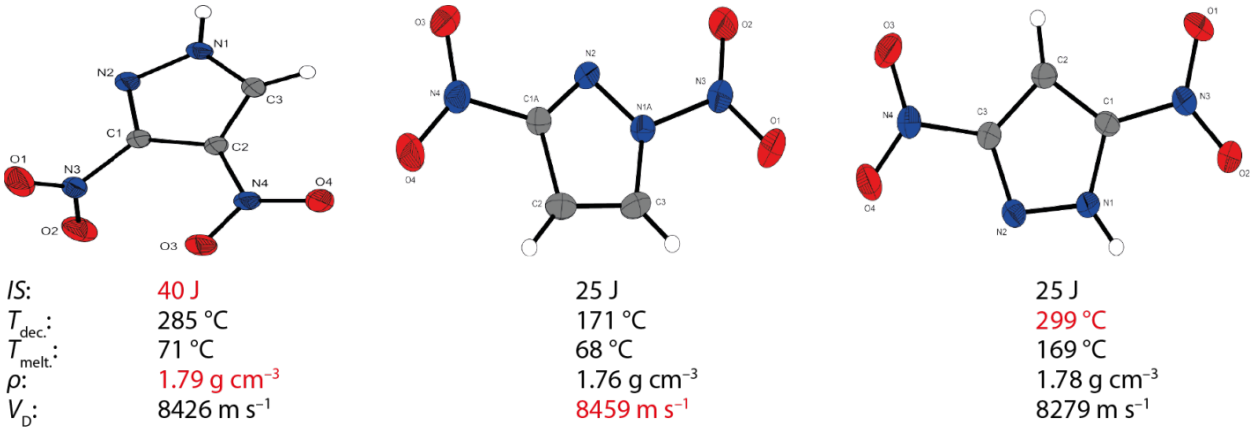

Figure 2.1. Crystal structures and selected properties of 3,4-dinitropyrazole (left), 1,3-dinitropyrazole (middle) and 3,5-dinitro-pyrazole (right).

Additionally, the sodium and potassium as well as six selected nitrogen rich (ammonium, hydrazinium, hydroxylammonium, guanidinium and 3,6,7-triamino-[1,2,4]triazolo[4,3-b][1,2,4]triazole (TATOT)) salts of 3,4-DNP and 3,5-DNP were synthesized in order to tune performance and sensitivity values (Figure 2.2). The salts show in general high decomposition temperatures, low sensitivity values and acceptable energetic parameters. Most compounds with exception of the hydrazinium and water free potassium salt are not sensitive to impact (IS: > 40 J) or friction (FS: 360 N). The most energetic compounds are the hydrazinium salts with detonation velocities between 8369 and 8610 m s^{-1}, which are close to the one of RDX (V_D: 8861 m s^{-1}).

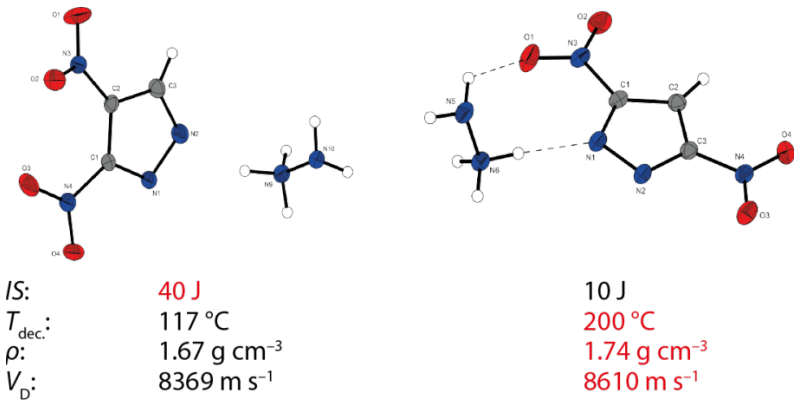

Figure 2.2. Crystal structures and selected properties of the hydrazinium salts of 3,4-DNP (left) and 3,5-DNP (right).

As a result of the toxicity measurement using the luminescent marine bacterium *Vibrio fischeri* the potassium salt of 3,5-DNP was observed to be less toxic than RDX, 3,5-DNP and the potassium salt of 3,4-DNP.

2.2 Improving the Energetic Properties of Dinitropyrazoles by Utilization of Current Concepts

Three different concepts (*N*-oxidation, salt formation and methylene bridging) for the functionalization of two isomeric dinitropyrazoles were used in order to improve the energetic properties and sensitivity values. First, two nitrated pyrazoles (3,4-DNP and 3,5-DNP) were reacted using Oxone® and a pH buffer system to get the *N*-hydroxides of both pyrazoles in high yields. Second, energetic salts of both hydroxides were synthesized showing that the salts of 3,5-DNP-oxide indicate higher decomposition temperatures, higher densities, higher detonation parameters and acceptable sensitivity values compared to the salts without the *N*-oxide (Chapter 3).

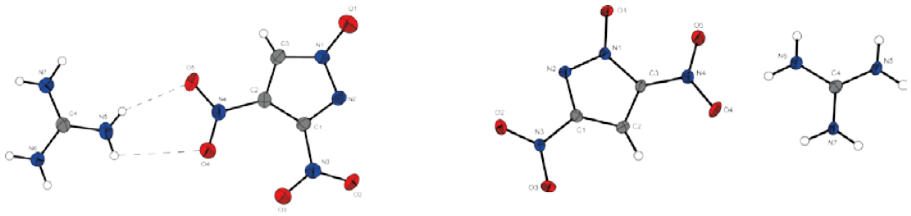

Figure 2.3. Crystal structures and selected properties of guanidinium 3,4-DNP-1-oxide (left) and guanidinium 3,5-DNP-1-oxide (right).

Third, two methylene bridged pyrazoles were synthesized and characterized using diodomethane in DMF (Figure 2.4). This class of compounds shows very high decomposition temperatures (up to 330 °C), low sensitivity values and acceptable detonation velocities (7966 and 8140 m^{-1}).

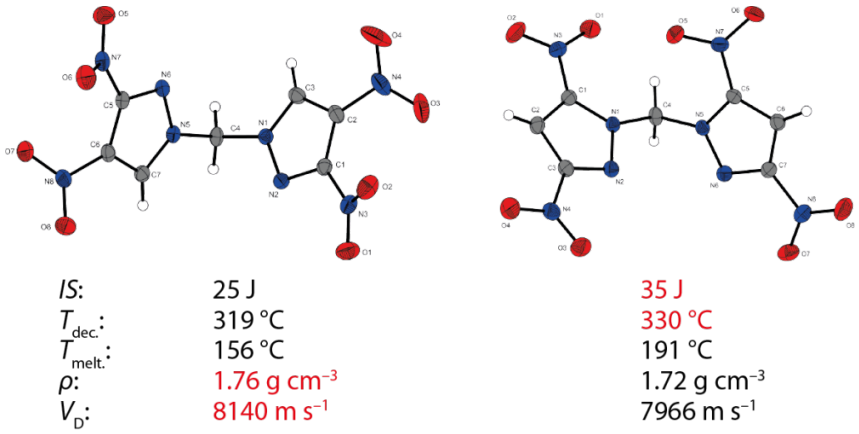

Figure 2.4. Crystal structures and selected properties of bis-(3,4-dinitro-1*H*-pyrazol-1-yl)-methane (left) and bis-(3,5-dinitro-1*H*-pyrazol-1-yl)-methane (right).

The toxicity to V*ibrio fischeri* was measured for both water soluble potassium salts due to their good water solubility. The measurement shows that the potassium salt of 3,4-DNP oxide is more toxic and the potassium salt of 3,5-DNP oxide is less toxic than RDX. Based on the relative high decomposition temperatures, rather high detonation parameters and appropriate sensitivity values both potassium salts and the bridged compounds have capability as future energetic materials.

2.3 Combination of Different Azoles – 1,2,4-Triazolyl-1,3,4-Oxadiazoles as Precursor for Energetic Materials

The synthesis of two new energetic derivatives based on the heterocycles 1,2,4-1*H*-triazole and 1,3,4-oxadiazole are described. 2-Amino-5-(5-amino-1*H*-1,2,4-triazol-3-yl)-1,3,4-oxadiazole can be synthesized in a three-step procedure and 2-amino-5-(5-nitro-1*H*-1,2,4-triazol-3-yl)-1,3,4-oxadiazole in a four-step procedure by using 5-amino-1*H*-1,2,4-triazole-3-carboxylic acid as starting material. The ring closing toward the 1,3,4-oxadiazole was carried out using cyanogen bromide and the corresponding triazole-carbohydrazides (Figure 2.5).

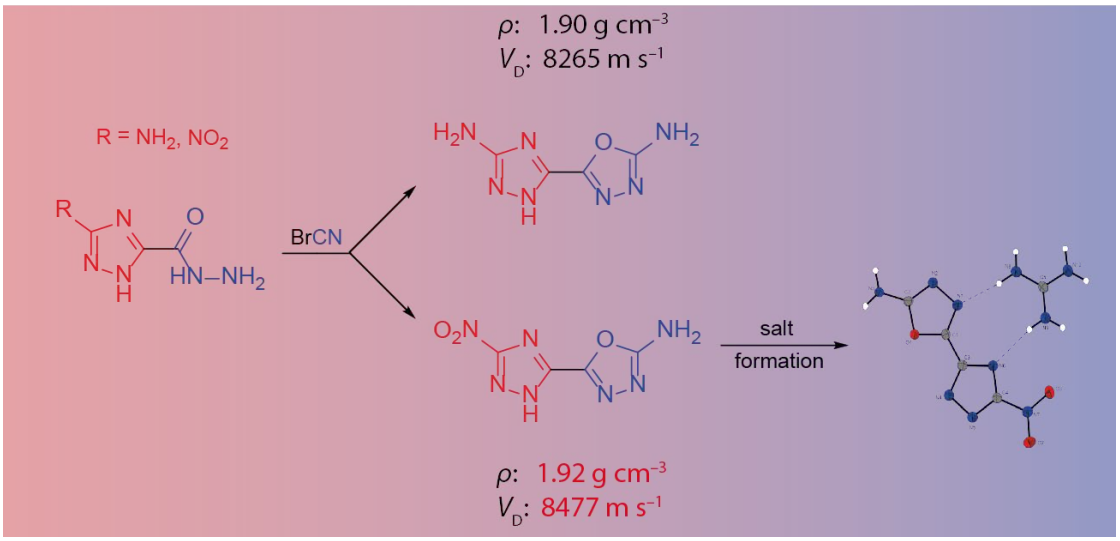

Figure 2.5. Overview of the synthetic pathway toward both triazole-oxadiazoles and the salts of the nitro derivative.

Both biheterocycles show high thermal stabilities, high densities (ρ = 1.90 and 1.92 g cm^{-3}) and acceptable detonation performances (V_D = 8265 and 8477 m^{-1}). Both heterocycles are not sensitive toward impact friction or ESD. The nitro derivative **6** was further functionalized by reacting it with four bases to yield the potassium, ammonium, guanidinium and aminoguanidinium salt. The salts were intensively characterized and the crystal structures were determined (Figure 2.6).

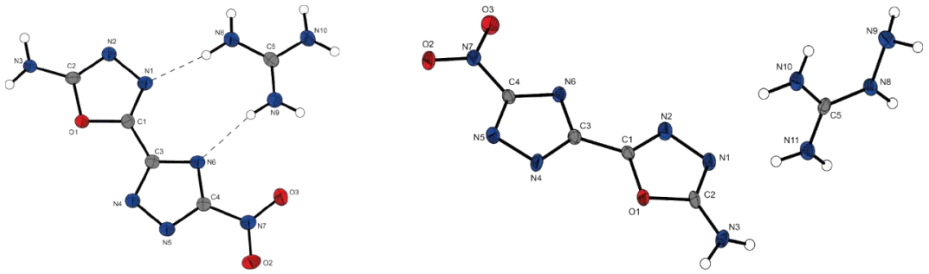

IS:	40 J	40 J
$T_{dec.}$:	296 °C	246 °C
ρ:	1.66 g cm^{-3}	1.64 g cm^{-3}
V_D:	7500 m s^{-1}	7672 m s^{-1}

Figure 2.6. Crystal structures and selected properties of the guandinium (left) and aminoguanidinium (right) salt of 2-amino-5-(5-nitro-1*H*-1,2,4-triazol-3-yl)-1,3,4-oxadiazole.

The synthesized ionic compounds are insensitive toward external stimuli with sensitivity values for impact of 40 J and for friction with 360 N, each. The thermal stability of all four compounds ranges from 246 °C for the aminoguanidinium salt to 296 °C for the guanidinium salt. 2-Amino-5-(5-amino-1*H*-1,2,4-triazol-3-yl)-1,3,4-oxadiazole and 2-amino-5-(5-nitro-1*H*-1,2,4-triazol-3-yl)-1,3,4-oxadiazole are suitable as precursors for new energetic materials. Their energetic behavior can be improved by nitration, amination, *N*-oxidation or *N*-functionalization

2.4 3,5-Ditetrazolyl-Pyrazoles as Precursor for New Energetic Materials – New Mixed Heterocycles Combining Pyrazoles and Tetrazoles (unpublished)

The first synthesis of the two triheterocyclic compounds 5,5'-(1*H*-pyrazole-3,5-diyl)-bis-1*H*-tetrazole and 5,5'-(4-nitro-1*H*-pyrazole-3,5-diyl)-bis-1*H*-tetrazole consisting of one pyrazole and two tetrazoles with high nitrogen content is described. The compounds were synthesized in a five or six-step synthesis using commercially available reagents and show high yields and facile reaction conditions (Figure 2.7).

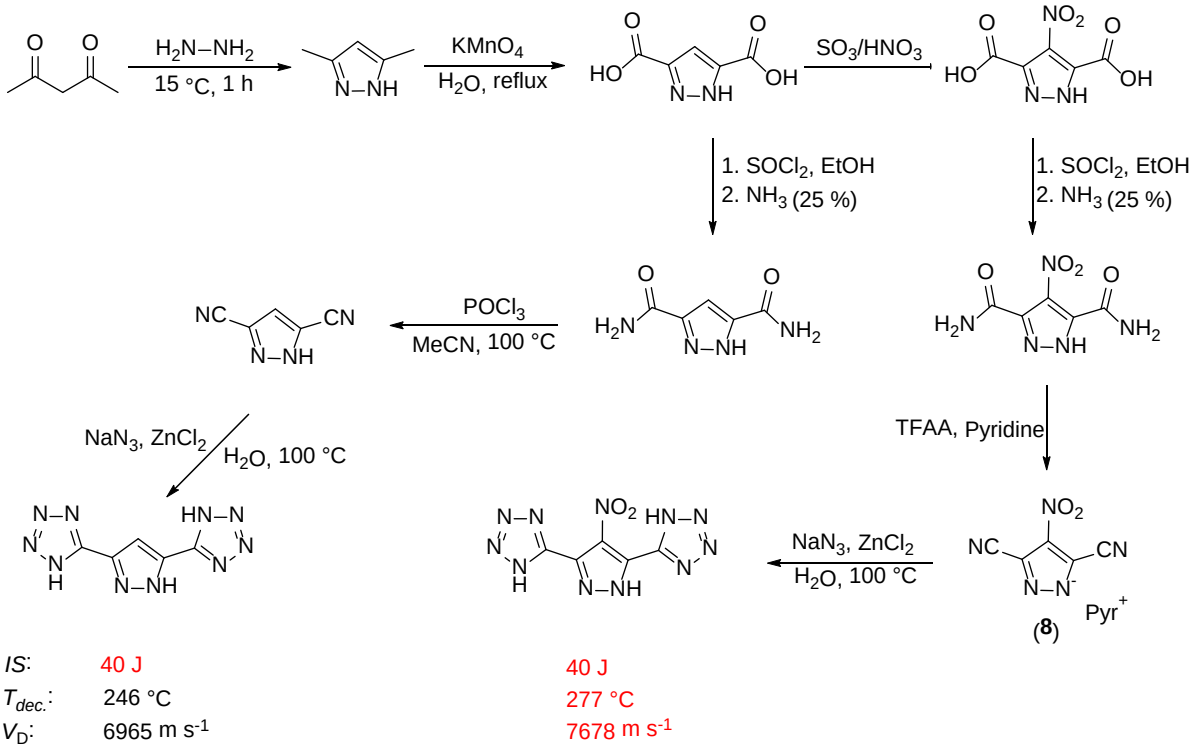

Figure 2.7. Synthetic pathway toward 5,5'-(1*H*-pyrazole-3,5-diyl)-bis-1*H*-tetrazole and 5,5'-(4-nitro-1*H*-pyrazole-3,5-diyl)-bis-1*H*-tetrazole and selected properties thereof.

Both compounds show high decomposition temperatures of 277 °C and 246 °C. Their sensitivity values as hydrates are > 40 J for impact and 360 N for friction, for which reason they are classified as not sensitive. The calculated detonation velocities of both compounds (V_D = 6965 and 7678 m s^{-1}) are lower than RDX.

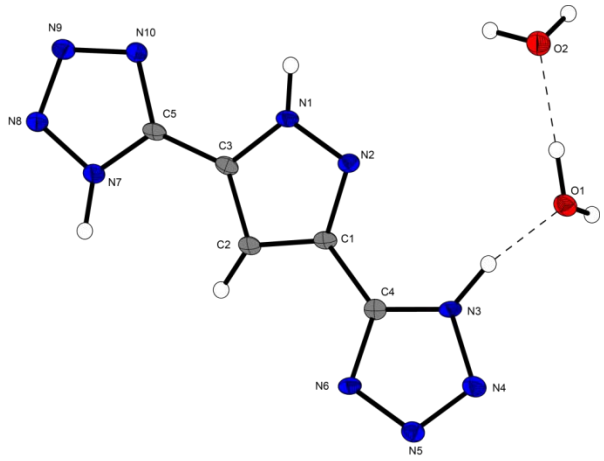

Figure 2.8. Crystal structure of 5,5'-(1*H*-pyrazole-3,5-diyl)-bis-1*H*-tetrazole as dihydrate.

According to their high decomposition temperatures and low sensitivity values, both triheterocylces are suitable as precursor for high energetic materials or due to their high nitrogen content as propellant charges. Their energetic characteristics can be improved by different concepts mentioned in the introduction of this thesis such as *N*-functionalization, *N*-oxidation or salt formation. Both compounds own three acidic protons, which can be functionalized individually to obtain mono-, di- or tri-substituted compounds implicating different energetic characteristics.

2.5 Metal Salts and Complexes of 1,1'-Dinitramino-5,5'-bitetrazole

The synthesis and characterization of several new metal salts (Li, Na, Rb, Cs, Ca, Sr and Ba) and complexes (Ni, Cu and Zn) of 1,1'-dinitramino-5,5'-bitetrazole (H_2DNABT) is described. Since the potassium salt **K_2DNABT** is a very promising environmentally benign primary explosive the remaining alkaline salts as well as selected alkaline earth and transition metal complexes should be investigated toward their energetic behavior. Within the group of alkali metal salts (Li, Na, K_2DNABT, Rb, Cs) the lithium and sodium salts form dihydrates which can reversibly be dehydrated. Two polymorphs of the sodium salt were explored formed by recrystallization from water and ethanol, respectively (Figure 2.9).

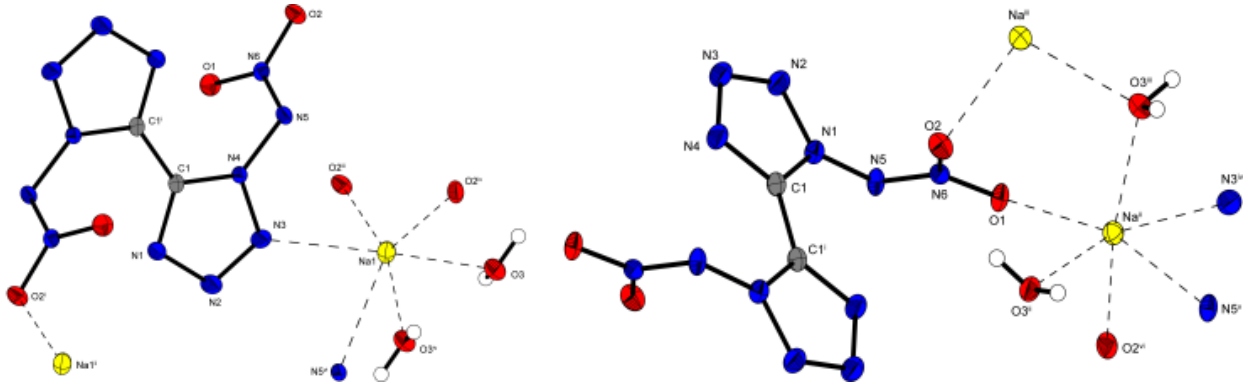

Space group:	$P2_1/c$	$Pbca$
IS:	< 1 J	< 1 J
ρ:	1.889 g cm^{-3}	1.887 g cm^{-3}

Figure 2.9. Crystal structures of two different polymorphs of disodium 1,1'-dinitramino-5,5'-bitetrazololate dihydrate from water (left) and ethanol (right).

The rubidium, cesium and silver salts are poorly soluble in water. All are highly sensitive showing a super fast "deflagration to detonation" behavior on contact with flame or hot surfaces. The silver salt usually explodes during drying, latest on lightest touch when dry. The alkaline earth metal salts (Ca, Sr, Ba) are highly soluble in water and could not be purified sufficiently. They are forming tetra- (Ca and Sr) and hexahydrates (Ba) in the solid state. Neat transition metal complexes could only be synthesized with Ni(II), Cu(II) and Zn(II) under addition and coordination of ammonia (Figure 2.10). The nickel and copper salts could be successfully initiated by laser irradiation. For the first time the cations hexaamminenickel(II) and tetraamminezinc(II) were combined with energetic counterions.

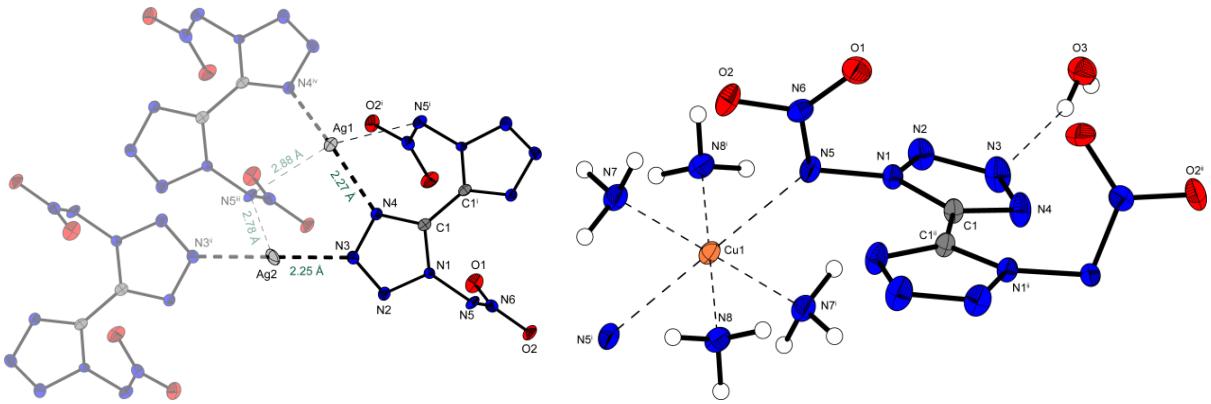

IS:	n.d.	2 J
$T_{dec.}$:	n.d.	155 °C
ρ:	3.177 g cm^{-3}	1.809 g cm^{-3}

Figure 2.10. Crystal structures of silver salt (left) and Cu(II) complex under addition of ammonia (right).

The crystal structure of all compounds except for calcium could be determined by low temperature X-ray diffraction, which gave insight in the coordination of the metal centers and hydrogen bond interactions. Sensitivities of the alkaline and transition metal salts were measured showing extremely high values partly much more susceptible. The lowest thermal stability of 155 °C was observed for the tetrammine-copper(II) complex which might be caused by the loss of ammonia. The highest value (247 °C) was observed for the dehydrated sodium salt. With respect to potential application in priming charges the potassium salt is still the most promising due to its manageable sensitivities in combination with a thermal stability of 200 °C.

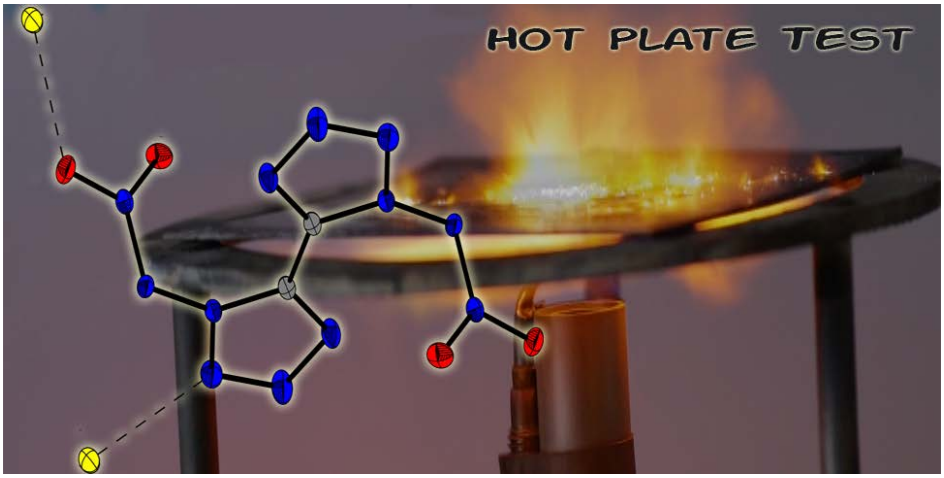

Figure 2.11. Overview of the sodium salt and the hot plate test of the synthesized salts and complexes.

3 Isomers of Dinitropyrazoles: Synthesis, Comparison and Tuning of their Physicochemical Properties

Marc F. Bölter, Alexander Harter, Thomas M. Klapötke and Jörg Stierstorfer

as published in

ChemPlusChem **2018**, 83, 804–811. (DOI: 10.1002/cplu.201800318)

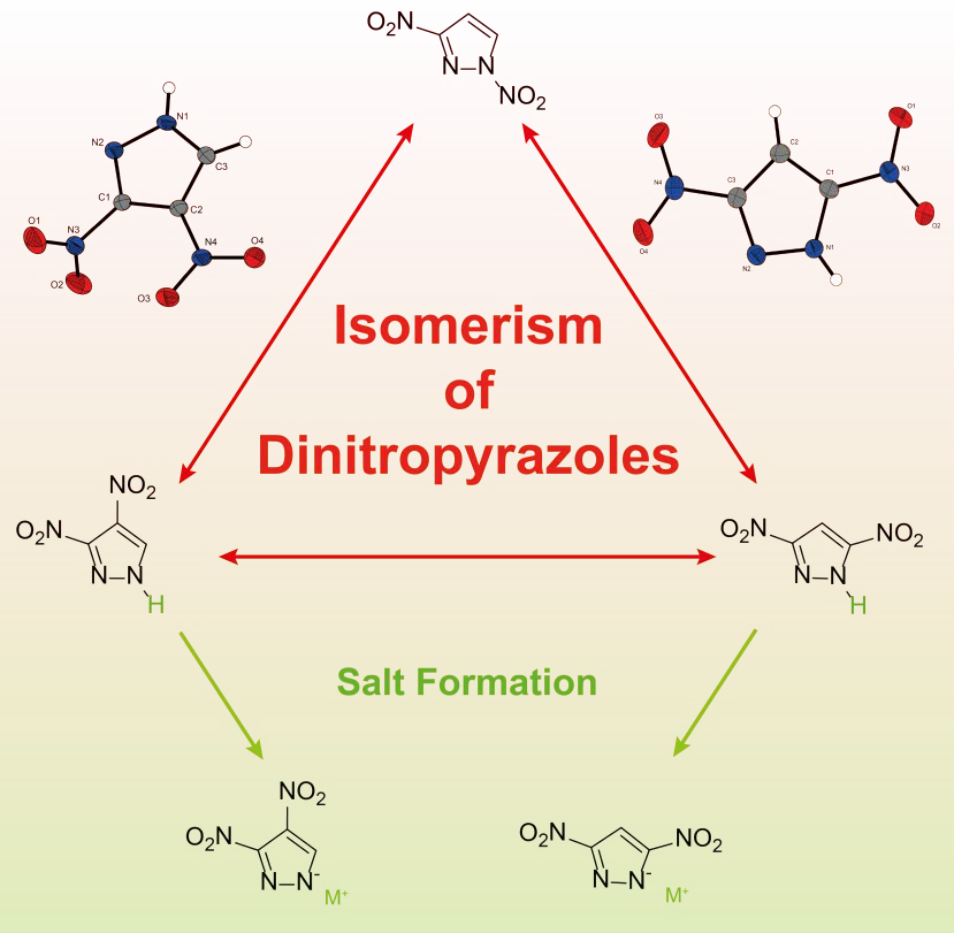

Abstract: Three isomeric dinitropyrazoles (DNPs) were synthesized starting from readily available 1*H*-pyrazole by slightly improved methods than described in the literature. 3,4-Dinitropyrazole (**3**), 1,3-dinitropyrazole (**4**), and 3,5-dinitropyrazole (**5**) were obtained and compared to each other with respect to thermal stability, crystallography, sensitivity and energetic performance. Two isomers (**3** and **4**) show high densities (1.79 and 1.76 g cm^{-3}) and interesting thermal behavior as melt-castable materials (**3**: $T_{melt.}$ = 71 °C, $T_{dec.}$ = 285 °C; **5**: $T_{melt.}$ = 68 °C, $T_{dec.}$ = 171 °C). Furthermore, eight salts (sodium, potassium, ammonium, hydrazinium, hydroxylammonium, guanidinium, aminoguanidinium and TATOT) of **3** and **5** were synthesized in order to tune performance and sensitivity values. These compounds were characterized using ^{1}H, ^{13}C, ^{14}N, ^{15}N NMR and IR spectroscopy as well as mass spectrometry, elemental analysis and thermal analysis (DSC). Crystal structures could be obtained of 14 compounds (**3**–**7**, **10**–**12** and **15**–**20**) by low temperature single crystal X-ray diffraction. Impact, friction and electrostatic discharge (ESD) values were also determined by standard methods. The sensitivity values range between 8.5 and 40 J for impact and 240 N and 360 N for friction and show mainly insensitive character. The energetic performances were calculated using recalculated X-ray densities, heats of formation and the EXPLO5 code and support the energetic character of the title compounds. The calculated energetic performances (V_D: 6245–8610 m s^{-1}; p_{CJ}: 14.1–30.8 GPa) were compared to RDX.

3.1 Introduction

Modern high energy density materials (HEDMs) have to fulfill different requirements depending on their application such as high energetic performance, high density, high heat of formation, low sensitivity toward external stimuli, thermal stability and environmental impact to replace the widely used RDX.[1] In contrast to the carcinogenic and hepatoxic RDX nitrogen-rich materials release mostly environmentally friendly dinitrogen after decomposition.[2] These goals could be achieved by azoles, such as tetrazoles[3], triazoles[4], imidazoles[5], oxadiazoles[6], furazanes[7] or pyrazoles[8]. In general the deprotonation of azoles by bases result in higher performances and thermal stabilities such as 5,5‘-bistetrazole-1,1-dioxide dihydrate (V_D: 8764 m s^{-1}, $T_{dec.}$: 214 °C) and its dihydroxylammonium salt (TKX-50 V_D: 9698 m s^{-1}, $T_{dec.}$: 221 °C) or its potassium salt ($T_{dec.}$: 335 °C).[3, 9] Nitrated pyrazoles arouse interest in the past due to their different characteristics and achieve the requirements mentioned before (Figure 3.1).[10] The nitro groups decrease the electron density inside the pyrazole, whereas the acidity of the *N* bonded proton rises and the pKa value decreases (1*H*-pyrazole: 14.2; 3-nitropyrazole 9.81; 3,4-dinitropyrazole: 5.14, 3,5-dinitropyrazole: 3.14 and 3,4,5-trinitropyrazole: 2.35).[11]

Hence, only the *C* nitrated dinitropyrazoles and trinitropyrazole (TNP) are acidic enough to get deprotonated by adding common bases (Figure 1). Shreeve *et al.* reported a series of nitrogen-rich salts of TNP with rather high energetic properties, low sensitivities and high thermal stabilities.[8]

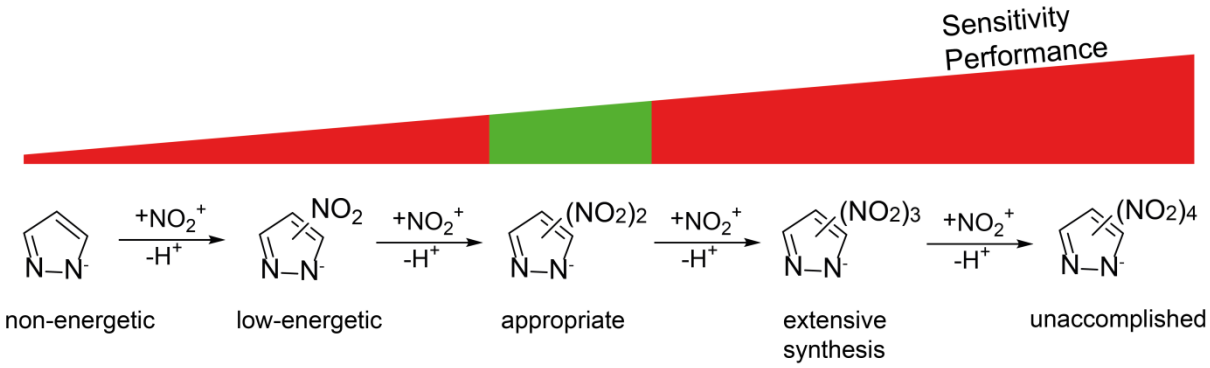

Figure 3.1. Overview of nitrated pyrazolates arranged according to their rising sensitivity and energetic performance.

Comparing the densities of di- and trinitrated pyrazoles the calculated density of TNP (1.867 g cm^{-3}) is marginally higher than the ones of the two DNP isomers (1.76 and 1.79 g cm^{-3}).[8] But the sensitivity values are with 17 J for impact and 92 N for friction higher than for TNP.[8] Nitrogen-rich salts of dinitrated pyrazoles (DNPs) have not been mentioned in the literature yet. In this work three different isomeric DNPs were synthesized by partly different methods than literature and selected alkaline metal and nitrogen-rich salts of 3,4-DNP and 3,5-DNP were prepared, intensively characterized and compared to each other.

3.2 Results and Discussion

The synthesis of the three DNPs is described by. Janssen *et al.* starting from *N*-nitration of pyrazole, followed by thermal rearrangement in anisole (**2**) (Scheme 3.1).[12] A selective C4 nitration of compound **2** was carried out by using nitric acid and sulfuric acid yielding 3,4-DNP (**3**).[12a] Similar nitration conditions to the first step were used for the synthesis of 1,3-DNP (**4**).[12a] A further thermal rearrangement in benzonitrile and an easier work-up from literature gave **5** in good yields.[12a]

Starting from compounds **3** and **5** different ionic derivatives (**6**–**21**) were synthesized by deprotonation. The salts were prepared using sodium hydroxide, potassium hydroxide, ammonia, hydroxylamine, hydrazine, guanidine bicarbonate, aminoguanidine bicarbonate and TATOT (3,6,7-

triamino-[1,2,4]triazolo[4,3-b][1,2,4]triazole). Salts of compound **5** show a much better and faster crystallization behavior than the salts of compound **3**.

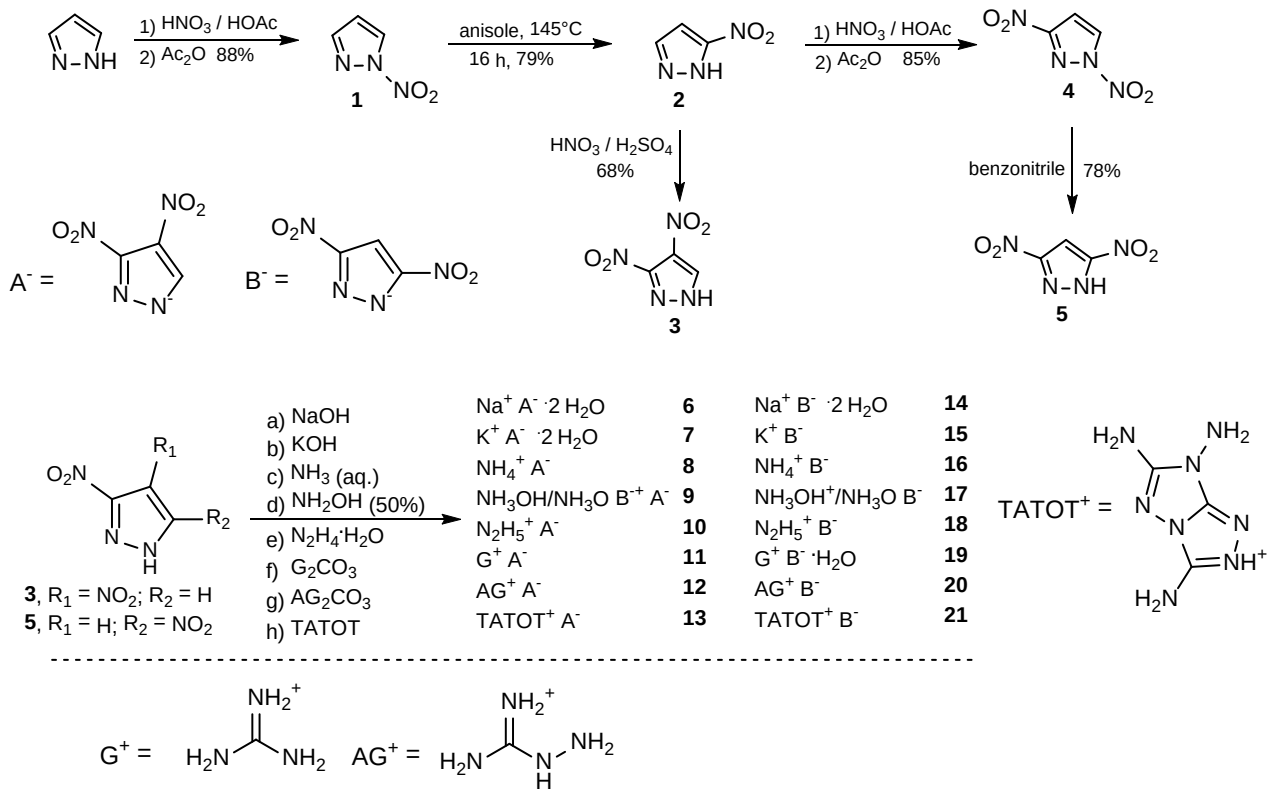

Scheme 3.1. Synthesis of 1,3-dinitropyrazole (**4**), 3,4-dinitropyrazole (**3**) and 3,5-dinitropyrazole (**5**) as well as their ionic derivatives.

3.2.1 Crystal structures

In this work the crystal structures of compounds **3**–**7**, **10**–**12** and **15**–**20** were obtained**.** Selected data and parameters from the low temperature X-ray data collection and refinements are given in the supporting information. Further information regarding the crystal-structure determinations have been deposited with the Cambridge Crystallographic Data Centre as supplementary publication Nos. 1835056 (**3**), 1835054 (**4**), 1835062 (**5**), 1835053 (**6**), 1835066 (**7**), 1835061 (**10**), 1835065 (**11**), 1835063 (**12**), 1835060 (**15**), 1835055 (**16**), 1835057 (**17**), 1835059 (**18**), 1835058 (**19**) and 1835064 (**20**).

Dinitropyrazoles **3**–**5** crystallize in common space groups (**3**: $P2_1/c$; **4**: $P2_1/c$; **5**: $Pca2_1$) with crystal densities between 1.796 g cm^{-3} (**4**) and 1.827 g cm^{-3} (**5**) at 173 K.

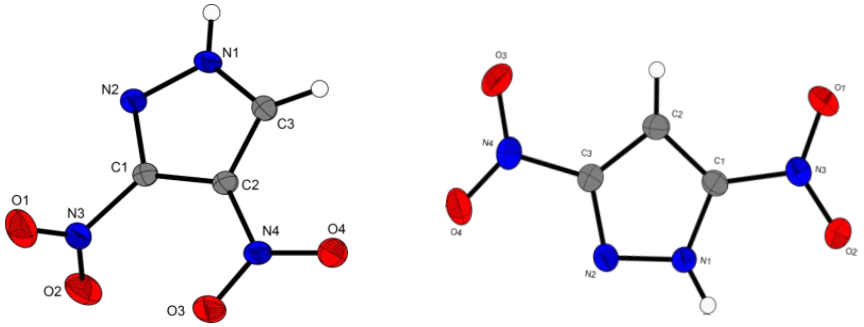

Figure 3.2. Molecular units of **3** (left) and **5** (right). Ellipsoids are drawn at the 50% probability level.

The molecular units of compounds **3**–**5** are shown in Figures 3.2 and 3.3. Compound **4** is disordered along the axis of rotation through atom N2. The bond lengths within the ring nitrogen atoms of the nitropyrazoles are between the values of a N–N single bond (1.47 Å) and a N=N double bond (1.25 Å).

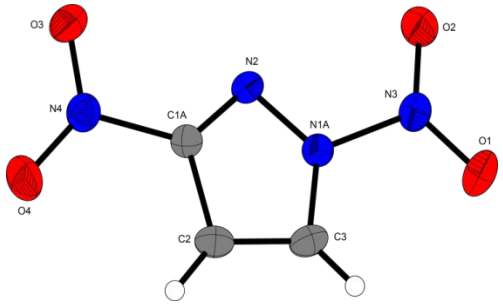

Figure 3.3. Molecular unit of **4**. Ellipsoids are drawn at the 50% probability level.

The nitro groups of **3** are most twisted toward the planar pyrazole ring due to their steric hindrance (**3**: –7.8(2)°, –78.83(18)°; **4**: –3.1(5)°, 17.1(8)°; **5**: –1.7(4)°, –8.9(3)°). Further, 3,4-DNP (**3**) is stabilized due to hydrogen bonding resulting in a high decomposition temperature ($T_{dec.}$: 285 °C). On the one hand classical hydrogen bonds are found involving N–H···N/O interactions and showing H···N/O distances between 2.9540(16) and 3.0572(16) Å.[13] Further, weak non-classical hydrogen bonds implicating C–H···O correlations are visible.

The molecular moieties of water free salts are depicted in Figures 3.4–3.7. The remaining crystal structures can be found in the supporting information. The potassium (**15**) and ammonium (**16**) salt of 3,5-DNP crystallize in the space group *P*–1. The crystal density of **15** shows the highest value of all compounds with 2.037 g cm^{-3} whereas the density of **16** is 1.732 g cm^{-3} at 173 K.

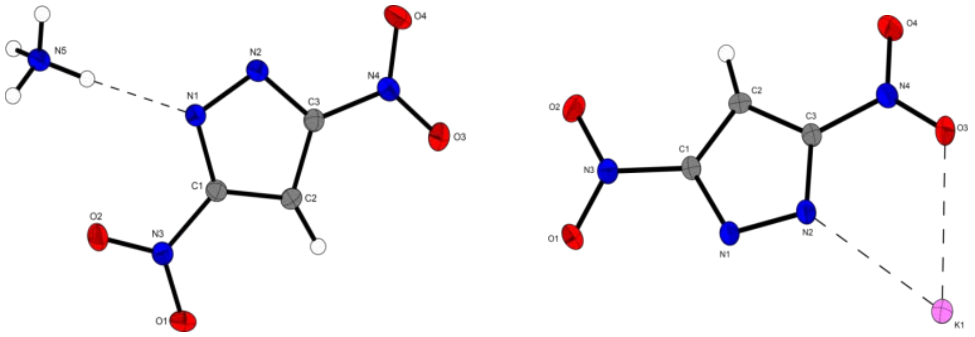

Figure 3.4. Molecular units of **15** (left) and **16** (right). Ellipsoids are drawn at the 50% probability level.

The bond lengths and angles of **15** and **16** are similar to the neutral compound **3**. Compound **16** is stabilized by various H-bonds between the ammonium cation and the anion e.g. N5–H5A···O3, N5–H5A···O1, N5–H5A···O4, N5–H5B···O2 N5–H5C···N1, N5–H5D···N2. The nitro groups of **16** (5.3°; 5.1°) are more twisted toward the planar pyrazole ring system compared to the ammonium salt (2.8(2)°; 1.3(2)°).

The hydrazinium salts of both isomers (**10**, **18**) are crystallizing in the monoclinic space groups $P2_1/c$ and $P2_1/n$, respectively. The nitro groups of hydrazinium salt **10** are further twisted toward the planar ring. The density of **10** (1.704 g cm^{-3}) is higher than that of compound **18** (1.682 g cm^{-3}). This relates to the slightly higher density of the neutral compounds **3** and **5**. The nitrogen bond lengths of both hydrazines are very similar (**10**: N9–N10 1.444(4); **18**: N5–N6 1.446(2)) and are in the range of a typical N–N single bond.

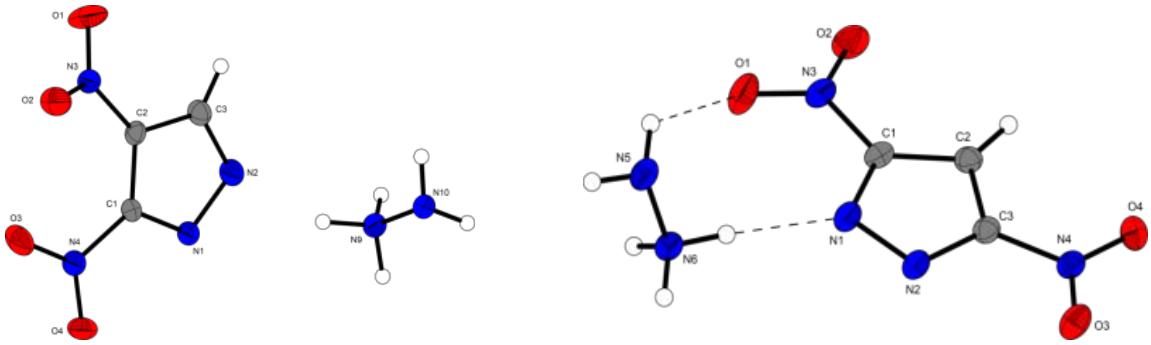

Figure 3.5. Molecular units of **10** (left) and **18** (right). Ellipsoids are drawn at the 50% probability level.

Both hydrazinium cations show hydrogen bonding to the pyrazole ring nitrogen and to the oxygen of the nitro groups. The better hydrogen interaction of **18** leads to a higher decomposition temperature (Figure 3.5).

Figures 3.6 and 3.7 depict the molecular units of the guanidinium derivatives (**11**, **12** and **20**). They all crystallize in the common space groups *P*–1 (**11**), $P2_12_12_1$ (**12**) and *C*2/c (**20**) with densities of 1.657 g cm^{-3} (**11**, 173 K), 1.647 g cm^{-3} (**12**, 173 K) and 1.695 g cm^{-3} (**20**, 100 K). The structure of **11** is dominated by strong hydrogen bonds involving all guanidinium protons and both nitro groups are twisted out of the pyrazole plane (O1–N3–C1–N1: 24.4(2)° and O4–N4–C2–C1: -168.89(16)°) due to their steric hindrance.

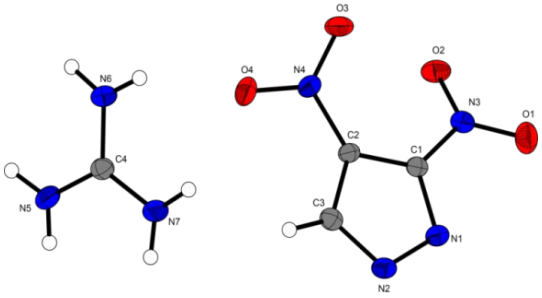

Figure 3.6. Molecular unit of **11**. Ellipsoids are drawn at the 50% probability level.

Also the nitro groups of compound **12** are twisted toward the planar pyrazole ring with torsion angles of 28.28(19)° (O4–N4–C1–N1) and 24.7(2)° (O1–N3–C2–C3). Comparing the twist of the nitro groups of compound **12** and **20** they are only distorted slightly for the latter (-3.1(3)° and 4.3(2)°).

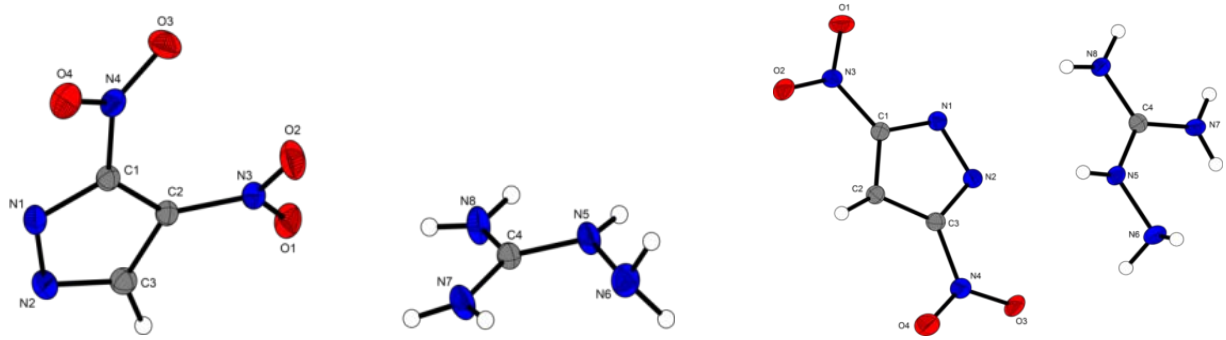

Figure 3.7. Molecular units of **12** (left) and **18** (bottom). Ellipsoids are drawn at the 50% probability level.

The N–N bond lengths of aminoguanidinium cations are close to a N–N single bond with distances between 1.4030(18) Å (**12**) and 1.410(2) Å (**20**). Both structures show hydrogen bonding involving all protons of the aminoguanidinium and the carbon bonded hydrogen.

3.2.2 Spectroscopy

The three isomers **3**–**5** can easily be distinguished by ^{1}H, ^{13}C, ^{14}N and ^{15}N NMR spectroscopy as well as IR and Raman spectroscopy. Further a two dimensional $^{1}H/^{15}N$ NMR HMBC spectrum was recorded for compound **4**.The NMR shifts of **3**–**5, 8, 11, 16** and **19** are listed in Table 3.1. In the ^{1}H NMR spectra, two hydrogen signals were observed for 1,3-DNP (9.09 and 7.44 ppm) and for 3,4-DNP (14.84 and 9.10 ppm) and one for 3,5-DNP (7.92 ppm). The reason for the missing N-H peak of 3,5-DNP might be the fact that the molecule is deprotonated in solution because of the high pK_a = 3.14 value.[11a] In the ^{13}C NMR spectra, two signals were determined for 3,5-DNP (151.5 and 98.8 ppm) and three for 1,3-DNP (152.6, 130.0 and 104.7 ppm) and 3,4-DNP (148.2, 132.7 and 126.3 ppm).

Table 3.1. NMR signals of compounds **3**–**5, 8, 11, 16** and **19**.

compound	^{1}H [ppm]	$^{13}C\{^{1}H\}$ [ppm]	^{15}N [ppm]
3	14.84, 9.10	148.2, 132.7, 126.3	−175.5, −85.0, −26.1, −25.5
4	9.09, 7.44	152.6, 130.0, 104.7	−113.5, −95.0, −63.2, −25.1
5	7.92	151.5, 98.9	−123.4, −26.4
8	8.14, 7.12	163.5, 138.0, 125.8	–
11	8.03, 6.94	157.9, 150.9, 138.1, 125.3	–
16	7.30, 7.10	156.4, 98.3	–
19	7.30, 6.93	157.9, 156.4, 98.4	–

In the ^{14}N NMR spectra the resonances for the nitro groups of **3**–**5** are in the typical range between −10 and −40 ppm for carbon bonded and between −40 and −70 ppm for *N* nitrated species (**4**). The three isomers can further be distinguished by ^{15}N NMR spectroscopy (supporting information). The ^{15}N spectra of 3,5-DNP (**5**) shows two signals (−123.4 and −26.4 ppm) due to its symmetry and **3** (−175.5 ; −85.0, −26.1 and −25.5 ppm) and **4** (−113.5, −95.0, −63.2 and −25.1 ppm) show four, respectively. In the two dimensional HMBC NMR spectra the protons can be assigned to the carbon atoms (Figure 3.8). Due to the signal splitting into a doublet of doublet of the nitrogen atom at −113.5 ppm it can be assigned to the pyrazole nitrogen (N4). The larger coupling belongs to N–C–H (^{2}J) and the smaller to the N–C–C–H (^{3}J) coupling. The ^{3}J coupling of the proton at 9.09 ppm with the carbon bonded nitro group (N1) indicates the proton (a) to be bonded at C-4.

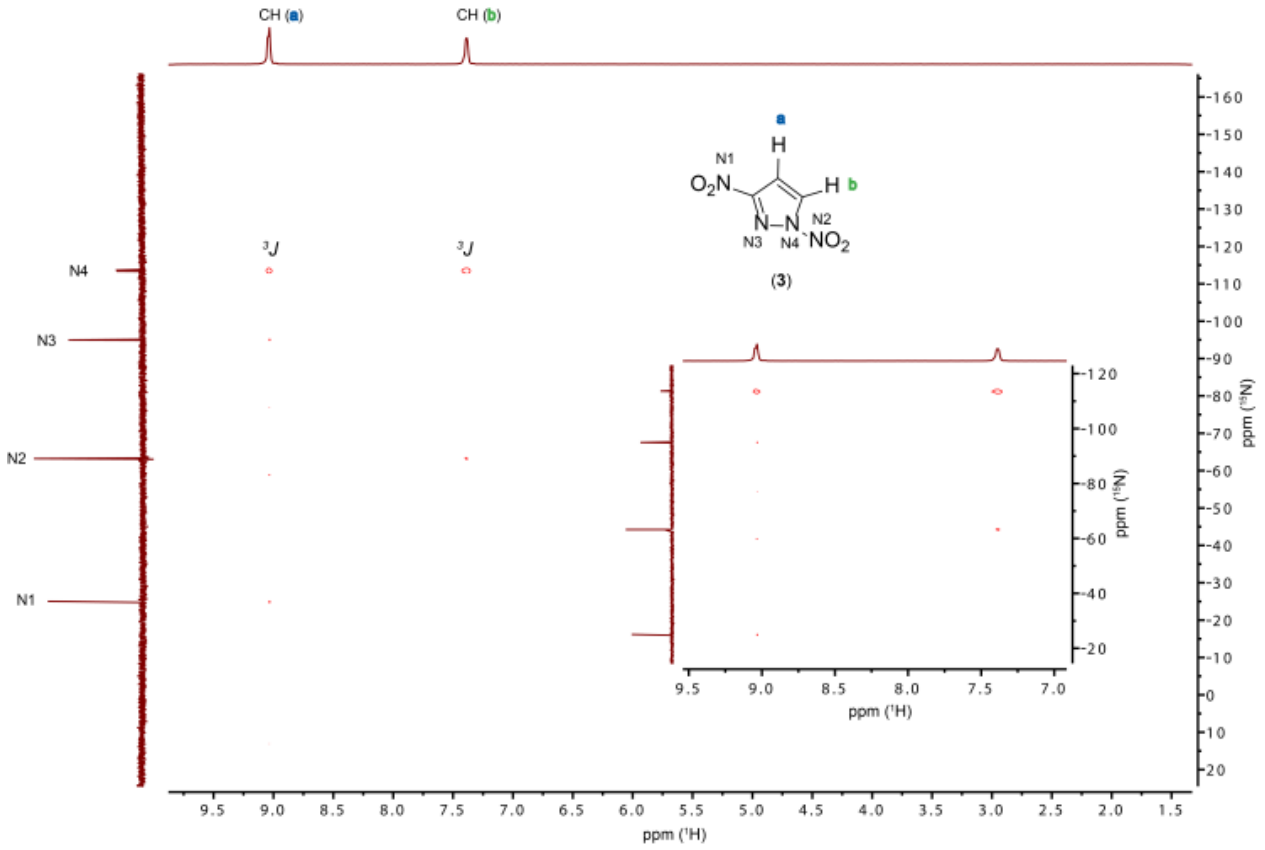

Figure3.8. Two dimensional ^{1}H, ^{15}N HMBC spectrum of compound **3**.

The characteristic absorption bands for nitro groups can be found at 1560/1329 cm^{-1} for (3,5-DNP), 1518/1346 cm^{-1} for (3,4-DNP) and 1351/1281 cm^{-1} for 1,3-DNP. The bands at 1637 and 1548 cm^{-1} were assigned to the *N*-nitro group of 1,3-DNP.

In the ^{1}H NMR spectra of 3,4-DNP salts **6–13** the hydrogen signal of DNP is observed between 8.03 and 8.30 ppm. For 3,5-DNP salts **14-21** the shift ranges from 7.28 to 7.30 ppm. In the ^{13}C NMR spectra, three resonances for the 3,4-DNP anion were observed and two for 3,5-DNP anion due to its symmetry. The signals range from 125.3–127.3 ppm (C-H), 136.9–139.1 ppm (C-NO_2) and 150.3–163.5 ppm (C-NO_2) for 3,4-DNP and from 98.3–98.4 ppm (C-H), 156.1–156.4 ppm (C-NO_2) for 3,5-DNP.

IR spectra of compounds **6–21** were measured and the frequencies were assigned according to observed data reported in the literature.[14] The characteristic absorption bands for nitro groups of salts **6–21** were found in the region from 1527–1556 cm^{-1} and 1335–1369 cm^{-1}. Further the absorption bands of the primary amines were found for the nitrogen-rich cations (**8-13** and **16–21**) in the range of 3125 and 3580 cm^{-1}. Triazole ring vibrations for **13** and **21** were found in the regions between 1583–1446 cm^{-1}.[1h]

3.2.3 Thermal Analysis, Sensitivities, Physicochemical and Energetic Properties

The different compounds were investigated in regard to their thermal behavior, sensitivities as well as their energetic properties. The decomposition temperatures were measured by differential scanning calorimetry (DSC) or differential thermal analysis (DTA) with a heating rate of 5 °C min^{-1}. Heats of formation were calculated by the atomization method using electronic energies (CBS-4M method). The energetic parameters were calculated with EXPLO5 V6.03.[15]

The isomers **3**–**5** only differ in the position of the nitro groups. The melting and decomposition temperatures rise from the most instable 1,3-DNP (**4**) with 68 °C and 171 °C over compound (**3**) with 71 °C and 285 °C to compound (**5**) with 169 °C and decomposition temperature of 299 °C (Figure 3.9).

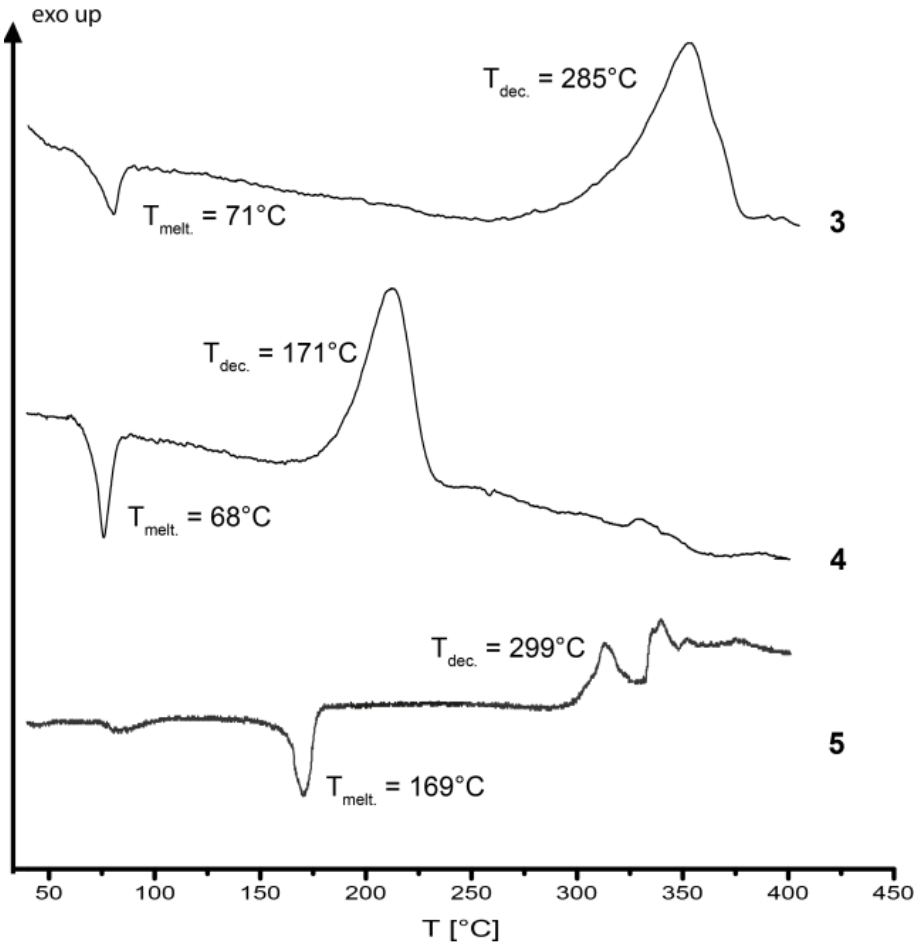

Figure 3.9. DSC plots of compounds **3**–**4** and DTA plot of **5** measured with a heating rate of 5 °C min^{-1}. Critical temperatures are given as onset temperatures.

As expected all of the DNPs are not or less sensitive with IS values of 25 to 40 J, 360 N for friction sensitivity and ca. 1.5 J for electrostatic discharge sensitivity. 1,3-DNP (**4**) implies the lowest value of 25 J, which refers to the nitramino part, but is still higher than RDX (IS: 7.5 J). The densities of **3**–**5** are in between 1.76 and 1.79 g m^{-3} at 298 K, which is nearby the density of RDX.[16]

All three DNPs are isomers and therefore have the same nitrogen content and a negative oxygen balance. The compounds have positive heat of formations in the range of 73.2 kJ mol^{-1} to 189.1 kJ mol^{-1}. 3,5-DNP (**5**) represent the lowest value (73.2 kJ mol^{-1}), followed by 3,4-DNP **3** (124.2 kJ mol^{-1}) and **5** (189.1 kJ mol^{-1}) with the highest. The detonation pressures (p_{CJ}) lie between 28.9 and 30.8 GPa increasing from compound (**5**) to compound (**3**). The detonation velocities (V_D) show the same trend with values between 8279 m s^{-1} and 8459 m s^{-1}. Regarding the melting and decomposition behavior of the DNP salts they strongly vary with the corresponding cation (Figure 3.10).

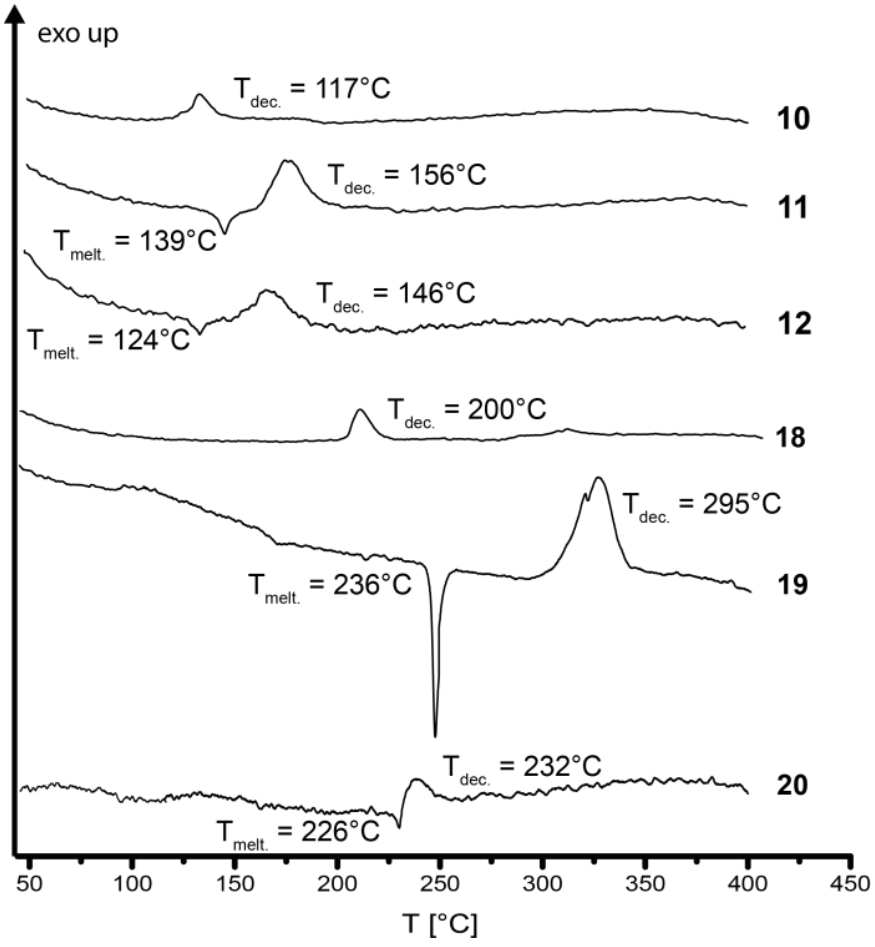

Figure 3.10. DSC plots of compounds **10–12** and **18–21** measured with a heating rate of 5 °C min^{-1}. Critical temperatures are given as onset temperatures.

The sodium (**6**) and potassium (**7**) salts of 3,4-DNP compounds dehydrate at 80 °C or 88 °C followed by decomposition at 142 °C and 174 °C, respectively. Beside compound **12,** which melts at 124 °C, all other decompose at temperatures between 101 °C and 180 °C with **13** as the highest. One reason could be the close position of the nitro groups destabilizing the molecule.

As shown in Table 3.2, all 3,4-DNP salts are insensitive toward impact, friction and electrostatic discharge. The two exceptions are the hydrazinium (IS: 10 J) and TATOT (IS: 30 J) salt, but nevertheless they are less sensitive than RDX (IS: 7.5 J) and are classified as less sensitive. All salts have friction sensitivity values of 360 N and the ESD value varies between 1.0 and 1.5 J, which also shows their insensitive behavior toward external stimuli. The heats of formation $\Delta_f H°$ lie in the range from negative values for the hydrates (**6:** –1071 kJ mol^{-1}, **7:** –675.4 kJ mol^{-1}) to 221.2 kJ mol^{-1} for **10**. The sodium (**6**), potassium (**7**) and guanidinium (**11**) salt have lower heat of formations compared to the neutral compound **3**. The densities lie between 1.61 and 1.74 g cm^{-3} at 298 K with **6** as the highest. The calculated detonation pressures (p_{CJ}) are in the range from 14.1 GPa (**6**) to 27.5 GPa (**10**). The highest p_{CJ} value of 275 bar belongs to the hydrazinium salt (**10**) as well as the highest detonation velocity (V_D) with a value of 8369 m s^{-1}. Table 3 shows the properties of different 3,5-DNP salts compared to RDX. In contrast to the 3,4-DNP salts they have higher decomposition temperatures (Figure 10). Compound **15** and **16** show the best thermal stability with values of 307 °C (**15**) and 300 °C (**16**). One reason for the relatively high decomposition temperature is the hydrogen bonding of **16**. The heats of formation lie between –298.7 kJ mol^{-1} (**19**) and 187.8 kJ mol^{-1} (**18**). Therefore, the hydrazinium (**18**) and aminoguanidinium (**19**) salt have a higher heat of formation than the neutral compound **5** (Table 3.3).

Regarding sensitivity values most 3,5-DNP salts are not sensitive toward friction, impact and electrostatic discharge with exception of the water free potassium salt (IS: 8.5 J) and the hydrazinium (IS: 10 J) salt. The densities lie between 1.59 and 2.037 g cm^{-3} at 298 K. The potassium salt of 3,5-DNP has the highest density, which is also higher than the neutral compound **5**. The calculated detonation pressures (p_{CJ}) lie in the range from 19.1 GPa (**19**) to 29.6 GPa (**18**). The highest p_{CJ} value (29.6 GPa) and the highest detonation velocity (V_D: 8610 m s^{-1}) were achieved for the hydrazinium salt (**18**).

Overall both hydrazinium salts (**10** and **18**) and the ammonium salt **16** perform nearly as well as RDX regarding its detonation properties (V_D = 8109–8610 m s^{-1}) and are less sensitive. Further the ammonium salt is not sensitive toward impact, friction and electrostatic discharge and shows a high thermal stability of 300 °C.

Table 3.2. Energetic Properties and detonation parameters of compounds **3–11** compared to **RDX**.

	3	**4**	**5**	**6·2H$_2$O**	**7·2H$_2$O**	**8**	**9**	**10**	**11**	**RDX**
Formula	$C_3H_2N_4O_4$	$C_3H_2N_4O_4$	$C_3H_2N_4O_4$	$C_3H_5N_4O_6Na$	$C_3H_5N_4O_6K$	$C_3H_5N_5O_4$	$C_3H_5N_5O_5$	$C_3H_6N_6O_4$	$C_4H_7N_7O_4$	$C_3H_6N_6O_6$
FW [g mol^{-1}]	158.07	158.07	158.07	216.08	232.19	175.03	191.03	190.05	217.06	221.12
IS [J][a]	40	25	25	40	40	40	10	40	40	7.5
FS [N][b]	360	360	360	360	360	360	360	360	360	120
ESD [J][c]	1.5	1.0	1.5	1.0	1.5	1.5	1.0	1.0	1.0	0.2
N [%][d]	35.44	35.44	35.44	25.93	24.13	40.00	36.65	44.20	45.15	37.84
Ω [%][e]	−30.36	−30.36	−30.36	−22.1	−20.7	−41.1	−29.3	−42.08	−55.26	−21.6
$T_{dec.}$ [°C][f]	71 (m.p.)	68 (m.p.)	169 (m.p.)	80 (H_2O)	88 (H_2O)	127	101	117	139 (m.p.)	205[18]
	285 (dec.)	171 (dec.)	299 (dec.)	142 (dec.)	174 (dec.)				156 (dec.)	
ρ [g cm^{-3}] (298K)[g]	1.79	1.76	1.78	1.74	1.72	1.69[o]	1.72[o]	1.67	1.63	1.81[16]
$\Delta_f H°$ [kJ mol^{-1}][h]	124.2	189.1	73.2	−1071	−675.4	–	–	221.2	40.4	70.3
$\Delta_f U°$ [kJ kg^{-1}][i]	864	1274	542	−4871	−2829	–	–	1268	288.7	417.0
EXPLO5 V6.03 values:[g]										
$-\Delta_E U°$ [kJ kg^{-1}][j]	5409	5752	5106	2070	3543	–	–	5402	3975	5845
T_E [K][k]	3956	4183	3786	1841	2665	–	–	3573	2866	3810
p_{CJ} [GPa][l]	30.6	30.8	28.9	14.1	17.8	–	–	27.6	21.1	34.5
V_D [m s^{-1}][m]	8426	8459	8279	6245	6800	–	–	8369	7585	8861
V_0 [L kg^{-1}][n]	711	721	428	612	581	–	–	832	815	785
Toxicity:										
EC_{50} (15 min) [g L^{-1}]	–	–	0.27	–	0.10	–	–	–	–	0.327
EC_{50} (30 min) [g L^{-1}]	–	–	0.19	–	0.08	–	–	–	–	0.239

[a] impact sensitivity (BAM drophammer, 1 of 6); [b] friction sensitivity (BAM friction tester, 1 of 6); [c] electrostatic discharge device (OZM); [d] nitrogen content; [e] oxygen balance; [f] decomposition temperature from DSC (β = 5°C); [g] recalculated from low temperature X-ray densities ($\rho_{298K} = \rho_T / (1+\alpha_V(298-T_0)$; $\alpha_V = 1.5\ 10^{-4}\ K^{-1}$); [h] calculated (CBS-4M) heat of formation; [i] calculated energy of formation; [j] energy of explosion; [k] explosion temperature; [l] detonation pressure; [m] detonation velocity; [n] assuming only gaseous products; [o] measured pycnometrically at room temperature.

Table 3.3. Energetic Properties and detonation parameters of compounds **12–21**.

	12	**13**	**14·2H$_2$O**	**15**	**16**	**17**	**18**	**19·H$_2$O**	**20**	**21**
Formula	$C_4H_8N_8O_4$	$C_6H_8N_{12}O_4$	$C_3H_5N_4O_6Na$	$C_3HN_4O_4K$	$C_3H_5N_5O_4$	$C_3H_8N_6O_4$	$C_3H_6N_6O_4$	$C_4H_9N_7O_5$	$C_4H_8N_8O_4$	$C_6H_8N_{12}O_4$
FW [g mol^{-1}]	232.18	312.08	216.08	196.16	175.03	191.03	190.05	217.06	232.18	312.08
IS [J][a]	40	30	40	8.5	40	40	10	40	40	40
FS [N][b]	360	360	360	240	360	360	360	360	360	360
ESD [J][c]	1.5	1.5	1.5	0.4	1.5	1.0	1.0	1.0	1.0	1.0
N [%][d]	48.27	53.84	25.93	28.56	40.00	36.65	44.20	45.15	48.27	53.84
Ω [%][e]	–55.2	–61.5	–22.1	–25.5	–41.1	–29.3	–42.1	–55.3	–55.2	–61.5
$T_{dec.}$ [°C][f]	124 (m.p.) 146 (dec.)	180	99 (H_2O) 297	307	251 (m.p.) 300 (dec.)	141	200	236 (m.p.) 295 (dec.)	226 (m.p.) 232 (dec.)	225 (m.p.) 234 (dec.)
ρ [g cm^{-3}] (298K)[g]	1.61	1.71[o]	1.72[o]	1.99	1.70	1.72[o]	1.74	1.59	1.64	1.62[o]
$\Delta_f H°$ [kJ mol^{-1}][h]	149.4	–	–	–194.8	34.0	–	187.8	–298.7	108.1	–
$\Delta_f U°$ [kJ kg^{-1}][i]	750.3	–	–	–936.1	293.4	–	1091.8	–1159.4	572.4	–
EXPLO5 V6.03 values:[g]										
$-\Delta_E U°$ [kJ kg^{-1}][j]	4273	–	–	4235	4764	–	5315	3295	4113	–
T_E [K][k]	2982	–	–	3064	3298	–	3481	2486	2893	–
p_{CJ} [GPa][l]	22.2	–	–	22.5	25.9	–	29.6	19.1	22.6	–
V_D [m s^{-1}][m]	7788	–	–	7557	8109	–	8610	7319	7848	–
V_0 [L kg^{-1}][n]	841	–	–	397	794	–	823	488	473	–
Toxicity:										
EC_{50} (15 min) [g L^{-1}]	–	–	–	1.21	–	–	–	–	–	–
EC_{50} (30 min) [g L^{-1}]	–	–	–	0.95	–	–	–	–	–	–

[a] impact sensitivity (BAM drophammer, 1 of 6); [b] friction sensitivity (BAM friction tester, 1 of 6); [c] electrostatic discharge device (OZM); [d] nitrogen content; [e] oxygen balance; [f] decomposition temperature from DSC (β = 5°C); [g] recalculated from low temperature X-ray densities ($\rho_{298K} = \rho_T / (1+\alpha_V(298-T_0)$; $\alpha_V = 1.5\ 10^{-4}\ K^{-1}$; [h] calculated (CBS-4M) heat of formation; [i] calculated energy of formation; [j] energy of explosion; [k] explosion temperature; [l] detonation pressure; [m] detonation velocity; [n] assuming only gaseous products; [o] measured pycnometrically at room temperature.

3.2.4 Toxicity Assessment

To determine the toxicity to aquatic life of **5**, **7** and **15** using the luminescent marine bacterium *Vibrio fischeri* (see supporting information) was used.[17] The EC50 value (half-maximal effective concentration) of compound **5** and **7** are lower than that of RDX (see Tables 2 and 3), which implies that **5** and **7** is more toxic than RDX. Hence, the potassium salt **15** has a higher EC_{50} value, which means that **15** is classified to be less toxic than RDX. Interestingly, the potassium salt of 3,5-DNP (**15**) is less toxic than the free acid (**5**).

3.3 Conclusion

Nitropyrazoles are valuable energetic materials due to their large variety of substitution patterns. While mono-nitropyrazoles are low energetic, trinitropyrazoles are characterized by an intensive synthetic protocol as well as higher sensitiveness which do not comply with new insensitive munitions regulations. Therefore in the present work, the three different dinitropyrazoles (3,4-DNP (**3**)**,** 1,3-DNP (**4**) and 3,5-DNP (**5**) are synthesized, characterized and compared to each other. Their interesting thermal behavior, high detonation properties and rather low sensitivity was identified. In addition the potassium and sodium as well as six selected nitrogen-rich salts were synthesized of 3,4- (**3**) and 3,5-DNP (**5**). Densities vary between 1.59 and 1.99 g cm^{-3}. Using EXPLO5, their detonation parameters were calculated. Their detonation velocity ranges from 6245 to 8610 m s^{-1}. With exception of **9** (10 J), **15** (8.5 J) and **18** (10 J) their IS values are higher than 40 J. According to their rather high thermal stabilities, low sensitivity values and detonation performances they can be used as HEDM.

3.4 Experimental Section

The complete experimental procedures for the synthesis of salts can be found in the supporting information.

CAUTION! All investigated compounds are potentially explosive energetic materials, although no hazards were observed during preparation and handling these compounds. Nevertheless, this necessitates additional meticulous safety precautions (earthed equipment, Kevlar® gloves, Kevlar® sleeves, face shield, leather coat, and ear plugs).

1-*N*-Nitropyrazole (1):[12b] 1*H*-Pyrazole (30.0 g, 495 mmol, 1.0 eq.) was dissolved in concentrated acetic acid (90 mL) and was cooled to 10 °C. Subsequently, fuming nitric acid (100 %, 21 mL, 504 mmol, 1.1 eq.) was added dropwise over 1 h, while keeping the temperature at 10 °C. The suspension was stirred for 30 min at 10 °C. Afterwards, the mixture was allowed to warm to room temperature and acetic anhydride (60 mL, 636 mmol, 1.4 eq.) was added slowly. The suspension was stirred for 1 h to receive a yellow solution, which was poured on ice afterwards. The resulting precipitate was filtered and dried on air to obtain **1** as a colorless solid (49.5 g, 438 mmol, 88 %).

^{1}H NMR (400MHz, DMSO d_6): δ (ppm) = 8.79 (dd, 1H, ^3J = 3.0 Hz, ^3J = 1.7 Hz, NO_2-N-CH), 7.87 (s, 1H, N=CH), 6.70 (dd, 1H, ^3J = 3.0 Hz, ^3J = 1.7 Hz, CH); **^{13}C NMR** (101 MHz, DMSO d_6): δ (ppm) = 141.5 (NO_2-N-CH), 126.8 (N=CH), 109.7 (C-H). **IR** (ATR, rel. int.): $\tilde{\nu}$ (cm^{-1}) = 3150 (w), 3121 (m), 1739 (w), 1608 (m), 1528 (w), 1477 (w), 1404 (w), 1371 (w), 1317 (m), 1283 (m), 1253 (m), 1228 (m), 1160 (m), 1062 (m), 1028 (m), 936 (m), 903 (m), 774 (s), 630 (s), 563 (m), 457 (m).

5-Nitropyrazole (2):[12a] Compound 1 (12.5 g, 111 mmol, 1.0 eq.) was suspended in anisole (250 mL) and heated for 16 h at 145 °C. Afterwards, the solution was cooled to 0 °C and the resulting precipitate was filtered, washed with cold anisole and dried on air. Compound 2 was obtained as a yellowish solid (9.91 g, 87.7 mmol, 79 %).

^{1}H NMR (400 MHz, DMSO d_6): δ (ppm) = 13.94 (s, 1H, NH), 8.02 (d, 1H, ^3J = 2.5 Hz, N=CH), 7.03 (d, 1H, ^3J = 2.5 Hz, CH); **^{13}C NMR** (101 MHz, DMSO d_6): δ (ppm) = 156.3 (C-NO_2), 132.3 (N=CH), 101.8 (CH); **IR** (ATR, rel. int.): $\tilde{\nu}$ (cm^{-1}) = 3141 (m), 3021 (w), 2974 (w), 2926 (m), 2882 (m), 1556 (s), 1510 (s), 1422 (m), 1379 (s), 1350 (s), 1249 (m), 1209 (m), 1144 (w), 1090 (m), 1048 (m), 990 (m), 928 (w), 903 (w), 821 (s), 783 (s), 752 (s), 613 (m), 537 (w).

3,4-Dinitropyrazole (3):[12a] Compound **2** (9.0 g, 79.6 mmol, 1.0 eq.) was dissolved in concentrated sulfuric acid (96 %, 15 mL) and the viscous solution was cooled to 0 °C. Subsequently, concentrated nitric acid (100 %, 10 mL) was added drop wise over 30 min, while keeping the temperature at 0 °C. Afterwards, further sulfuric acid (96 %, 30 mL) was added and the solution was allowed to warm to room temperature and heated at 80 °C for 3 h. The mixture was poured on ice and was extracted with diethyl ether (3x50 mL). The combined organic layers were dried over magnesium sulfate and the solvent was concentrated in vacuum. The residue was allowed to stand for crystallization. Compound (**3**) was obtained as yellowish crystals (8.56 g, 54.2 mmol, 68 %).

^{1}H NMR (400 MHz, DMSO d_6): δ (ppm) = 14.84 (s, 1H, NH), 9.10 (s, 1H, CH); **^{13}C NMR** (101 MHz, DMSO d_6): δ (ppm) = 148.2 (N=C-NO_2), 132.7 (CH), 126.3 (C-NO_2); **^{14}N NMR** (DMSO d_6): δ (ppm) = –25.3 (NO_2); **^{15}N NMR** (DMSO d_6): δ (ppm) = –175.5 (N-H), –85.0 (N), –26.1 (NO_2), –25.5 (NO_2); **IR** (ATR, rel. int.): $\tilde{\nu}$ (cm^{-1}) = 3298 (m), 3265 (m), 3148 (m), 3134 (m), 1766 (w), 1518 (s), 1446 (m),

1342 (s), 1273 (m), 1155 (m), 1091 (m), 1067 (m), 989 (w), 935 (w), 888 (w), 848 (m), 795 (s), 738 (s), 607 (s), 575 (s), 470 (m); **Raman** (1064 nm, 200 mW, cm^{-1}): $\tilde{\nu}$ = 3152(5), 1565(2), 1545(8), 1534(13), 1514(25), 1479(12), 1447(8), 1429(34), 1402(3), 1383(100), 1354(48), 1321(2), 1270(5), 1166(73), 1098(4), 1069(18), 932(18), 851(47), 810(6), 572(6), 484(5), 388(11), 279(4), 210(5), 183(23), 103(55); **Elemental analysis**: calcd. (%) for $C_3H_2N_4O_4$ (M = 158.07 g mol^{-1}): C 22.80, H 1.28, N 35.44; found: C 22.83, H 1.36, N 35.18.; **DSC** (5 °C min^{-1}): $T_{melt.}$ = 71 °C, $T_{dec.}$ = 285 °C, **Sensitivities** (grain size: < 100 µm): **BAM impact**: 40 J, **BAM friction**: 360 N, **ESD**: 1.5 J.

1,3-Dinitropyrazole (4):[12a] Compound **2** (5.0 g, 43 mmol 1.0 eq.) was suspended in acetic acid (100 %, 31 mL) and concentrated nitric acid (100 %, 4.14 mL) was added at r.t. to the suspension. The reaction was stirred for 30 min. at which the solution turned purple. Afterwards acetic anhydride (10 mL) was added and the solution was stirred for 24 h at room temperature. The mixture was poured on ice and extracted with ethyl acetate (3x50 mL). The combined organic layers were dried over magnesium sulfate and the solvent was concentrated in vacuum. The residue was stand for crystallization to give **4** as yellowish needles (5.77 g, 36.6 mmol, 85 %).

^{1}H NMR (400 MHz, DMSO d_6): δ (ppm) = 9.09 (s, 1H, CH), 7.44 (s, 1H, CH); **^{13}C NMR** (101 MHz, DMSO d_6): δ (ppm) = 152.55 (N=C-NO_2), 129.97 (CH), 104.73 (CH); **^{14}N NMR** (DMSO d_6): δ (ppm) = –62.4 (*N*-NO_2), –23.5 (*C*-NO_2); **^{15}N NMR** (DMSO d_6): δ (ppm) = –113.5 (N), –95.0 (N-NO_2), –63.2 (*N*-NO_2), –25.1 (*C*-NO_2); **IR** (ATR, rel. int.): $\tilde{\nu}$ (cm^{-1}) = 3170 (w), 3156 (w), 1740 (w), 1637 (m), 1548 (m), 1515 (w), 1471 (w), 1435 (w), 1398 (m), 1351 (m), 1323 (m), 1281 (s), 1237 (s), 1113 (s), 1039 (s), 983 (m), 961 (m), 899 (w), 810 (s), 781 (s), 753 (s), 616 (w), 567 (m), 523 (w), 485 (w); **Raman** (1064 nm, 200 mW, cm^{-1}): $\tilde{\nu}$ = 3173(17), 3159(11), 2836(8), 2753(5), 1638(16), 1549(22), 1521(17), 1474(14), 1437(58), 1400(100), 1320(21), 1324(21), 1289(31), 1238(16), 1212(10), 1116(13), 1102(11), 1044(10), 986(25), 964(37), 932(9), 986(9), 823(17), 788(9), 569(9); **Elemental analysis**: calcd. (%) for $C_3H_2N_4O_4$ (M = 158.07 g mol^{-1}): C 22.80, H 1.28, N 35.44; found: C 23.8, H 1.37, N 35.34.; **DSC** (5 °C min^{-1}): $T_{melt.}$ = 68 °C, $T_{dec.}$ = 175 °C. **Sensitivities** (grain size: < 100 µm): **BAM impact**: 25 J, **BAM friction**: 360 N, **ESD**: 1.0 J.

3,5-Dinitropyrazole (5):[12a] Compound **4** (9.0 g, 56.6 mmol, 1.0 eq.) was suspended in benzonitrile (250 mL) and heated at 180 °C for 3 hours. After cooling down the solution aqueous sodium hydroxide (2 M, 200 mL) was added and the precipitate was collected by filtration. The precipitate was acidified with conc. HCl to pH=1 and extracted with diethyl ether (3x100 mL). The combined organic layers were dried over magnesium sulfate and the solvent removed to yield **5** (7.0 g, 44 mmol, 78 %).

^{1}H NMR (400 MHz, DMSO d_6): δ (ppm) = 7.92 (s, 1H, CH) **^{13}C NMR** (101 MHz, DMSO d_6): δ (ppm) = 151.53 (N=C-NO_2), 99.78 (CH); **^{14}N NMR** (DMSO d_6): δ (ppm) = –24.8 (NO_2); **^{15}N NMR** (DMSO d_6): δ (ppm) = –123.4 (N), –26.4 (NO_2); **IR** (ATR, rel. int.): $\tilde{\nu}$ (cm^{-1}) = 3156 (w), 1712 (w), 1640 (m), 1550 (m), 1510 (m), 1436 (w), 1398 (m), 1329 (m), 1282 (s), 1237 (s), 1174 (w), 1111 (s), 1039 (s), 983 (m), 809 (s), 779 (s), 751 (s), 618 (w); **Raman** (1064 nm, 200 mW, cm^{-1}): $\tilde{\nu}$ = 3151(4), 1600(2), 1576(4), 1571(4), 1552(9), 1541(8), 1504(2), 1486(3), 1447(15), 1442(14),1431(11), 1401(100), 1358(4), 1341(5), 1273(4), 1196(4), 1025(1), 1015(3), 1005(3), 985(4), 848(1), 833(1), 762(1), 350(4), 286(6), 96(25), 75(6); **Elemental analysis**: calcd. (%) for $C_3H_2N_4O_4$ (M = 158.07 g mol^{-1}): C 22.80, H 1.28, N 35.44; found: C 23.04, H 1.28, N 35.76.; **DTA** (5 °C min^{-1}): $T_{melt.}$ = 171 °C, $T_{dec.}$ = 299 °C; **Sensitivities** (grain size: < 100 µm): **BAM impact**: 25 J, **BAM friction**: 360 N, **ESD**: 1.0 J.

3.5 References

[1] a) P. Yin, L. A. Mitchell, D. A. Parrish, J. M. Shreeve, *Chem. Asian J.* **2017**, *12*, 378–384; b) R. Haiges, K. O. Christe, *Inorg. Chem.* **2013**, *52*, 7249–7260; c) G. A. Parker, G. Reddy, M. A. Major, *Int. J. Tox.* **2006**, *25*, 373–378; d) R. Meyer, J. Köhler, A. Homburg, *Explosives*, Wiley-VCH, Weinheim, **2016**; e) M. Zhang, W. Fu, C. Li, H. Gao, L. Tang, Z. Zhou, *Eur. J. Inorg. Chem.* **2017**, 2017, 2883–2891; f) V. Thottempudi, H. Gao, J. M. Shreeve, *J. Am. Chem. Soc.* **2011**, *133*, 6464–6471; g) H. Xue, S. W. Arritt, B. Twamley, J. M. Shreeve, *Inorg. Chem.* **2004**, *43*, 7972–7977; h) T. M. Klapötke, P. C. Schmid, S. Schnell, J. Stierstorfer, *Chem. Eur. J.* **2015**, *21*, 9219–9228; i) T. M. Klapötke, *High Energy Density Materials*, Springer, Berlin, Heidelberg, **2007**.

[2] a) L. M. Sweeney, C. P. Gut, M. L. Gargas, G. Reddy, L. R. Williams, M. S. Johnson, *Reg. Tox. Pharmacol.* **2012**, *62*, 107–114; b) J. Giles, *Nature* **2004**, *427*, 580–581; c) M. B. Talawar, R. Sivabalan, T. Mukundan, H. Muthurajan, A. K. Sikder, B. R. Gandhe, A. S. Rao, *J. Hazard. Mater.* **2009**, *161*, 589–607.

[3] N. Fischer, D. Fischer, T. M. Klapötke, D. G. Piercey, J. Stierstorfer, *J. Mat. Chem.* **2012**, *22*, 20418–20422.

[4] T. M. Klapötke, P. C. Schmid, S. Schnell, J. Stierstorfer, *J. Mat. Chem. A* **2015**, *3*, 2658–2668.

[5] T. M. Klapötke, A. Preimesser, J. Stierstorfer, *Z. anorg. allg. Chem.* **2012**, *638*, 1278–1286.

[6] H. Wei, C. He, J. Zhang, J. M. Shreeve, *Angew. Chem. Int. Ed.* **2015**, *54*, 9367–9371.

[7] Y. Liu, J. Zhang, K. Wang, J. Li, Q. Zhang, J. M. Shreeve, *Angew. Chem. Int. Ed.***2016**, *55*, 11548–11551.

[8] Y. Zhang, Y. Guo, Y.-H. Joo, D. A. Parrish, J. M. Shreeve, *Chem. Eur. J.* **2010**, *16*, 10778–10784.

[9] a) T. M. Klapötke, M. Leroux, P. C. Schmid, J. Stierstorfer, *Chem. Asian J.* **2016**, *11*, 844–851; b) N. Fischer, T. M. Klapötke, M. Reymann, J. Stierstorfer, *Eur. J. Inorg. Chem.* **2013**, *2013*, 2167–2180.

[10] P. Yin, J. Zhang, D. A. Parrish, J. M. Shreeve, *Chem. Eur. J.* **2014**, *20*, 16529–16536.

[11] a) J. Catalan, J. Elguero, *Adv. Heterocycl. Chem.,* **1987**, *Vol. 41*, 187–274; b) G. Hervé, C. Roussel, H. Graindorge, *Angew. Chem. Int. Ed.* **2010**, *49*, 3177–3181.

[12] a) J. W. A. M. Janssen, H. J. Koeners, C. G. Kruse, C. L. Habrakern, *J. Org. Chem.* **1973**, *38*, 1777–1782; b) R. Hüttel, F. Büchele, P. Jochum, *Chem. Ber.* **1955**, *88*, 1577–1585.

[13] S. Thomas, *Angew. Chem. Int. Ed.* **2002**, *41*, 48–76.

[14] M. Hesse, H. Meier, B. Zeeh, *Spektroskopische Methoden in der Organischen Chemie,* 7th edn., Thieme, Stuttgart, New York, **2005**.

[15] T. Altenburger, T. M. Klapötke, A. Penger, J. Stierstorfer, *Z. anorg. allg. Chem.* **2010**, *636*, 463–471.

[16] C. S. Choi, E. Prince, *Acta Cryst. B* **1972**, *28*, 2857–2862.

[17] G. I. Sunahara, S. Dodard, M. Sarrazin, L. Paquet, G. Ampleman, S. Thiboutot, J. Hawari, A. Y. Renoux, *Ecotoxicol. Environ. Saf.* **1998**, *39*, 185–194.

[18] H. Maruizumi, D. Fukuma, K. Shirota, N. Kubota, *Propellants, Explos., Pyrotech.* **1982**, *7*, 40–45.

3.6 Supplementary Information

3.6.1 X-ray Diffraction

Single crystals were picked and measured on an Oxford Xcalibur3 diffractometer with a Spellman generator (voltage 50 kV, current 40 mA) and a CCD area detector for data collection using Mo-*K*α radiation (λ = 0.71073 Å). The data collection was carried out using CRYSALISPRO software[S1] and the reduction were performed. The structures were solved using direct methods (SIR-92,[S2] SIR-97[S3] or SHELXS-97[S4]) and refined by full-matrix least-squares on *F*2 (SHELXL[S4]): The final check was done with the PLATON software[S5] integrated in the WinGX software suite. The non-hydrogen atoms were refined anisotropically and the hydrogen atoms were located and freely refined. The absorptions were corrected by a SCALE3 ABSPACK multiscan method.[S6] The DIAMOND2 plots are shown with thermal ellipsoids at the 50% probability level and hydrogen atoms are shown as small spheres of arbitrary radii. The SADABS program embedded in the Bruker APEX3 software has been used for multi-scan absorption corrections in all structures.[S7]

Table 3.S1. Crystallographic data and refinement parameters of compound **3**, **4, 5** and **6**.

	3	**4**	**5**	**6**
Formula	$C_3H_2N_4O_4$	$C_3H_2N_4O_4$	$C_3H_2N_4O_4$	$C_3H_5N_4O_6Na$
FW [g mol^{-1}]	158.09	158.09	158.09	216.10
Crystal system	Monoclinic	Monoclinic	Orthorhombic	Monoclinic
Space Group	$P2_1/c$	$P2_1/c$	$Pca2_1$	Cc
Color / Habit	Light yellow block	Colorless block	Colorless block	Colorless block
Size [mm]	0.10 × 0.22 × 0.28	0.10 × 0.25 × 0.40	0.15 × 0.3 × 0.3	0.35 x 0.25 x 0.04
a [Å]	9.8326(4)	5.7084(6)	10.6055(3)	9.4273(6)
b [Å]	12.0559(4)	9.2664(8)	10.3711(3)	16.9108(9)
c [Å]	9.7190(4)	11.3570(11)	10.4933(3)	6.7574(4)
α [°]	90	90	90	90
β [°]	93.959(4)	103.315(10)	90	131.349(3)
γ [°]	90	90	90	90
V [Å^3]	1149.35(8)	584.60(10)	1154.17(6)	808.72 (9)
Z	8	4	8	4
$\rho_{calc.}$ [g cm^{-3}]	1.827	1.796	1.82	1.775
μ [mm^{-1}]	0.170	0.167	0.169	0.211
F(000)	640	320	640	440
$\lambda_{MoK\alpha}$[Å]	0.71073	0.71073	0.71073	0.71073
T [K]	123	173	173	173
ϑ min-max [°]	4.2, 26.0	4.3, 29.0	4.3, 27.0	4.6, 27.0
Dataset h; k; l	−12:12;−12:14;−11:11	−7:7;−12:12; −15:11	−13:13;−13:13; −13:13	−12:12 ; −21:21 ; −8: 8
Reflect. coll.	8674	5289	17350	6163
Independ. refl.	2236	1546	2502	1763
R_{int}	0.019	0.025	0.028	0.026
Reflection obs.	1918	1211	2337	1697
No. parameters	215	127	215	147
R_1 (obs)	0.0324	0.0339	0.0266	0.0256
wR_2 (all data)	0.0930	0.0899	0.0683	0.0637
S	1.04	1.04	1.04	1.06
Resd. Dens.[e Å^{-3}]	−0.22, 0.31	−0.23, 0.15	−0.18, 0.14	−0.13, 0.20
Device type	Oxford XCalibur3 CCD	Oxford XCalibur3 CCD	Oxford XCalibur3 CCD	Oxford XCalibur3 CCD
Solution	SIR-92	SIR-92	SIR-92	SIR-92
Refinement	SHELXL-2013	SHELXL-2013	SHELXL-2013	SHELXL-2013
Absorpt. corr.	multi-scan	multi-scan	multi-scan	multi-scan
CCDC	1835056	1835054	1835062	1835053

Table 3.S2. Crystallographic data and refinement parameters of compound **7, 10, 11** and **12**.

	7	**10**	**11**	**12**
Formula	$C_3H_5N_4O_6K$	$C_3H_6N_6O_4$	$C_3H_7N_7O_4$	$C_4H_8N_7O_4$
FW [g mol^{-1}]	232.21	190.14	217.17	232.18
Crystal system	Monoclinic	Monoclinic	Triclinic	Orthorhombic
Space Group	*P2$_1$/n*	*P2$_1$/c*	*P-1*	*P2$_1$2$_1$2$_1$*
Color / Habit	Colorless block	Colorless needle	Colorless block	Colorless block
Size [mm]	0.05 x 0.05 x 0.25	0.03 × 0.11 × 0.37	0.27 × 0.34 × 0.4	0.26 x 0.40 x 0.46
a [Å]	7.1818(4)	7.6584(6)	7.6007(7)	6.5366(2)
b [Å]	7.3770(4)	19.6060(11)	7.6465(8)	7.3548(2)
c [Å]	16.7871(8)	9.9145(5)	9.0964(9)	19.4770(5)
α [°]	90	90	107.092(9)	90
β [°]	98.243(5)	95.476(5)	91.714(8)	90
γ [°]	90	90	118.419(10)	90
V [Å^3]	880.20(8)	1481.87(16)	435.27(9)	936.36(5)
Z	4	8	2	4
$\rho_{calc.}$ [g cm^{-3}]	1.752	1.704	1.657	1.647
μ [mm^{-1}]	0.619	0.154	0.146	0.144
F(000)	472	784	224	480
$\lambda_{MoK\alpha}$[Å]	0.71073	0.71073	0.71073	0.71073
T [K]	173	173	173	173
ϑ min-max [°]	4.3, 26.0	4.3, 26.5	4.3, 26.5	4.2, 28.0
Dataset h; k; l	−8:8; −9:9; −20:19	−9:9;−24:19;−11:12	−9:9;−9:9;−11:9	−8:8;−9:9;−25:25
Reflect. coll.	6313	11369	3379	16498
Independ. refl.	1719	3057	1803	2255
R_{int}	0.028	0.06	0.018	0.024
Reflection obs.	1377	1719	1500	2167
No. parameters	147	283	164	177
R_1 (obs)	0.0299	0.0546	0.035	0.0260
wR_2 (all data)	0.0730	0.1408	0.0903	0.0688
S	1.02	1.01	1.06	1.05
Resd. Dens.[e Å^{-3}]	−0.25, 0.27	−0.25, 0.37	−0.28, 0.18	−0.18, 0.24
Device type	Oxford XCalibur3 CCD	Oxford XCalibur3 CCD	Oxford XCalibur3 CCD	Oxford XCalibur3 CCD
Solution	SIR-92	SIR-92	SIR-92	SIR-92
Refinement	SHELXL-2013	SHELXL-2013	SHELXL-2013	SHELXL-2013
Absorpt. corr.	multi-scan	multi-scan	multi-scan	multi-scan
CCDC	1835066	1835061	1835065	1835063

Table 3.S3. Crystallographic data and refinement parameters of compound **15**, **16**, **17** and **18**.

	15	**16**	**17**	**18**
Formula	$C_3HN_4O_4K$	$C_3H_5N_5O_4$	$C_3H_8N_6O_6$	$C_3H_6N_6O_4$
FW [g mol^{-1}]	196.18	175.12	224.15	190.14
Crystal system	Triclinic	Triclinic	Triclinic	Monoclinic
Space Group	*P*-1	*P*-1	*P*-1	$P2_1/n$
Color / Habit	Yellow block	Light yellow block	Yellow block	Light yellow needle
Size [mm]	0.03 × 0.10 × 0.20	0.05 × 0.10 × 0.35	0.09 × 0.10 × 0.40	0.09 × 0.10 × 0.37
a [Å]	4.7286(4)	4.9061(4)	3.6667(3)	12.0613(5)
b [Å]	8.0597(9)	8.0368(8)	9.8416(9)	3.7121(2)
c [Å]	9.0922(10)	9.1951(9)	11.7909(10)	16.7722(7)
α [°]	105.45(1)	103.753(9)	94.309(7)	90
β [°]	102.488(9)	104.226(8)	90.645(6)	91.217(4)
γ [°]	97.285(8)	96.410(7)	98.004(7)	90
V [Å^3]	319.77(6)	335.75(6)	420.05(6)	750.77(6)
Z	2	2	2	4
$\rho_{calc.}$ [g cm^{-3}]	2.037	1.732	1.772	1.682
μ [mm^{-1}]	0.809	0.158	0.168	0.152
F(000)	196	180	232	392
$\lambda_{MoK\alpha}$[Å]	0.71073	0.71073	0.71073	0.71073
T [K]	173	173	173	173
ϑ min-max [°]	4.5, 26.0	4.3, 26.5	4.2, 26.5	4.1, 26.5
Dataset h; k; l	−4:5; −9:9; −11:11	−6:6;−10:10;−11:11	−4:4;−12:12;−14:14	−15:15;−4:4;−21:21
Reflect. coll.	2343	4807	6055	10224
Independ. refl.	1249	1387	1755	1545
R_{int}	0.025	0.0308	0.0342	0.041
Reflection obs.	1091	1203	1455	1250
No. parameters	113	129	168	142
R_1 (obs)	0.0298	0.0308	0.0342	0.0382
wR_2 (all data)	0.0732	0.0794	0.0866	0.1023
S	1.07	1.05	1.06	1.07
Resd. Dens.[e Å^{-3}]	−0.31, 0.23	−0.28, 0.18	−0.27, 0.18	−0.22, 0.18
Device type	Oxford XCalibur3 CCD	Oxford XCalibur3 CCD	Oxford XCalibur3 CCD	Oxford XCalibur3 CCD
Solution	SIR-92	SIR-92	SIR-92	SIR-92
Refinement	SHELXL-2013	SHELXL-2013	SHELXL-2013	SHELXL-2013
Absorpt. corr.	multi-scan	multi-scan	multi-scan	multi-scan
CCDC	1835060	1835055	1835057	1835059

Table 3.S4. Crystallographic data and refinement parameters of compound **19** and **20**.

	19	**20**
Formula	$C_4H_9N_7O_5$	$C_4H_8N_8O_4$
FW [g mol^{-1}]	235.18	232.15
Crystal system	Monoclinic	Monoclinic
Space Group	$P2_1/c$	$C2/c$
Color / Habit	Light yellow block	Yellow rod
Size [mm]	0.09 × 0.41 × 0.49	0.02 x 0.02 x 0.01
a [Å]	3.5832(2)	20.5017(10)
b [Å]	11.5459(5)	3.5483(2)
c [Å]	23.3490(8)	26.5002(11)
α [°]	90	90
β [°]	93.152(4)	109.304(2)
γ [°]	90	90
V [Å^3]	964.52(8)	1819.40
Z	4	8
$\rho_{calc.}$ [g cm^{-3}]	1.620	1.695
μ [mm^{-1}]	0.146	0.149
$F(000)$	488	960
$\lambda_{MoK\alpha}$[Å]	0.71073	0.71073
T [K]	173	100
ϑ min-max [°]	4.4, 26.6	3.1, 26.4
Dataset h; k; l	−4:4;−13:14; -25:29	−24:23;−4:4; -33:33
Reflect. coll.	7399	8407
Independ. refl.	2001	1866
R_{int}	0.025	0.036
Reflection obs.	1663	1546
No. parameters	181	177
R_1 (obs)	0.0305	0.0420
wR_2 (all data)	0.0815	0.0915
S	1.04	1.10
Resd. Dens.[e Å^{-3}]	−0.22, 0.20	−0.28, 0.22
Device type	Oxford XCalibur3 CCD	Bruker D8 Venture
Solution	SIR-92	SIR-92
Refinement	SHELXL-2013	SHELXL-2013
Absorpt. corr.	multi-scan	multi-scan
CCDC	1835058	1835064

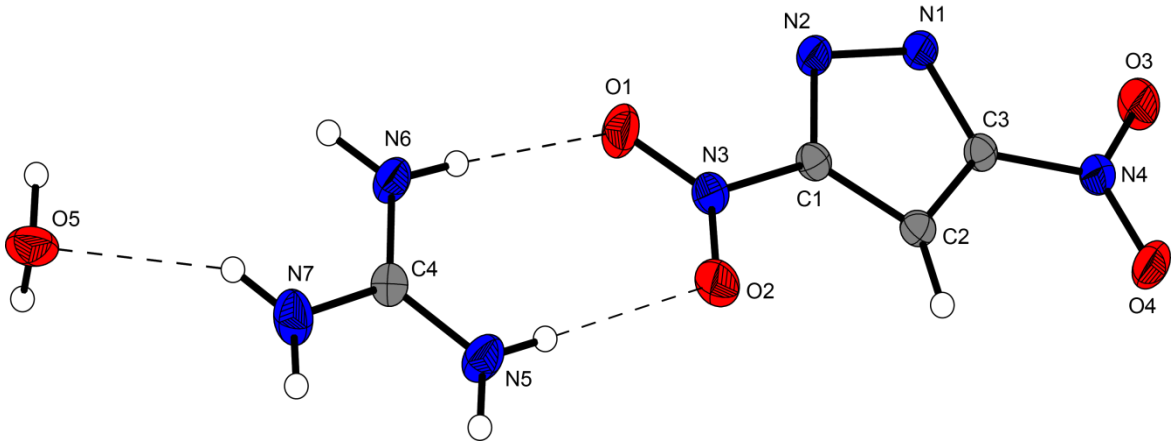

Figure 3.S1. Molecular structure of **19** showing the atom-labelling scheme. Thermal ellipsoids represent the 50% probability level.

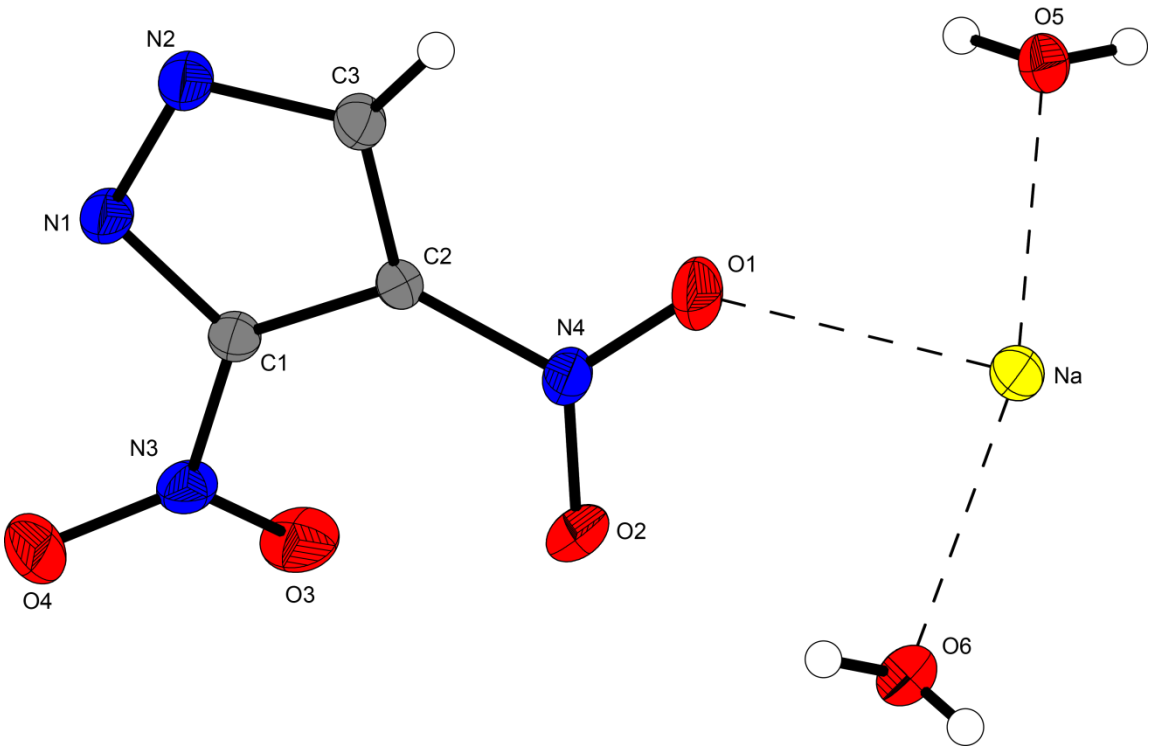

Figure 3.S2. Extended molecular structure of **6** showing the atom-labelling scheme. Thermal ellipsoids represent the 50% probability level.

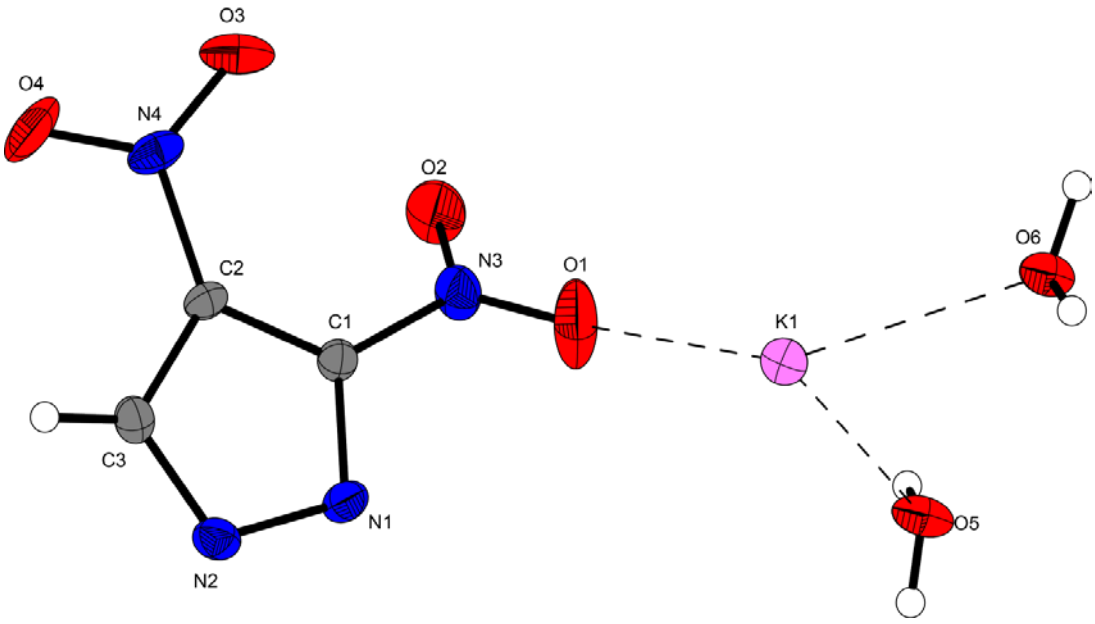

Figure 3.S3. Extended molecular structure of **7** showing the atom-labelling scheme. Thermal ellipsoids represent the 50% probability level.

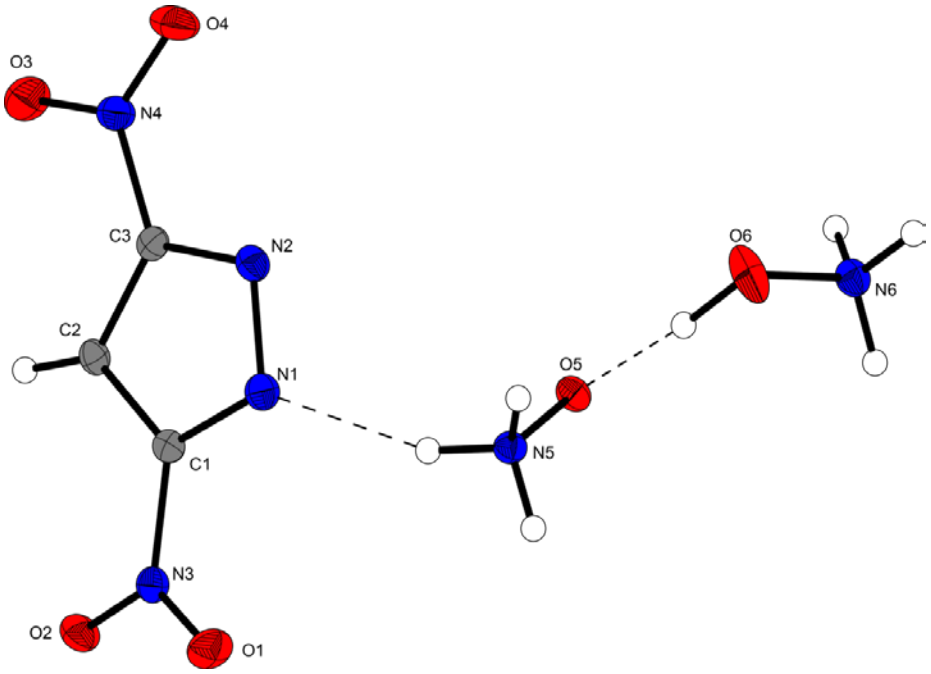

Figure 3.S4 Extended molecular structure of **17** showing the atom-labelling scheme. Thermal ellipsoids represent the 50% probability level.

3.6.2 Heat of formation calculations

All quantum chemical calculations were carried out using the Gaussian G09 program package.[S8] The enthalpies (H) and free energies (G) were calculated using the complete basis set (CBS) method of Petersson and coworkers in order to obtain very accurate energies. The CBS models are using the known asymptotic convergence of pair natural orbital expressions to extrapolate from calculations using a finite basis set to the estimated CBS limit. CBS-4 starts with an HF/3-21G(d) geometry optimization; the zero point energy is computed at the same level. It then uses a large basis set SCF calculation as a base energy, and an MP2/6- 31+G calculation with a CBS extrapolation to correct the energy through second order. A MP4(SDQ)/6-31+ (d,p) calculation is used to approximate higher order contributions. In this study, we applied the modified CBS-4M.

Heats of formation of the synthesized ionic compounds were calculated using the atomization method (equation E1) using room temperature CBS-4M enthalpies, which are summarized in Table 3.S5.[S9,S10]

$$\Delta_f H^\circ_{(g,\,M,\,298)} = H_{(Molecule,\,298)} - \sum H^\circ_{(Atoms,\,298)} + \sum \Delta_f H^\circ_{(Atoms,\,298)} \qquad (E1)$$

Table 3.S5. CBS-4M enthalpies for atoms C, H, N and O and their literature values for atomic $\Delta H^\circ_f{}^{298}$ / kJ mol^{-1}

	$-H^{298}$ [a.u.]	NIST [S11]
H	0.500991	218.2
C	37.786156	717.2
N	54.522462	473.1
O	74.991202	249.5

For neutral compounds the sublimation enthalpy, which is needed to convert the gas phase enthalpy of formation to the solid state one, was calculated by the *Trouton* rule.[S12] For ionic compounds, the lattice energy (U_L) and lattice enthalpy (ΔH_L) were calculated from the corresponding X-ray molecular volumes according to the equations provided by *Jenkins* and *Glasser*.[S13] With the calculated lattice enthalpy the gas-phase enthalpy of formation was converted into the solid state (standard conditions) enthalpy of formation. These molar standard enthalpies of formation (ΔH_m) were used to calculate the molar solid state energies of formation (ΔU_m) according to equation E2.

$$\Delta U_m = \Delta H_m - \Delta n\, RT \qquad (E2)$$

(Δn being the change of moles of gaseous components)

The calculation results are summarized in Table 3.S6.

Table 3.S6. Heat of formation calculation results.

M	$-H^{298}$ [a] [a.u.]	$\Delta_f H°$(g,M) [kJ mol^{-1}] [b]	V_M [Å^3] [c]	$\Delta U_L, \Delta H_L$;[d] [kJ mol^{-1}]	$\Delta_f H°$(s) [e] [kJ mol^{-1}]	Δn [f]	$\Delta_f U$(s) [g] [kJ kg^{-1}]
3	634.428441	188.9			124.2	5	864.1
4	634.404341	252.2			189.1	5	1274.0
5	634.438612	162.2			73.2	5	541.5
3 anion	633.930253	–36.6					
Na+	161.661926	596.8					
K+	599.035967	487.4					
NH4+	56.796608	635.8					
N2H5+	112.030523	773.4					
NH4O+	131.863249	686.4					
G+	205.453192	571.9					
AG+	260.701802	671.6					
TATOT+	555.474133	1080.0					
6		541.1	808.7	650.9, 657.1	–1071.1	–7.5	–4870.8
7		541.1	880.2	635.0, 641.2	–675.4	–7.5	–2828.5
10		737.5	1481.9	512.8, 516.3	221.2	8	1267.8
11		535.3	435.3	491.4, 494.9	40.4	9	288.7
12		635.0	936.4	482.1, 485.6	149.4	10	750.3
5 anion	633.943669	–71.9					
15		415.8	319.8	613.9, 613.7	–197.8	4.5	–951.6
16		564.0	335.8	526.4,529.9	34.0	7	293.4
18		702.3	750.8	511.0, 514.5	187.8	8	1091.8
19		541.1	964.5	548.7, 554.9	–298.7	10.5	–1159.4
20		599.7	1819.4	488.1, 491.6	108.1	10	572.4

[a] CBS-4M electronic enthalpy; [b] gas phase enthalpy of formation; [c] molecular volumes taken from X-ray structures and corrected to room temperature; [d] lattice energy and enthalpy (calculated using Jenkins and Glasser equations); [e] standard solid state enthalpy of formation; [f] Δn being the change of moles of gaseous components when formed; [g] solid state energy of formation.

3.6.3 Experimental Part

General Procedures

Differential Scanning Calorimetry (DSC) was recorded on a LINSEIS DSC PT10 with about 1 mg substance in a perforated aluminum vessel with a heating rate of 5 K·min^{-1} and a nitrogen flow of 5 dm^3·h^{-1}. The NMR spectra were carried out using a 400 MHz instruments JEOL Eclipse 270, JEOL EX 400 or a JEOL Eclipse 400 (^{1}H 399.8 MHz, ^{13}C 100.5 MHz, ^{14}N 28.9 MHz, and ^{15}N 40.6 MHz). Chemical shifts are given in parts per million (ppm) relative to tetramethylsilane (^{1}H, ^{13}C) and nitromethane (^{14}N, ^{15}N). Infrared spectra were measured with a Perkin-Elmer Spectrum BX-FTIR spectrometer equipped with a Smiths DuraSamplIR II ATR device. Transmittance values are qualitatively described as "very strong" (vs), "strong" (s), "medium" (m), and "weak" (w). Raman spectra were recorded using a Bruker MultiRAM FT-Raman instrument fitted with a liquid-nitrogen cooled germanium detector and a Nd:YAG laser (λ = 1064 nm). The intensities are quoted as percentages of the most intense peak and are given in parentheses. DTA spectra were carried out using a OZM DTA 551-EX with a heating rate of 5 K·min^{-1}. Low-resolution mass spectra were recorded with a JEOL MStation JMS 700 (DEI+ / FAB+/−). Elemental analysis (C/H/N) was carried out using a Vario Micro from the Elementar Company. TGA spectra were recorded on a Perkin Elmer TGA 4000 with a heating rate of 5 K min^{-1}.

Impact sensitivity tests were performed according to STANAG 4489[S14] modified instruction[S15] using a Bundesanstalt für Materialforschung (BAM) drophammer.[S16] Friction sensitivity tests were carried out according to STANAG 4487[S17] modified instruction[S18] using a BAM friction tester. The grading of the tested compounds results from the "UN Recommendations on the Transport of Dangerous Goods".[S19] ESD values were carried out using the Electric Spark Tester ESD 2010 EN.[S20]

1-*N*-Nitropyrazole (1)[S21]

1*H*-Pyrazole (30.0 g, 495 mmol, 1.0 eq.) was dissolved in concentrated acetic acid (90 mL) and was cooled to 10 °C. Subsequently, fuming nitric acid (100 %, 21 mL, 504 mmol, 1.1 eq.) was added dropwise over 1 h, while keeping the temperature at 10 °C. The suspension was stirred for 30 min at 10 °C. Afterwards, the mixture was allowed to warm to room temperature and acetic anhydride (60 mL, 636 mmol, 1.4 eq.) was added slowly. The suspension was stirred for 1 h to receive a yellow solution, which was poured on ice afterwards. The resulting precipitate was filtered and dried on air to obtain **1** as a colorless solid (49.5 g, 438 mmol, 88 %).

^{1}H NMR (400MHz, DMSO d_6): δ (ppm) = 8.79 (dd, 1H, ^{3}J = 3.0 Hz, ^{3}J = 1.7 Hz, NO_2-N-CH), 7.87 (s, 1H, N=CH), 6.70 (dd, 1H, ^{3}J = 3.0 Hz, ^{3}J = 1.7 Hz, CH); **^{13}C NMR** (101 MHz, DMSO d_6): δ (ppm) = 141.5 (NO_2-N-CH), 126.8 (N=CH), 109.7 (C-H). **IR** (ATR, rel. int.): $\tilde{\nu}$ (cm^{-1}) = 3150 (w), 3121 (m), 1739 (w), 1608 (m), 1528 (w), 1477 (w), 1404 (w), 1371 (w), 1317 (m), 1283 (m), 1253 (m), 1228 (m), 1160 (m), 1062 (m), 1028 (m), 936 (m), 903 (m), 774 (s), 630 (s), 563 (m), 457 (m).

5-Nitropyrazole (2) [S22]

1 (12.5 g, 111 mmol, 1.0 eq.) was suspended in anisole (250 mL) and heated for 16 h at 145 °C. Afterwards, the solution was cooled to 0 °C and the resulting precipitate was filtered, washed with cold anisole and dried on air. Compound **2** was obtained as a yellowish solid (9.91 g, 87.7 mmol, 79 %).

^{1}H NMR (400 MHz, DMSO d_6): δ (ppm) = 13.94 (s, 1H, NH), 8.02 (d, 1H, ^{3}J = 2.5 Hz, N=CH), 7.03 (d, 1H, ^{3}J = 2.5 Hz, CH); **^{13}C NMR** (101 MHz, DMSO d_6): δ (ppm) = 156.3 (C-NO_2), 132.3 (N=CH), 101.8 (CH); **IR** (ATR, rel. int.): $\tilde{\nu}$ (cm^{-1}) = 3141 (m), 3021 (w), 2974 (w), 2926 (m), 2882 (m), 1556 (s), 1510 (s), 1422 (m), 1379 (s), 1350 (s), 1249 (m), 1209 (m), 1144 (w), 1090 (m), 1048 (m), 990 (m), 928 (w), 903 (w), 821 (s), 783 (s), 752 (s), 613 (m), 537 (w).

3,4-Dinitropyrazole (3) [S22]

Compound **2** (9.0 g, 79.6 mmol, 1.0 eq.) was dissolved in concentrated sulfuric acid (96 %, 15 mL) and the viscous solution was cooled to 0 °C. Subsequently, concentrated nitric acid (100 %, 10 mL) was added drop wise over 30 min, while keeping the temperature at 0 °C. Afterwards, further sulfuric acid (96 %, 30 mL) was added and the solution was allowed to warm to room temperature and heated at 80 °C for 3 h. The mixture was poured on ice and was extracted with diethyl ether (3x50 mL). The combined organic layers were dried over magnesium sulfate and the solvent was concentrated in vacuum. The residue was allowed to stand for crystallization. Compound (**3**) was obtained as yellowish crystals (8.56 g, 54.2 mmol, 68 %).

^{1}H NMR (400 MHz, DMSO d_6): δ (ppm) = 14.84 (s, 1H, NH), 9.10 (s, 1H, CH); **^{13}C NMR** (101 MHz, DMSO d_6): δ (ppm) = 148.2 (N=C-NO_2), 132.7 (CH), 126.3 (C-NO_2); **^{14}N NMR** (DMSO d_6): δ (ppm) = –25.3 (NO_2); **^{15}N NMR** (DMSO d_6): δ (ppm) = –175.5 (N-H), –85.0 (N), –26.1 (NO_2), –25.5 (NO_2); **IR** (ATR, rel. int.): $\tilde{\nu}$ (cm^{-1}) = 3298 (m), 3265 (m), 3148 (m), 3134 (m), 1766 (w), 1518 (s), 1446 (m), 1342 (s), 1273 (m), 1155 (m), 1091 (m), 1067 (m), 989 (w), 935 (w), 888 (w), 848 (m), 795 (s), 738 (s), 607 (s), 575 (s), 470 (m); **Raman** (1064 nm, 200 mW, cm^{-1}): $\tilde{\nu}$ = 3152(5), 1565(2), 1545(8),

1534(13), 1514(25), 1479(12), 1447(8), 1429(34), 1402(3), 1383(100), 1354(48), 1321(2), 1270(5), 1166(73), 1098(4), 1069(18), 932(18), 851(47), 810(6), 572(6), 484(5), 388(11), 279(4), 210(5), 183(23), 103(55); **Elemental analysis**: calcd. (%) for $C_3H_2N_4O_4$ (M = 158.07 g mol^{-1}): C 22.80, H 1.28, N 35.44; found: C 22.83, H 1.36, N 35.18.; **DSC** (5 °C min^{-1}): $T_{melt.}$ = 71 °C, $T_{dec.}$ = 285 °C, **Sensitivities** (grain size: < 100 μm): **BAM impact**: 40 J, **BAM friction**: 360 N, **ESD**: 1.5 J.

1,3-Dinitropyrazole (4) [S22]

Compound **2** (5.0 g, 43 mmol 1.0 eq.) was suspended in acetic acid (100 %, 31 mL) and concentrated nitric acid (100 %, 4.14 mL) was added at r.t. to the suspension. The reaction was stirred for 30 min. at which the solution turned purple. Afterwards acetic anhydride (10 mL) was added and the solution was stirred for 24 h at room temperature. The mixture was poured on ice and extracted with ethyl acetate (3x50 mL). The combined organic layers were dried over magnesium sulfate and the solvent was concentrated in vacuum. The residue was stand for crystallization to give **4** as yellowish needles (5.77 g, 36.6 mmol, 85 %).

^{1}H NMR (400 MHz, DMSO d_6): δ (ppm) = 9.09 (s, 1H, CH), 7.44 (s, 1H, CH); **^{13}C NMR** (101 MHz, DMSO d_6): δ (ppm) = 152.55 (N=C-NO_2), 129.97 (CH), 104.73 (CH); **^{14}N NMR** (DMSO d_6): δ (ppm) = –62.4 (*N*-NO_2), –23.5 (*C*-NO_2); **^{15}N NMR** (DMSO d_6): δ (ppm) = –113.5 (N), –95.0 (N-NO_2), –63.2 (*N*-NO_2), –25.1 (*C*-NO_2); **IR** (ATR, rel. int.): $\tilde{\nu}$ (cm^{-1}) = 3170 (w), 3156 (w), 1740 (w), 1637 (m), 1548 (m), 1515 (w), 1471 (w), 1435 (w), 1398 (m), 1351 (m), 1323 (m), 1281 (s), 1237 (s), 1113 (s), 1039 (s), 983 (m), 961 (m), 899 (w), 810 (s), 781 (s), 753 (s), 616 (w), 567 (m), 523 (w), 485 (w); **Raman** (1064 nm, 200 mW, cm^{-1}): $\tilde{\nu}$ = 3173(17), 3159(11), 2836(8), 2753(5), 1638(16), 1549(22), 1521(17), 1474(14), 1437(58), 1400(100), 1320(21), 1324(21), 1289(31), 1238(16), 1212(10), 1116(13), 1102(11), 1044(10), 986(25), 964(37), 932(9), 986(9), 823(17), 788(9), 569(9); **Elemental analysis**: calcd. (%) for $C_3H_2N_4O_4$ (M = 158.07 g mol^{-1}): C 22.80, H 1.28, N 35.44; found: C 23.8, H 1.37, N 35.34.; **DSC** (5 °C min^{-1}): $T_{melt.}$ = 68 °C, $T_{dec.}$ = 175 °C. **Sensitivities** (grain size: < 100 μm): **BAM impact**: 25 J, **BAM friction**: 360 N, **ESD**: 1.0 J.

3,5-Dinitropyrazole (5) [S22]

Compound **4** (9.0 g, 56.6 mmol, 1.0 eq.) was suspended in benzonitrile (250 mL) and heated at 180 °C for 3 hours. After cooling down the solution aqueous sodium hydroxide (2 M, 200 mL) was added and the precipitate was collected by filtration. The precipitate was acidified with conc. HCl to pH=1

and extracted with diethyl ether (3x100 mL). The combined organic layers were dried over magnesium sulfate and the solvent removed to yield **5** (7.0 g, 44 mmol, 78 %).

^{1}H NMR (400 MHz, DMSO d_6): δ (ppm) = 7.92 (s, 1H, CH) **^{13}C NMR** (101 MHz, DMSO d_6): δ (ppm) = 151.53 (N=C-NO_2), 99.78 (CH); **^{14}N NMR** (DMSO d_6): δ (ppm) = –24.8 (NO_2); **^{15}N NMR** (DMSO d_6): δ (ppm) = –123.4 (N), –26.4 (NO_2); **IR** (ATR, rel. int.): $\tilde{\nu}$ (cm^{-1}) = 3156 (w), 1712 (w), 1640 (m), 1550 (m), 1510 (m), 1436 (w), 1398 (m), 1329 (m), 1282 (s), 1237 (s), 1174 (w), 1111 (s), 1039 (s), 983 (m), 809 (s), 779 (s), 751 (s), 618 (w); **Raman** (1064 nm, 200 mW, cm^{-1}): $\tilde{\nu}$ = 3151(4), 1600(2), 1576(4), 1571(4), 1552(9), 1541(8), 1504(2), 1486(3), 1447(15), 1442(14),1431(11), 1401(100), 1358(4), 1341(5), 1273(4), 1196(4), 1025(1), 1015(3), 1005(3), 985(4), 848(1), 833(1), 762(1), 350(4), 286(6), 96(25), 75(6); **Elemental analysis**: calcd. (%) for $C_3H_2N_4O_4$ (M = 158.07 g mol^{-1}): C 22.80, H 1.28, N 35.44; found: C 23.04, H 1.28, N 35.76.; **DTA** (5 °C min^{-1}): $T_{melt.}$ = 171 °C, $T_{dec.}$ = 299 °C; **Sensitivities** (grain size: < 100 μm): **BAM impact**: 25 J, **BAM friction**: 360 N, **ESD**: 1.0 J.

General procedure for the preparation of salts

To a water/ethanol 1:1 solution of **3** or **5** (0.5 g, 3.16 mmol) the corresponding base (**6/14**: NaOH 0.126 g, 3.16 mmol; **7/15**: KOH 0.174 g, 3.16 mmol; **8/16**: ammonia solution 1.6 mL, 2 M, 3.16 mmol; **9/17**: NH_2OH 0.21 mL, 50% in water, 3.16 mmol; **10/18**: $N_2H_4 \cdot H_2O$ 0.16 g, 3.16 mmol; **11/19**: guanidine carbonate 0.284 g, 3.16 mmol; **12/20**: aminoguanidine bicarbonate 0.43 g, 3.16 mmol; **13/20**: 3,6,7-triamino-7*H* -[1,2,4]triazolo[4,3-b][1,2,4]triazol-2-ium (TATOT) 0.49 g, 3.16 mmol) was added and heated until everything was dissolved. The solutions were filtered and left for crystallization.

3,4-Dinitro-1*H*-pyrazole salts

Sodium 3,4-dinitropyrazolate dihydrate (6)

Yield: (0.5 g, 2.3 mmol, 74 %) as colorless crystals.

^{1}H NMR (400MHz, DMSO d_6): δ (ppm) = 8.02 (s, 1H, CH); **^{13}C NMR** (101 MHz, DMSO d_6): δ (ppm) = 151.0, 138.2, 125.3; **IR** (ATR, rel. int.): $\tilde{\nu}$ (cm^{-1}) = 3131(w), 2203(w), 2173(w), 1637(w), 1538(w), 1493(w), 1403(w), 1317(w), 1346(w), 1271(w), 1150(w), 1116(w), 1050(w), 998(w), 938(w), 847(w), 808(w), 755(w), 595(s), 507(w), **Mass spectroscopy**: m/z (FAB+) = 23.0 (Na+), m/z (FAB–) = 157.1 ($C_3HN_4O_4^-$); **Elemental analysis**: calcd. (%) for $C_3H_5N_4O_6Na$ (M = 216.09 g mol^{-1}): C 16.68,

H 2.33, N 25.93; found: C 17.06, H 2.42, N 25.10; **DSC** (5 °C min^{-1}): T_{H2O} = 80 °C, $T_{dec.}$ = 142 °C; **Sensitivities** (grain size: < 500 µm): **BAM impact**: 40 J, **BAM friction**: 360 N, ESD: 1.0 J;

Potassium 3,4-dinitropyrazolate dihydrate (7)

Yield: (0.56 g, 2.41 mmol, 76 %) as colorless crystals.

^{1}H NMR (400MHz, DMSO d_6): δ (ppm) = 8.07 (s, 1H, CH); **^{13}C NMR** (101 MHz, DMSO d_6): δ (ppm) = 150.9, 137.9, 125.3; **IR** (ATR, rel. int.): $\tilde{\nu}$ (cm^{-1}) = 3988(w), 3128(w), 1977(w), 1493(s), 1436(s), 1342(s), 1288(s), 1163(s), 1113(s), 983(s), 885(s), 852(s), 807(s), 750(s), 631(s), 546(s); **Mass spectroscopy**: m/z (FAB+) = 39.0 (K+), m/z (FAB–) = 157.1 ($C_3HN_4O_4^-$); **Elemental analysis**: calcd. (%) for $C_3H_5N_4O_6K$ (M = 232.18 g mol^{-1}): C 15.52, H 2.17, N 24.13; found: C 15.39, H 2.26, N 24.39; **DSC** (5 °C min^{-1}): T_{H2O} = 88 °C $T_{dec.}$ = 174 °C; **Sensitivities** (grain size: < 500 µm): **BAM impact**: 40 J, **BAM friction**: 360 N, ESD: 1.5 J;

Ammonium 3,4-dinitropyrazolate (8)

Yield: (0.4 g, 2.3 mmol, 73 %) as colorless crystals.

^{1}HNMR (400MHz, DMSO d_6): δ (ppm) = 7.12 (s, 4H, NH_4), 8.14 (s, 1H, CH); **^{13}C NMR** (101 MHz, DMSO d_6): δ (ppm) = 163.5, 138.0, 125.8; **IR** (ATR, rel. int.): $\tilde{\nu}$ (cm^{-1}) = 3125 (s), 2007 (m), 1538 (s), 1493 (s), 1433 (s), 1363 (s), 1335 (s), 1279 (s), 1156 (s), 1110 (s), 1090 (s), 1076 (s), 992 (s), 945 (s), 882 (s), 848 (s), 806 (s), 750 (s), 669 (s), 630 (s), 607 (s); **Mass spectroscopy**: m/z (FAB+) = 18.1 (NH_4+), m/z (FAB–) = 157.1 ($C_3HN_4O_4^-$); **Elemental analysis**: calcd. (%) for $C_3H_5N_5O_4$ (M = 175.03 g mol^{-1}): C 20.58, H 2.88, N 40.0; found: C 21.01, H 2.54, N 38.39; **DSC** (5 °C min^{-1}): $T_{dec.}$ = 127 °C; **Sensitivities** (grain size: < 500 µm): **BAM impact**: 40 J, **BAM friction**: 360 N, ESD: 1.5 J.

Hydroxylammonium ammoniumoxide 3,4-dinitropyrazolate (9)

Yield: (0.3 g, 1.3 mmol, 42 %) as colorless crystals.

^{1}H NMR (400 MHz, DMSO d_6): δ (ppm) = 8.72 (NH_3OH), 8.30 (s, 1H, CH); **^{13}C NMR** (101 MHz, DMSO d_6): δ (ppm) = 150.3, 136.9, 125.6; **IR** (ATR, rel. int.): $\tilde{\nu}$ (cm^{-1}) = 3588 (w), 3298 (m), 3264 (m), 3149 (m), 3134 (m), 2898 (m), 1767 (w), 1624 (w), 1545 (s), 1518 (s), 1446 (m), 1410 (m), 1369 (s), 1343 (s), 1274 (m), 1182 (m), 1156 (m), 1089 (s), 1069 (s), 934 (m), 888 (m), 849 (s), 806 (s), 741 (s), 607 (s); **Mass spectroscopy**: m/z (FAB+) = 31.1 (NH_3OH+), m/z (FAB–) = 157.1 ($C_3HN_4O_4^-$);

Elemental analysis: calcd. (%) for $C_3H_8N_6O_6$ (M = 224.13 g mol^{-1}): C 16.08, H 3.60, N 37.50; found: C 16.43, H 3.47, N 36.62; **DSC** (5 °C min^{-1}): $T_{dec.}$ = 101 °C; **Sensitivities** (grain size: < 500 µm): **BAM impact**: 10 J, **BAM friction**: 360 N, ESD: 1.0 J.

Hydrazinium 3,4-dinitropyrazolate (10)

Yield: (0.4 g, 2.1 mmol, 68 %) as colorless crystals.

^{1}HNMR (400MHz, DMSO d_6): δ (ppm) = 7.19 (s, 5H, N_2H_5), 7.29 (s, 1H, CH); **^{13}C NMR** (101 MHz, DMSO d_6): δ (ppm) = 158.1, 139.1 , 127.3; **IR** (ATR, rel. int.): $\tilde{\nu}$ (cm^{-1}) = 3467 (s), 3418 (s), 3382 (s), 3298 (s), 3151 (s), 1651 (s), 1532 (s), 1471 (s), 1440 (s), 1348 (s), 1316 (s), 1274 (s), 1210 (s), 1155 (s), 1092 (s), 1065 (s), 1008 (s), 994 (s), 882 (m), 834 (s), 747 (s), 718 (s), 654 (s); **Mass spectroscopy**: m/z (FAB+) = (), m/z (FAB–) = 157.1 ($C_3HN_4O_4^-$); **Elemental analysis**: calcd. (%) for $C_3H_6N_6O_4$ (M = 190.11 g mol^{-1}): C 18.95, H 3.18, N 44.20; found: C 18.75, H 3.15, N 43.40 ; **DSC** (5 °C min^{-1}): $T_{dec.}$ = 117 °C; **Sensitivities** (grain size: < 500 µm): **BAM impact**: 40 J, **BAM friction**: 360 N, ESD: 1.0 J.

Guanidinium 3,4-dinitropyrazolate (11)

Yield: (0.4 g, 1.8 mmol, 58 %) as colorless crystals.

^{1}H NMR (400MHz, DMSO d_6): δ (ppm) = 6.94 (s, 6H, CH_6N_3), 8.03 (s, 1H, CH); **^{13}C NMR** (101 MHz, DMSO d_6): δ (ppm) = 157.9 (CH_6N_3), 150.9, 138.1, 125.3; **IR** (ATR, rel. int.): $\tilde{\nu}$ (cm^{-1}) = 3588 (w), 3298 (m), 3264 (m), 3149 (m), 3134 (m), 2898 (w), 1767 (w), 1624 (w), 1545 (s), 1518 (s), 1446 (m), 1410 (m), 1369 (s), 1343 (s), 1274 (m), 1182 (m), 1156 (m), 1089 (s), 1069 (s), 934 (m), 888 (m), 849 (s), 806 (s), 741 (s), 607 (s); **Mass spectroscopy**: m/z (FAB+) = 60.1 (CH_6N_3), m/z (FAB–) = 157.1 ($C_3HN_4O_4^-$); **Elemental analysis**: calcd. (%) for $C_4H_7N_7O_4$ (M = 217.14 g mol^{-1}): C 22.14, H 3.25, N 45.15; found: C 22.40, H 3.25, N 45.17; **DSC** (5 °C min^{-1}): $T_{melt.}$ = 139 °C, $T_{dec.}$ = 156 °C; **Sensitivities** (grain size: < 500 µm): **BAM impact**: 40 J, **BAM friction**: 360 N, ESD: 1.0 J.

Aminoguanidinium 3,4-dinitropyrazolate (12)

Yield: (0.5 g, 2.2 mmol, 70 %) as colorless crystals.

^{1}H NMR (400 MHz, DMSO d_6): δ (ppm) = 8.59 (s, 1H, N-H), 8.02 (s, 1H, CH), 7.21 (s, 2H, NH_2) , 4.68 (4H, NH_2) **^{13}C NMR** (101 MHz, DMSO d_6): δ (ppm) = 158.7, 150.9, 138.1, 125.1; **IR** (ATR, rel. int.): $\tilde{\nu}$

(cm^{-1}) = 3423 (m), 3367 (m), 3316 (m), 3126 (m), 1660 (s), 1531 (m), 1490 (s), 1422 (m), 1367 (s), 1341 (s), 1278 (s), 1206 (m), 1163 (m), 1112 (m), 1050 (s), 950 (s), 877 (m), 847 (m), 810 (m), 753 (s), 619 (s); **Elemental analysis**: calcd. (%) for $C_4H_8N_8O_4$ (M = 232.18 g mol^{-1}): C 20.69, H 3.47, N 48.27; found: C 20.98, H 3.47, N 47.64.; **Mass spectroscopy**: m/z (FAB+) = 75.1 (CH_7N_4+), m/z (FAB–) = 157.1 ($C_3HN_4O_4^-$); **DSC** (5 °C min^{-1}): $T_{melt.}$ = 124 °C, $T_{dec.}$ = 146 °C; **Sensitivities** (grain size: < 500 µm): **BAM impact**: 40 J, **BAM friction**: 360 N, ESD: 1.0 J.

TATOT 3,4-dinitropyrazolate (13)

Yield: (0.38 g, 1.26 mmol, 40 %) as colorless powder.

^{1}H NMR (400 MHz, DMSO d_6): δ (ppm) =8.26 (s, 1H, CH), 7.67, 7.07, 5.73; **^{13}C NMR** (101 MHz, DMSO d_6): δ (ppm) = 159.8, 147.7 141.6, 137.1, 125.5, 150.6; **IR** (ATR, rel. int.): $\tilde{\nu}$ (cm^{-1}) = 3555 (m), 3487 (m), 3994 (w), 3336 (m), 3295 (m), 3159 (m), 3116 (m), 2243 (w), 2184 (w), 2046 (w), 2014 (w), 1670 (m), 1630 (m), 1581 (w), 1537 (m), 1485 (s), 1446 (m), 1356 (s), 1326 (m), 1285 (m), 1285 (m), 1186 (m), 1097 (w), 1001 (m), 971 (m), 891 (m), 817 (m), 745 (m), 704 (m), 632 (m); **Mass spectroscopy**: m/z (FAB+) = 155.2 ($C_3H_7N_8$+), m/z (FAB–) = 157.1 ($C_3HN_4O_4^-$); **Elemental analysis**: calcd. (%) for $C_6H_8N_{12}O_4$ (M = 312.21 g mol^{-1}): C 23.08, H 2.58, N 53.84; found: C 23.23, H 2.64, N 52.68; **DSC** (5 °C min^{-1}): $T_{dec.}$ = 180 °C; **Sensitivities** (grain size: < 500 µm): **BAM impact**: 40 J, **BAM friction**: 360 N, ESD: 1.0 J.

3,5-Dinitro-1*H*-pyrazole salts

Sodium 3,5-dinitropyrazolate dihydrate (14)

Yield: (0.47 g, 2.17 mmol, 70 %) as colorless crystal.

^{1}H NMR (400MHz, DMSO d_6): δ (ppm) = 7.30 (s, 1H, CH); **^{13}C NMR** (101 MHz, DMSO d_6): δ (ppm) = 156.5, 98.3; **IR** (ATR, rel. int.): $\tilde{\nu}$ (cm^{-1}) = 3643 (w), 3552 (w), 3281(w), 3149(w), 2809(w), 2167(w), 1682(w), 1621(w), 1531(s), 1470(s), 1351(s), 1316(s), 1273(s), 1168(s), 1072(w), 1011(s), 839(s), 750(s), 666(w), 562(s); **Mass spectroscopy**: m/z (FAB+) = 23.0 (Na^+), m/z (FAB–) = 157.1 ($C_3HN_4O_4^-$); **Elemental analysis**: calcd. (%) for $C_3H_5N_4O_6Na$ (M = 216.08 g mol^{-1}): C 16.68, H 2.33, N 25.93; found: C 16.51, H 2.46, N 25.02; **DSC** (5 °C min^{-1}): T_{H2O} = 99 °C, $T_{dec.}$ = 297 °C; **Sensitivities** (grain size: < 500 µm): **BAM impact**: 40 J, **BAM friction**: 360 N, ESD: 1.5 J.

Potassium 3,5-dinitropyrazolate (15)

Yield: (0.56 g, 2.84 mmol, 92 %) as colorless powder.

^{1}H NMR (400MHz, DMSO d_6): δ (ppm) = 8.07 (s, 1H, CH); **^{13}C NMR** (101 MHz, DMSO d_6): δ (ppm) = 156.4, 98.3; **IR** (ATR, rel. int.): $\tilde{\nu}$ (cm^{-1}) = 3988(w), 3157(w), 2806(w), 2597(w), 1535(s), 1471(s), 1441(s), 1337(s), 1309(s), 1269(s), 1149(s), 1063(w), 1002(s), 829(s), 752(s), 672(w), 611(s), 580(s), 520(w); **Mass spectroscopy**: m/z (FAB+) = 39.0 (K+), m/z (FAB–) = 157.1 ($C_3HN_4O_4^-$); **Elemental analysis**: calcd. (%) for $C_3HN_4O_4K$ (M = 196.07 g mol^{-1}): C 18.80, H 0.51, N 28.56; found: C 19.22, H 0.89, N 29.20; **DSC** (5 °C min^{-1}): $T_{dec.}$ = 307 °C; **Sensitivities** (grain size: < 500 µm): **BAM impact**: 8.5 J, **BAM friction**: 240 N, ESD: 0.4 J.

Ammonium 3,5-dinitropyrazolate (16)

Yield: (0.44 g, 2.53 mmol, 80 %) as colorless powder.

^{1}H NMR (400MHz, DMSO d_6): δ (ppm) = 7.10 (s, 4H, NH_4), 7.30 (s, 1H, CH); **^{13}C NMR** (101 MHz, DMSO d_6): δ (ppm) = 156.4, 98.3; **IR** (ATR, rel. int.): $\tilde{\nu}$ (cm^{-1}) = 3305 (w), 3255 (w), 3155 (m), 3019 (w), 2971 (m), 2926 (m), 2887 (m), 2829 (m), 2777 (m), 2614 (w), 2592 (w), 2509 (w), 2479 (w), 2442 (w), 2410 (w), 2366 (w), 2191 (w), 2168 (w), 1737 (w), 1717 (w), 1671 (w), 1608 (w), 1556 (m), 1513 (m), 1480 (m), 1438 (m), 1423 (m), 1378 (s), 1350 (s), 1318 (m), 1276 (m), 1250 (m), 1209 (m), 1162 (m), 1091 (m), 1048 (m), 1012 (m), 991 (m), 928 (m), 902 (m), 862 (m), 823 (s), 784 (m), 752 (s), 720 (m), 638 (m), 609 (m); **Mass spectroscopy**: m/z (FAB+) = 18.1 (NH_4+), m/z (FAB–) = 157.1 ($C_3HN_4O_4^-$); **Elemental analysis**: calcd. (%) for $C_3H_5N_5O_4$ (M = 175.10 g mol^{-1}): C 20.58, H 2.88, N 40.00; found: C 20.86, H 2.95, N 39.50; **DSC** (5 °C min^{-1}): $T_{melt.}$ = 251 °C, $T_{dec.}$ = 300 °C; **Sensitivities** (grain size: 500 – 1000 µm): **BAM impact**: 40 J, **BAM friction**: 360 N, ESD: 1.5 J.

Hydroxylammonium ammonium oxide 3,5-dinitropyrazolate (17)

Yield: (0.23 g, 1.0 mmol, 82 %) as colorless powder.

^{1}H NMR (400MHz, DMSO d_6): δ (ppm) = 9.48 (s, 4H, NH_3OH), 7.30 (s, 1H, CH); **^{13}C NMR** (101 MHz, DMSO d_6): δ (ppm) = 156.4, 98.3; **IR** (ATR, rel. int.): $\tilde{\nu}$ (cm^{-1}) = 3580 (w), 3526 (w), 3211 (m), 3155 (m), 2866 (m), 2593 (m), 2509 (m), 2239 (m), 2213 (m), 2191 (m), 2167 (m), 2101 (m), 2076 (m), 2051 (m), 2034 (m), 1998 (m), 1979 (m), 1738 (m), 1618 (m), 1527 (s), 1479 (s), 1445 (s), 1350 (s), 1320 (s), 1278 (s), 1209 (s), 1165 (s), 1073 (s), 1010 (s), 992 (s), 822 (s), 748 (s), 670 (m), 607 (m);

Mass spectroscopy: m/z (FAB+) = 31.1 (NH_3OH^+), m/z (FAB–) = 157.1 ($C_3HN_4O_4^-$); **Elemental analysis**: calcd. (%) for $C_3H_8N_6O_6$ (M = 224.13 g mol^{-1}): C 16.08, H 3.60, N 37.50; found: C 16.06, H 3.56, N 37.45; **DSC** (5 °C min^{-1}): $T_{dec.}$ = 141 °C; **Sensitivities** (grain size: < 500 µm): **BAM impact**: 40 J, **BAM friction**: 360 N, ESD: 1.0 J.

Hydrazinium 3,5-dinitropyrazolate (18)

Yield: (0.56 g, 2.95 mmol, 80 %) as colorless solid.

^{1}H NMR (400MHz, DMSO d_6): δ (ppm) = 7.08 (s, 5H, N_2H_5), 7.29 (s, 1H, CH); **^{13}C NMR** (101 MHz, DMSO d_6): δ (ppm) = 156.4, 98.3; **IR** (ATR, rel. int.): $\tilde{\nu}$ (cm^{-1}) = 3352 (m), 3294 (m), 3188 (w), 3153 (m), 2826 (m), 2744 (m), 2616 (m), 2356 (m), 2325 (m), 2232 (w), 2213 (w), 2193 (m), 2169 (m), 2141 (w), 2088 (w), 2027 (w), 2008 (w), 1979 (w), 1925 (w), 1911 (w), 1645 (m), 1594 (m), 1535 (s), 1487 (s), 1444 (s), 1373 (s), 1352 (s), 1322 (s), 1283 (s), 1172 (s), 1135 (m), 1097 (s), 1069 (m), 1016 (s), 998 (s), 963 (s), 834 (s), 812 (s), 747 (s), 715 (m); **Mass spectroscopy**: m/z (FAB+) = 33.1 ($N_2H_5^+$), m/z (FAB–) = 157.1 ($C_3HN_4O_4^-$); **Elemental analysis**: calcd. (%) for $C_3H_7N_6O_{4.5}$ (M = 199.13 g mol^{-1}): C 18.10, H 3.54, N 42.20; found: C 17.98, H 3.71, N 42.65; **DSC** (5 °C min^{-1}): $T_{dec.}$ = 200 °C; **Sensitivities** (grain size: < 500 µm): **BAM impact**: 10 J, **BAM friction**: 360 N, ESD: 1.5 J.

Guanidinium 3,5-dinitropyrazolate hydrate (19)

Yield: (0.39 g, 1.79 mmol, 57 %) as colorless solid.

^{1}H NMR (400MHz, DMSO d_6): δ (ppm) = 6.93 (s, 6H, CH_6N_3), 7.30 (s, 1H, CH); **^{13}C NMR** (101 MHz, DMSO d_6): δ (ppm) = 157.9 (CH_6N_3), 156.4, 98.4; **IR** (ATR, rel. int.): $\tilde{\nu}$ (cm^{-1}) = 3993 (w), 3975 (w), 3940 (w), 3914 (w), 3884 (w), 3823 (w), 3467 (m), 3424 (m), 3382 (m), 3151 (m), 3005 (m), 2716 (w), 2463 (w), 2435 (w), 2340 (w), 2320 (w), 2296 (w), 2247 (w), 2212 (w), 2191 (w), 2167 (w), 2148 (w), 2126 (w), 2076 (w), 2039 (w), 2007 (w), 1648 (m), 1570 (m), 1533 (m), 1472 (s), 1441 (m), 1348 (s), 1315 (s), 1275 (m), 1154 (m), 1068 (m), 1008 (s), 833 (s), 748 (s), 654 (m), 606 (m); **Mass spectroscopy**: m/z (FAB+) = 60.1 ($CH_6N_3^+$), m/z (FAB–) = 157.1 ($C_3HN_4O_4^-$); **Elemental analysis**: calcd. (%) for $C_4H_9N_7O_5$ (M = 235.16 g mol^{-1}): C 20.43, H 3.86, N 41.69; found: C 20.76, H 3.88, N 41.56; **DSC** (5 °C min^{-1}): $T_{melt.}$ = 236 °C, $T_{dec.}$ = 295 °C; **Sensitivities** (grain size: < 500 µm): **BAM impact**: 40 J, **BAM friction**: 360 N, ESD: 1.0 J.

Aminoguanidinium 3,5-dinitropyrazolate (20)

Yield: (0.3 g, 1.3 mmol, 42 %) as colorless crystals.

^{1}H NMR (400 MHz, DMSO d_6): δ (ppm) = 8.65 (s, 1H, N-H), 7.28 (s, 1H, CH), 7.14 (s, 2H, NH_2) , 4.67 (4H, NH_2) **^{13}C NMR** (101 MHz, DMSO d_6): δ (ppm) = 158.8, 156.4, 98.4; **IR** (ATR, rel. int.): $\tilde{\nu}$ (cm^{-1}) = 3475 (m), 3434 (m), 3370 (m), 3320 (m), 3299 (m), 3174 (m), 3150 (s), 2750 (m), 2716 (m), 2595 (m), 2462 (w), 2293 (w), 2212 (w), 2193 (w), 2144 (w), 1635 (s), 1528 (m), 1480 (s), 1441 (s), 1345 (s), 1310 (s), 1274 (s), 1189 (s), 1155 (s), 1107 (m), 1069 (s), 1008 (s), 993 (s), 920 (s), 820 (s), 751 (s), 642 (s); **Mass spectroscopy**: m/z (FAB+) = 75.1 (CH_7N_4+), m/z (FAB–) = 157.1 ($C_3HN_4O_4^-$); **Elemental analysis**: calcd. (%) for $C_4H_8N_8O_4$ (M = 232.07 g mol^{-1}): C 20.69, H 3.47, N 48.27; found: C 20.83, H 3.47, N 48.30; **DSC** (5 °C min^{-1}): $T_{melt.}$ = 226 °C, $T_{dec.}$ = 232 °C; **Sensitivities** (grain size: < 500 µm): **BAM impact**: 40 J, **BAM friction**: 360 N, ESD: 1.0 J.

TATOT 3,5-dinitropyrazolate (21)

Yield: (0.4 g, 1.32 mmol, 42 %) as colorless solid.

^{1}H NMR (400 MHz, DMSO d_6): δ (ppm) =7.28 (s, 1H, CH) 5.76, 7.21, 8.15; **13C NMR** (101 MHz, DMSO d_6): δ (ppm) = 156.4, 98.4, 141.1, 147.4, 160.1; **IR** (ATR, rel. int.): $\tilde{\nu}$ (cm^{-1}) = 3555 (m), 3484 (m), 3427 (m), 3395 (m), 3336 (m), 3273 (m), 3159 (m), 2627 (m), 2333 (m), 2240 (m), 2213 (m), 2197 (m), 2118 (m), 2098 (m), 2084 (m), 2045 (m), 2021 (m), 1990 (m), 1966 (m), 1939 (w), 1867 (m), 1843 (m), 1826 (m), 1748 (m), 1703 (m), 1670 (s), 1631 (s), 1583 (m), 1537 (s), 1485 (s), 1446 (s), 1357 (s), 1327 (s), 1285 (s), 1260 (m), 1186 (s), 1153 (m), 1098 (m), 1071 (m), 1022 (s), 1001 (s), 971 (s), 890 (s), 849 (m), 833 (s), 817 (s), 747 (s), 722 (s), 704 (s), 633 (s); **Mass spectroscopy**: m/z (FAB+) = 155.2 ($C_3H_7N_8$+), m/z (FAB–) = 157.1 ($C_3HN_4O_4^-$); **Elemental analysis**: calcd. (%) for $C_6H_{10}N_{12}O_5$ (M = 330.23 g mol^{-1}): C 21.82, H 3.05, N 50.90; found: C 21.55, H 3.05, N 48.14; **DSC** (5 °C min^{-1}): $T_{melt.}$ = 225 °C, $T_{dec.}$ = 234 °C; **Sensitivities** (grain size: < 500 µm): **BAM impact**: 40 J, **BAM friction**: 360 N, ESD: 1.0 J.

3.6.4 ^{15}N NMR spectroscopy

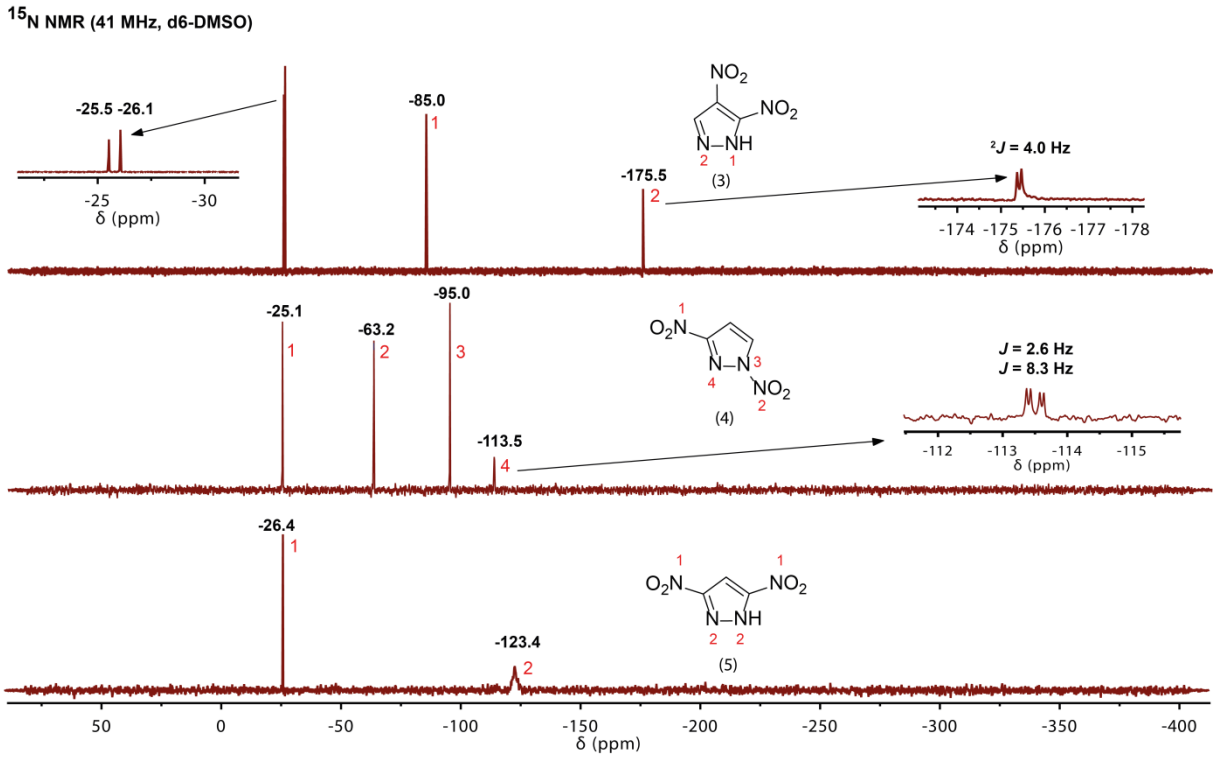

Figure 3.S5. ^{15}N NMR spectra of compounds **3**, **4** and **5**.

3.6.5 TGA spectra of 3 and 5

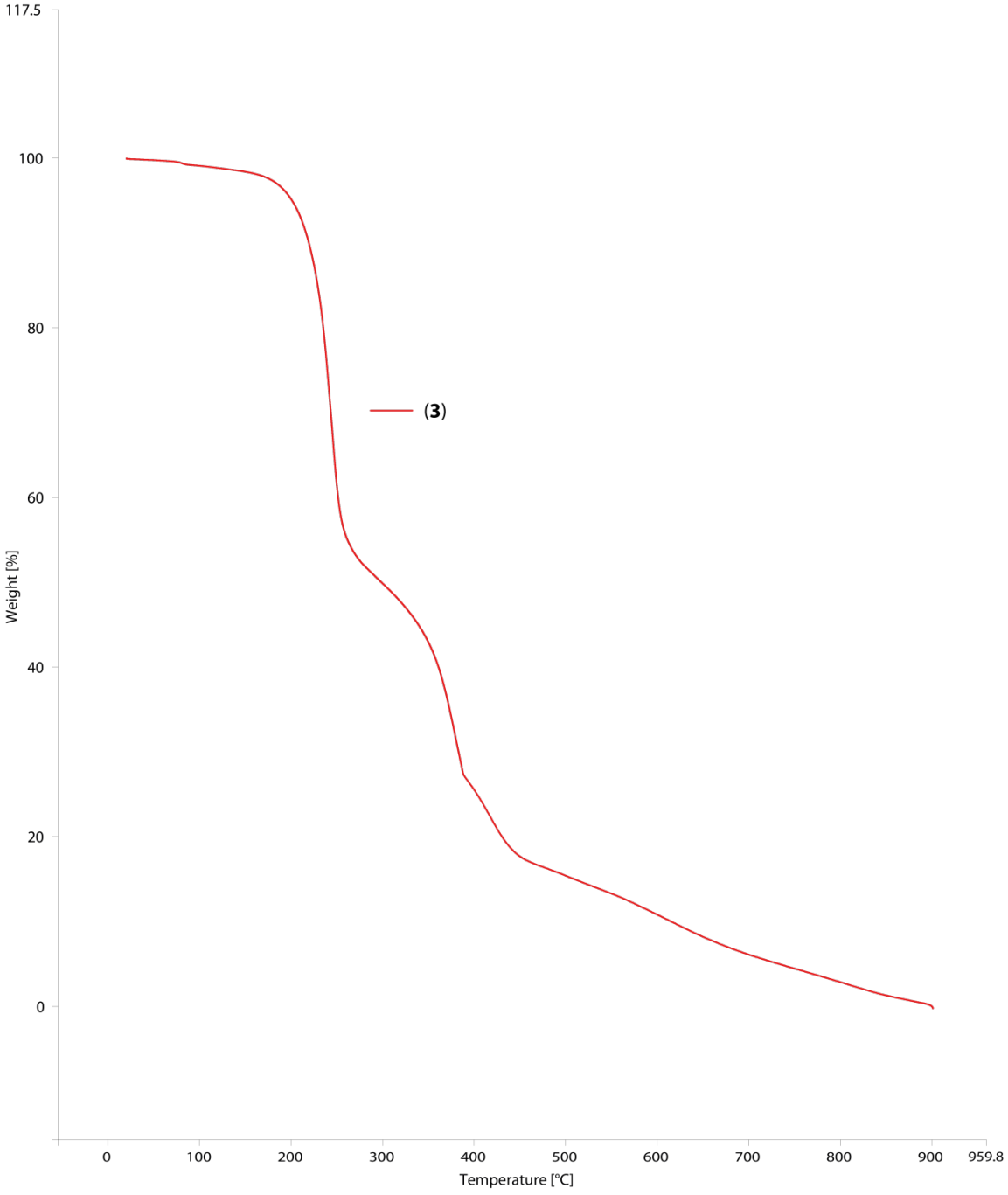

Figure 3.S6. TGA spectrum of 3,4-dinitropyrazole (**3**).

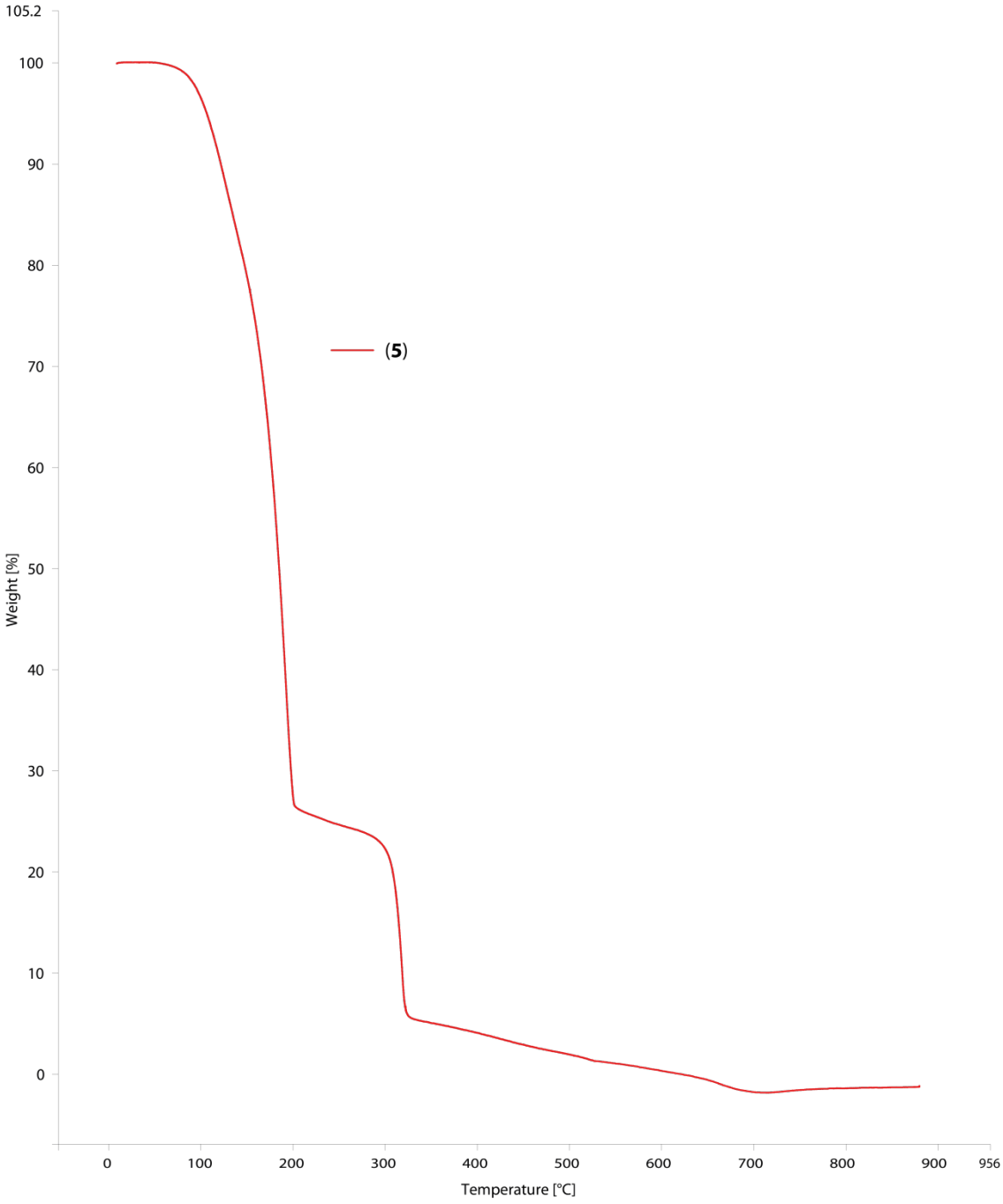

Figure 3.S7. TGA spectrum of 3,5-dinitropyrazole (**5**).

3.6.6 References

[S1] *CrysAlisPro*, Oxford Diffraction Ltd., version 171.33.41, **2009**.

[S2] *SIR-92*, *A program for crystal structure solution*: A. Altomare, G. Cascarano, C. Giacovazzo, A. Guagliardi, *J. Appl. Crystallogr.* **1993**, *26*, 343.

[S3] a) A. Altomare, G. Cascarano, C. Giacovazzo, A. Guagliardi, A. G. G. Moliterni, M. C. Burla, G. Polidori, M. Camalli, R. Spagna, *SIR97*, **1997**; b) A. Altomare, M. C. Burla, M. Camalli, G. L. Cascarano, C. Giacovazzo, A. Guagliardi, A. G. G. Moliterni, G. Polidori, R. Spagna, *J. Appl. Crystallogr.* **1999**, *32*, 115–119.

[S4] a) G. M. Sheldrick, *SHELX-97*, University of Göttingen, Göttingen, Germany, **1997**; b) G. M. Sheldrick, *Acta Crystallogr., Sect. A* **2008**, *64*, 112–122.

[S5] A. L. Spek, *PLATON*, *A Multipurpose Crystallographic Tool*, Utrecht University, The Netherlands, **1999**.

[S6] *SCALE3 ABSPACK – An Oxford Diffraction program* (1.0.4, gui: 1.0.3), Oxford Diffraction Ltd., **2005**.

[S7] *APEX3*. Bruker AXS Inc., Madison, Wisconsin, USA.

[S8] M. J. Frisch, G. W. Trucks, H. B. Schlegel, G. E. Scuseria, M. A. Robb, J. R. Cheeseman, G. Scalmani, V. Barone, B. Mennucci, G. A. Petersson, H. Nakatsuji, M. Caricato, X. Li, H.P. Hratchian, A. F. Izmaylov, J. Bloino, G. Zheng, J. L. Sonnenberg, M. Hada, M. Ehara, K. Toyota, R. Fukuda, J. Hasegawa, M. Ishida, T. Nakajima, Y. Honda, O. Kitao, H. Nakai, T. Vreven, J. A. Montgomery, Jr., J. E. Peralta, F. Ogliaro, M. Bearpark, J. J. Heyd, E. Brothers, K. N. Kudin, V. N. Staroverov, R. Kobayashi, J. Normand, K. Raghavachari, A. Rendell, J. C. Burant, S. S. Iyengar, J. Tomasi, M. Cossi, N. Rega, J. M. Millam, M. Klene, J. E. Knox, J. B. Cross, V. Bakken, C. Adamo, J. Jaramillo, R. Gomperts, R. E. Stratmann, O. Yazyev, A. J. Austin, R. Cammi, C. Pomelli, J. W. Ochterski, R. L. Martin, K. Morokuma, V. G. Zakrzewski, G. A. Voth, P. Salvador, J. J. Dannenberg, S. Dapprich, A. D. Daniels, O. Farkas, J.B. Foresman, J. V. Ortiz, J. Cioslowski, D. J. Fox, Gaussian 09 A.02, Gaussian, Inc., Wallingford, CT, USA, **2009**.

[S9] a) J. W. Ochterski, G. A. Petersson, and J. A. Montgomery Jr., *J. Chem. Phys.* **1996**, *104*, 2598–2619; b) J. A. Montgomery Jr., M. J. Frisch, J. W. Ochterski G. A. Petersson, *J. Chem. Phys.* **2000**, *112*, 6532–6542.

[S10] a) L. A. Curtiss, K. Raghavachari, P. C. Redfern, J. A. Pople, *J. Chem. Phys.* **1997**, *106*, 1063–1079; b) E. F. C. Byrd, B. M. Rice, *J. Phys. Chem*. A **2006**, *110*, 1005–1013; c) B. M. Rice, S. V. Pai, J. Hare, *Comb. Flame* **1999**, *118*, 445–458.

[S11] P. J. Lindstrom, W. G. Mallard (Editors), NIST Standard Reference Database Number 69, http://webbook.nist.gov/chemistry/ (accessed June **2011**).

[S12] M. S. Westwell, M. S. Searle, D. J. Wales, D. H. Williams, *J. Am. Chem. Soc*. **1995**, *117*, 5013–5015; b) F. Trouton, *Philos. Mag*. **1884**, *18*, 54–57.

[S13] a) H. D. B. Jenkins, H. K. Roobottom, J. Passmore, L. Glasser, *Inorg. Chem.* **1999,** *38,* 3609–3620; b) H. D. B. Jenkins, D. Tudela, L. Glasser, *Inorg. Chem.* **2002**, *41*, 2364–2367.

[S14] NATO standardization agreement (STANAG) on explosives, *impact sensitivity tests*, no. 4489, 1st ed., Sept. 17, **1999**.

[S15] WIWEB-Standardarbeitsanweisung 4-5.1.02, Ermittlung der Explosionsgefährlichkeit, hier der Schlagempfindlichkeit mit dem Fallhammer, Nov. 8, **2002**.

[S16] http://www.bam.de

[S17] NATO standardization agreement (STANAG) on explosive, *friction sensitivity tests*, no. 4487, 1st ed., Aug. 22, **2002**.

[S18] WIWEB-Standardarbeitsanweisung 4-5.1.03, Ermittlung der Explosionsgefährlichkeit oder der Reibeempfindlichkeit mit dem Reibeapparat, Nov. 8, **2002**.

[S19] Impact: insensitive > 40 J, less sensitive ≥ 35 J, sensitive ≥ 4 J, very sensitive ≤ 3 J; Friction: insensitive > 360 N, less sensitive = 360 N, sensitive < 360 N and > 80 N, very sensitive ≤ 80 N, extremely sensitive ≤ 10 N, According to: *Recommendations on the Transport of Dangerous Goods, Manual of Tests and Criteria*, 4th edition, United Nations, New York-Geneva, **1999**.

[S20] http://www.ozm.cz

[S21] R. Hüttel, F. Büchele, P. Jochum, *Chem. Ber*. **1955**, *88*, 1577–1585.

[S22] J. W. A. M. Janssen, H. J. Koeners, C. G. Kruse, C. L. Habrakern, *J. Org. Chem*. **1973**, *38*, 1777–1782.

4 Improving the Energetic Properties of Dinitropyrazoles by Utilization of Current Concepts

Marc F. Bölter, Thomas M. Klapötke, Tessa Kustermann, Tobias Lenz and Jörg Stierstorfer

as published in

Eur. J. Inorg. Chem. **2018**, 4125–4132 (DOI: 10.1002/ejic.201800781)

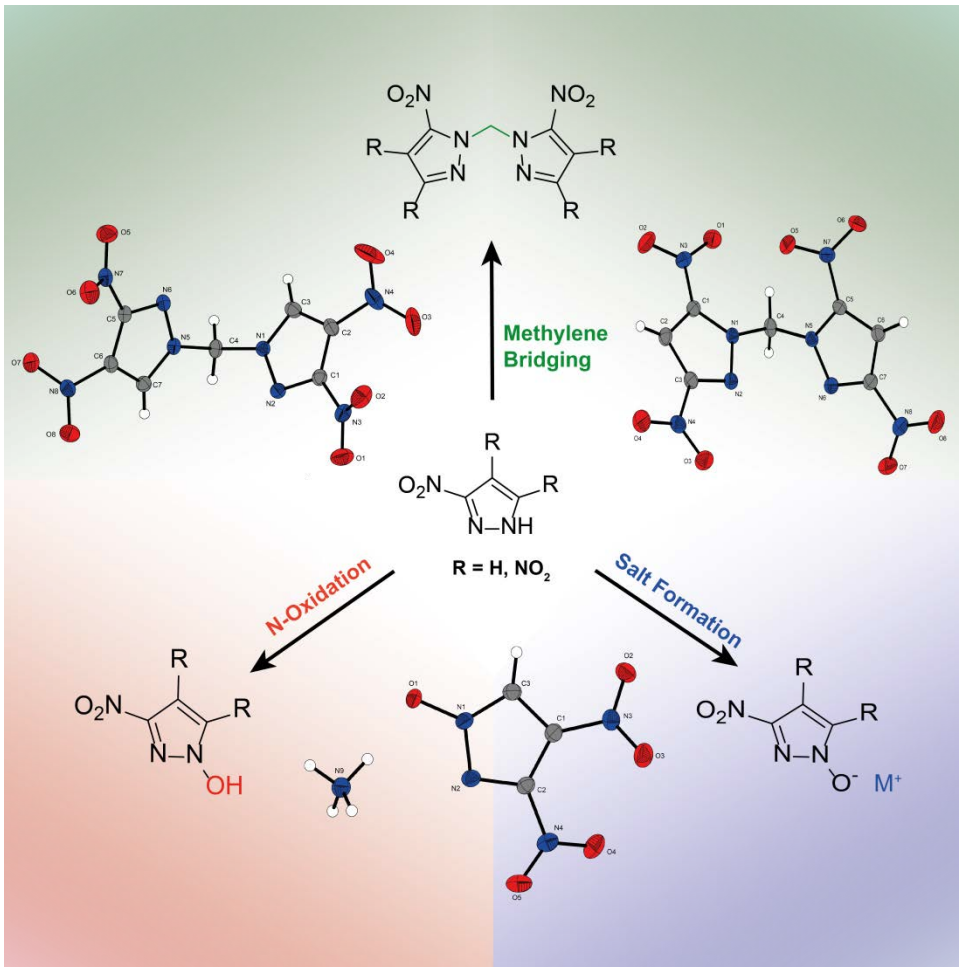

Abstract: The synthesis of two different isomeric dinitropyrazole-*N*-oxides is described and compared to each other. 3,4-Dinitropyrazole-1*N*-oxide (**2**) and 3,5-dinitropyrazole-1*N*-oxide (**4**) were used and four different nitrogen-rich salts were synthesized in order to enhance performance and sensitivity values. Further, two methylene bridged isomeric dinitropyrazoles were synthesized using diiodomethane. The obtained compounds were characterized using low temperature single crystal X-ray diffraction, IR spectroscopy, multinuclear NMR spectroscopy, mass spectrometry, elemental analysis and DSC measurements. The bridged compounds show a high thermal stability ($T_{dec.}$: 319 °C and 330 °C) whereas the ionic compounds have lower values ($T_{dec.}$: 131 °C–266 °C). Further, the sensitivity values toward impact, friction and electrostatic discharge were determined according to standard methods. Their sensitivity values lie in the range of **5** to 40 J for impact and 216 to 360 N for friction. Adapted from recalculated X-ray densities and calculated heats of formation the energetic performances were computed using the EXPLO5 code and support the high energetic character of the title compounds. The values (V_D: 7909–8279 m s^{-1}; p_{CJ}: 242–282 kbar) of the salts and bridged pyrazoles (V_D: 7966 and 8140 m s^{-1}; p_{CJ}: 263 and 280 kbar) were compared to RDX.

4.1 Introduction

The research of energetic materials currently attracts attention due to their broad application in both, the military and the civilian area [1]. Depending on their application, different requirements are needed such as good thermal stabilities for use in the mining and fracking industry or the application in aeronautics.[2] Nitrated pyrazoles are an interesting class in the research of new energetic materials due to their good thermal stability or the usage as melt-cast explosives[3]. Further they easily can be synthesized by nitration and rearrangement reactions.[4] One example for a melt-castable explosive is the already characterized 3,4-dinitro-1*H*-pyrazole (3,4-DNP, $T_{melt.}$ = 87, $T_{dec.}$ = 276 °C) that could already replace TNT as melt-cast explosives in compositions such as Composition B (RDX/TNT).[5]

The design of new nitrated pyrazole derivatives is an ongoing progress and many remarkable compounds were synthesized. The main concept for functionalization is to get rid of the acidic proton of the pyrazole ring which could cause compatibility problems. Various possibilities are known such as salt formation[6], methylation[7], *N*-functionalization[3, 8], azo bridging[9], amination[10], *N*-oxidation[11], ethylene[12] or methylene[1b] bridging (Figure 4.1).

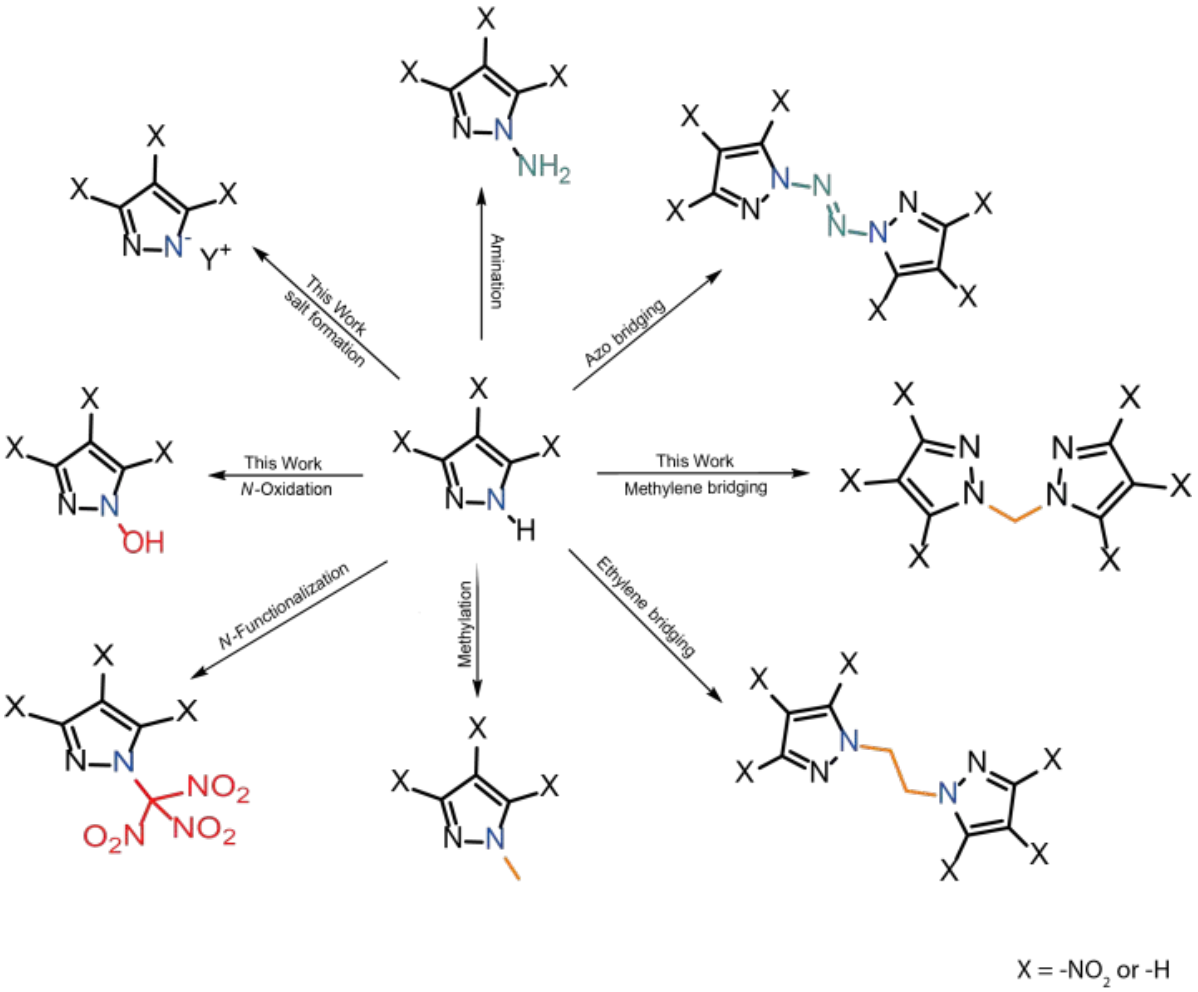

Figure 4.1. Functionalization of nitrated pyrazoles by detaching the acidic pyrazole proton.

Salt formation using nitrogen-rich cations generally improves the thermal stability and in some cases also the stability toward external stimuli caused by hydrogen bonding interactions.[13] *N*-functionalization such as the introduction of a trinitromethyl group to the nitrogen atom of 3,4-DNP and 3,5-DNP ($T_{dec.}$ = 141, 143 °C, V_D = 8668, 8733 m s^{-1}) or reacting bromonitromethane with trinitropyrazole (TNP) mainly increase the oxygen balance (OB) and the density, whereas these compounds can be classified as a high energetic density oxidizer (HEDO) due to their high oxygen content.[8, 14]

New pyrazole derivatives could further be synthesized by linking azoles via a *N,N´*-alkyl-bridge.[15] Examples are linked nitroamino or azido substituted nitropyrazoles with nitroimino-tetrazoles via an *N,N'*-ethylene-bridge to get thermal sensitive but powerful explosives ($T_{dec.}$ = 89–137°C, D = 8659–8804 m s^{-1}).[15b] Decreasing the carbon amount leads to *N,N'*-methylene-bridged compounds such as bispyrazolylmethanes, which were firstly described by Fischer *et al.*.

The hexanitro bridged pyrazole shows the highest detonation velocity (V_D = 9304 m s^{-1}) and a good thermal stability (T_{dec} = 205°C) and can therefore be compared to hexanitrohexaazaisowurtzitane (CL-20).[16]

Another concept is the introduction of *N*-oxides in tetrazoles, triazoles or pyrazoles which results in higher energetic performances due to a higher oxygen balance, as well as the density and hence the detonation parameters. [11b, 17] This class of compounds can easily be synthesized by using either Oxone® or hypofluorous acid (HOF).[18] Therefore, the *N*-oxide of TNP and some nitrogen-rich salts thereof were synthesized by using Oxone® and a corresponding base and some showed good properties as HEDMs (D = 8175–8676 m s^{-1}) with acceptable decomposition temperatures (T_{dec} = 118–186 °C).[19] Nevertheless the TNP oxide is a liquid and shows very high sensitivity values (IS: 1 J).[19]

We now report about the implementation of three of the concepts mentioned before using two isomeric dinitropyrazoles. Therefore, the literature known *N*-oxides of 3,4-DNP and 3,5-DNP were synthesized by a slightly different method increasing the yield. Further, their energetic salts were obtained and intensively characterized to compare the properties of these isomers.[11a] The literature mentioned bisdinitropyrazole-methanes[16b] (**1**, **3**) were synthesized by an easier method and also intensively characterized.

4.2 Results and Discussion

4.2.1 Synthesis

The synthesis of **2** (3,4-DNPO) and **4** (3,4-DNPO) is accomplished via *N*-oxidation of 3,4-DNP and 3,5-DNP using Oxone® instead of $KHSO_5$ in water holding the pH value close to their pK_a values (3,4-DNP: 5.14; 3,5-DNP: 3.14).[11a] The highest yields could be obtained for keeping the pH value at 6–8 (**2**) or 3–5 (**4**) by a phosphate buffer (NaH_2PO_4/NaOH) system (Scheme 4.1). Compounds **2** and **4** were obtained by extracting with diethyl ether and further purification with sodium acetate solution due its stronger acidity than the starting material. Another purification method is the better solubility of the oxides (**2**, **4**) in ice cold water.

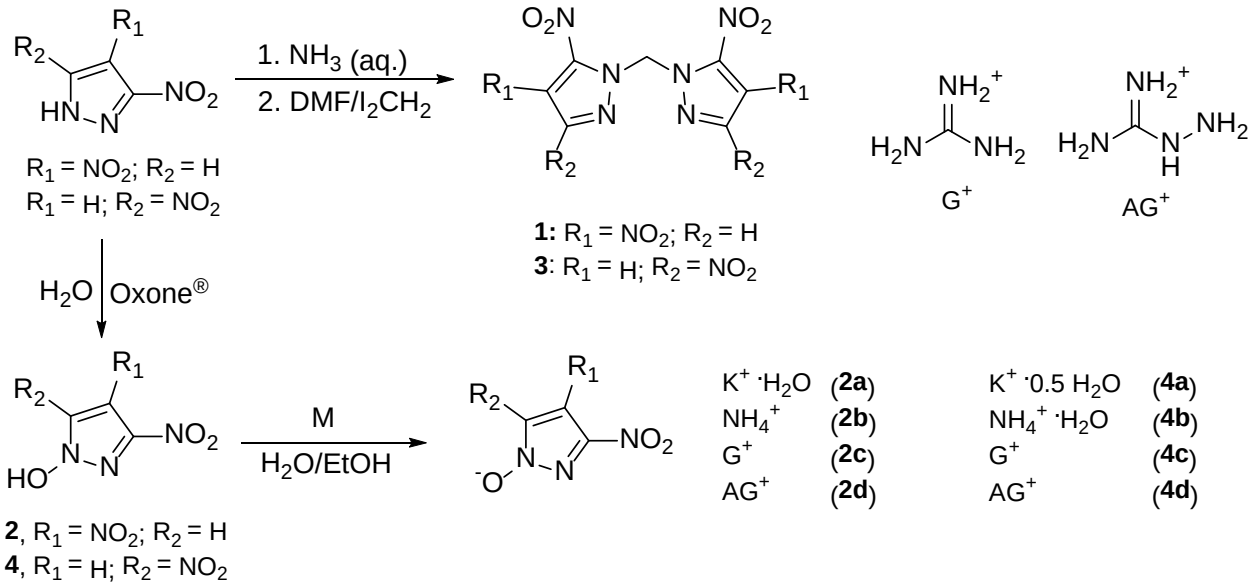

Scheme 4.1. Synthesis of bis-(3,5-dinitro-pyrazol-1-yl)methane (**1**), bis-(3,4-dinitro-pyrazol-1-yl)methane (**3**), 3,4-dinitropyrazol-1-oxide (**2**) and 3,5-dinitropyrazol-1-oxide (**4**) as well as the ionic derivatives of **2** and **4**.

The energetic salts **2a**–**2d** and **4a**–**4d** were obtained by deprotonation of the neutral compounds **2** and **4** in water/ethanol mixture by adding the corresponding bases. The mixtures were heated until everything was dissolved and left for crystallization to obtain the potassium (**2a, 4a**), ammonium (**2b, 4b**), guanidinium (**2c, 4c**) and aminoguanidinium (**2d, 4d**) salts. Further, the ammonium salts of 3,4-DNP and 3,5-DNP were synthesized in order to dissolve them in DMF and treating them with diidomethane (I_2CH_2) to get the isomeric methylene bridged compounds (**1, 3**).

4.2.2 Crystal Structures

In this work the crystal structures of compounds (**1**, **2**, **2a**–**2d**, **3**, **4a**–**4d**) were obtained by recrystallization in water/ethanol mixtures. The crystal structures of the water/ethanol containing compounds (**2**, **2a**, **4a** and **4b**) can be found in the supporting information. Further, selected parameters and data from the low temperature X-ray data collection and refinements are also given in the supporting information. Further information regarding the crystal-structure determinations have been deposited with the Cambridge Crystallographic Data Centre as supplementary publication Nos. 1836555 (**1**), 1836554 (**2·H₂O**), 1836556 (**2a·H₂O**), 1836562 (**2b**), 1836559 (**2c**), 1836558 (**2d**), 1836561 (**3**), 1836563 (**4a·EtOH**), 1836560 (**4b·H₂O**), 1836553 (**4c**) and 1836557 (**4d**).

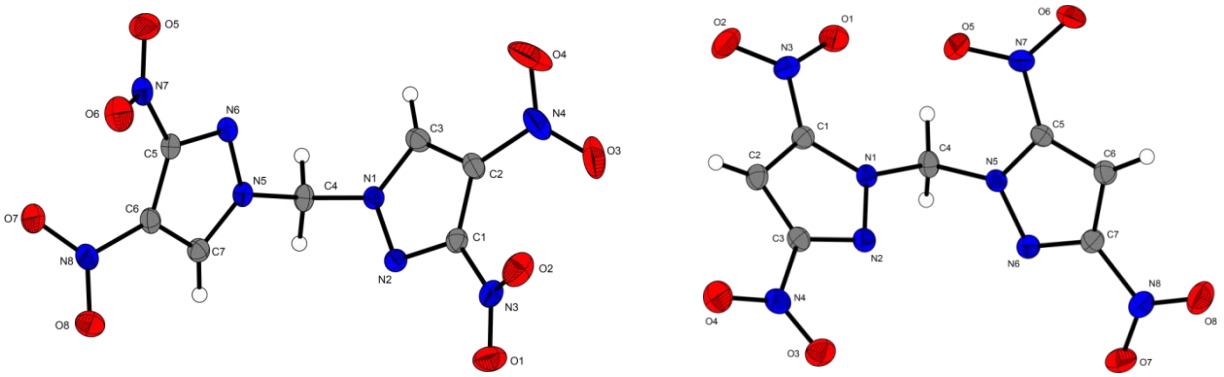

Figure 4.2. Molecular unit of **1** (left) and **3** (right). Ellipsoids are drawn at the 50% probability level.

Compounds **1** and **3** crystallize in the space groups *Cc* and $P2_12_12_1$ with densities of 1.799 (@173°C) and 1.756 g cm^{-3} (@173°C). The molecular units are depicted in Figure 4.2. The methylene bridged carbon atoms (N1–C4–N5) have similar bond angles of 110.43(19)° and 110.77(16)°. The pyrazole rings are arranged different toward the bridging C atom. For compound **1** the pyrazoles are ordered inversion symmetrically like and mirror-symmetrically for compound **3**. The nitro groups of **1** are twisted out of the planar pyrazole ring with torsion angle of O5–N7–C5–C6 = –153.4(3)°, O8–N8–C6–C7 = 32.7(4)°, O4–N4–C2–C3 = 28.1(5) and O2–N3–C1–C2 = 30.5(4). Compared to compound **1** the nitro groups of **3** are less twisted toward the plane pyrazole with angles of O1–N3–C1–C2 = 179.0(2)°, O8–N8–C7–C6 = 1.3(3)°, O4–N4–C3–C2 = –1.5(3)° and O5-N7-C5-C6 = –155.0(19)°. The bridging C–N bond lengths are very similar with values of 1.458(4) Å (N1–C4) and 1.451(4) Å (N5–C4) for **1** and 1.454(3) Å (N5–C4) and 1.463(2) Å (N1–C4) for **3**.

Compound **2b** crystallizes in the monoclinic space group $P2_1/n$ with a density of 1.730 g cm^{-3} at 100 K. The molecular unit is depicted in Figure 4.3. The bond length of the oxygen and the pyrazole nitrogen (O1–N1 = 1.332 Å) is the longest of all structures and similar to other azole oxides.[17c, 17d] The torsion angles (e.g. O1–N1–N2–C2, N3–C1–C2–N4) of the pyrazole show the plane arrangement. The nitro groups are twisted with 8.6° (N3–C1–C2–N4) against them self and with 31.0(5)° (O2–N3–C1–C3) and –21.5(5)° (O4–N4–C2–C1) to the planar ring system. Various hydrogen bonds between the pyrazole and the ammonium protons are build up, which explains the relative high decomposition temperature ($T_{dec.}$: 197°C).

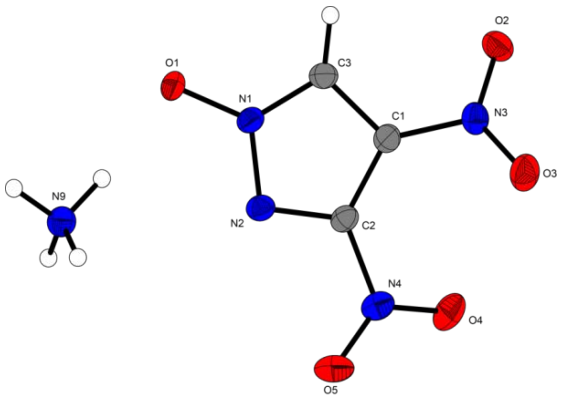

Figure 4.3. Molecular unit of **2b**. Ellipsoids are drawn at the 50% probability level.

Figures 4.4 and 4.5 depict the molecular units of the guanidinium derivatives of both isomers (**2c**, **2d**, **4c** and **4d**). They crystallize in the common space groups *P*-1 **(2c, 4c)** and $P2_1/n$ (**2d, 4d**). The densities lie between 1.664 (**2d**, 203 K) and 1.746 (**2c**, 143 K) g cm^{-3}.

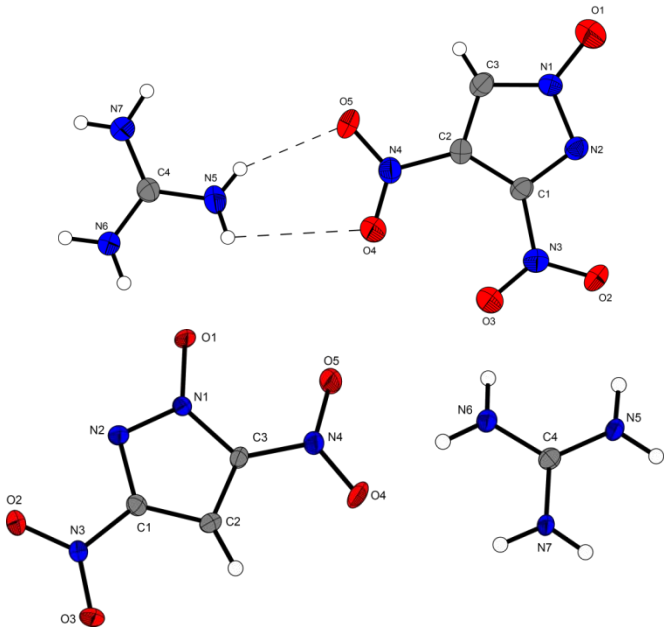

Figure 4.4. Molecular unit of **2c** (top) and **4c** (bottom). Ellipsoids are drawn at the 50% probability level.

All guanidinium and aminoguanidinium salts are dominated by strong hydrogen bonding resulting in a good thermal stability with exception of **4d** ($T_{dec.}$: 131 °C) and show an almost planar pyrazole ring system. Further, the oxygen atom attached to the pyrazole N atom of all four salts is located in the planar pyrazole heterocycle. The torsion angles of O1–N1–N2–C1 of **2c** (–177.2(3)) and **4c** (–178.47(19)) show the oxide is only slightly twisted toward the plane pyrazole. The nitro groups are

minimal twisted toward the pyrazole ring with torsions angles of O2–N3–C1–N2 = 4.1°(3) and O4–N4–C2–C1 = 5.7°(5) for **2c** and O2–N3–C1–N2 = –4.1°(3) and O4–N4–C3–C2 = 1.2°(4) for **4c**.

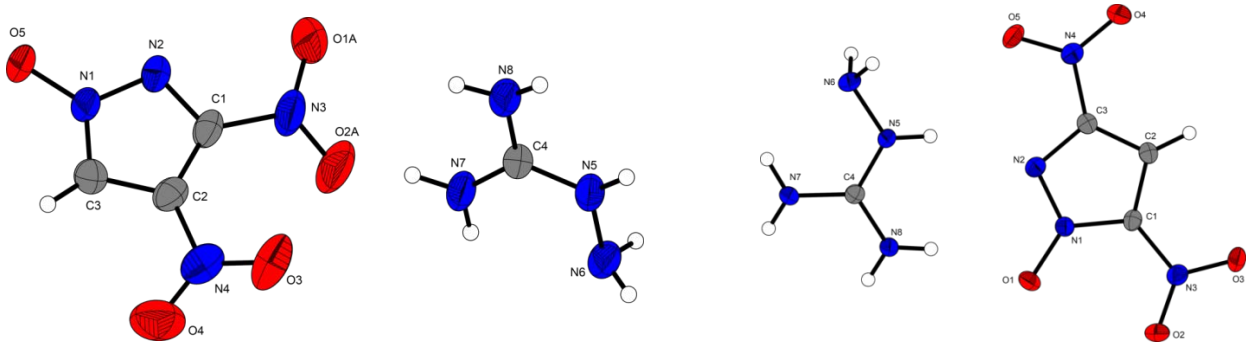

Figure 4.5. Molecular unit of **2d** (left) and **4d** (right). Ellipsoids are drawn at the 50% probability level.

The aminoguanidinium salts **2d** and **4d** show that the nitro groups of **2d** are twisted stronger out of the ring with torsion angles of O2A–N3–C1–N2 = –147.7(4)° and O4–N4–C2–C1 = –165.8(2)° compared to **4d** (–4.6(3) and 3.5(3)) due to its more sterical hindrance of the nearby nitro groups. The N–N bond length between N5–N6 of both aminoguanidinium cations show values close to an N–N single bond (**2d**: 1.413(2); **4d**: 1.408(3)).

4.2.3 Spectroscopy

All compounds are characterized by ^{1}H, ^{13}C NMR spectroscopy, elemental analysis, mass spectrometry and IR spectroscopy. The methylene bridged compounds **1** and **3** were further characterized by ^{15}N NMR spectroscopy. Both compounds **2** and **4** show one resonance in the ^{1}H spectrum (9.06 and 7.77 ppm) and three in the ^{13}C spectrum (**2**: 140.6, 126.0 and 124.4 ppm; **4**: 142.8, 138.6, 99.9 ppm). The OH protons were not observed due to the high acidity of both compounds. The IR spectra show several main absorption bands for OH (**2**: 2998 cm^{-1}; **4**: 2964 cm^{-1}), the nitro group (**2**: 1541/1354 cm^{-1}; **4**: 1528/1329 cm^{-1}) or CH stretching vibration (**2**: 3131 cm^{-1}; **4**: 3148 cm^{-1}). In the ^{1}H NMR spectra of compounds **1** and **3** two resonances are observed. The signals at 9.44 (**1**) and 8.31 (**3**) ppm can be assigned to the pyrazole hydrogen and the signals at 6.75 (**1**) and 7.42 (**3**) ppm to the bridged CH_2 group. In the IR spectra the main absorption bands 2998/2933 (C-H), 1544/1523 (NO_2-asym.) and 1357/1341 cm^{-1} (NO_2-sym.) are assigned to **1** and **3**. Measured mass spectra confirmed the synthesized compounds **1**, **2**, **3** and **4** as well.

In the ^{1}H NMR spectra of the salts (**2a**–**d**) the hydrogen signal of pyrazole is observed at 7.72–7.89 ppm and for **4a**–**d** at 7.44–7.74 ppm. Further, one proton resonance for the guanidinium (**2c**, **4c**) and three resonances for the aminoguanidinium (**2d**, **4d**) salts were observed in the ^{1}H NMR spectra. Three signals for the carbon atoms of the pyrazoles are found in the ^{13}C spectra between 98.6 and 159.7 ppm with an additional carbon signal for the guanidinium derivatives.

The absorption bands for nitro groups of salts **2a**–**d** and **4a**–**d** were found in the region from 1522–1564 cm^{-1} (asymmetrical) and 1320–1380 cm^{-1} (symetrical). Further the absorption bands of the primary amines were found for the nitrogen-rich cations (**2b**–**2d** and **4b**–**4d**) in the range from 3147 to 3499 cm^{-1}.

In addition to ^{1}H and ^{13}C NMR spectra, ^{15}N NMR spectra were recorded for the characterization of the methylene bridged compounds **1** and **3**. Both spectra show comparatively shifts for both isomers (Figure 4.6 and 4.7).

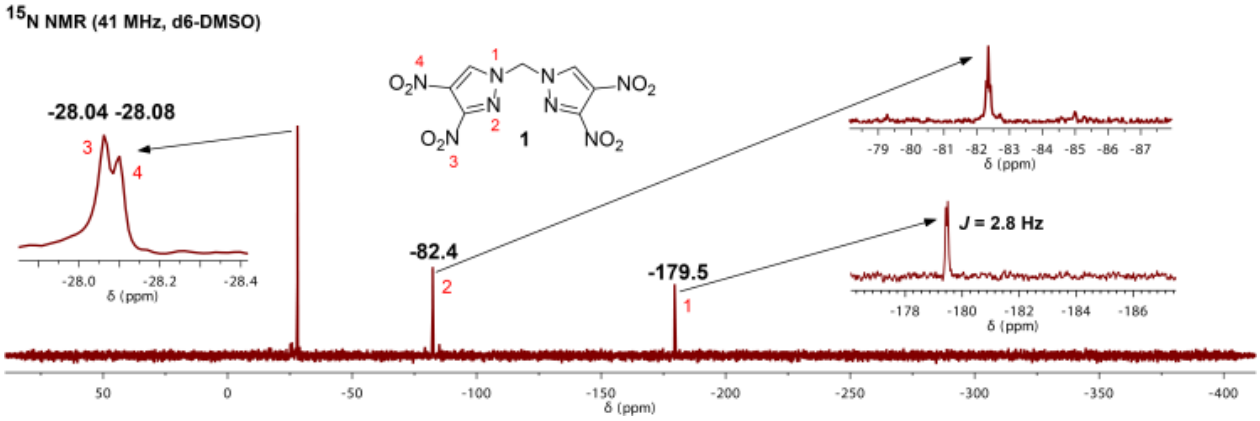

Figure 4.6. Proton coupled ^{15}N NMR spectra of compound **1**.

As shown in figure 6 the ^{15}N NMR spectrum shows four signals ranging from –28.04 to –179.5 ppm. The signals at –28.04 and –28.04 ppm can be assigned to the nitro groups, whereas nitrogen atom 4 belongs to the signal –28.08 due to its broader proton coupling. The resonance at –179.5 ppm (doublet) belongs to the bridged nitrogen atom and the one at –82.4 ppm (triplett) to the other pyrazole ring nitrogen because of the different coupling.

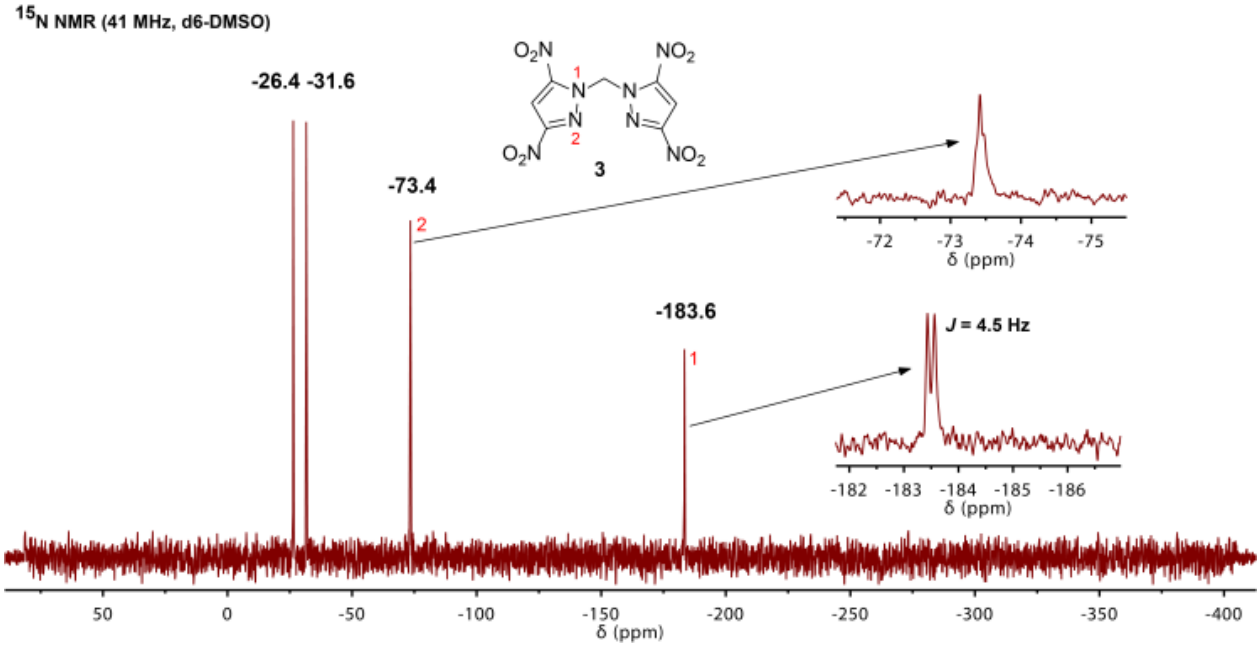

Figure 4.7. Proton coupled ^{15}N NMR spectra of compound **3**.

Compound **3** shows also four signals for the nitrogen atoms in the ^{15}N NMR spectrum (Figure 4.7). Nevertheless the coupling of both nitro groups is not visible for which reason the nitro groups cannot be assigned to the resonances (–26.4 and –31.6 ppm). The signal for the bridging nitrogen atom has a shift of –183.6 ppm (doublet) and the remaining pyrazole nitrogen at –73.4 ppm (triplett).

4.2.4 Thermal, Analysis, Sensitivities, Physicochemical and Energetic Properties

The thermal stabilities of all compounds were determined by DSC measurements (heating rate of 5 °C min^{-1}). Both methylene bridged compounds **1** and **3** show melting (**1**: 156 °C; **3**: 191 °C) and decomposition (**1**: 319 °C; **3**: 330 °C) behavior with similar values (Table 4.1). The decomposition temperatures are rather high and higher than the value of RDX or other methylene bridged pyrazoles (3,4,5-trinitropyrazole: 205 °C; 4-amino-3,5-dinitropyrazole: 310 °C)[1b]. Regarding the salts (**2a–d**, **4a–d**) the aminoguanidinium salt **2d** is the only compound that melts, whereas all other decompose at temperatures between 131 °C (**4d**) and 266 °C (**4c**). All salts of compound **4** have (with exception of **4d**) a higher thermal stability than the salts of **2** and RDX.

Compound **1** is with a value of 25 J slightly more sensitive than **3** (35 J) toward impact, whereas both are classified as not sensitive regarding their friction sensitivity values (>360 N). The impact sensitivity values of the salts (**2a–d** and **4a–d**) range from 5 J (**2a**) to 40 J (**4c**). Classified as sensitive toward impact are both potassium salts with values of 5 J (**2a,**·H_2O) and 6 J (**4a,** 0.5 H_2O), although both contain crystal water.[20] Comparing the salts of both isomers the ones of 3,4-DNP are more sensitive than the salts of 3,5-DNP. Furthermore, all salts are almost insensitive to friction and electrostatic discharge. Only compounds **2a** (216 N), **4a** (240 N) and **4b** (288 N) are slightly sensitive toward friction. Compared to RDX, only the potassium salts (**2a**, **4a**) are more sensitive toward impact, whereas all salts have lower friction and ESD values. The densities of the bridged compounds are (values of 1.76 and 1.72 g cm^{-3}) similar. Comparing the densities of the salts the values lie between 1.62 g cm^{-3} and 1.955 g cm^{-3} with the potassium salt (**2a**) as the highest. The calculated heats of formation ($\Delta_f H$) of the water containing compounds **2a** and **4b** are negative whereas all others are positive with values between 7 (**4c**) and 302 (**1**) kJ mol^{-1}. The isomers **1** and **3** have higher values for $\Delta_f H$ (301.7 and 266.4 kJ mol^{-1}) than RDX. Due to the similar $\Delta_f H$ also the detonation velocity and pressure are similar and range from 7966–8140 m s^{-1} and 263–280 kbar, respectively. Comparing the energetic parameters of the salts, the V_D vary from 7909 to 8279 m s^{-3} and the pressure from 242 (**4c**) to 269 (**2a**) kbar.

From the view of the functionalization strategies the bridged compounds show a higher thermal stability, higher heats of formation and an increasing of the sensitivity values compared to dinitropyrazole. The salts likewise show a higher thermal stability, higher density and better energetic properties than the similar salts of the dinitropyrazole isomers. Besides, the salts show a higher thermal stability as the salts of 3,4,5-trinitropyrazole-1-olate and only a slightly lower energetic performance.[19]

Table 4.1. Physicochemical properties and detonation parameters of **1**, **3**, **2a–2d** and **4a–4d** compared to RDX.

	1	**3**	**2a**	**2b**	**2c**	**2d**	**4a**	**4b**	**4c**	**4d**	**RDX**
Formula	$C_7H_4N_8O_8$	$C_7H_4N_8O_8$	$C_3HKN_4O_5 \cdot H_2O$	$C_3H_5N_5O_5$	$C_4H_7N_7O_5$	$C_4H_8N_8O_5$	$C_3HKN_4O_5 \cdot 0.5\ H_2O$	$C_3H_5N_5O_5 \cdot H_2O$	$C_4H_7N_7O_5$	$C_4H_8N_8O_5$	$C_3H_6N_6O_6$
FW [g mol^{-1}]	327.2	327.2	230.19	191.12	233.15	248.06	210.69	209.12	233.15	248.06	222.12
IS [J][a]	25	35	5	10	30	10	6	30	40	10	7.5
FS [N][b]	360	360	216	360	360	360	240	288	360	360	120
ESD [J][c]	1.5	1.0	0.7	1.5	1.5	1.5	n.d.	n.d.	n.d.	n.d.	0.20
N [%][d]	34.15	34.15	24.34	36.65	42.06	45.15	33.49	27.79	42.05	40.77	37.84
Ω [%][e]	–39.0	–39.0	–13.90	–29.30	–44.60	–45.13	–19.41	–26.77	–44.60	–45.12	–21.61
$T_{dec.}$ [°C][f]	319	330	197	167	180	169	229	224	266	131	205
T_{melt} [°C][f]	156	191				132					
ρ [g cm^{-3}] (298K)[g]	1.760	1.72	1.955	1.677	1.704	1.639	-	1.62	1.68	1.68	1.806
$\Delta_f H°$ [kJ mol^{-1}][h]	301.7	266.4	–391.7	68.7	27.0	144.9	-	–253.4	7.8	115.2	70.3
$\Delta_f U°$ [kJ kg^{-1}][i]	919.3	887.5	–1631.5	456.8	217.0	688.6	-	–1105.1	134.5	569.1	417.0
EXPLO5 V6.03 values:											
$-\Delta_E U°$ [kJ kg^{-1}][j]	5254	5119	4636	5482	4473	4738	-	4670	4388	4643	5845
T_E [K][k]	3895	3856	3182	3752	3119	3263	-	3242	3098	3186	3810
p_{CJ} [kbar][l]	280	263	269	282	251	247	-	244	242	257	345
V_D [m s^{-1}][m]	8140	7966	7920	8279	8063	8021	-	7909	7935	8159	8861
V_0 [L kg^{-1}][n]	432	441	399	795	804	835	-	468	459	458	785
Toxicity:											
EC_{50} (15 min) [g L^{-1}][o]	-	-	0.27	-	-	-	0.70	-	-	-	0.327 [21]
EC_{50} (30 min) [g L^{-1}] [o]	-	-	0.20	-	-	-	0.43	-	-	-	0.239 [21]

[a] impact sensitivity (BAM drophammer, 1 of 6); [b] friction sensitivity (BAM friction tester, 1 of 6); [c] electrostatic discharge device (OZM); [d] nitrogen content; [e] oxygen balance; [f] decomposition and melting temperature from DSC (β = 5°C); [g] recalculated from low temperature X-ray densities ($\rho_{298K} = \rho_T / (1+\alpha_V(298\text{-}T_0)$; $\alpha_V = 1.5\ 10^{-4}\ K^{-1}$); [h] calculated (CBS-4M) heat of formation; [i] calculated energy of formation; [j] energy of explosion; [k] explosion temperature; [l] detonation pressure; [m] detonation velocity; [n] assuming only gaseous products; [o] Toxicity measurements to aquatic life using the luminescent marine bacterium *Vibrio fischeri*.

4.3 Conclusion

In conclusion we report on the synthesis of 3,4-DNP-oxide (**2**) and 3,5-DNP-oxide (**4**) by *N*-oxidation using Oxone® and a phosphate buffer system with higher yields (68%; 61%) than mentioned in literature. Energetic salts of both isomers (**2a–d**; **4a–d**) and methylene bridged compounds (**1**, **3**) were obtained and intensively characterized. Compounds **4a–d** have higher decomposition temperatures than **2a–d** with the exception of **4d** ($T_{dec.}$: 131 °C). The decomposition temperatures are in between 131 °C up to 266 °C with the potassium salt **4a** as the highest. The methylene bridged compounds **1** and **3** show a similar thermal behavior with melting and high decomposition temperatures (319 and 330 °C). The sensitivity values of the salts are in the range from 5 to 40 J for impact and 216 N to 360 N for friction. Both potassium salts indicate the highest sensitivity values (**2a**: 5 J, **4a**: 6 J). Compounds **1** and **3** have impact sensitivity values of 25 J and 35 J and both a friction sensitivity value of 360 N. Densities for the salts lie between 1.62 (**4b**) to 1.955 (**2a**) g cm^{-3}. The calculated detonation velocities (V_D) range from 7909 (**4b**) to 8279 m s^{-1} (**2b**) and the detonation pressure (p_{CJ}) from 242 (**4c**) to 282 kbar (**2b**) and are lower compared to the values of RDX. The main properties of water-free salts are depicted in Figure 4.8. The toxicity to *vibrio fischeri* was measured for both potassium salts due to their good water solubility. The EC_{50} value of compound **2a** is lower and of compound **4a** higher than that of RDX, which means that **2a** is more toxic and **4a** less toxic than RDX[21]. Based on the relative high decomposition temperatures, rather high detonation parameters and appropriate sensitivity values both potassium salts (**2a**, **4a**) and the bridged compounds (**1**, **3**) have capability as future energetic materials.

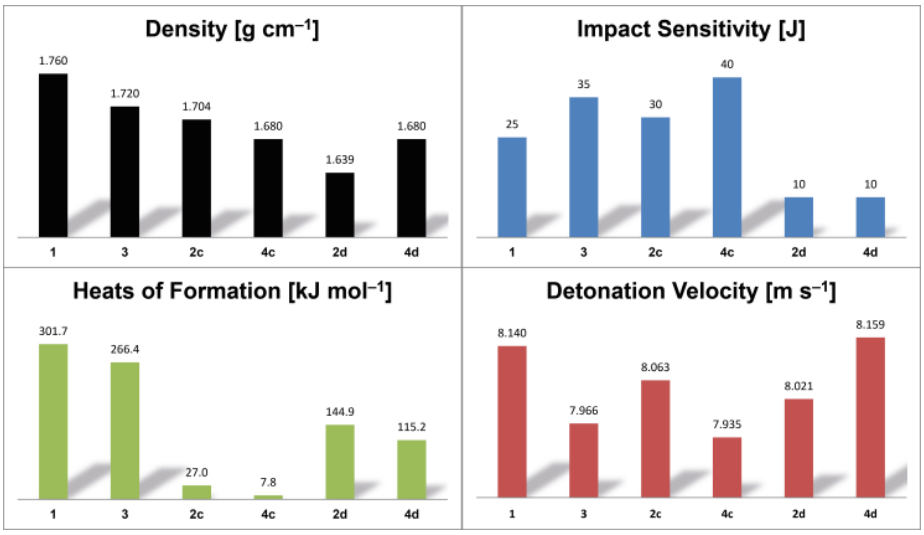

Figure 4.8. Overview of the densities, impact sensitivities, heat of formations and detonation velocities of water-free compounds **1**, **3**, **2c**, **2d**, **4c** and **4d**.

4.4 Experimental Section

The complete experimental procedures including the synthesis of salts can be found in the supporting information.

CAUTION! All investigated compounds are potentially explosive energetic materials, although no hazards were observed during preparation and handling these compounds. Nevertheless, this necessitates additional meticulous safety precautions (earthed equipment, Kevlar® gloves, Kevlar® sleeves, face shield, leather coat, and ear plugs).

Bis-(3,4-dinitro-1*H*-pyrazol-1-yl)methane (1): 3,4-Dinitro-1*H*-pyrazole[S22] (1.0 g, 6.2 mmol) was dissolved in water and aqueous ammonia solution (2 M, 3.2 mL, 6.2 mmol) was added. The mixture was stirred for 30 min and the solvent was removed in vacuum. The gained ammonium salt of 3,4-dinitro-1*H*-pyrazole (1.0 g, 5.71 mmol, 2.2 eq.) and diiodomethane (0.21 ml, 2.6 mmol, 1.0 eq.) were dissolved in DMF (15 ml). The solution was stirred overnight at 80 °C and afterwards poured on ice to obtain **1** after filtration (0.71 g, 2.16 mmol, 83 %).**^{1}H NMR** (400 MHz, DMSO *d6*): δ (ppm) = 9.44 (s, 2H, CH), 6.75 (s, 4H, CH_2); **^{13}C NMR** (101 MHz, DMSO *d6*): δ (ppm) = 147.9, 135.6, 127.0, 66.8; **^{15}N NMR** (41 MHz, DMSO *d6*): δ (ppm) = –28.1 (-NO_2), –28.1 (-NO_2), –82.4 (t, N), –179.5 (d, N_{bridge}); **IR** (ATR, rel. int.): $\tilde{\nu}$ (cm^{-1}) = 3124 (w), 3049(w), 2998 (w), 2161 (w), 2034 (w), 1544 (s), 1516 (s), 1462 (m), 1436 (m), 1357 (s), 1333 (s), 1281 (m), 1147 (m), 1119 (m), 1016 (w), 999 (w), 924 (w), 862 (m), 810 (s), 789 (m), 746 (s), 651 (m), 621 (w); **Elemental analysis:** calcd. (%) for $C_7H_4N_8O_8$ (327.20 g mol^{-1}): C 25.62, H 1.23, N 34.15; found: C 26.59, H 1.42, N 33.25; **Mass spectroscopy**: m/z (DEI) = 327.4 ($C_7H_4N_8O_8$); **DSC** (5°C min^{-1}): $T_{melt.}$ = 156°C, $T_{dec.}$ = 319°C.

3,4-Dinitropyrazol-1-oxide hydrate (2): 3,4-Dinitropyrazole[S22] (4.9 g, 31.0 mmol, 1.0 eq) was suspended in water (100 mL) and Oxone (65.3 g, 212.4 mmol, 6.9 eq) as well as basic buffer (NaH_2PO_4/2 M NaOH) was added alternately to hold the pH between 6-8. The solution was stirred at 55 C over 72 h, then sulfuric acid (50%, 100 mL) was added and the product was extracted with diethyl ether (3x 100mL). The combined organic layers were extracted with 5 % aqueous sodium acetate solution (3 x 100 mL). After acidification of the aqueous sodium acetate phase with hydrochloric acid (2 M) the product is isolated by extraction with diethyl ether (3x 100mL). The combined organic layers were dried over anhydrous magnesium sulfate, filtrated and the solvent was evaporated under reduced pressure to yield compound **2** (4.04 g, 21.1 mmol, 68 %) as yellowish crystals. **^{1}H NMR** (400MHz, DMSOd_6): δ (ppm) = 9.06 (s, 1H, CH); **^{13}C NMR** (101 MHz, DMSO d_6): δ (ppm) = 140.6, 126.0, 124.4; **IR** (ATR, rel. int.): $\tilde{\nu}$ (cm^{-1}) = 3565 (s), 3466 (s), 1710 (w), 1614 (m), 1541 (m), 1507 (s), 1464 (s), 1400 (s), 1354 (s), 1325 (s), 1270 (s), 1144 (s), 1117 (m),

1022 (m), 911 (s), 857 (s), 808 (m), 741 (m), 664 (m), 624 (m), 596 (m);); **Elemental analysis:** calcd. (%) for $C_3H_4N_4O_6$ (190.12 g mol^{-1}): C 18.76, H 2.10, N 29.17; found: C 18.96, H 2.16, N 28.27; **Mass spectroscopy**: m/z (FAB-) = 173.1 ($C_3HN_4O_5^-$); **DSC** (5°C min^{-1}): $T_{dec.}$ = 167°C; **Sensitivities** (grain size: < 500 μm): BAM impact: 35 J, BAM friction: 360 N, ESD: 1.0 J.

Bis-(3,5-dinitro-1*H*-pyrazol-1-yl)methane (3): 3,5-Dinitro-1*H*-pyrazole[S22] (1.0 g, 6.2 mmol) was dissolved in water and aqueous ammonia solution (2 M, 3.2 mL, 6.2 mmol) was added. The mixture was stirred for 30 min. and the solvent was removed in vacuum. The gained ammonium salt of 3,5-dinitro-1*H*-pyrazole (0.6 g, 3.43 mmol, 2.2 eq.) and diiodomethane (0.13 ml, 1.56 mmol, 1.1 eq.) were dissolved in DMF (15 ml). The solution was stirred overnight at 80 °C and afterwards poured on ice to obtain **3** after filtration (0.28 g, 0.85 mmol, 55 %). **^{1}H NMR** (400 MHz, DMSO *d6*): δ (ppm) = 8.31 (s, 2H, CH), 7.42 (s, 2H, CH_2); **^{13}C NMR** (101 MHz, DMSO *d6*): δ (ppm) = 153.2, 146.5, 103.5, 65.7; **IR** (ATR, rel. int.): $\tilde{\nu}$ (cm-1) = 3153 (w), 3093(w), 3013 (w), 2933 (w), 1563 (m), 1523 (s), 1463 (m), 1430 (w), 1343 (s), 1330 (s), 1273 (m), 1223 (m), 1143 (w), 1093 (m), 982 (m), 853 (m), 818 (m), 783 (m), 738 (s), 615 (w); **Elemental analysis:** calcd. (%) for $C_7H_4N_8O_8$ (327.20 g mol^{-1}): C 25.62, H 1.42, N 34.15; found: C 26.32, H 1.39, N 33.68; **Mass spectroscopy**: m/z (DEI) = 327.4 ($C_7H_4N_8O_8$); **DSC** (5°C min^{-1}): $T_{melt.}$ = 191°C, $T_{dec.}$ = 330°C; **Sensitivities** (grain size: < 500 μm): BAM impact: 35 J, BAM friction: 360 N, ESD: 1.0 J.

3,5-Dinitropyrazol-1-oxide hemihydrate (4): 3,5-Dinitropyrazole[S22] (6.3 g, 39.8 mmol, 1.0 eq) was suspended in water (100 mL) and Oxone (86.2 g, 280.0 mmol, 6.9 eq) as well as basic buffer (NaH_2PO_4/2 M NaOH) was added alternately to hold the pH between 3–5. The solution was stirred at 55 C over 72 h, then sulfuric acid (50 %, 100 mL) was added and the product was extracted with diethyl ether (3x 100mL). The ether phase was extracted with 5 % aqueous sodium acetate solution (3 x 100 mL). After acidification of the aqueous sodium acetate phase with hydrochloric acid (2 M) the product is isolated by extraction with diethyl ether (3x 100mL). The combined organic layers were dried over anhydrous magnesium sulfate, filtrated and the solvent was evaporated under reduced pressure to yield compound 4 (4.44 g, 24.3 mmol, 61 %) as colorless powder. **^{1}H NMR** (400MHz, DMSOd_6): δ (ppm) = 7.77 (s, 1H, CH); **^{13}C NMR** (101 MHz, DMSO d_6): δ (ppm) = 142.8, 138.6, 99.9; **IR** (ATR, rel. int.): $\tilde{\nu}$ (cm^{-1}) = 3215 (m), 3148 (m), 2964 (w), 2168 (w), 1692 (w), 1555 (m), 1528 (m), 1475 (m), 1445 (s), 1332 (s), 1202 (m), 1141 (m), 1083 (m), 1014 (m), 983 (s), 831 (s), 741 (s), 686 (s), 573 (m), 512 (m); **Elemental analysis:** calcd. (%) for $C_3H_3N_4O_{5.5}$ (183.08 g mol^{-1}): C 19.68, H 1.65, N 30.60; found: C 20.26, H 1.54, N 30.02; **Mass spectroscopy**: m/z (DEI) = 173.9 ($C_3HN_4O_5$); **DSC** (5°C min^{-1}): $T_{dec.}$ = 158°C; **Sensitivities** (grain size: < 500 μm): BAM impact: 35 J, BAM friction: 360 N, ESD: 1.0 J.

4.5 References

[1] a) J. P. Agrawal, R. Hodgson, *Organic Chemistry of Explosives*, Wiley, New York, **2007**; b) D. Fischer, J. L. Gottfried, T. M. Klapötke, K. Karaghiosoff, J. Stierstorfer, T. G. Witkowski, *Angew. Chem. Int. Ed.* **2016**, *55*, 16132–16135; c) G. Bélanger-Chabot, M. Rahm, R. Haiges, K. O. Christe, *Angew. Chem. Int. Ed.* **2015**, *127*, 11896–11900; d) Y. Tang, D. Kumar, J. M. Shreeve, *J. Am. Chem. Soc.* **2017**, *139*, 13684–13687.

[2] a) T. M. Klapötke, *Chemistry of High-Energy Materials*, 3rd ed., De Gruyter, Berlin, **2015**; b) J. P. Agrawal, *Propellants Explos. Pyrotech.* **2005**, *30*, 316–328.

[3] I. L. Dalinger, K. Y. Suponitsky, A. N. Pivkina, A. B. Sheremetev, *Propellants Explos., Pyrotech.* **2016**, *41*, 789–792.

[4] J. W. A. M. Janssen, H. J. Koeners, C. G. Kruse, C. L. Habrakern, *J. Org. Chem.* **1973**, *38*, 1777–1782.

[5] T. M. Klapötke, *Chemistry of high-energy materials, Vol. 3. ed.*, De Gruyter, Berlin, **2015**.

[6] Y. Zhang, Y. Guo, Y.-H. Joo, D. A. Parrish, J. M. Shreeve, *Chem. Eur. J.* **2010**, *16*, 10778–10784.

[7] M. W. Holladay, WO Patent 2017019804 A2, **2017**.

[8] I. L. Dalinger, I. A. Vatsadze, T. K. Shkineva, A. V. Kormanov, M. I. Struchkova, K. Y. Suponitsky, A. A. Bragin, K. A. Monogarov, V. P. Sinditskii, A. B. Sheremetev, *Chem. Asian J.* **2015**, *10*, 1987–1996.

[9] P. Yin, D. A. Parrish, J. M. Shreeve, *Chem. Eur. J.* **2014**, *20*, 6707–6712.

[10] a) P. Yin, J. Zhang, C. He, D. A. Parrish, J. M. Shreeve, *J. Mat. Chem. A* **2014**, *2*, 3200–3208; b) X. Zhao, C. Qi, L. Zhang, Y. Wang, S. Li, F. Zhao, S. Pang, *Molecules* **2014**, *19*, 896.

[11] a) V. M. Vinogradov, I. L. Dalinger, B. I. Ugrak, S. A. Shevelev, *Mendeleev Commun.* **1996**, *6*, 139–140; b) P. Yin, L. A. Mitchell, D. A. Parrish, J. M. Shreeve, *Chem. Asian J.* **2017**, *12*, 378–384.

[12] D. Kumar, L. A. Mitchell, D. A. Parrish, J. M. Shreeve, *J. Mat. Chem. A* **2016**, *4*, 9931–9940.

[13] T. Fendt, N. Fischer, T. M. Klapötke, J. Stierstorfer, *Eur. J. Inorg. Chem.* **2011**, *50*, 1447–1458.

[14] D. Kumar, G. H. Imler, D. A. Parrish, J. M. Shreeve, *J. Mat. Chem. A* **2017**, *5*, 10437–10441.

[15] a) D. Kumar, G. H. Imler, D. A. Parrish, J. M. Shreeve, *Chem. Eur. J.* **2017**, *23*, 7876–7881; b) D. Kumar, G. H. Imler, D. A. Parrish, J. M. Shreeve, *New J. Chem.* **2017**, *41*, 4040–4047.

[16] a) D. Fischer, J. L. Gottfried, T. M. Klapötke, K. Karaghiosoff, J. Stierstorfer, T. G. Witkowski, *Angew. Chem. Int. Ed.* **2016**, *128*, 16366–16369; b) M. H. Kim, B. Lee, N. Kim, M. Shin, H. J. Shin, K. Kwon, J. S. Kim, S. K. Lee, Y. G. Kim, *Bull. Korean Chem. Soc.* **2017**, *38*, 751–755.

[17] a) P. Yin, L. A. Mitchell, D. A. Parrish, J. M. Shreeve, *Angew. Chem. Int. Ed.* **2016**, *55*, 14409–14411; bM. Göbel, K. Karaghiosoff, T. M. Klapötke, D. G. Piercey, J. Stierstorfer, *J. Am. Chem. Soc.* **2010**, *132*, 17216–17226; c) N. Fischer, D. Fischer, T. M. Klapötke, D. G. Piercey, J. Stierstorfer, *J. Mater. Chem.* **2012**, *22*, 20418–20422; d) A. A. Dippold, T. M. Klapötke, *J. Am. Chem. Soc.* **2013**, *135*, 9931–9938; e) D. Fischer, T. M. Klapötke, M. Reymann, P. C. Schmid, J. Stierstorfer, M. Sućeska, *Propellants Explos. Pyrotech.* **2014**, *39*, 550–557.

[18] a) T. Harel, S. Rozen, *J. Org. Chem.* **2010**, *75*, 3141–3143; b) T. M. Klapötke, M. Q. Kurz, P. C. Schmid, J. Stierstorfer, *J. Energ. Mat.* **2015**, *33*, 191–201.

[19] Y. Zhang, D. A. Parrish, J. M. Shreeve, *J. Mater. Chem.* **2012**, *22*, 12659–12665.

[20] Impact: Insensitive > 40 J, less sensitive ≥ 35 J, sensitive ≥ 4, very sensitive ≤ 3 J; friction: Insensitive > 360 N, less sensitive = 360 N, sensitive < 360 N a. > 80 N, very sensitive ≤ 80 N, extreme sensitive ≤ 10 N; According to the UN Recommendations on the Transport of Dangerous Goods (+) indicates: not safe for transport.

[21] R. Scharf, Dissertation thesis, LMU München **2016**.

[22] M. F. Bölter, T. M. Klapötke, J. Stierstorfer, *21th New Trends in Research of Energetic Materials Seminar*, Pardubice, Czech, **2018**, 504–512.

4.6 Supplementary Information

4.6.1 X-ray Diffraction

Single crystals were picked and measured on an Oxford Xcalibur3 diffractometer with a Spellman generator (voltage 50 kV, current 40 mA) and a CCD area detector for data collection using Mo-*K*α radiation (λ = 0.71073 Å). The crystal structures of compounds **2b**, **2d, 4a, 4b, 4c** and **4d** were determined on a Bruker D8 Venture TXS diffractometer equipped with a multilayer monochromator, a Photon 2 detector, and a rotating-anode generator (MoKα radiation). The data collection was carried out using CRYSALISPRO software[S1] and the reduction were performed. The structures were solved using direct methods (SIR-92, [S3] SIR-97[S3] or SHELXS-97[S4]) and refined by full-matrix least-squares on *F*2 (SHELXL [S4]): The final check was done with the PLATON software [S5] integrated in the WinGX software suite. The non-hydrogen atoms were refined anisotropically and the hydrogen atoms were located and freely refined. The absorptions were corrected by a SCALE3 ABSPACK multiscan method.[S6] The DIAMOND2 plots are shown with thermal ellipsoids at the 50% probability level and hydrogen atoms are shown as small spheres of arbitrary radii. The SADABS program embedded in the Bruker APEX3 software has been used for multi-scan absorption corrections in all structures.[S7]

Table 4.S1. Crystallographic data and refinement parameters of compound **1**, **2, 2a** and **2b**.

	1	**2·H₂O**	**2a·H₂O**	**2b**
Formula	$C_7H_4N_8O_8$	$C_3H_4N_4O_6$	$C_3H_3N_4O_6K$	$C_3H_5N_5O_5$
FW [g mol⁻¹]	328.18	192.10	230.19	191.12
Crystal system	Monoclinic	Monoclinic	Monoclinic	Monoclinic
Space Group	*Cc*	*P21*	*P21/c*	*P21/n*
Color / Habit	Colorless rod	Colorless block	Orange plate	Orange rod
Size [mm]	0.14 × 0.17 × 0.34	0.20 × 0.40 × 0.40	0.09 × 0.22 × 0.24	0.03 × 0.03 × 0.1
a [Å]	10.9540(8)	4.9308(2)	9.1277(5)	18.418(3)
b [Å]	12.5712(5)	8.5502(3)	12.3808(6)	4.8418(7)
c [Å]	10.3265(5)	8.4683(4)	6.7712(4)	18.434(3)
α [°]	90	90	90	90
β [°]	121.575(7)	91.521(4)	95.614(5)	116.748(4)
γ [°]	90	90	90	90
V [Å³]	1211.49(15)	356.89(3)	761.53(7)	1468.0(4)
Z	4	2	4	8
$\rho_{calc.}$ [g cm⁻³]	1.799	1.788	2.008	1.730
μ [mm⁻¹]	0.165	0.174	0.714	0.162
F(000)	664	196	464	784
$\lambda_{MoK\alpha}$[Å]	0.71073	0.71073	0.71073	0.71073
T [K]	173	173	130	100
ϑ min-max [°]	4.3, 27.5	4.7, 27.5	4.3, 26.0	2.1, 26.4
Dataset h; k; l	−14:14;−16:15;−11:13	−6:6;−11:10;−9:10	−11:11;−15:15;−8:5	−23:23;−6:6; −23:23
Reflect. coll.	5095	2835	5548	18097
Independ. refl.	2468	1460	1498	2979
R_{int}	0.016	0.013	0.028	0.075
Reflection obs.	2371	1417	1276	2511
No. parameters	224	134	139	269
R_1 (obs)	0.028	0.0225	0.0266	0.0445
wR_2 (all data)	0.0719	0.0550	0.0653	0.1156
S	1.05	1.09	1.04	1.10
Resd. Dens.[e Å⁻³]	−0.17, 0.20	−0.16, 0.16	−0.25, 0.30	−0.35, 0.36
Device type	Xcalibur Sapphire 3	Xcalibur Sapphire 3	Xcalibur Sapphire 3	Bruker D8 Venture
Solution	SIR-92	SIR-92	SIR-92	SIR-92
Refinement	SHELXL-2013	SHELXL-2013	SHELXL-2013	SHELXL-2013
Absorpt. corr.	multi-scan	multi-scan	multi-scan	multi-scan
CCDC	1836555	1836554	1836556	1836562

Table 4.S2. Crystallographic data and refinement parameters of compounds **2c, 2d, 3** and **4a**.

	2c	**2d**	**3**	**4a·EtOH**
Formula	$C_4H_7N_7O_5$	$C_4H_8N_8O_5$	$C_7H_4N_8O_8$	$C_5H_7N_4O_6K$
FW [g mol^{-1}]	233.17	248.18	328.18	258.35
Crystal system	Triclinic	Monoclinic	Orthorhombic	Monoclinic
Space Group	*P–1*	*P21/n*	*P*212121	P21/n
Color / Habit	Orange plate	Orange-yellow block	Colorless rod	Yellow rod
Size [mm]	0.06 × 0.14 × 0.34	0.22 × 0.32 × 0.43	0.11 × 0.17 × 0.32	0.03 x 0.08 x 0.09
a [Å]	6.9088(8)	9.5342(8)	8.6423(2)	4.5793(3)
b [Å]	7.079(1)	8.3482(5)	9.8451(2)	14.819(1)
c [Å]	9.5185(11)	13.2118(9)	14.5917(4)	14.7285(10)
α [°]	72.814(11)	90	90	90
β [°]	87.039(9)	109.608(9)	90	90.993(2)
γ [°]	86.113(10)	90	90	90
V [Å^3]	443.47(10)	990.59(13)	1241.53(5)	999.35(12)
Z	2	4	4	4
$\rho_{calc.}$ [g cm^{-3}]	1.746	1.664	1.756	1.716
μ [mm^{-1}]	0.158	0.150	0.161	0.554
F(000)	240	512	664	528
$\lambda_{MoK\alpha}$[Å]	0.71073	0.71073	0.71073	0.71073
T [K]	143	203	173	103
ϑ min-max [°]	4.2, 26.0	4.5, 26.5	4.1, 27.5	3.1, 26.0
Dataset h; k; l	−7:8;−8:8;−11:11	−10:11;−10:10;−16:16	−11:11;−12:12;−18:18	−5:5;−18:18; −18:18
Reflect. coll.	3328	8092	20754	13684
Independ. refl.	1739	2040	2835	1960
R_{int}	0.031	0.027	0.038	0.036
Reflection obs.	1320	1591	2582	1801
No. parameters	173	205	127	150
R_1 (obs)	0.0514	0.0426	0.0273	0.0245
wR_2 (all data)	0.1392	0.1202	0.0680	0.0608
S	1.05	1.04	1.06	1.06
Resd. Dens. [e Å^{-3}]	−0.38, 0.49	−0.30, 0.33	−0.17, 0.17	−0.23, 0.26
Device type	Xcalibur Sapphire 3	Bruker D8 Venture	Xcalibur Sapphire 3	Bruker D8 Venture
Solution	SIR-92	SIR-92	SIR-92	SIR-92
Refinement	SHELXL-2013	SHELXL-2013	SHELXL-2013	SHELXL-2013
Absorpt. corr.	multi-scan	multi-scan	multi-scan	multi-scan
CCDC	1836559	1836558	1836561	1836563

Table 4.S3. Crystallographic data and refinement parameters of compounds **4b**, **4c** and **4d**.

	4b·H_2O	**4c**	**4d**
Formula	$C_3H_7N_8O_6$	$C_4H_7N_7O_5$	$C_4H_8N_8O_5$
FW [g mol^{-1}]	209.14	233.17	248.18
Crystal system	Triclinic	Triclinic	Monoclinic
Space Group	*P–1*	*P–1*	P21/n
Color / Habit	Yellow plate	Yellow block	Brown platelet
Size [mm]	0.02 × 0.07 × 0.08	0.02 × 0.02 × 0.03	0.02 × 0.05 × 0.09
a [Å]	4.7398(4)	3.6558(2)	10.9035(7)
b [Å]	9.0434(9)	11.3428(6)	3.5661(2)
c [Å]	10.0417(9)	11.7421(6)	24.5303(14)
α [°]	101.309(4)	112.789(2)	90
β [°]	97.471(3)	94.275(2)	94.867(2)
γ [°]	95.925(4)	90.277(2)	90
V [Å^3]	414.80(7)	447.35(4)	950.37(10)
Z	2	2	4
$\rho_{calc.}$ [g cm^{-3}]	1.674	1.731	1.735
μ [mm^{-1}]	0.160	0.157	0.156
F(000)	216	240	512
$\lambda_{MoK\alpha}$[Å]	0.71073	0.71073	0.71073
T [K]	103	103	100
ϑ min-max [°]	3.4, 26.4	3.2, 26.4	3.3, 26.4
Dataset h; k; l	−5:5;−11:11;−11:12	−4:4;−14:13;0:14	−13:12;−4:4; −28:30
Reflect. coll.	4286	1823	5074
Independ. refl.	1684	1823	1959
R_{int}	0.024	0.038	0.034
Reflection obs.	1449	1604	1478
No. parameters	160	170	186
R_1 (obs)	0.0389	0.0397	0.0464
wR_2 (all data)	0.0885	0.0957	0.1083
S	1.14	1.15	1.05
Resd. Dens. [e Å^{-3}]	−0.31, 0.24	−0.29, 0.31	−0.28, 0.30
Device type	Bruker D8 Venture	Bruker D8 Venture	Bruker D8 Venture
Solution	SIR-92	SIR-92	SIR-92
Refinement	SHELXL-2013	SHELXL-2013	SHELXL-2013
Absorpt. corr.	multi-scan	multi-scan	multi-scan
CCDC	1836560	1836553	1836557

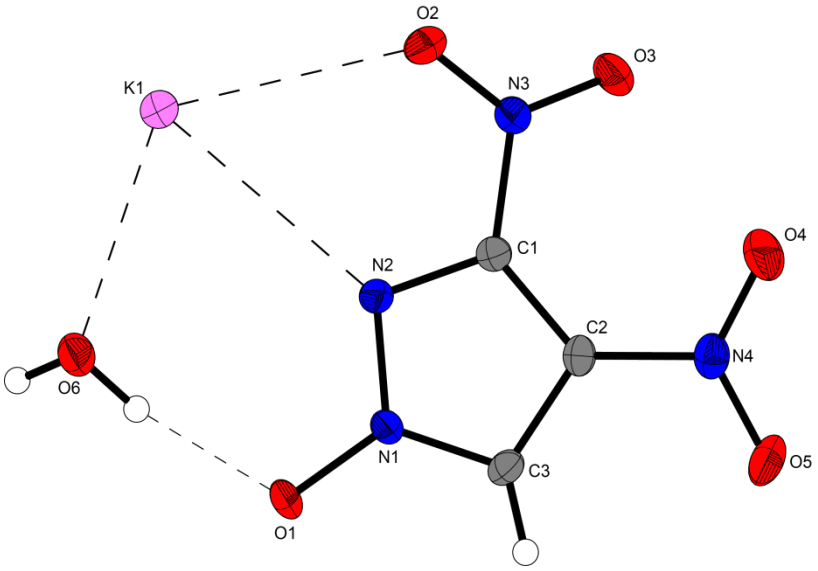

Figure 4.S1. Molecular structure of **2a** showing the atom-labelling scheme. Thermal ellipsoids represent the 50% probability level.

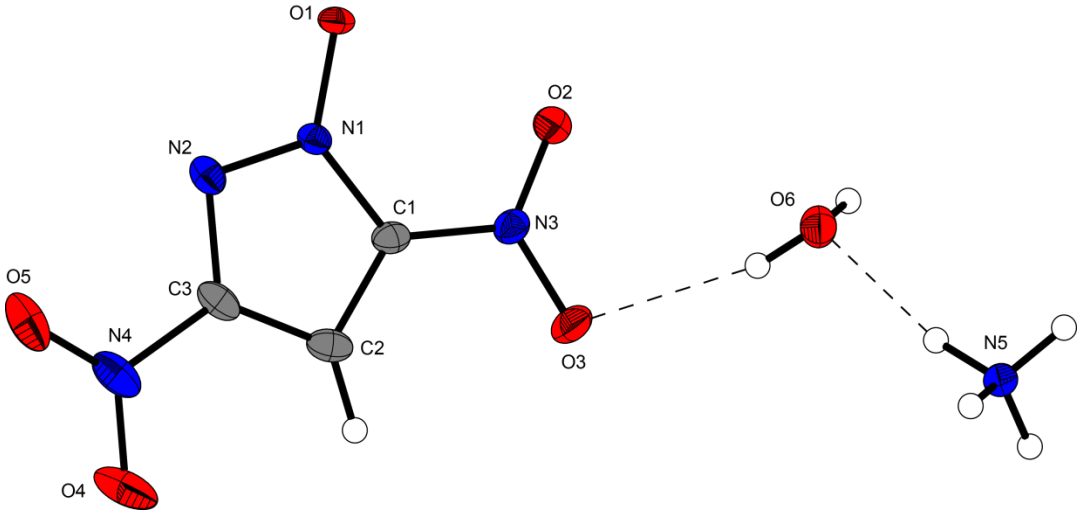

Figure 4.S2. Extended molecular structure of **4b** showing the atom-labelling scheme. Thermal ellipsoids represent the 50% probability level.

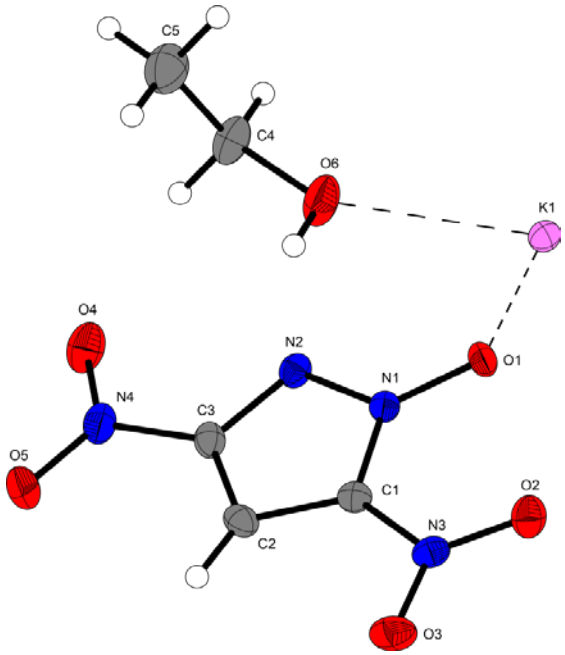

Figure 4.S3. Extended molecular structure of **4a** showing the atom-labelling scheme. Thermal ellipsoids represent the 50% probability level.

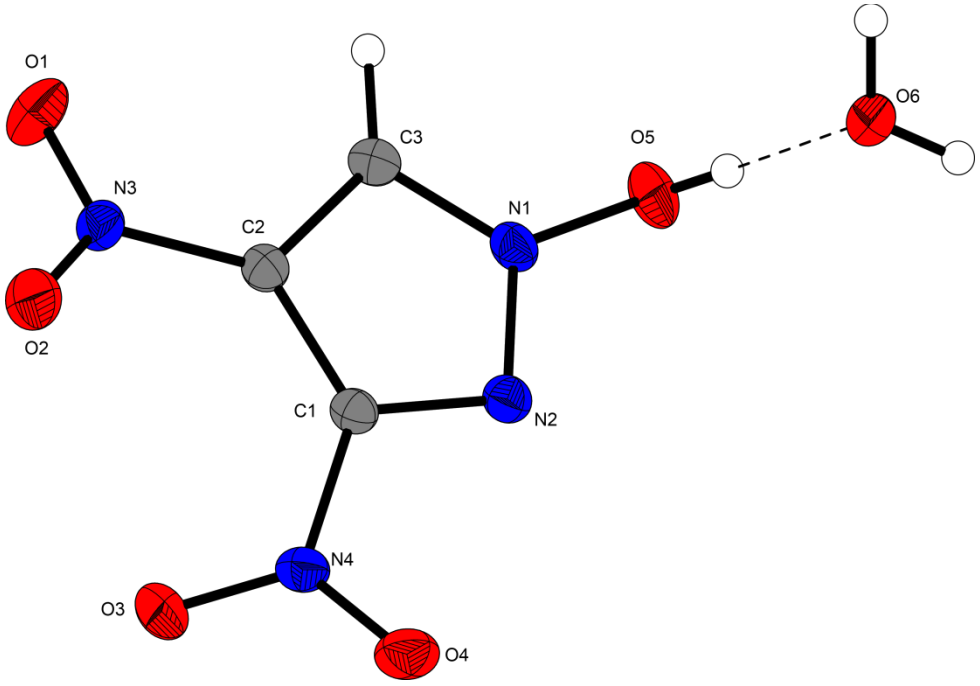

Figure 4.S4. Extended molecular structure of **2** showing the atom-labelling scheme. Thermal ellipsoids represent the 50% probability level.

4.6.2 Heat of formation calculations

All quantum chemical calculations were carried out using the Gaussian G09 program package.[S8] The enthalpies (H) and free energies (G) were calculated using the complete basis set (CBS) method of Petersson and coworkers in order to obtain very accurate energies. The CBS models are using the known asymptotic convergence of pair natural orbital expressions to extrapolate from calculations using a finite basis set to the estimated CBS limit. CBS-4 starts with an HF/3-21G(d) geometry optimization; the zero point energy is computed at the same level. It then uses a large basis set SCF calculation as a base energy, and an MP2/6- 31+G calculation with a CBS extrapolation to correct the energy through second order. A MP4(SDQ)/6-31+ (d,p) calculation is used to approximate higher order contributions. In this study, we applied the modified CBS-4M.

Heats of formation of the synthesized ionic compounds were calculated using the atomization method (equation E1) using room temperature CBS-4M enthalpies, which are summarized in Table 4.S5.[S9,S10]

$$\Delta_f H^\circ_{(g,\,M,\,298)} = H_{(Molecule,\,298)} - \sum H^\circ_{(Atoms,\,298)} + \sum \Delta_f H^\circ_{(Atoms,\,298)} \qquad (E1)$$

Table 4.S5. CBS-4M enthalpies for atoms C, H, N and O and their literature values for atomic $\Delta H^\circ_f{}^{298}$ / kJ mol^{-1}

	$-H^{298}$ [a.u.]	NIST [S11]
H	0.500991	218.2
C	37.786156	717.2
N	54.522462	473.1
O	74.991202	249.5

For neutral compounds the sublimation enthalpy, which is needed to convert the gas phase enthalpy of formation to the solid state one, was calculated by the *Trouton* rule.[S12] For ionic compounds, the lattice energy (U_L) and lattice enthalpy (ΔH_L) were calculated from the corresponding X-ray molecular volumes according to the equations provided by *Jenkins* and *Glasser*.[S13] With the calculated lattice enthalpy the gas-phase enthalpy of formation was converted into the solid state (standard conditions) enthalpy of formation. These molar standard enthalpies of formation (ΔH_m) were used to calculate the molar solid state energies of formation (ΔU_m) according to equation E2.

$$\Delta U_m = \Delta H_m - \Delta n\, RT \qquad (E2)$$

(Δn being the change of moles of gaseous components)

The calculation results are summarized in Table 4.S6.

Table 4.S6. Heat of formation calculation results.

M	$-H^{298}$ [a] [a.u.]	$\Delta_f H°$(g,M) [kJ mol^{-1}] [b]	V_M [Å^3] [c]	$\Delta U_L, \Delta H_L$;[d] [kJ mol^{-1}]	$\Delta_f H°$(s) [e] [kJ mol^{-1}]	Δn [f]	$\Delta_f U$(s) [g] [kJ kg^{-1}]
1	1306.907808	389.0			301.7	10	995.0
3	1306.921244	353.7			266.4	10	887.5
2 anion	709.020387	–47.0					
K+	599.035967	487.4					
NH4+	56.796608	635.8					
G+	205.453192	571.9					
AG+	260.701802	671.6					
2a		541.1	761.5	585.1, 588.8	–391.7	–6.5	–1631.5
2b		588.8	1468.0	516.6, 124.2	68.7	7.5	456.8
2c		524.9	443.5	494.4, 118.9	27.0	9.5	217.0
2d		624.6	990.6	476.3, 479.7	144.9	10.5	688.6
4 anion	709.029271	–71.8					
4b		541.1	414.8	571.4, 575.1	–253.4	–9	–1105.1
4c		501.6	447.4	490.3, 493.8	7.8	9.5	134.5
4d		601.3	950.4	482.6, 486.1	115.2	10.5	569.0

[a] CBS-4M electronic enthalpy; [b] gas phase enthalpy of formation; [c] molecular volumes taken from X-ray structures and corrected to room temperature; [d] lattice energy and enthalpy (calculated using Jenkins and Glasser equations); [e] standard solid state enthalpy of formation; [f] Δn being the change of moles of gaseous components when formed; [g] solid state energy of formation.

4.6.3 Experimental Part

General Procedures

Thermal analysis by Differential Scanning Calorimetry (DSC) was performed on a LINSEIS DSC PT10 with about 1–2 mg substance in a perforated aluminum vessel with a heating rate of 5 K·min^{-1} and a nitrogen flow of 5 dm^3·h^{-1}. The NMR spectra were recorded on a 400 MHz instruments JEOL Eclipse 270, JEOL EX 400 or a JEOL Eclipse 400 (^{1}H 399.8 MHz, ^{13}C 100.5 MHz, ^{14}N 28.9 MHz, and ^{15}N 40.6 MHz). Chemical shifts are given in parts per million (ppm) relative to Si(Me)$_4$ (^{1}H, ^{13}C) and nitromethane (^{14}N, ^{15}N). Infrared spectra were measured with a Perkin-Elmer Spectrum BX-FTIR spectrometer equipped with a Smiths DuraSamplIR II ATR device. Transmittance values are qualitatively depicted as “very strong” (vs), “strong” (s), “medium” (m), and “weak” (w). Mass spectra were recorded with a JEOL MStation JMS 700 (DEI+ / FAB+/−). Elemental analysis was performed using a Vario Micro from the Elementar Company.

Impact sensitivity tests were carried out according to STANAG 4489[S8] modified instruction[S9] using a Bundesanstalt für Materialforschung (BAM) drophammer.[S10] Friction sensitivity tests were carried out according to STANAG 4487[S11] modified instruction[S12] using the BAM friction tester. The classification of the compounds results from the “UN Recommendations on the Transport of Dangerous Goods”.[S13] The sensitivity toward electrical discharge was tested upon using the Electric Spark Tester ESD 2010 EN.[S14] Bis-(3,4-dinitro-1*H*-pyrazol-1-yl)methane (**1**) and bis-(3,5-dinitro-1*H*-pyrazol-1-yl)methane (**3**) were synthesized in a different way than mentioned in literature.[S23]

Bis-(3,4-dinitro-1*H*-pyrazol-1-yl)methane (1)

3,4-Dinitro-1*H*-pyrazole[S22] (1.0 g, 6.2 mmol) was dissolved in water and aqueous ammonia solution (2 M, 3.2 mL, 6.2 mmol) was added. The mixture was stirred for 30 min and the solvent was removed in vacuum. The gained ammonium salt of 3,4-dinitro-1*H*-pyrazole (1.0 g, 5.71 mmol, 2.2 eq.) and diiodomethane (0.21 ml, 2.6 mmol, 1.0 eq.) were dissolved in DMF (15 ml). The solution was stirred overnight at 80 °C and afterwards poured on ice to obtain **1** after filtration (0.71 g, 2.16 mmol, 83 %).

^{1}H NMR (400 MHz, DMSO *d6*): δ (ppm) = 9.44 (s, 2H, CH), 6.75 (s, 4H, CH_2); **^{13}C NMR** (101 MHz, DMSO *d6*): δ (ppm) = 147.9, 135.6, 127.0, 66.8; **^{15}N NMR** (41 MHz, DMSO *d6*): δ (ppm) = –28.1 (-NO_2), –28.1 (-NO_2), –82.4 (t, N), –179.5 (d, N_{bridge}); **IR** (ATR, rel. int.): $\tilde{\nu}$ (cm^{-1}) = 3124 (w), 3049(w), 2998 (w), 2161 (w), 2034 (w), 1544 (s), 1516 (s), 1462 (m), 1436 (m), 1357 (s), 1333 (s), 1281 (m), 1147 (m), 1119 (m), 1016 (w), 999 (w), 924 (w), 862 (m), 810 (s), 789 (m), 746 (s), 651 (m), 621

(w); **Elemental analysis:** calcd. (%) for $C_7H_4N_8O_8$ (327.20 g mol^{-1}): C 25.62, H 1.23, N 34.15; found: C 26.59, H 1.42, N 33.25; **Mass spectroscopy**: m/z (DEI) = 327.4 ($C_7H_4N_8O_8$); **DSC** (5°C min^{-1}): $T_{melt.}$ = 156°C, $T_{dec.}$ = 319°C.

3,4-Dinitropyrazol-1-oxide hydrate (2) [S21]

3,4-Dinitropyrazole[S22] (4.9 g, 31.0 mmol, 1.0 eq) was suspended in water (100 mL) and Oxone (65.3 g, 212.4 mmol, 6.9 eq) as well as basic buffer (NaH_2PO_4/2 M NaOH) was added alternately to hold the pH between 6-8. The solution was stirred at 55 C over 72 h, then sulfuric acid (50%, 100 mL) was added and the product was extracted with diethyl ether (3x 100mL). The combined organic layers were extracted with 5 % aqueous sodium acetate solution (3 x 100 mL). After acidification of the aqueous sodium acetate phase with hydrochloric acid (2 M) the product is isolated by extraction with diethyl ether (3x 100mL). The combined organic layers were dried over anhydrous magnesium sulfate, filtrated and the solvent was evaporated under reduced pressure to yield compound **2** (4.04 g, 21.1 mmol, 68 %) as yellowish crystals.

^{1}H NMR (400MHz, DMSOd_6): δ (ppm) = 9.06 (s, 1H, CH); **^{13}C NMR** (101 MHz, DMSO d_6): δ (ppm) = 140.6, 126.0, 124.4; **IR** (ATR, rel. int.): $\tilde{\nu}$ (cm^{-1}) = 3565 (s), 3466 (s), 1710 (w), 1614 (m), 1541 (m), 1507 (s), 1464 (s), 1400 (s), 1354 (s), 1325 (s), 1270 (s), 1144 (s), 1117 (m), 1022 (m), 911 (s), 857 (s), 808 (m), 741 (m), 664 (m), 624 (m), 596 (m); **Elemental analysis:** calcd. (%) for $C_3H_4N_4O_6$ (190.12 g mol^{-1}): C 18.76, H 2.10, N 29.17; found: C 18.96, H 2.16, N 28.27; **Mass spectroscopy**: m/z (FAB-) = 173.1 ($C_3HN_4O_5^-$); **DSC** (5°C min^{-1}): $T_{dec.}$ = 167°C; **Sensitivities** (grain size: < 500 μm): BAM impact: 35 J, BAM friction: 360 N, ESD: 1.0 J.

General procedure for the preparation of salts of 2

A water/ethanol 1:1 solution of **2** (**2a**: 0.5 g, 2.6 mmol; **2b**: 0.16 g, 0.92 mmol, **2c**: 0.22 g, 1.26 mmol; **2d**: 0.55 g, 3.17 mmol) was treated with the corresponding base (**2a**: KOH 0.15 g, 2.6 mmol; **2b**: ammonia solution 25%, 0.48 mL, 0.92 mmol; **2c**: guanidine carbonate 0.22 g,1.26 mmol; **2d**: aminoguanidine bicarbonate 0.43 g, 3.17 mmol) and heated at 80 °C for 30 min. The solutions were filtered and left for crystallization.

Potassium 3,4-dinitropyrazol-1-olate hydrate (2a)

Yield: (0.44 g, 2.1 mmol, 81 %) as orange crystals.

^{1}H NMR (400 MHz, DMSO d_6**)**: δ(ppm) = 7.73 (s, 1H, CH); **^{13}C NMR (**101 MHz, DMSO d_6**)**: δ(ppm) = 136.7, 122.6, 118.7; **IR** (ATR, rel. int.): $\tilde{\nu}$ (cm^{-1}) = 3614 (m), 3319 (w), 3236 (w), 3147 (m), 1647 (m), 1526 (m), 1496 (s), 1459 (s), 1429 (m), 1376 (s), 1318 (s), 1191 (s), 1144 (m), 1114 (m), 1008 (m), 802 (s), 737 (s), 643 (m), 600(m); **Elemental analysis:** calcd. (%) for $C_3H_3KN_4O_6$ (212.16 g mol^{-1}): C 15.65, H 1.31, N 24.34; found: C 15.61, H 1.37, N 23.93; **DSC** (5°C min^{-1}): $T_{dec.}$ =197°C; **Sensitivities** (grain size: 100–500 μm): BAM impact: 5 J, BAM friction: 216 N, ESD: 0.7 J.

Ammonium 3,4-dinitropyrazol-1-olate (2b)

Yield: (0.13 g, 0.68 mmol, 74 %) as orange crystals.

^{1}H NMR (400 MHz, DMSO d_6): δ(ppm) =7.89 (s, 1H, CH), 7.13 (m, 4H, NH_4); **^{13}C NMR** (101 MHz, DMSO d_6): δ(ppm) = 137.3, 122.7, 119.5; **IR** (ATR, rel. int.): $\tilde{\nu}$ (cm^{-1}) = 3324 (w), 3148 (m), 1625 (w), 1496 (m), 1564 (s), 1429 (s), 1380 (s), 1339 (s), 1310 (s), 1201 (s), 1151 (s), 1113 (s), 1011 (m), 866 (w), 805 (s), 741 (s), 670 (m), 638 (m), 609 (m), 501 (m); **Elemental analysis:** calcd. (%) for $C_3H_5N_5O_5$ (191.10 g mol^{-1}): C 18.86, H 2.64, N 36.65; found: C 19.25, H 2.62, N 34.89; **DSC** (5°C min^{-1}): $T_{dec.}$ =167°C; **Sensitivities** (grain size: 100–500 μm): BAM impact: 10 J, BAM friction: 360 N, ESD: 1.5 J.

Guanidinium 3,4-dinitropyrazol-1-olate (2c)

Yield: (0.20 g, 0.86 mmol, 68 %) as dark red crystals.

^{1}H NMR (400 MHz, DMSO d_6): δ(ppm) =7.74 (s, 1H, CH), 6.95 (s, 6H, NH_2); **^{13}C NMR** (101 MHz, DMSO d_6): δ(ppm) = 157.9 (Gua+), 136.7, 122.6, 118.7; **IR** (ATR, rel. int.): $\tilde{\nu}$ (cm^{-1}) = 3474 (m), 3425 (m), 3367 (m), 3258 (m), 3172 (m), 3150 (m), 1650 (s), 1580 (m), 1527 (m), 1495 (s), 1465 (s), 1428 (s), 1369 (m), 1320 (s), 1300 (s), 1188 (s), 1148 (s), 1110 (m), 1063 (m), 1024 (m), 929 (m), 866 (m), 847 (m), 806 (s), 744 (s), 653 (s), 514 (s); **Elemental analysis:** calcd. (%) for $C_4H_7N_7O_5$ (233.14 g mol^{-1}): C 20.61, H 3.03, N 42.06; found: C 20.87, H 3.13, N 41.70; **DSC** (5 °C min^{-1}): $T_{dec.}$ = 180°C; **Sensitivities** (grain size: 100–500 μm): BAM impact: 30 J, BAM friction: 360 N, ESD: 1.5 J.

Aminoguanidinium 3,4-dinitropyrazol-1-olate (2d)

Yield: (0.46 g, 1.85 mmol, 58 %) as orange crystals.

^{1}H NMR (400 MHz, DMSO d_6): δ(ppm) = 8.60 (s, 1H, NH), 7.72 (s, 1H, CH), 7.22 (s, 2H, NH_2) , 4.68 (4H, NH_2); **^{13}C NMR** (101 MHz, DMSO d_6): δ(ppm) = 158.8 (AG+), 136.7, 122.6, 118.6; **IR** (ATR, rel. int.): $\tilde{\nu}$ (cm^{-1}) = 3359 (m), 3234 (m), 3151 (m), 1659 (s), 1522 (s), 1466 (s), 1434 (s), 1380 (m), 1332 (s), 1309 (s), 1202 (s), 1152 (m), 1113 (m), 1005 (m), 798 (m), 742 (s), 513 (s); **Elemental analysis:** calcd. (%) for $C_4H_7N_7O_5$ (248.16 g mol^{-1}): C 19.36, H 3.25, N 45.15; found: C 19.31, H 3.34, N 45.37; **DSC** (5°C min^{-1}): $T_{melt.}$ = 132°C, $T_{dec.}$ = 169°C. **Sensitivities** (grain size: 100–500 μm): BAM impact: 10 J, BAM friction: 360 N, ESD: 1.5 J.

Bis- (3,5-dinitro-1*H*-pyrazol-1-yl)methane (3)

3,5-Dinitro-1*H*-pyrazole[S22] (1.0 g, 6.2 mmol) was dissolved in water and aqueous ammonia solution (2 M, 3.2 mL, 6.2 mmol) was added. The mixture was stirred for 30 min. and the solvent was removed in vacuum. The gained ammonium salt of 3,5-dinitro-1*H*-pyrazole (0.6 g, 3.43 mmol, 2.2 eq.) and diiodomethane (0.13 ml, 1.56 mmol, 1.1 eq.) were dissolved in DMF (15 ml). The solution was stirred overnight at 80 °C and afterwards poured on ice to obtain **3** after filtration (0.28 g, 0.85 mmol, 55 %).

^{1}H NMR (400 MHz, DMSO d_6): δ (ppm) = 8.31 (s, 2H, CH), 7.42 (s, 2H, CH_2); **^{13}C NMR** (101 MHz, DMSO d_6): δ (ppm) = 153.2, 146.5, 103.5, 65.7; **IR** (ATR, rel. int.): $\tilde{\nu}$ (cm^{-1}) = 3153 (w), 3093(w), 3013 (w), 2933 (w), 1563 (m), 1523 (s), 1463 (m), 1430 (w), 1343 (s), 1330 (s), 1273 (m), 1223 (m), 1143 (w), 1093 (m), 982 (m), 853 (m), 818 (m), 783 (m), 738 (s), 615 (w); **Elemental analysis:** calcd. (%) for $C_7H_4N_8O_8$ (327.20 g mol^{-1}): C 25.62, H 1.42, N 34.15; found: C 26.32, H 1.39, N 33.68; **Mass spectroscopy**: m/z (DEI) = 327.4 ($C_7H_4N_8O_8$); **DSC** (5°C min^{-1}): $T_{melt.}$ = 191°C, $T_{dec.}$ = 330°C; **Sensitivities** (grain size: < 500 μm): BAM impact: 35 J, BAM friction: 360 N, ESD: 1.0 J.

3,5-Dinitropyrazol-1-oxide hemihydrate (4) [S21]

3,5-Dinitropyrazole[S22] (6.3 g, 39.8 mmol, 1.0 eq) was suspended in water (100 mL) and Oxone (86.2 g, 280.0 mmol, 6.9 eq) as well as basic buffer (NaH_2PO_4/2 M NaOH) was added alternately to hold the pH between 3–5. The solution was stirred at 55 C for 72 h, then sulfuric acid (50 %, 100 mL) was added and the product was extracted with diethyl ether (3 x 100mL). The ether phase was extracted with 5 % aqueous sodium acetate solution (3 x 100 mL). After acidification of the

aqueous sodium acetate phase with hydrochloric acid (2 M) the product is isolated by extraction with diethyl ether (3x 100mL). The combined organic layers were dried over anhydrous magnesium sulfate, filtrated and the solvent was evaporated under reduced pressure to yield compound 4 (4.44 g, 24.3 mmol, 61 %) as colorless powder.

^{1}H NMR (400MHz, DMSOd_6): δ (ppm) = 7.77 (s, 1H, CH); **^{13}C NMR** (101 MHz, DMSO d_6): δ (ppm) = 142.8, 138.6, 99.9; **IR** (ATR, rel. int.): $\tilde{\nu}$ (cm^{-1}) = 3215 (m), 3148 (m), 2964 (w), 2168 (w), 1692 (w), 1555 (m), 1528 (m), 1475 (m), 1445 (s), 1332 (s), 1202 (m), 1141 (m), 1083 (m), 1014 (m), 983 (s), 831 (s), 741 (s), 686 (s), 573 (m), 512 (m); **Elemental analysis:** calcd. (%) for $C_3H_3N_4O_{5.5}$ (183.08 g mol^{-1}): C 19.68, H 1.65, N 30.60; found: C 20.26, H 1.54, N 30.02; **Mass spectroscopy**: m/z (DEI) = 173.9 ($C_3HN_4O_5$); **DSC** (5°C min^{-1}): $T_{dec.}$ = 158°C; **Sensitivities** (grain size: < 500 μm): BAM impact: 35 J, BAM friction: 360 N, ESD: 1.0 J.

General procedure for the preparation of salts of 4

A water/ethanol 1:1 solution of **4** (**4a**: 0.31 g, 1.78 mmol; **4b**: 0.2 g, 1.15 mmol, **4c**: 0.30 g, 1.72 mmol; **4d**: 0.25 g, 1.44 mmol) was treated with the corresponding base (**4a**: KOH 0.10 g, 1.78 mmol; **4b**: aqueous ammonia solution 2 M, 0.6 mL, 1.15 mmol; **4c**: guanidine carbonate 0.15 g,1.72 mmol; **4d**: aminoguanidine bicarbonate 0.20 g, 1.44 mmol) and heated at 80 °C for 30 min. The solutions were filtered and left for crystallization.

Potassium 3,5-dinitropyrazol-1-olate hemihydrate (4a)

Yield: (0.30 g, 1.41 mmol, 79 %) as orange solid.

^{1}H NMR (400 MHz, DMSO d_6**)**: δ(ppm) = 7.45 (s, 1H, CH); **^{13}C NMR (**101 MHz, DMSO d_6**)**: δ(ppm) = 159.7, 139.2, 98.6; **IR** (ATR, rel. int.): $\tilde{\nu}$ (cm^{-1}) = 3594 (w), 3393 (w), 3149 (w), 1626 (m), 1537 (s), 1514 (m), 1465 (s), 1399 (s), 1322 (s), 1281 (s), 1232 (s), 1138 (s), 998 (m), 925 (m), 866 (m), 815(s), 758 (s), 652 (m), 540 (m); **Elemental analysis:** calcd. (%) for $C_3H_2KN_4O_{5.5}$ (221.17 g mol^{-1}): C 16.29, H 0.91, N 25.33; found: C 16.31, H 0.85, N 23.63; **DSC** (5°C min^{-1}): $T_{dec.}$ =224°C; **Sensitivities** (grain size: 100–500 μm): BAM impact: 6 J, BAM friction: 240 N, ESD: - .

Ammonium 3,5-dinitropyrazol-1-olate hydrate (4b)

Yield: (0.21 g, 1.09 mmol, 94 %) as yellow crystals.

^{1}H NMR (400 MHz, DMSO d_6): δ(ppm) =7.49 (s, 1H, CH), 7.10 (m, 4H, NH_4); **^{13}C NMR** (101 MHz, DMSO d_6): δ(ppm) = 158.9, 138.1, 98.8; **IR** (ATR, rel. int.): $\tilde{\nu}$ (cm^{-1}) = 3308 (w), 3160 (m), 2960 (m), 2903 (m), 1547 (s), 1462 (s), 1464 (s), 1394 (s), 1321 (s), 1286 (s), 1132 (s), 1090 (s), 1002 (m), 860 (m), 826 (m), 866 (w), 756 (m), 738 (s), 639 (m), 602 (m), 538 (m); **Elemental analysis:** calcd. (%) for $C_3H_5N_5O_5$ (191.10 g mol^{-1}): C 18.86, H 2.64, N 36.65; found: C 19.04, H 2.55, N 34.71; **DSC** (5°C min^{-1}): $T_{dec.}$ =229°C; **Sensitivities** (grain size: 100–500 μm): BAM impact: 30 J, BAM friction: 288 N, ESD: - .

Guanidinium 3,5-dinitropyrazol-1-olate (4c)

Yield: (0.32 g, 0.93 mmol, 80 %) as yellow crystals.

^{1}H NMR (400 MHz, DMSO d_6): δ(ppm) =7.44 (s, 1H, CH), 6.91 (s, 6H, NH_2); **^{13}C NMR** (101 MHz, DMSO d_6): δ(ppm) = 159.6, 157.9 (Gua+), 139.2, 98.6; **IR** (ATR, rel. int.): $\tilde{\nu}$ (cm^{-1}) = 3499 (m), 3408 (m), 3345 (m), 3206 (m), 3172 (m), 3144 (m), 2197 (w), 2032 (w), 1973 (w), 1653 (s), 1532 (m), 1460 (s), 1401 (s), 1327 (s), 1289 (m), 1238 (m), 1153 (m), 1088 (m), 1045 (m), 1003 (m), 867 (m), 822 (m), 736 (s), 655 (s), 586 (s), 545 (s); **Elemental analysis:** calcd. (%) for $C_4H_7N_7O_5$ (233.14 g mol^{-1}): C 20.61, H 3.03, N 42.06; found: C 20.88, H 3.04, N 42.03; **DSC** (5 °C min^{-1}): $T_{dec.}$ = 266°C; **Sensitivities** (grain size: 100–500 μm): BAM impact: 40 J, BAM friction: 360 N, ESD: - .

Aminoguanidinium 3,5-dinitropyrazol-1-olate (4d)

Yield: (0.23 g, 1.85 mmol, 64 %) as brown crystals.

^{1}H NMR (400 MHz, DMSO d_6): δ(ppm) = 8.55 (s, 1H, NH), 7.74 (s, 1H, CH), 7.24 (s, 2H, NH_2), 4.68 (4H, NH_2); **^{13}C NMR** (101 MHz, DMSO d_6): δ(ppm) = 159.6, 158.7 (AG+), 139.1, 98.6; **IR** (ATR, rel. int.): $\tilde{\nu}$ (cm^{-1}) = 3446 (m), 3278 (m), 3147 (m), 1661 (s), 1538 (s), 1467 (s), 1404 (m), 1339 (s), 1300 (m), 1247 (m), 1198 (m), 1146 (s), 1084 (m), 896 (m), 865 (m), 815 (m), 737 (s), 615 (m), 516 (s); **Elemental analysis:** calcd. (%) for $C_4H_8N_8O_5$ (248.16 g mol^{-1}): C 19.36, H 3.25, N 45.15; found: C 19.36, H 3.30, N 45.43; **DSC** (5°C min^{-1}): $T_{dec.}$ = 131°C; **Sensitivities** (grain size: 100–500 μm): BAM impact: 10 J, BAM friction: 360 N, ESD: - .

4.6.4 References

[S1] *CrysAlisPro*, Oxford Diffraction Ltd., version 171.33.41, **2009**.

[S2] *SIR-92*, *A program for crystal structure solution*: A. Altomare, G. Cascarano, C. Giacovazzo, A. Guagliardi, *J. Appl. Crystallogr.* **1993**, *26*, 343.

[S3] a) A. Altomare, G. Cascarano, C. Giacovazzo, A. Guagliardi, A. G. G. Moliterni, M. C. Burla, G. Polidori, M. Camalli, R. Spagna, *SIR97*, **1997**; b) A. Altomare, M. C. Burla, M. Camalli, G. L. Cascarano, C. Giacovazzo, A. Guagliardi, A. G. G. Moliterni, G. Polidori, R. Spagna, *J. Appl. Crystallogr.* **1999**, *32*, 115–119.

[S4] a) G. M. Sheldrick, *SHELX-97*, University of Göttingen, Göttingen, Germany, **1997**; b) G. M. Sheldrick, *Acta Crystallogr., Sect. A* **2008**, *64*, 112–122.

[S5] A. L. Spek, *PLATON*, *A Multipurpose Crystallographic Tool*, Utrecht University, The Netherlands, **1999**.

[S6] *SCALE3 ABSPACK – An Oxford Diffraction program* (1.0.4, gui: 1.0.3), Oxford Diffraction Ltd., **2005**.

[S7] *APEX3*. Bruker AXS Inc., Madison, Wisconsin, USA.

[S8] M. J. Frisch, G. W. Trucks, H. B. Schlegel, G. E. Scuseria, M. A. Robb, J. R. Cheeseman, G. Scalmani, V. Barone, B. Mennucci, G. A. Petersson, H. Nakatsuji, M. Caricato, X. Li, H.P. Hratchian, A. F. Izmaylov, J. Bloino, G. Zheng, J. L. Sonnenberg, M. Hada, M. Ehara, K. Toyota, R. Fukuda, J. Hasegawa, M. Ishida, T. Nakajima, Y. Honda, O. Kitao, H. Nakai, T. Vreven, J. A. Montgomery, Jr., J. E. Peralta, F. Ogliaro, M. Bearpark, J. J. Heyd, E. Brothers, K. N. Kudin, V. N. Staroverov, R. Kobayashi, J. Normand, K. Raghavachari, A. Rendell, J. C. Burant, S. S. Iyengar, J. Tomasi, M. Cossi, N. Rega, J. M. Millam, M. Klene, J. E. Knox, J. B. Cross, V. Bakken, C. Adamo, J. Jaramillo, R. Gomperts, R. E. Stratmann, O. Yazyev, A. J. Austin, R. Cammi, C. Pomelli, J. W. Ochterski, R. L. Martin, K. Morokuma, V. G. Zakrzewski, G. A. Voth, P. Salvador, J. J. Dannenberg, S. Dapprich, A. D. Daniels, O. Farkas, J.B. Foresman, J. V. Ortiz, J. Cioslowski, D. J. Fox, Gaussian 09 A.02, Gaussian, Inc., Wallingford, CT, USA, **2009**.

[S9] a) J. W. Ochterski, G. A. Petersson, and J. A. Montgomery Jr., *J. Chem. Phys.* **1996**, *104*, 2598–2619; b) J. A. Montgomery Jr., M. J. Frisch, J. W. Ochterski G. A. Petersson, *J. Chem. Phys.* **2000**, *112*, 6532–6542.

[S10] a) L. A. Curtiss, K. Raghavachari, P. C. Redfern, J. A. Pople, *J. Chem. Phys.* **1997**, *106*, 1063–1079; b) E. F. C. Byrd, B. M. Rice, *J. Phys. Chem*. A **2006**, *110*, 1005–1013; c) B. M. Rice, S. V. Pai, J. Hare, *Comb. Flame* **1999**, *118*, 445–458.

[S11] P. J. Lindstrom, W. G. Mallard (Editors), NIST Standard Reference Database Number 69, http://webbook.nist.gov/chemistry/ (accessed June **2011**).

[S12] M. S. Westwell, M. S. Searle, D. J. Wales, D. H. Williams, *J. Am. Chem. Soc*. **1995**, *117*, 5013–5015; (b) F. Trouton, *Philos. Mag*. **1884**, *18*, 54–57.

[S13] a) H. D. B. Jenkins, H. K. Roobottom, J. Passmore, L. Glasser, *Inorg. Chem.* **1999,** *38,* 3609–3620; b) H. D. B. Jenkins, D. Tudela, L. Glasser, *Inorg. Chem.* **2002**, *41*, 2364–2367.

[S14] NATO standardization agreement (STANAG) on explosives, *impact sensitivity tests*, no. 4489, 1st ed., Sept. 17, **1999**.

[S15] WIWEB-Standardarbeitsanweisung 4-5.1.02, Ermittlung der Explosionsgefährlichkeit, hier der Schlagempfindlichkeit mit dem Fallhammer, Nov. 8, **2002**.

[S16] http://www.bam.de

[S17] NATO standardization agreement (STANAG) on explosive, *friction sensitivity tests*, no. 4487, 1st ed., Aug. 22, **2002**.

[S18] WIWEB-Standardarbeitsanweisung 4-5.1.03, Ermittlung der Explosionsgefährlichkeit oder der Reibeempfindlichkeit mit dem Reibeapparat, Nov. 8, **2002**.

[S19] Impact: insensitive > 40 J, less sensitive ≥ 35 J, sensitive ≥ 4 J, very sensitive ≤ 3 J; Friction: insensitive > 360 N, less sensitive = 360 N, sensitive < 360 N and > 80 N, very sensitive ≤ 80 N, extremely sensitive ≤ 10 N, According to: *Recommendations on the Transport of Dangerous Goods, Manual of Tests and Criteria*, 4th edition, United Nations, New York-Geneva, **1999**.

[S20] http://www.ozm.cz

[S21] V. M. Vinogradov, I. L. Dalinger, B. I. Ugrak, S. A. Shevelev, *Mendeleev Commun.* **1996**, *6*, 139–140.

[S22] J. W. A. M. Janssen, H. J. Koeners, C. G. Kruse, C. L. Habrakern, *J. Org. Chem.* **1973**, *38*, 1777–1782.

[S23] M. H. Kim, B. Lee, N. Kim, M. Shin, H. J. Shin, K. Kwon, J. S. Kim, S. K. Lee, Y. G. Kim, *Bull. Korean Chem. Soc.* **2017**, *38*, 751–755.

5 Combination of Different Azoles – 1,2,4-Triazolyl-1,3,4-Oxadiazoles as Precursor for Energetic Materials

Marc F. Bölter, Ivan Gospodinov, Thomas M. Klapötke and Jörg Stierstorfer

will be published in Zeitschrift für Anorganische und Allgemeine Chemie

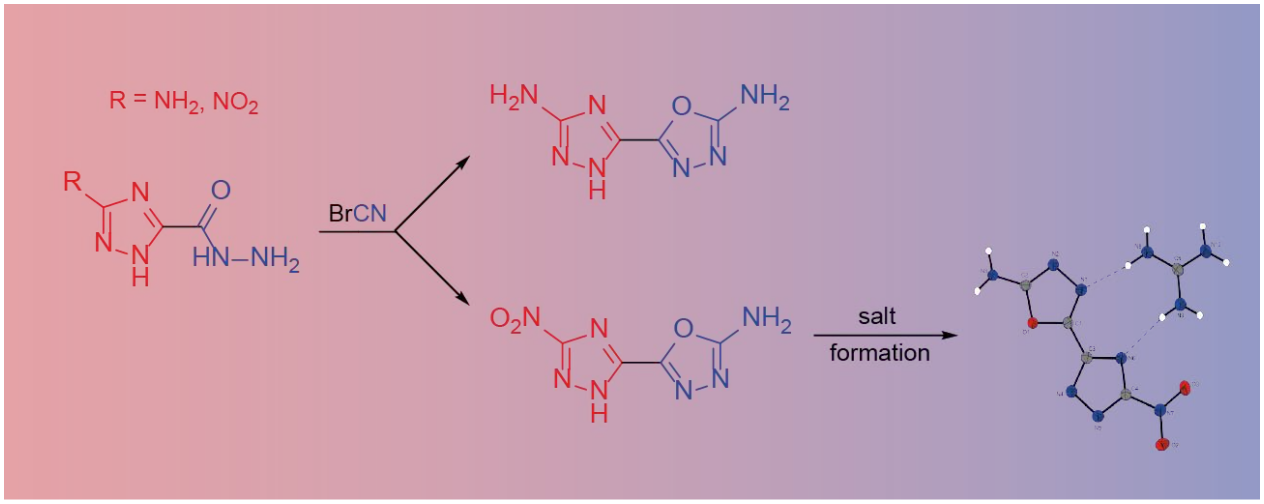

Abstract: Two new bisheterocyclic compounds 2-amino-5-(5-amino-1*H*-1,2,4-triazol-3-yl)-1,3,4-oxadiazole (**5**) and 2-amino-5-(5-nitro-1*H*-1,2,4-triazol-3-yl)-1,3,4-oxadiazole (**6**) were synthesized and compared to each other. Further, four energetic salts of compound **6** were synthesized in order to improve the energetic performance and sensitivity values. The obtained compounds were characterized using IR, NMR (^{1}H, ^{13}C, ^{14}N), mass, elemental analysis and thermal analysis (DSC). Crystal structures could be obtained of five compounds (**3, 7**–**10**) by low temperature single crystal X-ray diffraction. Impact, friction and ESD values were determined according to *Bundesamt für Materialforschung* (BAM) standard methods. Both bisheterocyclic compounds and obtained salts are not sensitive toward external stimuli and show a thermal stability up to 296 °C. The energetic performance of the energetic salts was calculated using recalculated X-ray densities, heats of formation and the EXPLO5 code. Their detonation velocity and pressure lie in the range of 6965–7672 m s^{-1} and 179–206 kbar. Both bisheterocycles (**5** and **6**) are suitable as precursors for new energetic materials indicating a high thermal stability.

5.1 Introduction

The research on new powerful explosives is an ongoing field of study due to their application in military and civilian areas.[1] Depending on their usage, high energetic dense materials (HEDMs) have to fulfil different requirements such as a safe handling, high detonation properties or high thermal stability.[2] The main goal is to substitute the current mostly used secondary explosive RDX and TNT due to its high toxicity to the environment and humans.[3] Modern research for alternatives to RDX and TNT focus on nitrogen-rich azoles, which show good sensitivity values, possess high positive heats of formation and mainly generate environmentally friendly dinitrogen gas during decomposition.[4] The heats of formation increase with the number of nitrogen atoms within the ring from imidazoles tetrazoles (Figure 5.1).[5] 1,2,4-Triazoles are suitable heterocycles as building blocks for energetic materials due to the high nitrogen content, positive heat of formation and good thermal stability.[6] The introduction of oxygen to an azole leads to oxadiazoles, which combine a good oxygen balance, high energetic performance and likewise high thermal stability.[2c, 7]

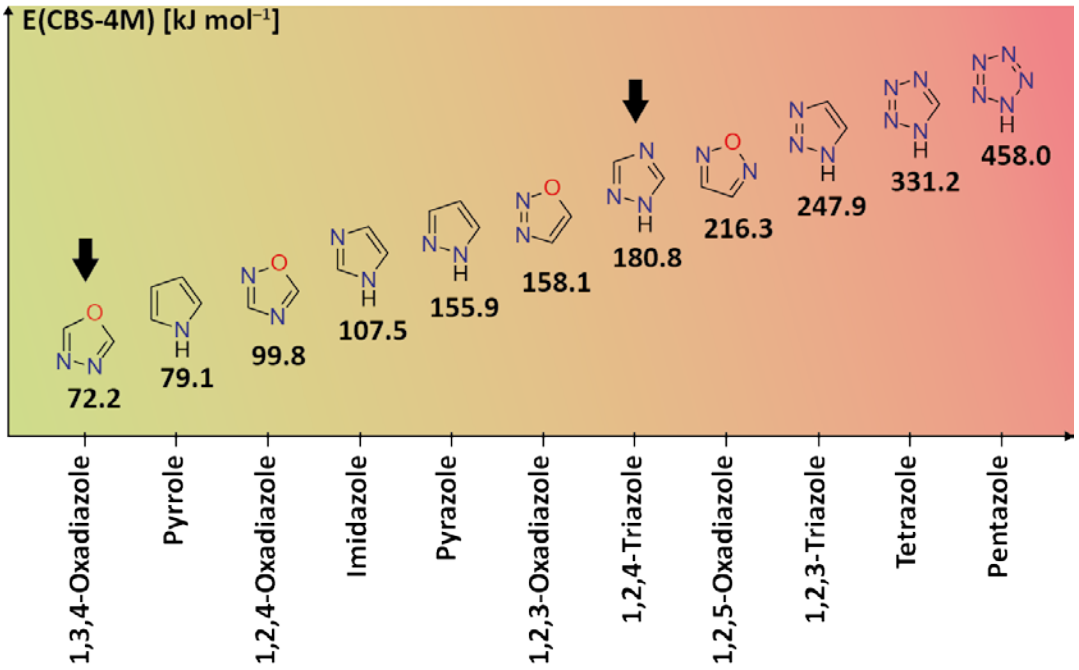

Figure 5.1. Overview of the heat of formation in kJ mol^{-1} of selected azoles.

A huge number of C–C bonded bisheterocyclic nitrogen-rich compounds combining triazoles, tetrazoles, pyrazoles and oxadiazoles have been synthesized in the past showing promising physicochemical and energetic properties (Figure 5.2).[6b, 7b, 8]

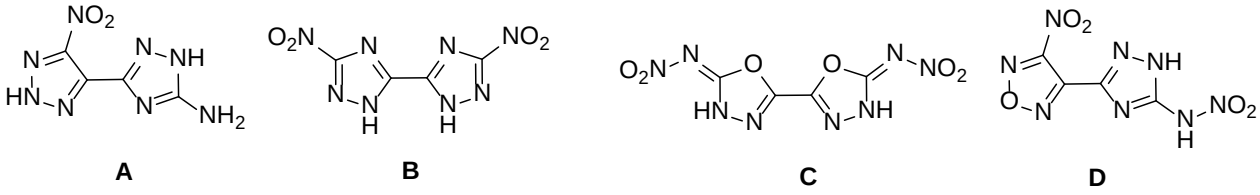

Figure 5.2. Different energetic materials based on bisheterocyclic compounds: A) 4-Nitro-5-(5-amino-1,2,4-triazol-3-yl)-2H-1,2,3-triazole[6a], B) 3,3'-Dinitro-5,5'-bis(1H-1,2,4-triazole)[6b], C) 2,2'-Dinitramino-5,5'-bi(1-oxa-3,4-diazole)[7b], D) 3-Nitro-4-(5-nitramino-1,2,4-triazol-3-yl)furazane[8a].

Bisheterocyclic compounds consisting of a 1,2,4-triazole and a 1,3,4-oxadiazole have not been reported in the literature yet. This contribution reports on the synthesis and intensive characterization of 3-amino-5-(5-amino-1*H*-1,2,4-triazol-3-yl)-1,3,4-oxadiazole (**5**) and 3-amino-5-(5-nitro-1*H*-1,2,4-triazol-3-yl)-(3-amino1,3,4-oxadiazole (**6**). In addition, four energetic salts with the derivative **6** were obtained. Both compounds **5** and **6** can be used as suitable precursors for the synthesis of energetic materials.

5.2 Results and Discussion

5.2.1 Synthesis

5-Amino-1*H*-1,2,4-triazole-3-carboxylic acid was used as the starting material for the synthesis of the heterocyclic compounds **5** and **6** (Scheme 5.1). The concept for the synthesis of 2-amino-5-(5-amino-1*H*-1,2,4-triazol-3-yl)-1,3,4-oxadiazole (**5**) was to obtain the triazole carboxylate, convert this compound into the triazole carbohydrazine (**3**) and perform a ring closure to yield the triazole-oxadiazole product. The first step was performed according to the know literature by reacting the starting material with thionyl chloride in abs. EtOH which lead to the formation of the carboxylic acid ester (**1**).[9] The reaction of compound **1** with hydrazine hydrate in MeOH was carried out similar to the work of Metelkina *et al.* leading to the formation of the triazole carbohydrazone derivative (**3**).[10] 2-Amino-5-(5-amino-1*H*-1,2,4-triazol-3-yl)-1,3,4-oxadiazole (**5**) was obtained by reacting **3** with the base KOH followed by the ring closure with BrCN.[11,12] 2-Amino-5-(5-nitro-1*H*-1,2,4-triazol-3-yl)-1,3,4-oxadiazole (**6**) was obtained similar to the synthesis of **5**. For this purpose, compound **1** was nitrated with $NaNO_2$ and H_2SO_4 according to the modified literature method to yield the nitro derivative **2**.[13,14] Subsequent reaction first with hydrazine hydrate leads to the formation of compound **4** which can be further converted to the desired product **6** with BrCN and KOH.

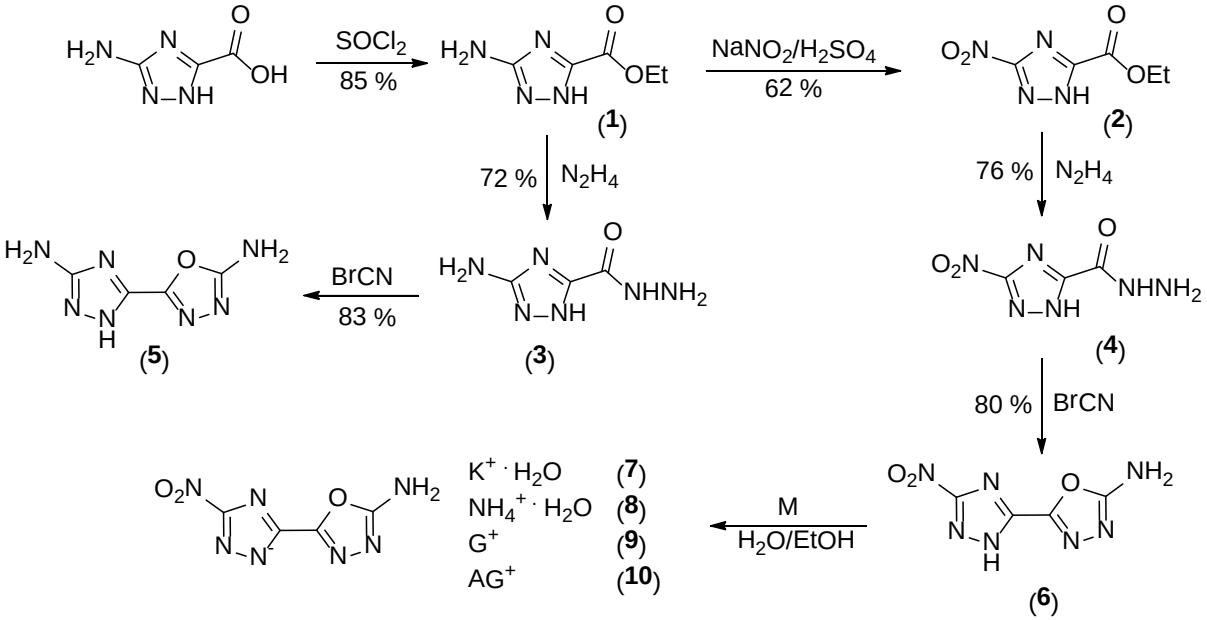

Scheme 5.2. Synthesis of 2-amino-5-(5-amino-1*H*-1,2,4-triazol-3-yl)-1,3,4-oxadiazole (**5**) and 2-amino-5-(5-nitro-1*H*-1,2,4-triazol-3-yl)-1,3,4-oxadiazole (**6**) and energetic salts (**7**–**10**).

Different methods for improving the energetic character of azoles are known such as salt formation, *N*-oxidation, *N* or *C* functionalization, methylene or ethylene bridging, methylation or azo bridging.[2a,8b,16] The bisheterocylic compounds (**5** and **6**) are suitable to serve as precursors for improving their energetic characteristics by synthesizing nitrogen-rich salts, *N*-oxidation or *N*-functionalization. For this purpose, compound **6** was reacted with the four different bases potassium carbonate, ammonia, guanidinium carbonate and aminoguanidinium carbonate.

5.2.2 NMR and Vibrational Spectroscopy

All compounds (**1**–**10**) were characterized by ^{1}H, ^{13}C NMR spectroscopy, elemental analysis and IR spectroscopy. In the ^{1}H NMR spectra, four signals were observed for compound **1** (12.60, 6.20, 4.22 and 1.26 ppm) and two for compound **2** (4.43 and 1.35 ppm). The carbohydrazide derivative **3** shows four signals (12.48–3.66 ppm) in the ^{1}H spectrum whereas compound **4** only two signals at 9.35 and 4.11 ppm. The desired heterocycle **5** exhibit three signals (12.61, 7.21 and 6.27 ppm) in the ^{1}H spectrum, whereas compound **6** shows only one resonance at 7.70 ppm. Both ester compounds **1** and **2** exhibit five resonances in the ^{13}C NMR spectrum in the range of 162.2–13.9 ppm and the carbohydrazides **3** and **4** show only three resonances. The heterocyclic compounds **5** and **6** show four resonances in the ^{13}C NMR spectra. For the energetic salts **7** and **8** were observed only four resonances in the ^{13}C NMR spectrum whereas for the compounds **9** and **10** exhibit five signals.

IR spectra of compounds **1**–**10** were measured and all observed frequencies are reported in the Supporting Information. The deformation vibration of the amino groups for the guanidinium and aminoguanidinium salts **9** and **10** were observed at 1655 and 1652 cm^{-1}, respectively. In addition, the asymmetric and symmetric vibration of the amino groups of compound **10** were observed at 3380 and 3328 cm^{-1}.[15]

5.2.3 X-Ray crystallography

Suitable crystals of compounds **3** and **7**–**10** were obtained by recrystallization. The structures are shown in Figures 5.3–5.5 and the structure of **3** and **8** can be found in the Supporting Information. Further information regarding the crystal-structure determinations have been deposited with the Cambridge Crystallographic Data Centre as supplementary publication Nos. 1869975 (**3**), 1869977 (**7**), 1869976 (**8**), 1869978 (**9**) and 1869979 (**10**).

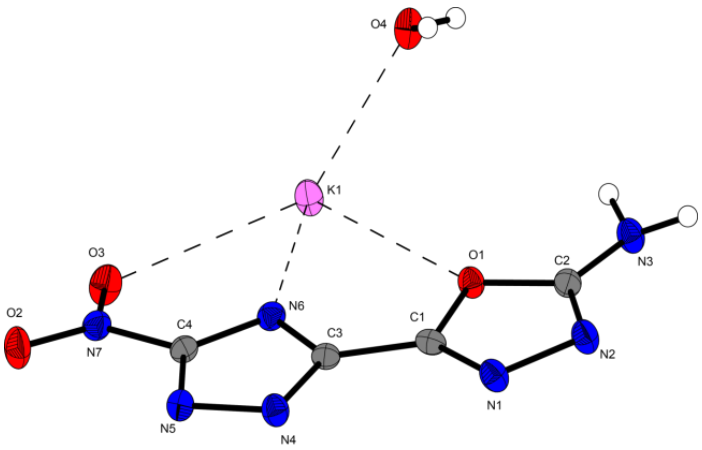

Figure 5.3. Molecular unit of compound **7** in the crystalline state. Ellipsoids correspond to 50% probability levels. Hydrogen radii are arbitrary. Selected bond lengths (Å) and angles [deg]: O1–C2 1.362(2), O1–C1 1.376(2), O1–K1 3.3846(13), N6–K1 2.7756(15), K1–O4 2.7078(15), N2–C2 1.305(2), N1–N2 1.414(2), N1–C1 1.286(2), N4–N5 1.364(2), O3–N7 1.2280(19), O2–N7 1.232(2), N6–C4 1.334(2), C1–C3 1.454(3), C1–N1–N2 106.09(14), C2–N2–N1 106.10(14), N2–C2–O1 112.46(15), C4–N6–C3 98.80(14), C2–O1–C1 102.32(13), O3–N7–O2 123.55(16), C1–N1–N2–C2 –0.1(2), C3–N4–N5–C4 –0.01(18), N2–N1–C1–C3 –179.28(18), N2–N1–C1–O1 0.1(2), C2–O1–C1–C3 179.44(15), N1–N2–C2–N3 –176.45(18), C1–O1–C2–N3 176.87(16), C4–N6–C3–N4 0.48(19), C4–N6–C3–C1 –179.62(16), O3–N7–C4–N5 –171.11(16).

The crystal structure of potassium 5-(2-amino-1,3,4-oxadiazolyl)-(3-nitrotriazolate) monohydrate **7** is shown in Figure 5. 4 with bond length and angles. Compound **7** crystallizes as colorless rods in the monoclinic space group $P\ 2_1/n$ with four molecules in the unit cell. The volume of the unit cell is 898.68(5) Å^3 and lattice constants are a = 6.6407(2) Å, b = 11.2308(4) Å, c = 12.3709(3) Å and β = 103.0810(10) °. The density is 1.872 g cm^{-3} measured at a temperature of 100(2) K. The potassium salt of 5-(5-nitro-4*H*-1,2,4-triazol-3-yl)-2-amino-1,3,4-oxadiazole crystallize with one molecule water. Looking on the torsion angles, it is visible that the triazole-oxadiazole scaffold is planar. Furthermore, the oxygen atom of the oxadiazole, nitrogen N6 of the triazole and one oxygen atom of the nitro group are aligned at the potassium cation, what leads to a torsion of the nitro group against the plane. The oxygen atom of the crystal water is coordinating the cation, too. The distances to the potassium atom vary from 2.7078(15) Å (K1–O4) up to 3.3846(13) Å. The bond lengths and angles in the triazole correspond to the known values, while the bond angle of the nitro group O3–N7–O2 123.55(16) ° is a bit reduced compared to the expected value of about 125 °.[18,20] The bond between the triazole and the oxadiazole has a length of 1.454(3) Å. Further to enhance the stability of the molecule small deformation of the oxadiazole scaffold are observable. This can be seen for example at elongation of N1–N2 (1.414(2) Å) or the reduction of N1–C1 (1.286(2) Å). The bond angles also differ a bit from the known values for 1,3,4-oxadiazoles, also the bond angle of the crystal water molecule is enlarged up to 108(3) °.[21,22]

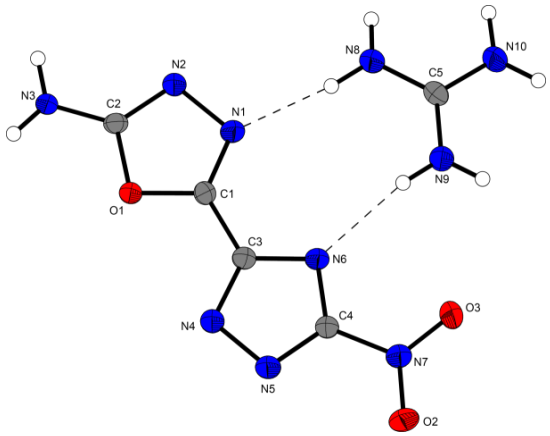

Figure 5.4. X-ray structure of compound **9**. Ellipsoids are drawn at the 50% probability level. Selected distances [Å]: C1–C3 1.448 (2), C4–N7 1.444 (2), C2–N3 1.329 (2). Selected bond angles [°]: O2–N7–C4 117.95 (15), N10–C5–N 9 120.12 (18), N3–C2–O1 118.65 (16). Selected torsion angles [°]: O1–C1–C3 N4 −0.8 (3), N6–C4–N7 O3 1.7 (3).

Compound **9** crystallizes in the monoclinic space group *C2/c* with a cell volume of 1991.0(3) Å^3 and eight formula units per cell. The cell constants are a = 20.3525(18) Å, b = 5.4863(4) Å and c = 18.5795(14) Å, while the density is 1.709 g cm^{-3}. The distance between the two heterocycles of the molecule is C1–C3 1.448(2) Å. It is in the range of single and double bond like in all the other heterocycle atoms.[23] One guanidinium cation is bound by two hydrogen bonds to the N1-atom and the N6-atom of the anion. The angle N10–C5–N9 is at 120.12(18) ° which is means the guanidine is planar and the positive charge is split over the whole cation. The torsion angles O1–C1–C3–N4 with 0.8(3)° and N6–C4–N7–O3 with 1.7(3) ° are close to zero, why the anion is almost planar.

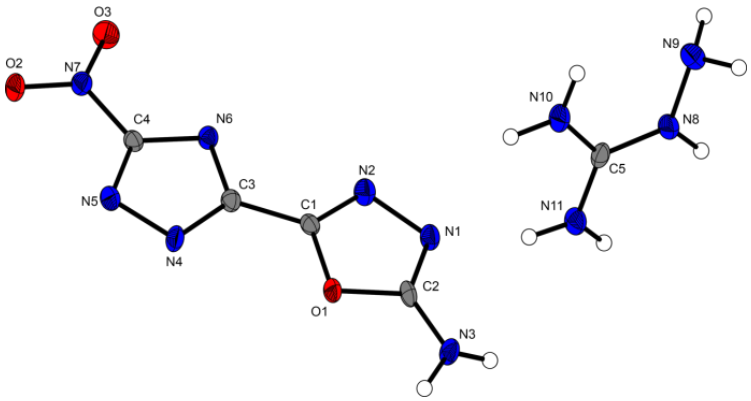

Figure 5.5. Crystal structure of aminoguanidinium 5-(5-amino-1,3,4-oxadiazol-2-yl)-3-nitro-1,2,4-triazolate (**10**). Ellipsoids of non-hydrogen atoms are drawn at the 50 % probability level. Selected distances [Å]: C4–N7 1.346(4), C2–N3 1.303(4), N7–C4 1.442(4), C2–N3 1.335(5). Selected bond angles [°]: C3–C1–O1 120.4(3), O1–C2–N3 118.0(3), C4–N6–C3 98.5(2), C1–O1–C2 101.6(2). Selected torsion angles [°]: N4–C3–C1–N2 176.5(3), O2–N7–C4–N5 −1762(3), N3–C2–N1–N2 −179.0(3), N6–C3–C1–N2 −1.0(5).

Compound **10** crystallizes in the monoclinic space group $P2_1/n$ with a cell volume of 1061.8 (2) Å^3 and four formula units per cell. The cell constants are a = 13.4494 (17) Å, b = 5.2321 (6) Å and c = 15.302 (2) Å, while the density is 1.697 g cm^{-3}. The distance between the two heterocycles of the molecule is C1-C3 1.454 (5) Å. It is in the range of single and double bond like in all the other heterocycle atoms.[23] One aminoguanidinium cation is bound by two hydrogen bonds to the N1-atom and the N2-atom of the anion. The angle N10 C5 N11 is at 120.5 (3) ° which means the aminoguanidine is planar and the positive charge is split over the whole cation. Also the torsion angle N11–C5–N8–N9 with -178.7(3) ° reinforces the assumption of a planar cation. The torsion angles O1–C1–C3–N4 with 0.3(5) ° and N6–C4–N7–O3 with 4.4(5) ° are close to zero which means that the anion is almost planar.

5.2.4 Thermal Analysis, Sensitivities, Physicochemical and energetic properties

Since compounds **7**–**10** can be classified as energetic materials their energetic behaviour was extensively investigated. All theoretical and experimentally determined values for the energetic salts of compound **6** are reported in Table 5.1. The thermal behaviour was investigated with a LINSEIS DSC PT10 instrument at a heating rate of 5 °C min^{-1}. The decomposition point of the energetic salts is in the range of 240 to 300 °C, whereas the lowest decomposition (onset) was observed for the aminoguanidinium salt (**10**, 246 °C) and the highest for the guanidinium salt (**9**, 296 °C). The sensitivities of all four compounds (**7**–**10**) were measured according the BAM standards.[24] The energetic salts show no sensitivity toward external stimuli with sensitivity values for friction of < 360 N and impact < 40 J, for each compound, and can be classified as insensitive. The reported detonation parameters were calculated using the EXPLO5_V6.03 computer code.[25] The EXPLO5 detonation parameters of the energetic salts **7**–**10** were calculated by using the room-temperature density values obtained from the X-ray structures as described in reference.[26] The potassium (**7**) and ammonium (**8**) salts were obtained as monohydrates with recalculated room temperature densities of 1.84 and 1.61 g cm^{-3}, respectively. The highest detonation pressure was calculated for the aminoguanidinium salt **10** (V_D = 7672 m s^{-1}) and the lowest for the potassium monohydrate salt **7** (V_D = 6965 m s^{-1}).

Table 5.3. Physicochemical properties and detonation parameters of **5–10** compared to RDX.

	5	**6**	**7 ·H_2O**	**8 ·H_2O**	**9**	**10**	**RDX[1d]**
Formula	$C_4H_5N_7O$	$C_4H_3N_7O_3$	$C_4H_2N_7O_3K$	$C_4H_6N_8O_3$	$C_5H_8N_{10}O_3$	$C_5H_9N_{11}O_3$	$C_3H_6N_6O_6$
FW [g mol^{-1}]	167.13	197.11	253.24	232.18	256.19	271.23	221.12
IS [J][a]	40	40	40	40	40	40	7.5
FS [N][b]	360	360	360	360	360	360	120
ESD [J][c]	1.5	1.5	1.5	1.5	1.5	1.5	0.2
N [%][d]	58.7	49.7	41.7	52.3	54.7	56.8	37.8
Ω [%][e]	–90.9	–52.8	–41.1	–55.1	–68.7	–67.8	–21.6
$T_{dec.}$ [°C][f]	309 (melt.)	245	254	276	296	246	205
ρ [g cm^{-3}] (298K)[g]	1.90	1.92[o]	1.84	1.61	1.66	1.64	1.81
$\Delta_f H°$ [kJ mol^{-1}][h]	140.3	224.2	–277.1	–123.6	133.4	241.0	70.3
$\Delta_f U°$ [kJ kg^{-1}][i]	935.6	1219.2	–1020.7	–425.5	622.2	993.7	417.0
EXPLO5 V6.03:[g]							
$-\Delta_E U°$ [kJ kg^{-1}][j]	1996	3933	3099	3153	2982	3281	5845
T_E [K][k]	1737	2936	2446	2440	2334	2462	3810
p_{CJ} [kbar][l]	238	285	179	190	197	206	345
V_D [m s^{-1}][m]	8265	8477	6965	7337	7500	7672	8861
V_0 [L kg^{-1}][n]	429	413	438	485	473	478	785

[a] impact sensitivity (BAM drophammer, 1 of 6); [b] friction sensitivity (BAM friction tester, 1 of 6); [c] electrostatic discharge device (OZM); [d] nitrogen content; [e] oxygen balance; [f] decomposition temperature from DTA (β = 5°C); [g] recalculated from low temperature X-ray densities ($\rho_{298K} = \rho_T / (1+\alpha_V(298-T_0)$; $\alpha_V = 1.5\ 10^{-4}$ K^{-1}); [h] calculated (CBS-4M) heat of formation; [i] calculated energy of formation; [j] energy of explosion; [k] explosion temperature; [l] detonation pressure; [m] detonation velocity; [n] assuming only gaseous products; [o] measured pycnometrically at room temperature.

5.3 Conclusion

In conclusion, we reported on the synthesis of two new energetic derivatives based on the heterocycles 1,2,4-1*H*-triazole and 1,3,4-oxadiazole. 2-Amino-5-(5-amino-1*H*-1,2,4-triazol-3-yl)-1,3,4-oxadiazole (**5**) can be synthesized in a three-step procedure and 2-amino-5-(5-nitro-1*H*-1,2,4-triazol-3-yl)-1,3,4-oxadiazole (**6**) in a four-step procedure by using 5-amino-1*H*-1,2,4-triazole-3-carboxylic acid as the starting material. The ring closing toward the 1,3,4-oxadiazole was carried out using cyanogen bromide and the corresponding triazole-carbohydrazides. Compounds **5** and **6** show high thermal stabilities, high densities (ρ = 1.90 and 1.92 g cm^{-3}) and accetable detonation performances (V_D = 8265 and 8477 m^{-1}). Both heterocycles are not sensitive toward impact friction or ESD. Compound **6** was further functionalized by reacting it with four bases to yield the potassium (**7**), ammonium (**8**), guanidinium (**9**) and aminoguanidinium (**10**) salt. The synthesized ionic derivatives of compound **6** are insensitive toward external stimuli with sensitivity values for impact of 40 J and for friction with 360 N, each. The thermal stability of all four compounds ranges from 246 °C for the aminoguanidinium salt (**10**) to 296 °C for the guanidinium salt (**9**). 2-Amino-5-(5-amino-1*H*-1,2,4-triazol-3-yl)-1,3,4-oxadiazole (**5**) and 2-amino-5-(5-nitro-1*H*-1,2,4-triazol-3-yl)-1,3,4-oxadiazole (**6**) can be used as precursors for the synthesis of new energetic materials.

5.4 References

[1] a) H. Gao, J. M. Shreeve, *Chem. Rev.* **2011**, *111*, 7377–7436; b) D. M. Badgujar, M. B. Talawar, S. N. Asthana, P. P. Mahulikar, *J. Hazard. Mater.* **2008**, *151*, 289–305; c) Y. Tang, C. He, G. H. Imler, D. A. Parrish, J. M. Shreeve, *J. Mater. Chem. A* **2018**, *6*, 5136–5142; d) T. M. Klapötke, *Chemistry of High-Energy Materials*, 4th ed., De Gruyter, Berlin, **2017**.

[2] a) D. Fischer, J. L. Gottfried, T. M. Klapötke, K. Karaghiosoff, J. Stierstorfer, T. G. Witkowski, *Angew. Chem. Int. Ed.* **2016**, *55*, 16132–16135; b) D. Kumar, G. H. Imler, D. A. Parrish, J. M. Shreeve, *New J. Chem.* **2017**, *41*, 4040–4047; c) T. M. Klapötke, T. G. Witkowski, *ChemPlusChem* **2016**, *81*, 357–360.

[3] a) J. K. Stanley, G. R. Lotufo, J. M. Biedenbach, P. Chappell, K. A. Gust, *Environ. Toxicol. Chem.* **2015**, *34*, 873–879; b) G. A. Parker, G. Reddy, M. A. Major, *International Journal of Toxicology* **2006**, *25*, 373–378; c) H. Abadin, C. Smith, *Toxicological Profile For RDX*, U.S. Department of Health and Human Serivces, Public Health Service, Agency for Toxic Substances and Disease

Registry, **2012**, available online at https://www.atsdr.cdc.gov/toxprofiles/tp78.pdf; d) Y. Weifei, L. Longyu, C. Feilan, H. Mingzhong, T. Dongmei, F. Guijuan, H. Shilong, L. Huanchang, *Int. J. Ecotoxicol Ecobiol.* **2016**, *1*, 88–93.

[4] a) D. Kumar, G. H. Imler, D. A. Parrish, J. M. Shreeve, *Chem. Eur. J.* **2017**, *23*, 7876–7881; b) P. Yin, L. A. Mitchell, D. A. Parrish, J. M. Shreeve, *Chem. Asian J.* **2017**, *12*, 378–384; c) T. M. Klapötke, P. C. Schmid, S. Schnell, J. Stierstorfer, *J. Mater. Chem. A* **2015**, *3*, 2658–2668; d) Y. Tang, C. He, L. A. Mitchell, D. A. Parrish, J. M. Shreeve, *J. Mater. Chem. A* **2016**, *4*, 3879–3885; e) Y. Liu, J. Zhang, K. Wang, J. Li, Q. Zhang, J. M. Shreeve, *Angew. Chem. Int. Ed.* **2016**, *55*, 11548–11551; f) M. B. Talawar, R. Sivabalan, T. Mukundan, H. Muthurajan, A. K. Sikder, B. R. Gandhe, A. S. Rao, *J. Hazard. Mater.* **2009**, *161*, 589–607; g) O. S. Bushuyev, P. Brown, A. Maiti, R. H. Gee, G. R. Peterson, B. L. Weeks, L. J. Hope-Weeks, *J. Am. Chem. Soc.* **2012**, *134*, 1422–1425.

[5] Z. Yu, E. R. Bernstein, *J. Phys. Chem. A* **2013**, *117*, 10889–10902.

[6] a) Z. Xu, G. Cheng, S. Zhu, Q. Lin, H. Yang, *J. Mater. Chem. A* **2018**, *6*, 2239–2248; b) A. A. Dippold, T. M. Klapötke, *Chem. Eur. J.* **2012**, *18*, 16742–16753.

[7] a) Y. Tang, H. Gao, L. A. Mitchell, D. A. Parrish, J. M. Shreeve, *Angew. Chem. Int. Ed.* **2016**, *55*, 3200–3203; b) T. S. Hermann, K. Karaghiosoff, T. M. Klapötke, J. Stierstorfer, *Chem. Eur. J.* **2017**, *23*, 12087–12091.

[8] a) Z. Xu, G. Cheng, H. Yang, J. Zhang, J. n. M. Shreeve, *Chem. Eur. J.* **2018**, *24*, 10488–10497; b) N. Fischer, D. Fischer, T. M. Klapötke, D. G. Piercey, J. Stierstorfer, *J. Mater. Chem.* **2012**, *22*, 20418–20422; c) D. Fischer, T. M. Klapötke, J. Stierstorfer, *Angew. Chem. Int. Ed.* **2014**, *53*, 8172–8175; d) T. M. Klapötke, M. Leroux, P. C. Schmid, J. Stierstorfer, *Chem. Asian J.* **2016**, *11*, 844–851; e) K. Hafner, T. M. Klapötke, P. C. Schmid, J. Stierstorfer, *Eur. J. Inorg. Chem.* **2015**, *2015*, 2794–2803; f) A. A. Dippold, T. M. Klapötke, *Chem. Asian J.* **2013**, *8*, 1463–1471.

[9] A. A. Dippold, T. M. Klapötke, *Chem. Asian J.* **2013**, *8*, 1463–1471.

[10] E. L. Metelkina, T. A. Novikova, S. N. Berdonosova, D. Y. Berdonosov, *Russ. J. Org. Chem.* **2005**, *41*, 440–443.

[11] H. Gehlen, K. H. Uteg, *Arch. Pharm.* **1968**, *301*, 911–922.

[12] S. Sanchit, P. S.N., *Int. J. Res. Ayurveda Pharm.* **2011**.

[13] L. I. Bagal, M. S. Pevzner, A. N. Frolov, N. I. Sheludyakova, *Chem. Heterocycl. Compd.* **1970**, *6*, 240–244.

[14] A. A. Dippold, D. Izsák, T. M. Klapötke, *Chem. Eur. J.* **2013**, *19*, 12042–12051.

[15] M. Hesse, H. Meier, B. Zeeh, *Spektroskopische Methoden in der organischen Chemie*, 7. überarbeitete Auflage ed., Georg Thieme Verlag, Stuttgart, New York, **2005**.

[16] F. H. Allen, O. Kennard, D. G. Watson, L. Brammer, A. G. Orpen, R. Taylor, *J. Chem. Soc., Perkin Trans. 2* **1987**, 1–19.

[17] E. Wiberg, N. Wiberg, *Lehrbuch der anorganischen Chemie*, 102. Auflage ed., De Gruyter, Berlin, New York, **2007**.

[18] L. Pauling, *The Nature of the Chemical Bond and the Structure of Molecules and Crystals: An Introduction to Modern Structural Chemistry*, Cornell University Press, New York, **1960**.

[19] J. Zhang, T. Zhang, K. Yu, *Struc. Chem.* **2006**, *17*, 249–254.

[20] A. D. Vasiliev, A. M. Astachov, R. S. Stepanov, S. D. Kirik, *Acta Cryst., Sect. C* **1999**, *55*, 830–832.

[21] R. D. Brown, B. A. W. Coller, J. E. Kent, *Theor. Chim. acta* **1968**, *10*, 435–446.

[22] A. R. Hoy, P. R. Bunker, *J. Mol. Spectrosc.* **1979**, *74*, 1–8.

[23] S. Sanchit, S. N. Pandeya, *Int. J. Res. Ayurveda Pharm.* **2011**, *2*, 459–468.

[24] a) Reichel & Partner GmbH, http://www.reichelt-partner.de; b) Test methods according to the UN Recommendations on the Transport of Dangerous Goods, Manual of Test and Criteria, 4th edn., United Nations Publication, New York and Geneva, **2003**, ISBN 92–1-139087 7, Sales No. E.03.VIII.2; 13.4.2 Test 3 a (ii) BAM Fallhammer.

[25] M. Sućeska, *EXPLO5 Version 6.03 User's Guide*, Zagreb, Croatia: OZM; **2015**.

[26] J. S. Murray, P. Politzer, *J. Mol. Model* **2014**, *20*, 2223–2227.

5.5 Supplementary Information

5.5.1 X-ray Diffraction

Single crystals were picked and measured on an Oxford Xcalibur3 diffractometer with a Spellman generator (voltage 50 kV, current 40 mA) and a CCD area detector for data collection using Mo-*K*α radiation (λ = 0.71073 Å). The crystal structures of compound **5** was determined on a Bruker D8 Venture TXS diffractometer equipped with a multilayer monochromator, a Photon 2 detector, and a rotating-anode generator (MoKα radiation). The data collection was carried out using CRYSALISPRO software[S1] and the reduction were performed. The structures were solved using direct methods (SIR-92,[S2] SIR-97[S3] or SHELXS-97[S4]) and refined by full-matrix least-squares on *F*2 (SHELXL[S4]): The final check was done with the PLATON software[S5] integrated in the WinGX software suite. The non-hydrogen atoms were refined anisotropically and the hydrogen atoms were located and freely refined. The absorptions were corrected by a SCALE3 ABSPACK multiscan method.[S6] The DIAMOND2 plots are shown with thermal ellipsoids at the 50% probability level and hydrogen atoms are shown as small spheres of arbitrary radii. The SADABS program embedded in the Bruker APEX3 software has been used for multi-scan absorption corrections in all structures.[S7]

Table 5.S1. Crystallographic data and refinement parameters of compound **3, 7**, **8, 9** and **10**.

	3	**7**	**8**	**9**	**10**
Formula	$C_3H_6N_6O$	$C_4H_4N_7O_4K$	$C_7H_4N_8O_8$	$C_5H_8N_{10}O_3$	$C_5H_9N_{14}O_3$
FW [g mol^{-1}]	142.14	253.24	232.18	256.21	271.23
Crystal system	Monoclinic	Monoclinic	Monoclinic	Monoclinic	Monoclinic
Space Group	*P*-21/n	$P2_1/c$	$P2_1$/n	$C2/c$	$P2_1/n$
Color / Habit	Colorless	Orange	Orange	Yellow	Colorless
Size [mm]	0.09 × 0.10 × 0.59	0.06 × 0.14 × 0.34	0.01 × 0.05 × 0.3	0.10 × 0.25 × 0.5	0.01 × 0.03 × 0.05
a [Å]	5.1775(5)	6.6407(2)	6.690(5)	20.3525(18)	13.4494(17)
b [Å]	8.5646(7)	11.2308(4)	11.426(5)	5.4863(4)	5.2321(6)
c [Å]	13.1752(12)	12.3709(3)	12.614(5)	18.5795(14)	15.302(2)
α [°]	90	90	90	90	90
β [°]	97.917(11)	103.081(1)	104.623(5)	106.316(9)	99.583(5)
γ [°]	90	90	90	90	90
V [Å^3]	578.66(9)	898.69(5)	933.0(9)	1991.0(3)	1061.8(2)
Z	4	4	4	8	4
$\rho_{calc.}$ [g cm^{-3}]	1.632	1.872	1.653	1.709	1.697
μ [mm^{-1}]	0.130	0.608	0.145	0.143	0.142
F(000)	296	512	480	1056	560
$\lambda_{MoK\alpha}$[Å]	0.71073	0.71073	0.71073	0.71073	0.71073
T [K]	173	100	123	130	100
ϑ min-max [°]	4.5, 26.2	3.1, 26.0	4.3, 26.5	4.2, 26.5	2.7, 25.4
Dataset h; k; l	−6:6;−10:10; −16:16	−8:8;−13:13; −15:15	−8:8;−14:13; −15:15	−25:25;−6:6; −23:16	−16:15;−6:5; −18:18
Reflect. coll.	4314	10517	7208	7599	6058
Independ. refl.	1171	1757	1925	2051	1946
R_{int}	0.032	0.040	0.057	0.042	0.049
Reflection obs.	943	1487	1398	1622	1566
No. parameters	115	161	177	195	208
R_1 (obs)	0.0394	0.0279	0.0531	0.0391	0.0613
wR_2 (all data)	0.1091	0.0682	0.1445	0.1020	0.1580
S	1.04	1.06	1.05	1.05	1.09
Resd. Dens.[e Å^{-3}]	−0.19, 0.30	−0.25, 0.23	−0.29, 0.44	−0.22, 0.27	−0.26, 0.47
Device type	Oxford Xcalibur3	Bruker D8 Venture TXS	Oxford Xcalibur3	Oxford Xcalibur3	Bruker D8 Venture TXS
Solution	SIR-92	SIR-92	SIR-92	SIR-92	SIR-92
Refinement	SHELXL-2013	SHELXL-2013	SHELXL-2013	SHELXL-2013	SHELXL-2013
Absorpt. corr.	multi-scan	multi-scan	multi-scan	multi-scan	multi-scan
CCDC	1869975	1869977	1869976	1869978	1869979

5.5.2 Heat of formation calculations

All quantum chemical calculations were carried out using the Gaussian G09 program package.[S8] The enthalpies (H) and free energies (G) were calculated using the complete basis set (CBS) method of Petersson and coworkers in order to obtain very accurate energies. The CBS models are using the known asymptotic convergence of pair natural orbital expressions to extrapolate from calculations using a finite basis set to the estimated CBS limit. CBS-4 starts with an HF/3-21G(d) geometry optimization; the zero point energy is computed at the same level. It then uses a large basis set SCF calculation as a base energy, and an MP2/6- 31+G calculation with a CBS extrapolation to correct the energy through second order. A MP4(SDQ)/6-31+ (d,p) calculation is used to approximate higher order contributions. In this study, we applied the modified CBS-4M.

Heats of formation of the synthesized ionic compounds were calculated using the atomization method (equation S1) using room temperature CBS-4M enthalpies, which are summarized in Table 5.S1.[S9,S10]

$$\Delta_f H^\circ_{(g,\,M,\,298)} = H_{(Molecule,\,298)} - \sum H^\circ_{(Atoms,\,298)} + \sum \Delta_f H^\circ_{(Atoms,\,298)} \qquad (E1)$$

Table 5.S2. CBS-4M enthalpies for atoms C, H, N and O and their literature values for atomic $\Delta H^\circ_f{}^{298}$ / kJ mol^{-1}

	$-H^{298}$ [a.u.]	NIST [S11]
H	0.500991	218.2
C	37.786156	717.2
N	54.522462	473.1
O	74.991202	249.5

For neutral compounds the sublimation enthalpy, which is needed to convert the gas phase enthalpy of formation to the solid state one, was calculated by the *Trouton* rule.[S12] For ionic compounds, the lattice energy (U_L) and lattice enthalpy (ΔH_L) were calculated from the corresponding X-ray molecular volumes according to the equations provided by *Jenkins* and *Glasser*.[S13] With the calculated lattice enthalpy the gas-phase enthalpy of formation was converted into the solid state (standard conditions) enthalpy of formation. These molar standard enthalpies of formation (ΔH_m) were used to calculate the molar solid state energies of formation (ΔU_m) according to equation E2.

$$\Delta U_m = \Delta H_m - \Delta n\, RT \qquad (E2)$$

(Δn being the change of moles of gaseous components)

The calculation results are summarized in Table 5.S3.

Table 5.S3. Heat of formation calculation results.

	$-H^{298}$ [a] [a.u.]	$\Delta_f H°$(g,M) [kJ mol^{-1}] [b]	V_M [Å^3][c]	$\Delta U_L, \Delta H_L$;[d] [kJ mol^{-1}]	$\Delta_f H°$(s) [e] [kJ mol^{-1}]	Δn [f]	$\Delta_f U$(s) [g] [kJ kg^{-1}]
5		59.6			140.3	6.5	935.6
6		275.6			224.2	6.5	1219.2
6 anion	761.565028	41.7					
K+	599.035967	487.4					
NH4+	56.796608	635.8					
G+	205.453192	571.9					
AG+	260.701802	671.6					
7 hydrate			898.69	599.1, 562.9	–277.1	–7.5	–1020.7
8 hydrate			933.00	553.6, 557.3	–123.6	–10	–425.5
9		613.6	1991.0	476.8, 480.2	133.4	10.5	822.2
10		713.3	1061.8	468.8, 472.3	241.0	11.5	993.7

[a] CBS-4M electronic enthalpy; [b] gas phase enthalpy of formation; [c] molecular volumes taken from X-ray structures and corrected to room temperature; [d] lattice energy and enthalpy (calculated using Jenkins and Glasser equations); [e] standard solid state enthalpy of formation; [f] Δn being the change of moles of gaseous components when formed; [g] solid state energy of formation.

5.5.3 Experimental Part

General Procedures

Differential Scanning Calorimetry (DSC) was recorded on a LINSEIS DSC PT10 with about 1 mg substance in a perforated aluminum vessel with a heating rate of 5 K·min^{-1} and a nitrogen flow of 5 dm^3·h^{-1}. The NMR spectra were carried out using a 400 MHz instruments JEOL Eclipse 270, JEOL EX 400 or a JEOL Eclipse 400 (^{1}H 399.8 MHz, ^{13}C 100.5 MHz, ^{14}N 28.9 MHz, and ^{15}N 40.6 MHz). Chemical shifts are given in parts per million (ppm) relative to tetramethylsilane (^{1}H, ^{13}C) and nitromethane (^{14}N, ^{15}N).

Infrared spectra were measured with a Perkin-Elmer Spectrum BX-FTIR spectrometer equipped with a Smiths DuraSamplIR II ATR device. Transmittance values are qualitatively described as “very strong” (vs), “strong” (s), “medium” (m), and “weak” (w). Raman spectra were recorded using a Bruker MultiRAM FT-Raman instrument fitted with a liquid-nitrogen cooled germanium detector and a Nd:YAG laser (λ = 1064 nm). The intensities are quoted as percentages of the most intense

peak and are given in parentheses. DTA spectra were carried out using a OZM DTA 551-EX with a heating rate of 5 K·min^{-1}. Low-resolution mass spectra were recorded with a JEOL MStation JMS 700 (DEI+ / FAB+/−). Elemental analysis (C/H/N) was carried out using a Vario Micro from the Elementar Company. Impact sensitivity tests were performed according to STANAG 4489[S14] modified instruction[S15] using a Bundesanstalt für Materialforschung (BAM) drophammer.[S16] Friction sensitivity tests were carried out according to STANAG 4487[S17] modified instruction[S18] using a BAM friction tester. The grading of the tested compounds results from the "UN Recommendations on the Transport of Dangerous Goods".[S19] ESD values were carried out using the Electric Spark Tester ESD 2010 EN.[S20]

Ethyl 5-amino-1*H*-1,2,4-triazole-3-carboxylate (1)[S21]

5-amino-1*H*-1,2,4-triazole-3-carboxylic acid (20.0 g, 137 mmol, 1.00 eq.) was suspended in ethanol (300 mL) and cooled down to 0 °C. Then thionyl chloride (26.2 g, 220 mmol, 1.60 eq.) was added dropwise at 0 °C and the mixture was stirred for 1 h at this temperature. Subsequently the solution was stirred for 3 d at 75 °C. The solvent was evaporated under reduced pressure and then saturated sodium acetate solution (180 mL) was added. The resulting solid was filtered and washed with water (50 mL) to yield compound (1) as a white powder (20.7 g, 133 mmol, 85 %).

^{1}H-NMR (400 MHz, DMSO-d_6): δ(ppm) = 12.60 (s, 1H, NH), 6.20 (s, 2H, NH_2), 4.21 (q, 2H, ^{3}J = 7.1 Hz, CH_2), 1.26 (t, 3H, ^{3}J = 7.1 Hz, CH_3);^{13}C NMR (101 MHz, DMSO-d_6): δ(ppm) = 160.4 (C=O), 157.4 ($C_{(triazole)}$), 151.9 ($C_{(triazole)}$), 60.3 (CH_2), 14.1 (CH_3); IR (ATR, rel. int.): ν (cm^{-1}) = 3447 (m), 3029 (w), 3000 (w), 2971 (w), 2918 (w), 1723 (s), 1635 (s), 1579 (w), 1507 (m), 1464 (m), 1443 (m), 1389 (m), 1356 (m), 1228 (s), 1155 (w), 1120 (s), 1051 (m), 1028 (s), 876 (w), 855 (m), 793 (m), 756 (m), 718 (s), 659 (m), 630 (m), 544 (w), 528 (w), 515 (w), DSC (5 °C min^{-1}): $T_{melt.}$= 239 °C.

Ethyl 5-nitro-1*H*-1,2,4-triazole-3-carboxylate (2)

Compound (1) (5.00 g, 32.0 mmol, 1.00 eq.) was dissolved in water (40 mL) and sodium nitrate (21.1 g, 320 mmol, 10.0 eq.) was added. Sulfuric acid (20 %, 34.0 mL) was added dropwise over 4 h. Afterwards the mixture was stirred 2 h at 50 °C. The mixture was cooled down to room temperature and sulfuric acid (50 %, 50 mL) was added. The product was extracted with ethyl acetate (3 x 100 mL), the organic layer was separated and saturated $NaHCO_3$ solution (100 mL) was added. The organic layer was separated and the hydrous layer was extracted with ethyl acetate (2 x 70 mL).

The combined organic layers were dried over anhydrous $MgSO_4$ and the solvent was evaporated under reduced pressure to yield compound (2) as a yellow solid (23.70g, 19.8 mmol, 62 %).

^{1}H-NMR (400 MHz, DMSO-d_6): δ(ppm) = 4.43 (q, 2H, ^{3}J = 7.1 Hz, CH_2), 1.35 (t, 3H, ^{3}J = 7.1 Hz, CH_3);^{13}C NMR (101 MHz, DMSO-d_6): δ(ppm) = 162.2 (C=O), 156.1 ($C_{(triazole)}$), 147.6 ($C_{(triazole)}$), 62.7 (CH_2), 13.9 (CH_3); ^{14}N NMR (29 MHz, DMSO-d_6): δ(ppm) = –26; IR (ATR, rel. int.): ν (cm^{-1}) = 3564 (w), 3433 (w), 1920 (m), 1722 (s), 1552 (s), 1485 (m), 1462 (m), 1424 (m), 1382 (m), 1319 (s), 1244 (s), 1185 (m), 1091 (m), 1038 (m), 1016 (s), 842 (m), 801 (m), 759 (m), 652 (s), 601 (s), 550 (s); Mass spectrometry: m/z (FAB$^-$) = 185.1 [M$^-$],

5-Amino-1*H*-1,2,4-triazole-3-carbohydrazide (3)

Compound (1) (12.0 g, 76.8 mmol, 1.00 eq.) was dissolved in methanol (80 mL), hydrazine-monohydrate (11.4 g, 230 mmol, 3.00 eq.) was added slowly. The mixture was stirred for 24 h at 75 °C and cooled down to room temperature. Hydrochloric acid (37 %, 20.0 mL) was added, the solid was filtered and the residue was washed with water (3 x 30 mL), ethyl acetate (2 x 30 mL) and diethylether (2 x 30 mL) to yield compound (3) as a white solid (9.60 g, 55.8 mmol, 72 %).

^{1}H-NMR (400 MHz, DMSO-d_6): δ(ppm) = 12.48 (s, 1H, $NH_{(triazole)}$), 9.30 (m, 1H, NH-NH_2), 6.07 (s, 2H, $NH_{2(triazole)}$), 3.66 (br s, 2H, NH_2-NH);^{13}C NMR (101 MHz, DMSO-d_6): δ(ppm) = 159.4 (C=O), 157.6 ($C_{(triazole)}$), 153.2 ($C_{(triazole)}$); ^{14}N NMR (29 MHz, DMSO-d_6): δ(ppm) = –26; IR (ATR, rel. int.): ν (cm^{-1}) = 3412 (w), 3311 (m), 3196 (w), 2938 (w), 2893 (w), 2571 (w), 2453 (w), 2265 (w), 2204 (w), 2166 (w), 2063 (w), 2051 (w), 2023 (w), 2004 (w), 1982 (w), 1955 (w), 1941 (w), 1921 (w), 1720 (w), 1681 (s), 1648 (s), 1621 (s), 1584 (s), 1533 (m), 1499 (s), 1388 (m), 1355 (m), 1294 (m), 1253 (s), 1132 (s), 1094 (m), 1047 (s), 1011 (m), 969 (m), 862 (s), 822 (s), 757 (m), 723 (s), 661 (m), 631 (m), 569 (s), 532 (s); Mass spectrometry: m/z (DEI+) = 142.1 [M$^+$], DSC (5 °C min^{-1}): $T_{melt.}$= 175 °C.

5-Nitro-1*H*-1,2,4-triazole-3-carbohydrazide (4)

Compound (2) (4.20 g, 24.4 mmol, 1.00 eq.) was dissolved in methanol (50 mL), hydrazine-monohydrate (3.80 mL, 73.2 mmol, 3.00 eq.) was added slowly. The mixture was stirred for 24 h at 75 °C and cooled down to room temperature. Hydrochloric acid (37 %, 12.0 mL) was added, the solid was filtered and the residue was washed with water (3 x 20 mL), ethyl acetate (2 x 20 mL) and diethylether (2 x 20 mL) to yield compound (4) as a brownish solid (3.20 g, 18.6 mmol, 76 %).

^{1}H-NMR (400 MHz, DMSO-d_6): δ(ppm) = 9.35 (s, 1H, NH-NH_2), 4.11 (br s, 2H, NH-NH_2); ^{13}C NMR (101 MHz, DMSO-d_6): δ(ppm) = 165.2 (C=O), 160.3 ($C_{(triazole)}$), 156.5 ($C_{(triazole)}$); IR (ATR, rel. int.): ν (cm^{-1}) = 3336 (w), 3312 (w), 3209 (w), 3119 (w), 2995 (w), 2861 (w), 2741 (w), 2637 (w), 1669 (m), 1623 (m), 1600 (m), 1540 (m), 1513 (m), 1468 (s), 1383 (s), 1332 (m), 1301 (m), 1280 (m), 1128 (m), 1102 (s), 1056 (m), 1033 (w), 986 (m), 967 (s), 892 (w), 871 (w), 838 (m), 803 (w), 785 (w), 770 (w), 720 (w), 640 (s), 585 (w), 520 (w), 502 (w); DSC (5 °C min^{-1}): $T_{melt.}$= 275 °C, $T_{dec.}$ = 295 °C.

2-Amino-5-(5-amino-1*H*-1,2,4-triazol-3-yl)-1,3,4-oxadiazole (5)

Compound (3) (3.00 g, 21.1 mmol, 1.00 eq.) was suspended in water (20 mL) and KOH (1.18 g, 21.1 mmol, 1.00 eq.) was added. The solution was cooled to 0 °C and cyanogen bromide (3.38 g, 31.7 mmol, 1.50 eq) was added slowly. The solution was stirred at 0 °C for 2 h and was further stirred at room temperature for 72 h. The formed residue was filtered under reduced pressure to yield compound (5) as a yellow solid (2.93 g, 17.5 mmol, 83 %).

^{1}H-NMR (400 MHz, DMSO-d_6): δ(ppm) = 12.48 (s, 1H, NH), 7.42 (s, 2H, $NH_{2(oxodiazole)}$), 6.25 (s, 2H, $NH_{2(triazole)}$); ^{13}C NMR (101 MHz, DMSO-d_6): δ(ppm) = 163.5 (C-$NH_{2(oxodiazole)}$), 159.3 (C-$NH_{2(triazole)}$), 157.8 ($C_{(oxodiazole)}$), 153.1 ($C_{(triazole)}$); IR (ATR, rel. int.): ν (cm^{-1}) = 3310 (m), 3153 (m), 2198 (w), 2166 (w), 2140 (w), 2050 (w), 2004 (w), 1979 (w), 1731 (w), 1635 (s), 1589 (s), 1518 (s), 1491 (m), 1394 (s), 1362 (s), 1288 (m), 1235 (m), 1192 (m), 1094 (m), 1043 (m), 1011 (m), 956 (w), 898 (w), 813 (m), 732 (s), 695 (s); Mass spectrometry: m/z (DEI+) = 167.1 [M^+], DSC (5 °C min^{-1}): $T_{melt.}$ = 309 °C

2-Amino-5-(5-nitro-1*H*-1,2,4-triazol-3-yl)-1,3,4-oxadiazole (6)

Compound (4) (4.11 g, 24.2 mmol, 1.00 eq.) was suspended in water (50 mL) and KOH (1.55 g, 26.6 mmol, 1.10 eq.) was added. The solution was cooled to 0 °C and cyanogen bromide (3.57 g, 33.9 mmol, 1.40 eq.) was added slowly. The solution was stirred at 0 °C for 2 h and was further stirred at room temperature for 72 h. The formed residue was filtered to yield compound (6) as a yellow solid (3.08 g, 19.3 mmol, 80 %).

^{1}H-NMR (400 MHz, DMSO-d_6): δ(ppm) = 7.70 (s, 2H, NH_2);^{13}C NMR (101 MHz, DMSO-d_6): δ(ppm) = 164.5 (C-NO_2), 162.9 (C-NH_2), 148.8 ($C_{(oxodiazole)}$), 144.5 ($C_{(triazole)}$); ^{14}N NMR (29 MHz, DMSO-d_6): δ(ppm) = –25; IR (ATR, rel. int.): ν (cm^{-1}) = 3593 (w), 3496 (w), 3440 (w), 3365 (m), 3248 (w), 3129 (w), 2464 (w), 2209 (w), 2182 (w), 2051 (w), 2027 (w), 2004 (w), 1980 (w), 1693 (s), 1632 (m),

1584 (m), 1547 (s), 1477 (m), 1445 (m), 1413 (m), 1379 (m), 1346 (w), 1308 (s), 1196 (w), 1179 (w), 1100 (m), 1063 (m), 1032 (m), 1009 (m), 957 (m), 933 (w), 842 (s), 770 (w), 745 (w), 728 (w), 668 (w), 646 (m), 598 (w); Mass spectrometry: m/z (FAB$^-$) = 196.0 [M$^-$], DSC (5 °C min^{-1}): $T_{dec.}$ = 245 °C.

General procedure for the synthesis of salts

To a water/methanol 1:1 solution (7 mL/7 mL) of 6 (300 mg, 1.52 mmol) the corresponding base (K_2CO_3: 210 mg, 1.52 mmol; ammonia solution: 0.5 mL, 25 %, 1.52 mmol; guanidine carbonate: 136 mg, 1.52 mmol; aminoguanidine bicarbonate: 207 mg, 1.52 mmol;) was added and heated until everything was dissolved. The solutions were filtered and left for crystallization.

Potassium 3-(5-amino-1,3,4-oxadiazol-2-yl)-5-nitro-1,2,4-triazolate hydrate (7)

Yield: (334 mg, 1.32 mmol, 87 %) as a dark red solid.

^{1}H-NMR (400 MHz, DMSO-d_6): δ(ppm) = 7.13 (s, 2H, NH_2); ^{13}C NMR (101 MHz, DMSO-d_6): δ(ppm) = 165.9 (C-NO_2), 163.4 (C-NH_2), 153.3 ($C_{(oxadiazole)}$), 150.4 ($C_{(triazole)}$); ^{14}N NMR (29 MHz, DMSO-d_6): δ(ppm) = –27; IR (ATR, rel. int.): ν (cm^{-1}) = 3288 (w), 3127 (w), 1647 (m), 1614 (m), 1589 (m), 1560 (w), 1521 (m), 1455 (m), 1393 (m), 1325 (m), 1301 (m), 1250 (m), 1197 (m), 1172 (m), 1098 (m), 1046 (m), 1017 (m), 960 (m), 844 (m), 799 (m), 732 (s), 683 (s), 657 (s), 642 (s), 590 (s), 525 (m); Elemental analysis: calc. (%) for $C_4H_4N_7O_4$ (M = 253.22 g mol^{-1}): C 18.97, N 38.72, H 1.59; found: C 23.13, N 52.68, H 3.37; DSC (5 °C min^{-1}): $T_{dec.}$ = 254 °C; Sensitivities: ESD: 1.5 J, Friction: 360 N, Impact: 40 J.

Ammonium 3-(5-amino-1,3,4-oxadiazol-2-yl)-5-nitro-1,2,4-triazolate hydrate (8)

Yield: (220 mg, 1.03 mmol, 68 %) as a dark red solid.

^{1}H-NMR (400 MHz, DMSO-d_6): δ(ppm) = 7.13 (s, 2H, NH_2); ^{13}C NMR (101 MHz, DMSO-d_6): δ(ppm) = 165.8 (C-NO_2), 163.4 (C-NH_2), 153.3 ($C_{(oxadiazole)}$), 150.4 ($C_{(triazole)}$); IR (ATR, rel. int.): ν (cm^{-1}) = 3142 (w), 1652 (s), 1583 (w), 1528 (m), 1461 (m), 1425 (m), 1397 (s), 1327 (w), 1304 (m), 1107 (w), 1051 (w), 1016 (w), 843 (m), 734 (w), 655 (m); Elemental analysis: calc. (%) for $C_4H_8N_8O_4$ (M = 232.18 g mol^{-1}): C 20.69, N 48.27, H 3.47; found: C 20.51, N 47.21, H 3.19; DSC (5 °C m in^{-1}): $T_{dec.}$ = 276 °C; Sensitivities: ESD: 1.5 J, Friction: 360 N, Impact: 40 J.

Guanidinium 3-(5-amino-1,3,4-oxadiazol-2-yl)-5-nitro-1,2,4-triazolate (9)

Yield: (210 mg, 0.82 mmol, 54 %) as a brown solid.

^{1}H-NMR (400 MHz, DMSO-d_6):δ(ppm) = 7.31 (s, 2H, $NH_{2(oxodiazole)}$), 6.92 (s, 6H, 3 x $NH_{2(guanidine)}$); ^{13}C NMR (101 MHz, DMSO-d_6): δ(ppm) = 164.9 (C-NO_2), 162.7 (C-NH_2), 157.8 ($C_{(guanidine)}$), 151.9 ($C_{(oxodiazole)}$), 148.6 ($C_{(triazole)}$); IR (ATR, rel. int.): ν (cm^{-1}) = 3565 (w), 3442 (m), 3130 (m), 2167 (w), 2003 (w), 1981 (w), 1655 (s), 1579 (m), 1517 (m), 1490 (m), 1436 (m), 1378 (s), 1317 (s), 1300 (s), 1201 (m), 1135 (w), 1092 (m), 1054 (m), 1036 (m), 1011 (m), 973 (w), 839 (s), 752 (m), 684 (m), 645 (s), 534 (s), 513 (s), Elemental analysis: calc. (%) for $C_5H_8N_{10}O_3$ (M = 256.18 g mol^{-1}): C 22.44, N 54.68, H 3.15; found: C 23.13, N 52.68, H 3.37; DSC (5 °C min^{-1}): $T_{dec.}$ = 296 °C; Sensitivities: ESD: 1.5 J, Friction: 360 N, Impact: 40 J.

Aminoguanidinium 3-(5-amino-1,3,4-oxadiazol-2-yl)-5-nitro-1,2,4-triazolate (10)

Yield: (310 mg, 1.13 mmol, 74 %) as a brown solid.

^{1}H-NMR (400 MHz, DMSO-d_6): δ(ppm) = 8.57 (s, 1H, NH), 7.25 (m, 2H, $NH_{2(aminoguanidine)}$), 7.13 (s, 2H, $NH_{2(oxodiazole)}$), 6.76 (m, 2H, $NH_{2(aminoguanidine)}$), 4.68 (s, 2H, $NH_{2(aminoguanidine)}$); ^{13}C NMR (101 MHz, DMSO-d_6): δ(ppm) = 165.8 (C-NO_2), 163.3 (C-NH_2), 158.7 ($C_{(aminoguanidine)}$), 153.3 ($C_{(oxodiazole)}$), 150.4 ($C_{(triazole)}$); IR (ATR, rel. int.): ν (cm^{-1}) = 3461 (m), 3380 (m), 3329 (m), 3303 (m), 3200 (s), 3152 (m), 3089 (s), 3076 (m), 1652 (s), 1602 (m), 1573 (m), 1551 (m), 1493 (m), 1439 (m), 1395 (m), 1325 (m), 1304 (m), 1199 (m), 1099 (m), 1057 (m), 1037 (m), 1021 (m), 974 (m), 952 (m), 839 (s), 686 (m), 648 (m), 613 (m), 592 (w), 544 (m), 522 (s); Elemental analysis: calc. (%) for $C_5H_9N_{11}O_3$ (M = 271.23 g mol^{-1}): C 22.14, N 56.81, H 3.34; found: C 22.30, N 55.81, H 3.32; DSC (5 °C min^{-1}): $T_{dec.}$ = 246 °C; Sensitivities: ESD: 1.5 J, Friction: 360 N, Impact: 40 J.

5.5.4 Crystal Structures

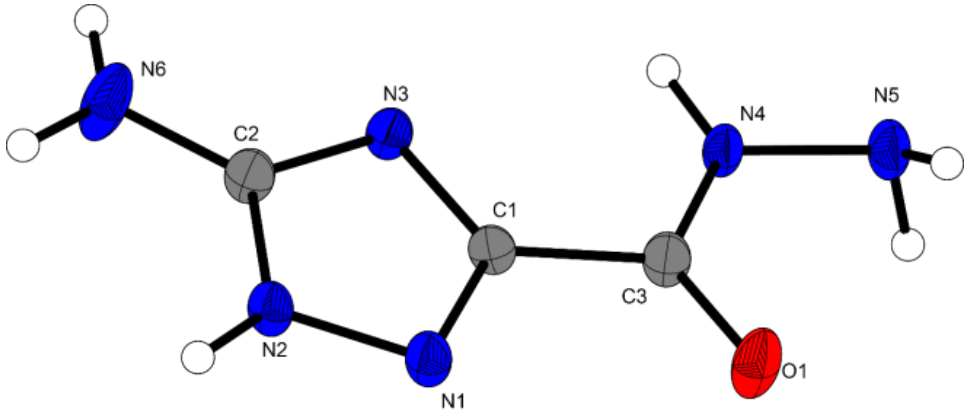

Figure 5.S1 Crystal Structure of **3**.

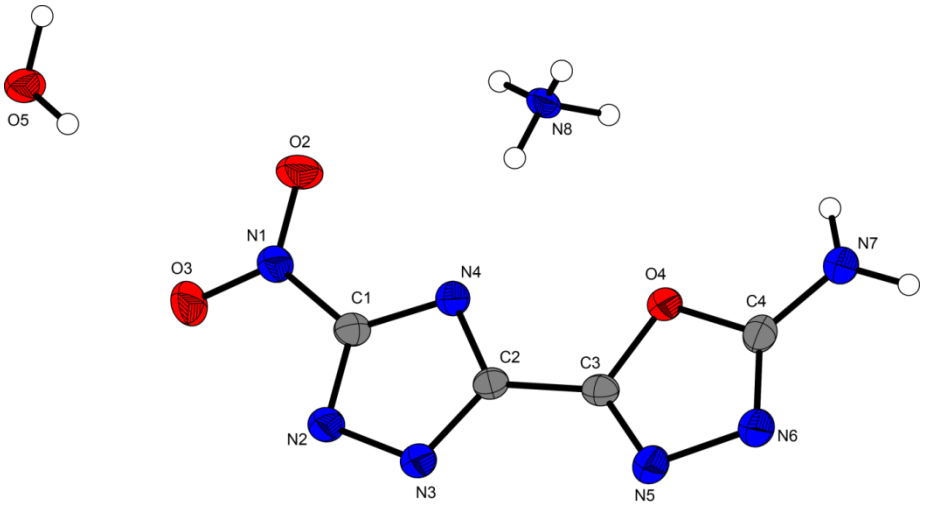

Figure 5.S2 Crystal Structure of **8** as hydrate.

5.5.5 References

[S1] *CrysAlisPro*, Oxford Diffraction Ltd., version 171.33.41, **2009**.

[S2] *SIR-92*, *A program for crystal structure solution*: A. Altomare, G. Cascarano, C. Giacovazzo, A. Guagliardi, *J. Appl. Crystallogr.* **1993**, *26*, 343.

[S3] a) A. Altomare, G. Cascarano, C. Giacovazzo, A. Guagliardi, A. G. G. Moliterni, M. C. Burla, G. Polidori, M. Camalli, R. Spagna, *SIR97*, **1997**; b) A. Altomare, M. C. Burla, M. Camalli, G. L. Cascarano, C. Giacovazzo, A. Guagliardi, A. G. G. Moliterni, G. Polidori, R. Spagna, *J. Appl. Crystallogr.* **1999**, *32*, 115–119.

[S4] a) G. M. Sheldrick, *SHELX-97*, University of Göttingen, Göttingen, Germany, **1997**; b) G. M. Sheldrick, *Acta Crystallogr., Sect. A* **2008**, *64*, 112–122.

[S5] A. L. Spek, *PLATON*, *A Multipurpose Crystallographic Tool*, Utrecht University, The Netherlands, **1999**.

[S6] *SCALE3 ABSPACK – An Oxford Diffraction program* (1.0.4, gui: 1.0.3), Oxford Diffraction Ltd., **2005**.

[S7] *APEX3*. Bruker AXS Inc., Madison, Wisconsin, USA.

[S8] M. J. Frisch, G. W. Trucks, H. B. Schlegel, G. E. Scuseria, M. A. Robb, J. R. Cheeseman, G. Scalmani, V. Barone, B. Mennucci, G. A. Petersson, H. Nakatsuji, M. Caricato, X. Li, H.P. Hratchian, A. F. Izmaylov, J. Bloino, G. Zheng, J. L. Sonnenberg, M. Hada, M. Ehara, K. Toyota, R. Fukuda, J. Hasegawa, M. Ishida, T. Nakajima, Y. Honda, O. Kitao, H. Nakai, T. Vreven, J. A. Montgomery, Jr., J. E. Peralta, F. Ogliaro, M. Bearpark, J. J. Heyd, E. Brothers, K. N. Kudin, V. N. Staroverov, R. Kobayashi, J. Normand, K. Raghavachari, A. Rendell, J. C. Burant, S. S. Iyengar, J. Tomasi, M. Cossi, N. Rega, J. M. Millam, M. Klene, J. E. Knox, J. B. Cross, V. Bakken, C. Adamo, J. Jaramillo, R. Gomperts, R. E. Stratmann, O. Yazyev, A. J. Austin, R. Cammi, C. Pomelli, J. W. Ochterski, R. L. Martin, K. Morokuma, V. G. Zakrzewski, G. A. Voth, P. Salvador, J. J. Dannenberg, S. Dapprich, A. D. Daniels, O. Farkas, J.B. Foresman, J. V. Ortiz, J. Cioslowski, D. J. Fox, Gaussian 09 A.02, Gaussian, Inc., Wallingford, CT, USA, **2009**.

[S9] a) J. W. Ochterski, G. A. Petersson, and J. A. Montgomery Jr., *J. Chem. Phys.* **1996**, *104*, 2598–2619; b) J. A. Montgomery Jr., M. J. Frisch, J. W. Ochterski G. A. Petersson, *J. Chem. Phys.* **2000**, *112*, 6532–6542.

[S10] a) L. A. Curtiss, K. Raghavachari, P. C. Redfern, J. A. Pople, *J. Chem. Phys.* **1997**, *106*, 1063–1079; b) E. F. C. Byrd, B. M. Rice, *J. Phys. Chem*. A **2006**, *110*, 1005–1013; c) B. M. Rice, S. V. Pai, J. Hare, *Comb. Flame* **1999**, *118*, 445–458.

[S11] P. J. Lindstrom, W. G. Mallard (Editors), NIST Standard Reference Database Number 69, http://webbook.nist.gov/chemistry/ (accessed June **2011**).

[S12] M. S. Westwell, M. S. Searle, D. J. Wales, D. H. Williams, *J. Am. Chem. Soc*. **1995**, *117*, 5013–5015; b) F. Trouton, *Philos. Mag*. **1884**, *18*, 54–57.

[S13] a) H. D. B. Jenkins, H. K. Roobottom, J. Passmore, L. Glasser, *Inorg. Chem.* **1999,** *38,* 3609–3620; b) H. D. B. Jenkins, D. Tudela, L. Glasser, *Inorg. Chem.* **2002**, *41*, 2364–2367.

[S14] NATO standardization agreement (STANAG) on explosives, *impact sensitivity tests*, no. 4489, 1st ed., Sept. 17, **1999**.

[S15] WIWEB-Standardarbeitsanweisung 4-5.1.02, Ermittlung der Explosionsgefährlichkeit, hier der Schlagempfindlichkeit mit dem Fallhammer, Nov. 8, **2002**.

[S16] http://www.bam.de

[S17] NATO standardization agreement (STANAG) on explosive, *friction sensitivity tests*, no. 4487, 1st ed., Aug. 22, **2002**.

[S18] WIWEB-Standardarbeitsanweisung 4-5.1.03, Ermittlung der Explosionsgefährlichkeit oder der Reibeempfindlichkeit mit dem Reibeapparat, Nov. 8, **2002**.

[S19] Impact: insensitive > 40 J, less sensitive ≥ 35 J, sensitive ≥ 4 J, very sensitive ≤ 3 J; Friction: insensitive > 360 N, less sensitive = 360 N, sensitive < 360 N and > 80 N, very sensitive ≤ 80 N, extremely sensitive ≤ 10 N, According to: *Recommendations on the Transport of Dangerous Goods, Manual of Tests and Criteria*, 4th edition, United Nations, New York-Geneva, **1999**.

[S20] http://www.ozm.cz

[S21] A. A. Dippold, T. M. Klapötke, *Chem. Asian J.* **2013**, *8*, 1463–1471.

6 3,5-Ditetrazolyl-Pyrazoles as Precursor for New Energetic Materials – New Mixed Heterocycles Combining Pyrazoles and Tetrazoles

Marc F. Bölter, Thomas M. Klapötke and Jörg Stierstorfer

unpublished

Abstract: The new triheterocyclic compounds 5,5'-(1*H*-pyrazole-3,5-diyl)-bis-1*H*-tetrazole and 5,5'-(4-Nitro-1*H*-pyrazole-3,5-diyl)-bis-1*H*-tetrazole combining one pyrazole and two tetrazoles were synthesized and compared to each other. These two compounds are suitable as precursors for new energetic materials based on azoles. The obtained compounds were characterized using IR, NMR (^{1}H, ^{13}C, ^{14}N), mass, elemental analysis and thermal analysis (DSC or DTA). Crystal structures could be obtained of four compounds by low temperature single crystal X-ray diffraction. Impact, friction and ESD values were determined according to BAM (*Bundesamt für Materialforschung)* standard methods. The energetic performance of both triheterocyclic compounds were calculated using recalculated X-ray densities, heats of formation and the EXPLO5 code. The energetic performance could be further improved by salt formation, *N*-functionalization or *N*-oxidation.

6.1 Introduction

Depending on their different application such as for military or civil usage, high energetic dense materials (HEDMs) have to fulfil different requirements.[1-2] The key characteristics for that class of compounds are in general a high energetic performance, high positive heat of formation, low sensitivity values, long term stability, a high thermal stability and low toxicity.[3-6] The main goal is to substitute the current mostly used secondary explosive RDX due to its high toxicity.[7-9] Therefore, suitable backbones, which attract attention in the past, are based on five-membered nitrogen-rich heterocycles containing two (pyrazole or imidazole), three (triazole) or four (tetrazole) nitrogen atoms.[10-14] A large number of C–C-bonded mono-, bi- or triheterocyclic nitrogen-rich compounds have been synthesized in the past showing promising physicochemical and energetic properties (Figure 6.1).[3, 5, 10, 15-24] Tetrazoles are suitable as building block for triheterocyclic compounds due to its high nitrogen content, high positive heat of formation (1*H*-tetrazole: 320 kJ mol^{-1})[25] and sufficient thermal stability deriving from its aromaticity.[5, 22, 26] A large number of different tetrazoles have been synthesized resulting in high detonation velocities and appropriate thermal stability, especially for bistetrazole-based compounds.[19, 27-31] Besides tetrazoles, (nitrated) pyrazoles were noticed in the past due to their different characteristics, positive heat of formation (1*H*-pyrazole: 180 kJ mol^{-1})[25], cheap price, facile synthesis and functionalization possibilities such as nitration, amination, bridging or hydroxylation to improve oxygen balance, density or both.[10, 32-35]

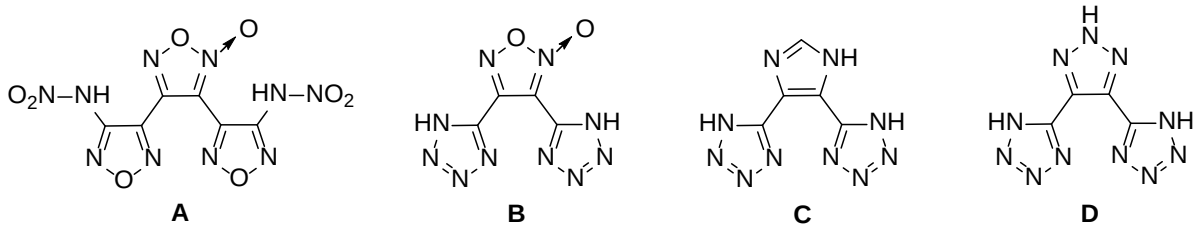

Figure 6.1. Different energetic materials based on triheterocyclic compounds: 3,4-Bis(4-nitramino-1,2,5-oxadiazol-3-yl)-1,2,5-furoxan[20] (**A**), 3,4-Bis(1*H*-5-tetrazolyl)-furoxan[36] (**B**), 4,5-Bis(1*H*-tetrazol-5-yl)-1*H*-imidazole[3] (**C**), 4,5-Bis(1*H*-tetrazol-5-yl)-2*H*-1,2,3-triazole[5] (**D**).

Triheterocyclic compounds containing one pyrazole and two tetrazoles moieties (nitrogen content of $C_5H_4N_{10}$: 69 %) have not been mentioned in literature yet. In this work, two different triheterocyclic compounds were prepared, intensively characterized and compared to each other. Both compounds could serve as precursor for high energetic dense materials.

6.2 Results and Discussion

The synthesis of 5,5'-(1*H*-pyrazole-3,5-diyl)-bis-1*H*-tetrazole (**5**) and 5,5'-(4-Nitro-1*H*-pyrazole-3,5-diyl)-bis-1*H*-tetrazole (**9**) starts with the condensation of acetyl acetone and hydrazine giving dimethylpyrazole (**1**) followed by oxidation of the methyl groups to carboxyl groups (**2**) using potassium permanganate (Scheme 6.1).[37] Compound **2** was further reacted using thionyl chloride in ethanol to form an intermediate diester,[38] which was treated with aqueous ammonia to obtain the carboxamide (**3**).[39] The carboxamide groups were dehydrated using phosphoryl chloride to form dinitrile-pyrazole (**4**).[39] The triheterocyclic compound **5** was obtained by a [3+2] cyclo addition using sodium azide and zinc chloride as catalyst.[40] The nitrated heterocyclic compound **9** is obtained by nitration using oleum (30 % SO_3) and nitric acid (100 %) of compound **2** to yield 4-nitro-1*H*-pyrazole-3,5-dicarboxylic acid (**6**).[41] The carboxylic acid (**6**) was esterified with thionyl chloride in ethanol and afterwards treated with aqueous ammonia to obtain the carboxamide (**7**).[39]

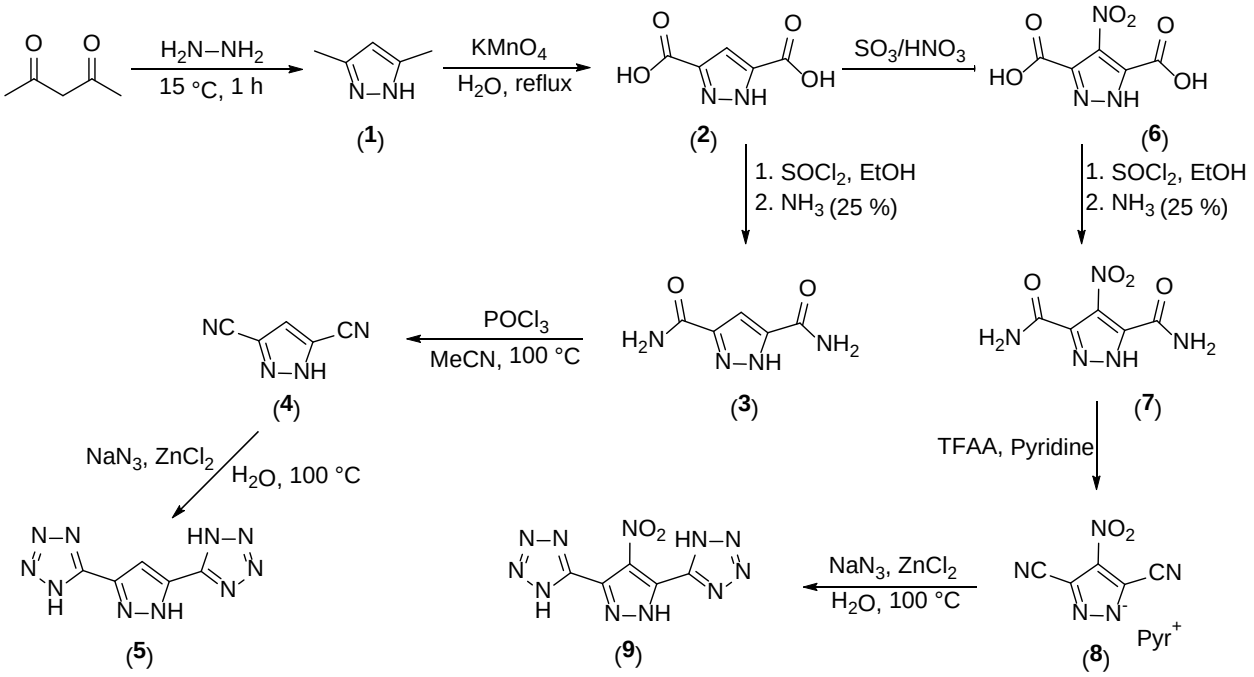

Scheme 6.1. Synthesis of 5,5'-(1H-pyrazole-3,5-diyl)-bis-1H-tetrazole (**5**) and 5,5'-(4-Nitro-1H-pyrazole-3,5-diyl)-bis-1H-tetrazole (**9**).

The dehydration of the carboxamide to the corresponding dinitrile (**8**) was investigated using phosphoryl chloride or phosphorus pentoxide in acetonitrile.[39, 42-43] However, both reactions led mainly to the monodehydrated compound. Therefore, a different method according to Fershtat *et al.* was tried out using trifluoro acetic acid in pyridine as dehydration reagents.[44] This method showed a successful dehydration obtaining the dinitrile pyrazole as pyridinium salt (**8**). Last, compound **8** was reacted with sodium azide and zinc chloride to yield the desired triheterocyclic pyrazole (**9**).[40]

Different methods for improving the energetic character of azoles are known such as salt formation, *N*-oxidation, *N*- or *C*-functionalization, methylene- or ethylene-bridging, methylation or azo-bridging.[1, 27, 45-51] The triheterocylic compounds (**5** and **9**) are suitable to serve as precursors for improving their energetic characteristics by synthesizing nitrogen-rich salts, *N*-oxidation or *N* functionalization.

6.2.1 NMR and Vibrational Spectroscopy

All compounds (**1**–**9**) were characterized by ^{1}H, ^{13}C NMR spectroscopy, mass, elemental analysis and IR spectroscopy. In the ^{1}H NMR spectra, three hydrogen signals were observed for compound **1** (11.99, 5.73 and 2.12 ppm) and one for compound **2** (6.98 ppm). For compounds **3**–**5** the shift

ranges from 7.21 (**3**) to 7.89 ppm (**4**) for the C-H signal. The disappearance of the signal at 6.98 ppm shows the successful nitration from **2** to **6**. The broad signals at 8.15 and 7.93 ppm indicate the amino group of compound **7**. The ^{1}H NMR spectra of **8** just displays the pyridine signals between 8.94 and 8.11 ppm, whereas for the ring-closed compound **9** no signals were observed.

In the ^{13}C NMR spectra, three signals were determined for **1** and **2**, whereas the signal at 161.5 ppm confirms the formation of the carboxyl group. The synthesis from **3** to **5** can be tracked by the emerging shift of the functional group in the ^{13}C NMR spectra. The carboxamide group (**3**) has a signal at 161.5 ppm, the dinitrile (**4**) at 118.7 ppm and the triheterocycle **5** at 149.7 ppm. The introduction of the nitro-group toward **6** is indicated by the shift of the signal from 109.9 to 135.5 ppm. The pyridine cation of **8** shows additional three signals (146.7 ppm, 142.0 ppm and 127.3 ppm) besides the signal at 113.1 ppm for the characteristic nitrile group.[52] After the successful ring-closing to compound **9**, the signals slightly shifted to 147.9 ppm, 142.7 ppm and 131.7 ppm.

IR spectra of compounds **1**–**9** were measured and the frequencies were assigned according to observed data reported in the literature.[52] The absorption bands between 1680–1704 cm^{-1} were assigned to the carbonyl moiety of **2**–**4** and **6**–**7**. The characteristic absorption bands for the nitrile groups of **4** and **8** were found at 2248 cm^{-1} and 2247 cm^{-1}. Further, the absorption bands in the region of 3000 cm^{-1} were assigned to the NH_2-stretching vibration and the ones in the region of 1600 cm^{-1} to the deformation vibration of the amino group. The vibration of the nitro groups (**6**–**9**) can be found in the range of 1558–1529 cm^{-1} for the asymmetric stretching and of 1361–1312 cm^{-1} for the symmetric stretching.

6.2.2 Thermal Analysis, Sensitivities, Physicochemical and energetic properties

Both triheterocylces (**5** and **9**) were investigated in regard to their thermal behaviour and sensitivities (Table 6.1). All decomposition temperatures were measured by differential scanning calorimetry (DSC) or differential thermal analysis (DTA) with a heating rate of 5 °C min^{-1}. For compound **5** the heat of formation was calculated by the atomization method using electronic energies (CBS-4M method). Further, the energetic parameters of **5** were calculated with EXPLO5 V6.03.[53]

Compound **5** and **9** only differ in the existence of a nitro group, which obviously led to a different thermal stability (Figure 6.2). DTA measurements indicated the high thermal stability of both compounds with decomposition temperatures of 246 °C (**9**) and 277 °C (**5**). The endothermic peaks validated a water loss at 88 °C (**5**) and 116 °C (**9**).

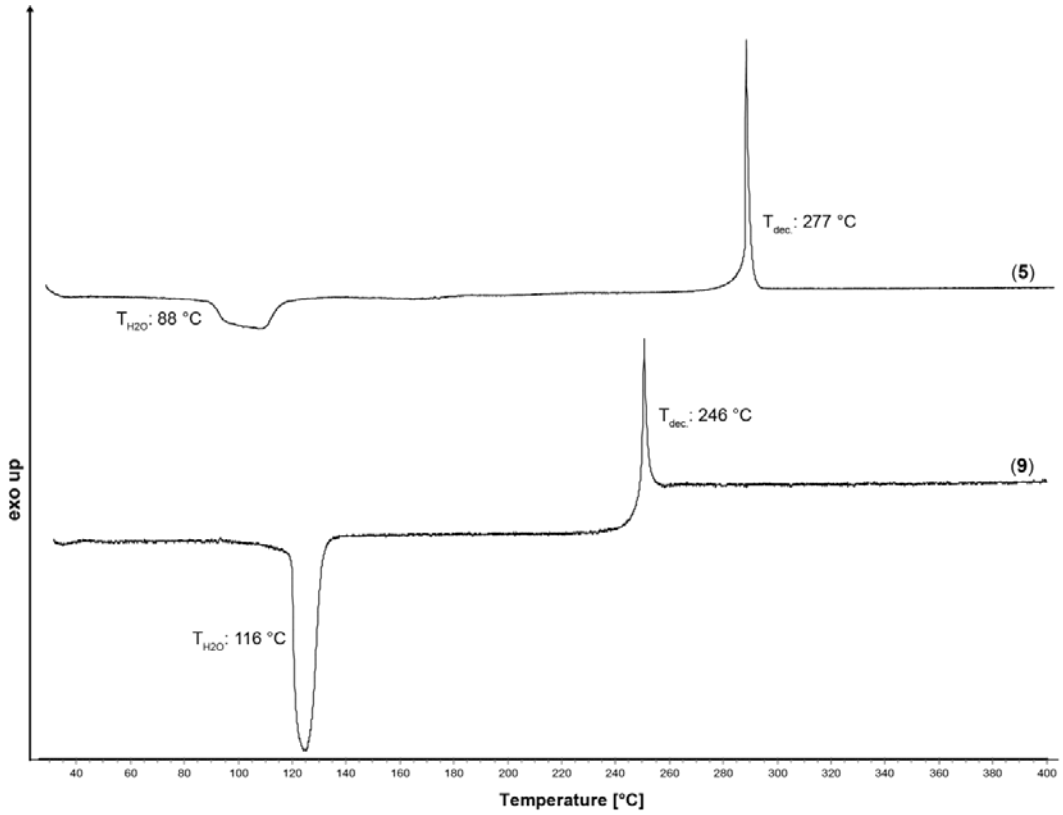

Figure 6.2. DTA plots of compounds **5** and **9** measured with a heating rate of 5 °C min^{-1}.

Both triheterocylces are due to their hydrates not sensitive toward impact (IS: <40 J) or friction (FS: 360 N) compared to RDX (IS: 7.5 J; FS: 120 N). The detonation velocity V_D (**5**: 6965 m s^{-1}, **9**: 7678 m s^{-1}) and pressure p_{CJ} (**5**: 161 kbar, **9**: 220 kbar) were calculated using the EXPLO5 code, however these values cannot surpass RDX (V_D = 8861 m s^{-1}, p_{CJ} = 345 kbar). Likewise, the densities at 298 K are lower for both triheterocylces than RDX.

Table 6.1. Physicochemical properties and detonation parameters of **5** and **9** compared to RDX.

	5 · 2 H_2O	**9 · H_2O**	**RDX[4]**
Formula	$C_5H_8N_{10}O_2$	$C_5H_5N_{11}O_3$	$C_3H_6N_6O_6$
M [g mol^{-1}]	240.21	267.17	221.12
IS [J][a]	<40	<40	7.5
FS [N][b]	360	360	120
ESD [J][c]	1.5	1.5	0.2
N [%][d]	58.32	57.67	37.84
Ω [%][e]	–94.04	–57.9	–21.6
$T_{dec.}$ [°C][f]	88 (H_2O) 277 (dec.)	119 (melt.) 246 (dec.)	205 (dec.)
ρ [g cm^{-3}] (298 K)[g]	1.579 1.44 [p] [54]	1.695 [o]	1.81
$\Delta_fH°$ [kJ mol^{-1}][h]	723.8 [p]	754.2 [p]	70.3
$\Delta_fU°$ [kJ kg^{-1}][i]	3629.5 [p]	3106.2 [p]	417.0
EXPLO5 V6.03:[g]			
$-\Delta_EU°$ [kJ kg^{-1}][j]	3277 [p]	4262 [p]	5845
T_E [K][k]	2558 [p]	3318 [p]	3810
p_{CJ} [kbar][l]	161 [p]	220 [p]	345
V_D [m s^{-1}][m]	6965 [p]	7678 [p]	8861
V_0 [L kg^{-1}][n]	499 [p]	725 [p]	785

[a] impact sensitivity (BAM drophammer, 1 of 6); [b] friction sensitivity (BAM friction tester, 1 of 6); [c] electrostatic discharge device (OZM); [d] nitrogen content; [e] oxygen balance; [f] decomposition temperature from DTA (β = 5 °C); [g] recalculated from low temperature X-ray densities ($\rho_{298K} = \rho_T / (1+\alpha_V(298-T_0)$; $\alpha_V = 1.5\ 10^{-4}$ K^{-1}); [h] calculated (CBS-4M) heat of formation; [i] calculated energy of formation; [j] energy of explosion; [k] explosion temperature; [l] detonation pressure; [m] detonation velocity; [n] assuming only gaseous products; [o] measured pycnometrically; [p] calculated without crystal water.

6.2.3 X-Ray crystallography

Suitable crystals of (**4**–**6** and **8**) were obtained by recrystallization. The structures are shown in Figures 6.3–6.5 and the structure of **6** can be found in the supporting information.

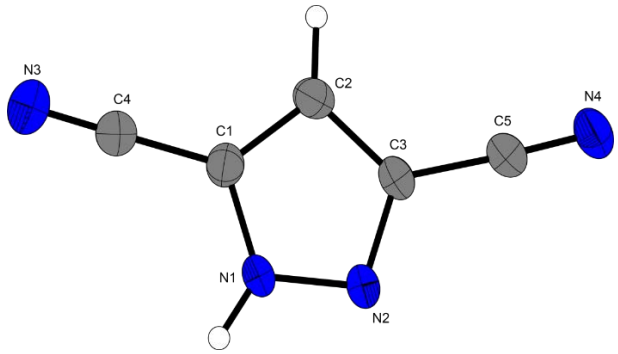

Figure 6.3. X-ray structure of compound **4**. Ellipsoids are drawn at the 50% probability level. Selected bond length in Ångstrom: N1–N2 1.3332(16), N1–C1 1.3559(18), N3–C4 1.1443(19), N4–C5 1.1414(19); selected bond angles in degree: N2–N1–C1 112.67(11), C1–C2–C3 103.65(12), N3–C4–C1 179.07(16), N4–C5–C3 177.51(16); selected torsion angles in degree:C1–N1–N2–C3 –0.04(15).

Dinitrile (**4**) crystallizes from acetonitrile in the monoclinic space group $P\,2_1/n$ with four molecules per unit cell and a density of 1.477 g cm^{-3} at 173 K, which is illustrated in Figure 6.3. Compound **4** is approximately planar and both nitrile groups are also in plane toward the plane pyrazole ring.

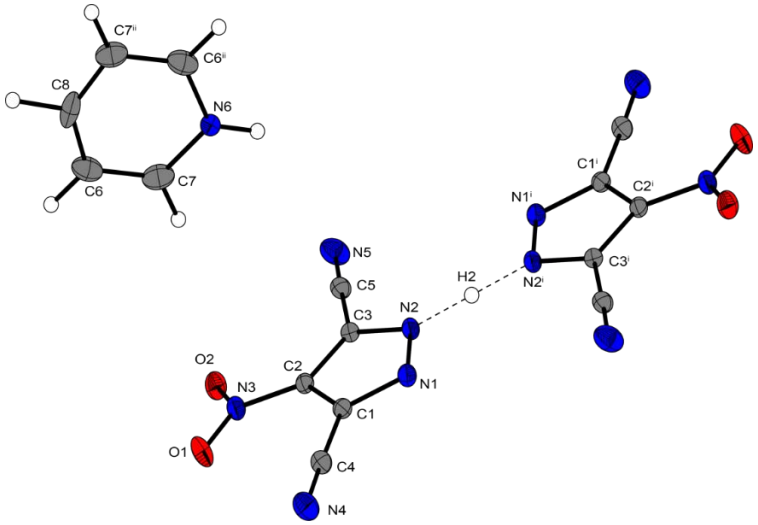

Figure 6.4. X-ray structure of compound **8**. Ellipsoids are drawn at the 50% probability level. Selected bond length Ångstrom: N1–N2 1.348(3), N4–C4 1.142(3), N5–C5 1.139(3), N3–C2 1.425(3); Selected bond angles in degree: N2–N1–C1 106.35(17), O1–N3–C2 117.77(19), O2 –N3–C2 117.49(18), N4–C4–C1 178.3(2), N5–C5–C3 178.2(2); selected torsion angles in degree: C1–N1–N2–C3 –0.6(2), N2–N1–C1–C4 179.57(19), O1–N3–C2–C3 –177.0(2), O2–N3–C2–C1 –171.6(2), selected hydrogen bonds d(D–H···A) in Ångstrom : N2–H2···N2 1.3200; symmetry code (i) –x, 0.5 + y, 0.5 – z.

Dinitrile (**8**) crystallizes from water in the monoclinic space group $P\,2_1/c$ with two molecules per unit cell and a density of 1.568 g cm^{-3} at 173 K, which is illustrated in Figure 6.4. A hydrogen bond between two pyrazoles stabalizes the molecule. The pyrazole ring system including the nitro and nitrile groups is approximately planar.

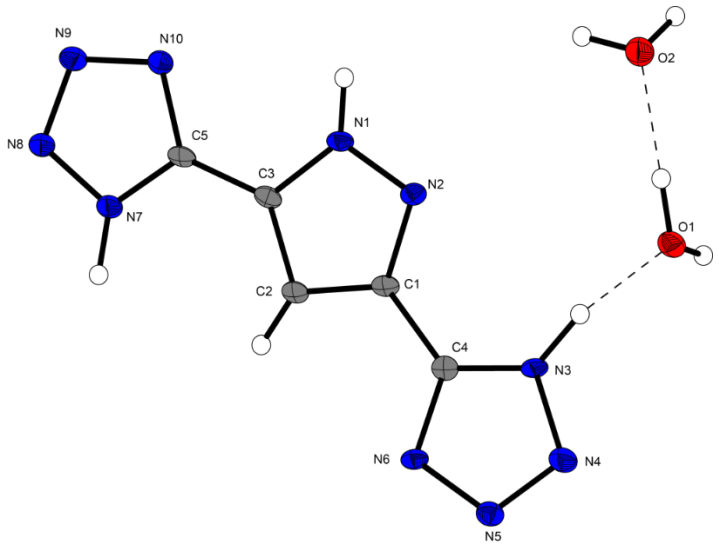

Figure 6.5. X-ray structure of compound **5**. Ellipsoids are drawn at the 50% probability level. Selected bond length Ångstrom: N1–N2 1.341(4), C3–C5 1.443(4), C1–C4 1.456(4), C2–H2 0.91(3); selected bond angles in degree: N2–N1–C3 112.5(2), N8–N7–H7 120(2), C5–N7–H7 129(2); selected torsion angles in degree: N2–N1–C3–C2 0.4(3), N2–C1–C4–N3 –9.6(4), N1–C3–C5–N7 176.3(3).

Triheterocycle (**5**) crystallizes as dihydrate from water in the monoclinic space group $P\,2_1/c$ with four molecules per unit cell and a density of 1.609 g cm^{-3} at 173 K, which is illustrated in Figure 6.5. The whole molecule is almost planar with torsion angles of –9.6°(4) and 3.7°(3) for the tetrazoles.

6.3 Conclusion and Outlook

In conclusion, we reported on the first synthesis of two triheterocyclic compounds (**5** and **9**) consisting of one pyrazole and two tetrazoles with high nitrogen content. The compounds were synthesized in a five-step (**5**) or six-step (**9**) synthesis using commercially available reagents and showing high yields and facile reaction conditions. The crystal density and the calculated heat of formation were used to calculate the detonation performances (heat of explosion, explosion temperature, detonation pressure, and velocity) with. Compounds **5** and **9** obtained high decomposition temperatures of 277 °C and 246 °C. Their sensitivity values are 40 J for impact and 360 N for friction, for which reason they are classified as not sensitive. The calculated detonation

properties of **5** (V_D = 6965 m s^{-1}) and **9** (V_D = 7678 m s^{-1}) are lower than RDX. According to their high decomposition temperatures and low sensitivity values, both triheterocylces (**5** and **9**) are suitable as precursor for high energetic materials or due to the high nitrogen content as propellant charges. Their energetic characteristics can be improved by different methods such as *N*-functionalization, *N*-oxidation or salt formation (Scheme 6.2). Both compounds own three acidic protons, which can be functionalized individually to obtain mono-, di- or tri-substituted compounds implicating different characteristics.

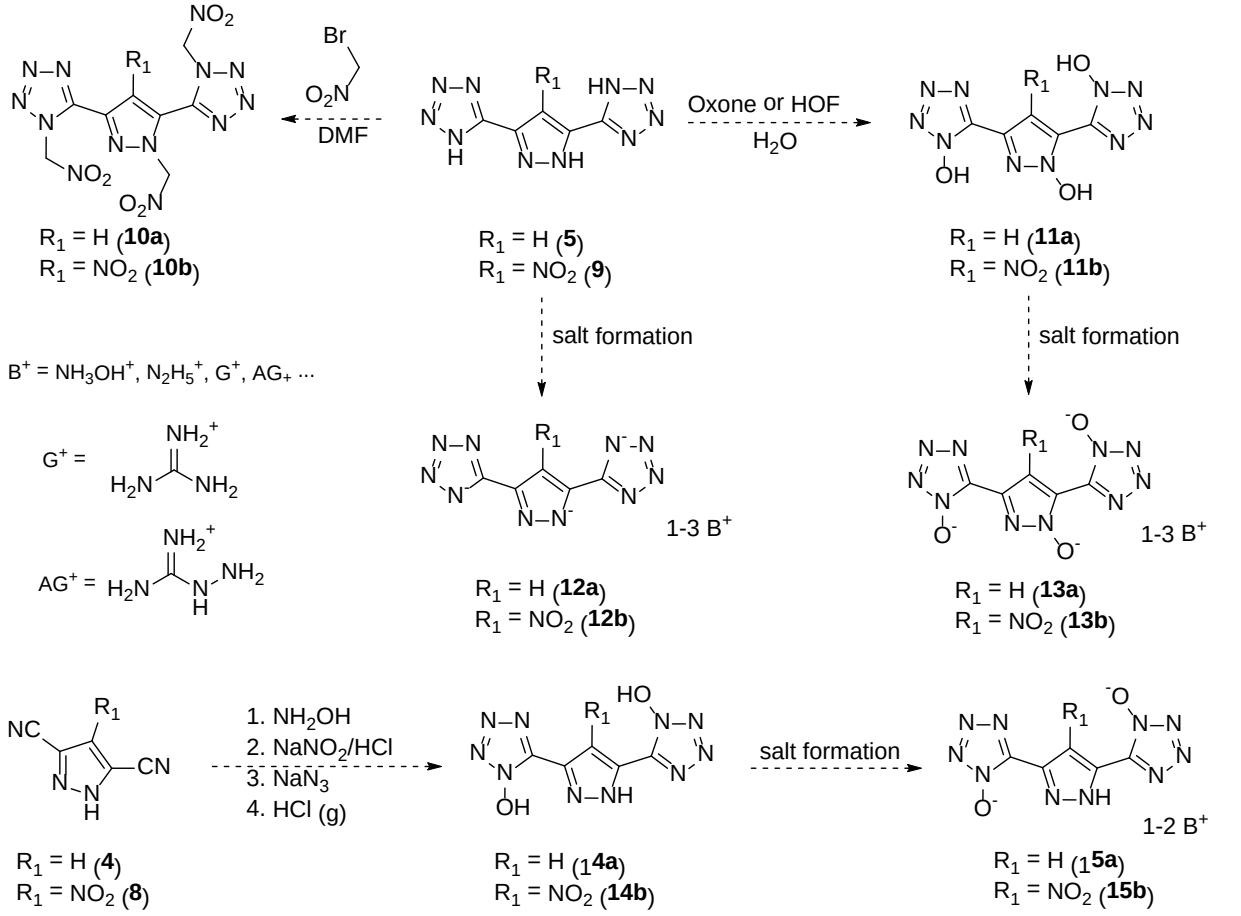

R$_1$ = H (**10a**)
R$_1$ = NO$_2$ (**10b**)

R$_1$ = H (**5**)
R$_1$ = NO$_2$ (**9**)

R$_1$ = H (**11a**)
R$_1$ = NO$_2$ (**11b**)

R$_1$ = H (**12a**)
R$_1$ = NO$_2$ (**12b**)

R$_1$ = H (**13a**)
R$_1$ = NO$_2$ (**13b**)

R$_1$ = H (**4**)
R$_1$ = NO$_2$ (**8**)

R$_1$ = H (1**4a**)
R$_1$ = NO$_2$ (**14b**)

R$_1$ = H (1**5a**)
R$_1$ = NO$_2$ (**15b**)

Scheme 6.2. Different functionalization possibilities using **4**, **5**, **8** or **9** as starting material.

The oxygen balance can be increased by substituting the acid protons of the three azoles with nitromethyl groups (**10a** or **10b**).[16] Another possibility to improve the thermal stability and the energetic performance is to perform salt formation using nitrogen-rich bases such as hydroxylamine, hydrazine, guanidine or aminoguanidine (**12a** or **12b**).[6, 20, 47] The introduction of the N–O functionality (*N*-oxidation) to azoles enhances the oxygen balance, the density and the detonation performance.[11, 17, 27] Therefore, on the one hand *N*-oxidation can be performed using Oxone/HOF (**11a** and **11b**) or on the other hand starting with the nitriles (**4** or **8**) in a four-step

synthesis (**14a** and **14b**) using hydroxylamine, $NaNO_2$, NaN_3 and gaseous HCl.[18] The N–O moiety plays an important role as proton acceptor in ionic derivatives leading to a high density and low sensitivity values.[11] Hence, the nitrogen-rich salts of the *N*-oxidized compounds (**13a**, **13b**, **15a** and **15b**) will presumably reach the highest densities, acceptable sensitivity values and the highest energetic performance compared to the salts **12a** and **12b**.

6.4 References

[1] D. Fischer, J. L. Gottfried, T. M. Klapötke, K. Karaghiosoff, J. Stierstorfer, T. G. Witkowski, *Angew. Chem. Int. Ed.* **2016**, *55*, 16132–16135.

[2] D. Kumar, G. H. Imler, D. A. Parrish, J. M. Shreeve, *New J. Chem.* **2017**, *41*, 4040–4047.

[3] Q. Yang, G. Yang, W. Zhang, S. Zhang, Z. Yang, G. Xie, Q. Wei, S. Chen, S. Gao, *Chem. Eur. J.* **2017**, *23*, 9149–9155.

[4] T. M. Klapötke, *Chemistry of High-Energy Materials*, 4th ed., De Gruyter, Berlin, **2017**.

[5] A. A. Dippold, D. Izsák, T. M. Klapötke, C. Pflüger, *Chem. Eur. J.* **2016**, *22*, 1768–1778.

[6] Y. Zhang, Y. Guo, Y.-H. Joo, D. A. Parrish, J. M. Shreeve, *Chem. Eur. J.* **2010**, *16*, 10778-10784.

[7] J. K. Stanley, G. R. Lotufo, J. M. Biedenbach, P. Chappell, K. A. Gust, *Environ. Toxicol. Chem.* **2015**, *34*, 873–879.

[8] G. A. Parker, G. Reddy, M. A. Major, *Int. J. Toxicol.* **2006**, *25*, 373–378.

[9] H. Abadin, C. Smith, in *Toxicological Profile For RDX*, U.S. Department of Health and Human Serivces, Public Health Service, Agency for Toxic Substances and Disease Registry, **2012**.

[10] D. Kumar, G. H. Imler, D. A. Parrish, J. M. Shreeve, *Chem. Eur. J.* **2017**, *23*, 7876–7881.

[11] P. Yin, L. A. Mitchell, D. A. Parrish, J. M. Shreeve, *Chem. Asian J.* **2017**, *12*, 378–384.

[12] T. M. Klapötke, P. C. Schmid, S. Schnell, J. Stierstorfer, *J. Mater. Chem. A* **2015**, *3*, 2658–2668.

[13] Y. Tang, C. He, L. A. Mitchell, D. A. Parrish, J. M. Shreeve, *J. Mater. Chem. A* **2016**, *4*, 3879–3885.

[14] Y. Liu, J. Zhang, K. Wang, J. Li, Q. Zhang, J. M. Shreeve, *Angew. Chem. Int. Ed.* **2016**, *55*, 11548–11551.

[15] G. Hervé, C. Roussel, H. Graindorge, *Angew. Chem. Int. Ed.* **2010**, *49*, 3177–3181.

[16] D. Kumar, G. H. Imler, D. A. Parrish, J. M. Shreeve, *J. Mater. Chem. A* **2017**, *5*, 10437–10441.

[17] A. A. Dippold, T. M. Klapötke, *J. Am. Chem. Soc.* **2013**, *135*, 9931–9938.

[18] A. A. Dippold, D. Izsák, T. M. Klapötke, *Chem. Eur. J.* **2013**, *19*, 12042–12051.

[19] D. Fischer, T. M. Klapötke, M. Reymann, P. C. Schmid, J. Stierstorfer, M. Sućeska, *Propellants Explos. Pyrotech.* **2014**, *39*, 550–557.

[20] I. Gospodinov, T. Hermann, T. M. Klapötke, J. Stierstorfer, *Propellants Explos. Pyrotech.* **2018**, *43*, 355–363.

[21] I. L. Dalinger, A. V. Kormanov, I. A. Vatsadze, O. V. Serushkina, T. K. Shkineva, K. Y. Suponitsky, A. N. Pivkina, A. B. Sheremetev, *Chem. Heterocycl. Compd.* **2016**, *52*, 1025–1034.

[22] D. Srinivas, V. D. Ghule, K. Muralidharan, *RSC Advances* **2014**, *4*, 7041–7051.

[23] R. Tsyshevsky, P. Pagoria, M. Zhang, A. Racoveanu, A. DeHope, D. Parrish, M. M. Kuklja, *J. Phys. Chem. C* **2015**, *119*, 3509–3521.

[24] P. Pagoria, M. Zhang, A. Racoveanu, A. DeHope, R. Tsyshevsky, M. Kuklja, *Molbank* **2014**, *M824*, 1–4.

[25] Z. Yu, E. R. Bernstein, *J. Phys. Chem. A* **2013**, *117*, 10889–10902.

[26] H. Huang, Z. Zhou, L. Liang, J. Song, K. Wang, D. Cao, W. Sun, C. Bian, M. Xue, *Chem. Asian J.* **2012**, *7*, 707–714.

[27] N. Fischer, D. Fischer, T. M. Klapötke, D. G. Piercey, J. Stierstorfer, *J. Mater. Chem.* **2012**, *22*, 20418–20422.

[28] K. Hafner, T. M. Klapötke, P. C. Schmid, J. Stierstorfer, *Eur. J. Inorg. Chem.* **2015**, *2015*, 2794–2803.

[29] Y.-H. Joo, J. M. Shreeve, *J. Am. Chem. Soc.* **2010**, *132*, 15081–15090.

[30] K. Karaghiosoff, T. M. Klapötke, C. M. Sabaté, *Eur. J. Inorg. Chem.* **2009**, *2009*, 238–250.

[31] Y. Guo, H. Gao, B. Twamley, J. M. Shreeve, *Adv. Mater.* **2007**, *19*, 2884–2888.

[32] V. M. Vinogradov, I. L. Dalinger, B. I. Ugrak, S. A. Shevelev, *Mendeleev Commun.* **1996**, *6*, 139–140.

[33] P. Yin, J. Zhang, C. He, D. A. Parrish, J. M. Shreeve, *J. Mater. Chem. A* **2014**, *2*, 3200-3208.

[34] P. Yin, J. Zhang, D. A. Parrish, J. M. Shreeve, *Chem. Eur. J.* **2014**, *20*, 16529–16536.

[35] O. Mó, M. Yáñez, M. V. Roux, P. Jiménez, J. Z. Dávalos, M. A. V. Ribeiro da Silva, M. d. D. M. C. Ribeiro da Silva, M. A. R. Matos, L. M. P. F. Amaral, A. Sánchez-Migallón, P. Cabildo, R. Claramunt, J. Elguero, J. F. Liebman, *J. Phys. Chem. A* **1999**, *103*, 9336–9344.

[36] H. Huang, Z. Zhou, L. Liang, J. Song, K. Wang, D. Cao, C. Bian, W. Sun, M. Xue, *Z. Anorg. Allg. Chem.* **2012**, *638*, 392–400.

[37] J. Bao, Z. Zhang, R. Tang, H. Han, Z. Yang, *J. Lumin.* **2013**, *136*, 68–74.

[38] M. Mochizuki, S. Miura, Takeda Pharmaceutical Company Limited, Japan, CA2718727A1, **2009**.

[39] A. A. Trabanco-Suárez, H. J. M. Gijsen, M. L. M. v. Gool, J. A. V. Ramiro, F. Delgado-Jiménez, Janssen Pharmaceutica NV, WO 2012/117027 A1, **2012**.

[40] Z. P. Demko, K. B. Sharpless, *J. Org. Chem.* **2001**, *66*, 7945–7950.

[41] M. E. Bunnage, G. Maw, D. Rawson, A. Wood, J. P. Mathias, Pfizer Ltd., *WO0024745 (A1)* **2000**.

[42] A. A. Dippold, T. M. Klapötke, *Chem. Asian J.* **2013**, *8*, 1463–1471.

[43] I. A. Korbukh, S. V. Kitaev, M. N. Probrazhenskaya, *Zh. Org. Khim.* **1976**, *12*, 682–683.

[44] L. L. Fershtat, M. A. Epishina, A. S. Kulikov, I. V. Ovchinnikov, I. V. Ananyev, N. N. Makhova, *Tetrahedron* **2015**, *71*, 6764–6775.

[45] D. Kumar, L. A. Mitchell, D. A. Parrish, J. M. Shreeve, *J. Mater. Chem. A* **2016**, *4*, 9931–9940.

[46] H. Xue, S. W. Arritt, B. Twamley, J. M. Shreeve, *Inorg. Chem.* **2004**, *43*, 7972–7977.

[47] N. Fischer, T. M. Klapötke, M. Reymann, J. Stierstorfer, *Eur. J. Inorg. Chem.* **2013**, *2013*, 2167–2180.

[48] A. R. Katritzky, E. F. V. Scriven, S. Majumder, R. G. Akhmedova, N. G. Akhmedov, A. V. Vakulenko, *ARKIVOC (Gainesville, FL, U. S.)* **2005**, 179–191.

[49] I. L. Dalinger, I. A. Vatsadze, T. K. Shkineva, A. V. Kormanov, M. I. Struchkova, K. Y. Suponitsky, A. A. Bragin, K. A. Monogarov, V. P. Sinditskii, A. B. Sheremetev, *Chem. Asian J.* **2015**, *10*, 1987–1996.

[50] X. Zhao, C. Qi, L. Zhang, Y. Wang, S. Li, F. Zhao, S. Pang, *Molecules* **2014**, *19*, 896.

[51] P. Yin, D. A. Parrish, J. M. Shreeve, *Chem. Eur. J.* **2014**, *20*, 6707–6712.

[52] M. Hesse, H. Meier, B. Zeeh, *Spektroskopische Methoden in der organischen Chemie*, Thieme, Stuttgart, **2012**.

[53] M. Sućeska, *EXPLO5 V6.03 program*, Zagreb, Croatia, **2015**.

[54] H. D. B. Jenkins, D. Tudela, L. Glasser, *Inorg. Chem.* **2002**, *41*, 2364–2367.

6.5 Supplementary Information

6.5.1 X-ray Diffraction

Single crystals were picked and measured on an Oxford Xcalibur3 diffractometer with a Spellman generator (voltage 50 kV, current 40 mA) and a CCD area detector for data collection using Mo-*K*α radiation (λ = 0.71073 Å). The crystal structures of compound **5** was determined on a Bruker D8 Venture TXS diffractometer equipped with a multilayer monochromator, a Photon 2 detector, and a rotating-anode generator (MoKα radiation). The data collection was carried out using CRYSALISPRO software[S1] and the reduction were performed. The structures were solved using direct methods (SIR-92,[S2] SIR-97[S3] or SHELXS-97[S4]) and refined by full-matrix least-squares on *F*2 (SHELXL[S4]): The final check was done with the PLATON software[S5] integrated in the WinGX software suite. The non-hydrogen atoms were refined anisotropically and the hydrogen atoms were located and freely refined. The absorptions were corrected by a SCALE3 ABSPACK multiscan method.[S6] The DIAMOND2 plots are shown with thermal ellipsoids at the 50% probability level and hydrogen atoms are shown as small spheres of arbitrary radii. The SADABS program embedded in the Bruker APEX3 software has been used for multi-scan absorption corrections in all structures.[S7]

Table 6.S1. Crystallographic data and refinement parameters of compound **4**, **5, 6** and **8**.

	4	**5 ·2H$_2$O**	**6**	**8**
Formula	$C_5H_2N_4$	$C_5H_8N_{10}O_2$	$C_{10}H_{14}N_6O_{16}$	$C_{15}H_7N_{11}O_4$
FW [g mol^{-1}]	118.11	240.21	474.27	405.32
Crystal system	Monoclinic	Monoclinic	Triclinic	Monoclinic
Space Group	$P2_1/n$	$P2_1$/c	P-1	$P2_1$/c
Color / Habit	Colorless Plate	Colorless Plate	Colorless Plate	Colorless Block
Size [mm]	0.05 × 0.22 × 0.38	0.01 × 0.04 × 0.05	0.12 x 0.36 x 0.45	0.10 x 0.15 x 0.25
a [Å]	3.7386(2)	4.8173(3)	8.4124(11)	10.4274(5)
b [Å]	6.5622(3)	8.2655(6)	9.1690(9)	6.0887(2)
c [Å]	21.7083(14)	24.9783(19)	13.3980(16)	14.4805(6)
α [°]	90	90	85.766(9)	90
β [°]	94.361(6)	94.229(3)	88.102(10)	111.007(5)
γ [°]	90	90	65.688(11)	90
V [Å^3]	531.04(5)	991.86(12)	939.2(2)	858.25(7)
Z	4	4	2	2
$\rho_{calc.}$ [g cm^{-3}]	1.477	1.609	1.677	1.568
μ [mm^{-1}]	0.103	0.13	0.162	0.122
F(000)	240	496	488	412
$\lambda_{MoK\alpha}$[Å]	0.71073	0.71073	0.71073	0.71073
T [K]	173	173	173	173
ϑ min-max [°]	4.2, 26.0	2.6, 25.4	4.3, 26.0	4.2, 32.3
Dataset h; k; l	−4:4;−8:7; −25:26	−5:5;−9:9; −30:30	−10:7;−11:10; −16:16	−15:15;−8:8; −19:21
Reflect. coll.	3386	12991	6312	9140
Independ. refl.	1043	1830	3682	2822
R_{int}	0.038	0.097	0.048	0.034
Reflection obs.	864	1396	1793	2332
No. parameters	90	186	345	153
R_1 (obs)	0.0366	0.0586	0.0689	0.0680
wR_2 (all data)	0.0999	0.1225	0.1865	0.1302
S	1.06	1.05	1.05	1.25
Resd. Dens.[e Å^{-3}]	−0.19, 0.19	−0.30, 0.30	−0.37, 0.31	−0.28, 0.39
Device type	Oxford Xcalibur3	Bruker D8 Venture TXS	Oxford Xcalibur3	Oxford Xcalibur3
Solution	SIR-92	SIR-92	SIR-92	SIR-92
Refinement	SHELXL-97	SHELXL-2013	SHELXL-97	SHELXL-2013
Absorpt. corr.	multi-scan	multi-scan	multi-scan	multi-scan
CCDC	-	-	-	-

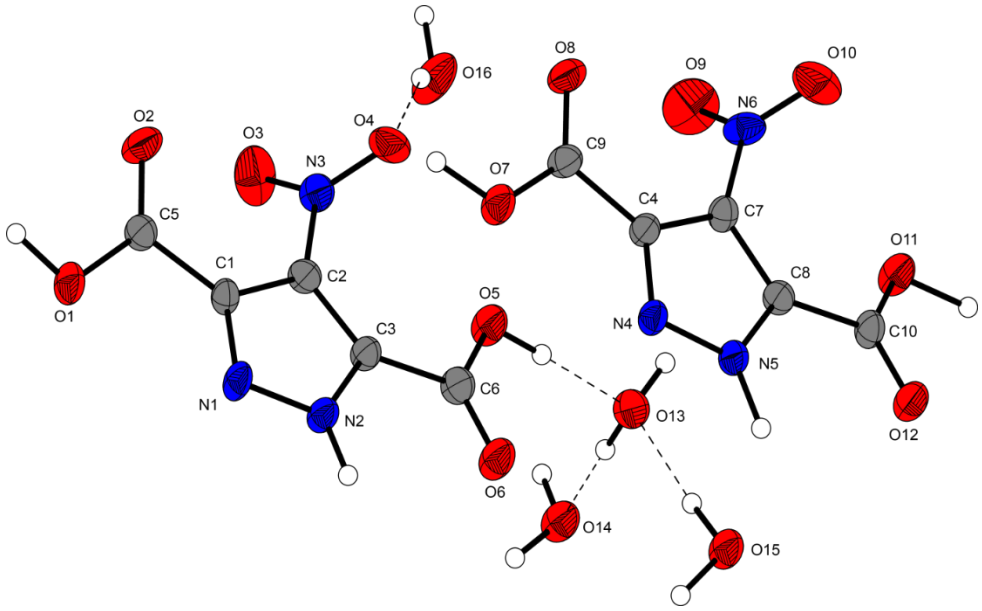

Figure 5.S1. Molecular structure of **6** showing the atom-labelling scheme. Thermal ellipsoids represent the 50% probability level.

6.5.2 Heat of formation calculations

All quantum chemical calculations were carried out using the Gaussian G09 program package.[S8] The enthalpies (H) and free energies (G) were calculated using the complete basis set (CBS) method of Petersson and coworkers in order to obtain very accurate energies. The CBS models are using the known asymptotic convergence of pair natural orbital expressions to extrapolate from calculations using a finite basis set to the estimated CBS limit. CBS-4 starts with an HF/3-21G(d) geometry optimization; the zero point energy is computed at the same level. It then uses a large basis set SCF calculation as a base energy, and an MP2/6- 31+G calculation with a CBS extrapolation to correct the energy through second order. A MP4(SDQ)/6-31+ (d,p) calculation is used to approximate higher order contributions. In this study, we applied the modified CBS-4M.

Heats of formation of the synthesized ionic compounds were calculated using the atomization method (equation E1) using room temperature CBS-4M enthalpies, which are summarized in Table 6.S2.[S9,S10]

$$\Delta_f H^\circ_{(g,\,M,\,298)} = H_{(Molecule,\,298)} - \sum H^\circ_{(Atoms,\,298)} + \sum \Delta_f H^\circ_{(Atoms,\,298)} \qquad (E1)$$

Table 6.S2. CBS-4M enthalpies for atoms C, H, N and O and their literature values for atomic $\Delta H°_f^{298}$ / kJ mol^{-1}

	$-H^{298}$ [a.u.]	NIST [S11]
H	0.500991	218.2
C	37.786156	717.2
N	54.522462	473.1
O	74.991202	249.5

For neutral compounds the sublimation enthalpy, which is needed to convert the gas phase enthalpy of formation to the solid state one, was calculated by the *Trouton* rule.[S12] For ionic compounds, the lattice energy (U_L) and lattice enthalpy (ΔH_L) were calculated from the corresponding X-ray molecular volumes according to the equations provided by *Jenkins* and *Glasser*.[S13] With the calculated lattice enthalpy the gas-phase enthalpy of formation was converted into the solid state (standard conditions) enthalpy of formation. These molar standard enthalpies of formation (ΔH_m) were used to calculate the molar solid state energies of formation (ΔU_m) according to equation E2.

$$\Delta U_m = \Delta H_m - \Delta n\, RT \qquad \text{(E2)}$$

(Δn being the change of moles of gaseous components)

The calculation results are summarized in Table 6.S3.

Table 6.S3. Heat of formation calculation results.

	$-H^{298}$ [a] [a.u.]	$\Delta_f H°$(g,M) [kJ mol^{-1}] [b]	V_M [Å^3] [c]	ΔU_L, ΔH_L ;[d] [kJ mol^{-}]^1	$\Delta_f H°$(s) [e] [kJ mol^{-1}]	Δn [f]	$\Delta_f U$(s) [g] [kJ kg^{-1}]
5	739.347837	812.72			723.76	7	3629.54
9	943.632928	827.93			754.21	8	3106.22

[a] CBS-4M electronic enthalpy; [b] gas phase enthalpy of formation; [c] molecular volumes taken from X-ray structures and corrected to room temperature; [d] lattice energy and enthalpy (calculated using Jenkins and Glasser equations); [e] standard solid state enthalpy of formation; [f] Δn being the change of moles of gaseous components when formed; [g] solid state energy of formation.

6.5.3 Experimental Part

General Procedures

Differential Scanning Calorimetry (DSC) was recorded on a LINSEIS DSC PT10 with about 1 mg substance in a perforated aluminum vessel with a heating rate of 5 K·min^{-1} and a nitrogen flow of 5 dm^3·h^{-1}. The NMR spectra were carried out using a 400 MHz instruments JEOL Eclipse 270, JEOL EX 400 or a JEOL Eclipse 400 (^{1}H 399.8 MHz, ^{13}C 100.5 MHz, ^{14}N 28.9 MHz, and ^{15}N 40.6 MHz). Chemical shifts are given in parts per million (ppm) relative to tetramethylsilane (^{1}H, ^{13}C) and nitromethane (^{14}N, ^{15}N). Infrared spectra were measured with a Perkin-Elmer Spectrum BX-FTIR spectrometer equipped with a Smiths DuraSamplIR II ATR device. Transmittance values are qualitatively described as "very strong" (vs), "strong" (s), "medium" (m), and "weak" (w). Raman spectra were recorded using a Bruker MultiRAM FT-Raman instrument fitted with a liquid-nitrogen cooled germanium detector and a Nd:YAG laser (λ = 1064 nm). The intensities are quoted as percentages of the most intense peak and are given in parentheses. DTA spectra were carried out using a OZM DTA 551-EX with a heating rate of 5 K·min^{-1}. Low-resolution mass spectra were recorded with a JEOL MStation JMS 700 (DEI+ / FAB+/−). Elemental analysis (C/H/N) was carried out using a Vario Micro from the Elementar Company. Impact sensitivity tests were performed according to STANAG 4489[S14] modified instruction[S15] using a Bundesanstalt für Materialforschung (BAM) drophammer.[S16] Friction sensitivity tests were carried out according to STANAG 4487[S17] modified instruction[S18] using a BAM friction tester. The grading of the tested compounds results from the "UN Recommendations on the Transport of Dangerous Goods".[S19] ESD values were carried out using the Electric Spark Tester ESD 2010 EN.[S20]

3,5-Dimethyl-1*H*-pyrazole (1) [S21]

Hydrazine monohydrate (100 %, 60 mL, 1.9 mol, 3.13 eq) was dissolved in water (150 mL) and the solution was cooled to 0 °C. Subsequently, acetylacetone (62 mL, 603 mmol, 1.00 eq) was added drop wise, whereby the temperature was kept below 15 °C. The resulting solution was allowed to warm to room temperature and stirred for 12 h. The precipitate was isolated by filtration, washed with water and dried. Compound **1** was obtained as colorless powder and used without further purification (60.7 g, 537 mmol, 89 %).

^{1}H NMR (400 MHz, DMSO d_6): δ = 11.99 (s, 1H, NH), 5.73 (s, 1H, CH), 2.12 (s, 6H, CH_3) ppm; **^{13}C NMR** (101 MHz, DMSO d_6): δ = 143.0 (C), 103.2 (CH), 11.8 (CH_3) ppm; **IR** (ATR, rel. int.): $\tilde{\nu}$ (cm^{-1}) = 3200 (m), 3131 (m), 3107 (m), 3037 (m), 2991 (m), 2940 (m), 2873 (s), 2787 (m), 2727 (m), 2608 (m),

1667 (w), 1594 (m), 1484 (m), 1421 (m), 1306 (s), 1149 (w), 1028 (s), 1008 (s), 839 (s), 777 (s), 737 (s), 661 (m), 590 (w); **DSC** (5 °C min^{-1}): 99 °C (melt.); **Elemental analysis:** calcd. (%) for $C_5H_8N_2$ (M = 96.13 g mol^{-1}): C 62.47, H 8.39, N 29.14; found: C 62.29, H 8.19, N 29.01; **Mass spectrometry:** m/z (DEI+) = 96.1 $[M]^+$.

1*H*-Pyrazole-3,5-dicarboxylic acid (2) hydrate [S21]

Compound **1** (20 g, 208 mmol, 1.00 eq) was suspended in water (500 mL) and the mixture was heated to 80 °C. Then potassium permanganate (160 g, 1.01 mol, 4.85 eq) was added portion wise, while keeping the temperature of the exothermic reaction between 90 and 95 °C by adding water. The resulting dark suspension was stirred under reflux for 4 h. Afterwards, the mixture was filtered hot and the colorless, clear filtrate was acidified with aqueous hydrochloric acid (37 %) to pH = 1. The precipitate was filtered off and dried to give compound **2** as a colorless powder (20.1 g, 129 mmol, 62 %).

^{1}H NMR (400 MHz, DMSO d_6**)**: δ = 6.98 (s, 1H, CH) ppm; **^{13}C NMR (**101 MHz, DMSO d_6**)**: δ = 161.5 (CO_2H), 140.4 (C), 109.9 (CH) ppm, **IR** (ATR, rel. int.): $\tilde{\nu}$ (cm^{-1}) = 3176 (w), 3126 (w), 2997 (w), 2363 (brw), 1692 (m), 1640 (m), 1556 (w), 1486 (w), 1456 (w), 1397 (w), 1318 (w), 1269 (m), 1196 (m), 1147 (brm), 1112 (m), 1010 (m), 989 (s), 857 (s), 809 (s), 800 (m), 780 (s), 655 (s); **DSC** (5 °C min^{-1}): 361 °C (dec.); **Elemental analysis:** calcd. (%) for $C_5H_6N_2O_5$ (M = 174.11 g mol^{-1}): C 33.49, H 3.47, N 16.09; found: C 33.05, H 3.35, N 15.40; **Mass spectrometry:** m/z (DEI+) = 156.1 $[C_5H_4N_2O_4]^+$.

1*H*-pyrazole-3,5-dicarboxamide (3) [S22 S23]

Compound **2** (25 g, 160 mmol, 1 eq.) was suspended in ethanol (400 ml) and cooled to 0 °C. Afterwards, thionyl chloride (30 ml, 412.67 mmol, 2.56 eq.) was added drop wise. The mixture was stirred for 72 hours at 40 °C and the solvent evaporated in vacuum. Ammonia (200 ml, 25 %) was added and it was stirred for 48 hours at 80 °C. The solvents were evaporated in vacuum and water was added to the solution. Then it was acidified with hydrochloric acid and after filtration compound **3** was obtained (18.25 g, 118.5 mmol, 74 %).

^{1}H NMR (400 MHz, DMSO d_6): δ = 7.84 (s, 2H, NH_2), 7.45 (s, 2H, NH_2), 7.21 (s, 1H, CH) ppm; **^{13}C NMR** (101 MHz, DMSO d_6): δ = 161.2 (CO_2H), 143.4 (C-CO_2H), 106.4 (C-H) ppm; **IR** (ATR, rel. int.): $\tilde{\nu}$ (cm^{-1}) = 3440 (w), 3379 (w), 3182 (w), 1680 (s), 1622 (w), 1519 (m), 1439 (m), 1456 (m), 1328 (m), 1250

(w), 1131 (m), 1007 (w), 844 (s), 790 (s), 736 (m), 624 (s), 524 (s); **DTA** (5 °C min^{-1}): 252 °C (melt.), 280 °C (dec.); **Elemental analysis:** calcd. (%) for $C_5H_6N_4O_2$ (M = 154.12 g mol^{-1}): C 38.96, H 3.92, N 36.35; found: C 38.75, H 3.38, N 36.98; **Mass spectrometry:** m/z (FAB-) = 153.1 $[C_5H_5N_4O_2]^-$.

1*H*-Pyrazole-3,5-dicarbonitrile (4) [S23]

Compound **3** (3.50 g, 18.2 mmol, 1.00 eq.) was suspended in acetonitrile (60 mL) and the reaction mixture was cooled to 0 °C. Then phosphoryl chloride (16.0 mL, 172 mmol, 9.45 eq.) was added drop wise at 0 °C and then the suspension was stirred at 120 °C for 6 h, during which the color changed to dark green. Then the mixture was cooled to room temperature and stirred overnight. Afterwards the solution was poured into an ice/water mixture (60 mL), whereby a solid precipitated and the color changed to purple. The suspension was filtered through kieselguhr and the filtrate was extracted with dichloromethane (3 x 100 mL). Subsequently, the combined organic layers were dried over magnesium sulfate and the solvent was evaporated in vacuum. The precipitate was dissolved in diethyl ether, filtered and the solvent was removed to yield **4** as a colorless powder (1.42 g, 12.0 mmol, 66 %).

^{1}H NMR (400MHz, DMSO d_6): δ = 7.89 (s, 1H, CH) ppm; **^{13}C NMR** (101MHz, DMSO d_6): δ =120.1 (C-CN), 118.7 (CN), 111.5 (CH) ppm; **IR** (ATR, rel. int.) $\tilde{\nu}$ (cm^{-1}) = 3233 (m), 3139 (w), 2262 (w), 2248 (w), 1704 (m), 1558 (w), 1537 (w), 1470 (w), 1447 (w), 1408 (w), 1377 (w), 1293 (m), 1271 (m), 1244 (m), 1200 (s), 1136 (w), 1016 (m), 994 (s), 876 (m), 843 (s), 793 (s), 769 (s), 680 (w), 661 (w); **DSC** (5 °C min^{-1}): 181 °C (melt.), 202 °C (dec.); **Elemental analysis:** calcd. (%) for $C_5H_2N_4$ (M = 118.09 g mol^{-1}): C 50.85, H 1.71, N 47.44; found: C 50.73, H 1.77, N 46.01; **Mass spectrometry:** m/z (DEI+) = 118.0 $[C_5H_2N_4]^+$, (FAB-) = 117.1 $[M-H]^-$.

5,5'-(1*H*-pyrazole-3,5-diyl)-bis-1*H*-tetrazole dihydrate (5)

Compound **4** (1.4 g, 11.86 mmol, 1 eq.) was dissolved in water (60 mL). Afterwards, sodium azide (1.85 g, 28.5 mmol, 2.4 eq.) and zinc chloride (1.94 g, 14.23 mmol, 1.2 eq) were added. Then the mixture was stirred for 24 hours at 100 °C. Afterwards, hydrochloric acid (50 mL, 2 M) was added and the mixture was extracted with ethyl acetate (3 x 100 mL). Compound **5** was obtained after evaporation of the solvents (1.34 g, 5.6 mmol, 47 %).

^{1}H NMR (400 MHz, DMSO d_6): δ =7.44 (s, 1H, CH) ppm; **^{13}C NMR** (101MHz, DMSO d_6): δ = 149.7, 108.0, 105.5 ppm; IR (ATR, rel. int.): $\tilde{\nu}$ (cm^{-1}) = 3509 (w), 3106 (m), 3039 (m), 2906 (m), 2681 (m), 2010 (w), 1737 (m), 1634 (m), 1532 (m), 1459 (m), 1386 (m), 1234 (m), 1177 (m), 1079 (m), 970

(s), 872 (s), 743 (s), 650 (m), 536 (s), 474 (s); **Mass spectrometry:** m/z (FAB+) = 205.2 $[C_5H_4N_{10}]^+$, (FAB-) = 203.3 $[C_5H_4N_{10}]^-$; **Elemental analysis:** calcd. (%) for $C_5H_8N_{10}O_2$ (M = 240.18 g mol^{-1}): C 25.00, H 3.36, N 58.32; found: C 25.14, H 3.36, N 58.65; **DTA** (5 °C min^{-1}): 87 °C (H_2O), 277 °C (dec.); **Sensitivities** (grain size: < 100 μm): **BAM impact**: >40 J, **BAM friction**: 360 N, **ESD**: 1.5 J.

4-Nitro-1*H*-pyrazole-3,5-dicarboxylic acid dihydrate (6) [S24]

Fuming sulfuric acid (Oleum, 30 %, 13 mL) was added over 45 min to ice-cooled fuming nitric acid (11 mL), so as to maintain a temperature below 15 °C during the addition. Subsequently, the mixture was warmed to 40 °C and compound **2** (15.0 g, 100 mmol) was added portion wise. The reaction then stirred at 60 °C for 12 h. Afterwards, the resulting suspension was poured on ice and stirred till all residues were solved. The solution was extracted with ethyl acetate (3×50 mL) and the organic layers were dried over magnesium sulfate. Then the organic solvent was evaporated in high vacuum and toluene (70 mL) was added to the remaining substance. After evaporation of the toluene compound **6** was obtained as colorless powder (13.0 g, 64.6 mmol, 65 %).

^{1}H NMR (400 MHz, DMSO d_6): δ = - ppm; **^{13}C NMR** (101 MHz, DMSO d_6): δ = 158.9 (CO_2H), 135.2 (C–NO_2), 132.8 (C–CO_2H) ppm; **^{14}N NMR** (DMSO d_6): δ = –21 (NO_2) ppm; **IR** (ATR, rel. int.): $\tilde{\nu}$ (cm^{-1}) = 3578 (w), 3513 (w), 3177 (m), 3019 (m), 1727 (s), 1697 (m), 1541 (m), 1512 (s), 1460 (m), 1393 (m), 1333 (m), 1232 (s), 1125 (m), 1022 (s), 893 (m), 814 (s), 738 (s), 599 (m), 553 (s), 491 (s); **DSC** (5 °C min^{-1}): 85 °C (H_2O), 199 °C (melt.), 216 °C (dec.), **Elemental analysis:** calcd. (%) for $C_{10}H_8N_6O_{13}$ (M = 420.21 g mol^{-1}): C 28.58, H 1.92, N 20.00; found: C 28.36, H 1.84, N 20.20, **Mass spectrometry:** m/z (FAB-) = 199.2 $[C_5HN_3O_6]^{2-}$.

4-Nitro-1*H*-pyrazole-3,5-dicarboxamide (7) [S25]

Compound **6** (12.5 g, 62.2 mmol, 1.00 eq) was dissolved in ethanol (150 mL) and thionyl chloride (29.2 mL, 404 mmol, 6.50 eq) was added drop wise to the solution over 2 h at 0 °C. Subsequently, the mixture was stirred under reflux for 36 h at 80 °C. The solvent of the resulting cooled solution was evaporated in vacuum and aqueous ammonia (25 %, 180 mL) was added and stirred under reflux at 70 °C for 2 d. Subsequently, the solution was cooled to room temperature and the solvent was evaporated in vacuum. Water (100 mL) was added and using HCl (37 %) the pH value was set to pH = 1. The precipitate was collected by filtration to yield compound **5** as yellowish solid (8.8 g, 44.1 mmol, 71 %).

^{1}H NMR (400 MHz, DMSO d_6): δ = 8.15 (s, 2H, NH_2), 7.93 (s, 2H, NH_2) ppm; **^{13}C NMR** (101 MHz, DMSO d_6): δ = 159.8 (CO_2H), 138.6 (C–NO_2), 130.5 (C–CO_2H) ppm; **IR** (ATR, rel. int.): ν (cm^{-1}) = 3440 (w), 3083 (w), 2887 (w), 2361 (w), 2340 (w), 1693 (m), 1614 (s), 1558 (w), 1529 (m), 1508 (s), 1492 (m), 1450 (s), 1404 (s), 1375 (m), 1354 (s), 1328 (s), 1281 (w), 1191 (w), 1127 (w), 1009 (w), 862 (w), 840 (s), 806 (s), 767 (s) 699 (w), 608 (w); **DSC** (5 °C min^{-1}): 254 °C (melt.), 280 °C(dec.); **Elemental analysis:** calcd. (%) for $C_4H_5N_5O_4$ (M = 199.13 g mol^{-1}): C 30.17, H 2.53, N 35.17; found: C 30.23, H 2.51, N 34.51.

Pyridinium-3,5-dicarbonitrile-4-nitropyrazolate (8)

Compound **7** (1.1 g, 5.5 mmol, 1.0 eq.) was dissolved in acetonitrile (30 mL) and pyridine (1.62 mL, 20.1 mmol, 3.7 eq.) and the solution was cooled to 0 °C. Subsequently, trifluoroacetic anhydride (2.65 mL, 18.8 mmol, 3.4 eq.) was added drop wise over 1 h, while keeping the temperature between 0–5 °C. The mixture was stirred at room temperature for 72 h. Afterwards, water (10 mL) was added and the solvent was concentrated in vacuum. The residue was allowed to stand for crystallization. Compound **8** was obtained as colorless crystals (0.31 g, 1.2 mmol, 22 %).

^{1}H NMR (400 MHz, DMSO d_6): δ = 8.94 (dd, 2H, *3J* = 6.6 Hz, *4J* = 1.5 Hz, $CH_{pyr.}$), 8.65 (tt, 1H, *3J* = 7.9 Hz, *4J* = 1.6 Hz, $CH_{pyr.}$), 8.11 (dd, 2H, *3J* = 7.8 Hz, *3J* = 6.5 Hz, $CH_{pyr.}$) ppm; **^{13}C NMR** (101 MHz, DMSO d_6): δ = 146.7 (N-$CH_{pyr.}$), 142.0 ($CH_{pyr.}$), 138.3 (C-NO_2), 127.3 ($CH_{pyr.}$), 120.5 (C-CN), 113.1 (CN) ppm; **IR** (ATR, rel. int.): $\tilde{\nu}$ (cm^{-1}) = 3278 (w), 3092 (w), 2247 (w), 1739 (m), 1680 (m), 1634 (m), 1607 (m), 1539 (m), 1485 (s), 1424 (w), 1361 (m), 1259 (w), 1190 (s), 1136 (s), 1079 (m), 1024 (m), 987 (m), 915 (w), 830 (s), 797 (m), 721 (m), 673 (s), 606 (s), 575 (s), 481 (s); **DSC** (5°C min^{-1}): 165 °C (melt.), 215 °C (dec.); **Elemental analysis:** calcd. (%) for $C_{10}H_7N_{11}O_4$ (M = 405.32 g mol^{-1}): C 44.45, H 1.74, N 38.02; found: C 44.13, H 1.85, N 37.28; **Mass spectroscopy:** m/z (FAB+) = 80.1 [$C_5H_6N^+$], m/z (FAB-) = 162.1 [$C_5N_5O_2^-$].

5,5'-(4-Nitro-1*H*-pyrazole-3,5-diyl)-bis-1*H*-tetrazole hydrate (9)

A mixture of compound **8** (1.57 g, 6.48 mmol, 1.00 eq), sodium azide (0.93 g, 14.26 mmol, 2.20 eq) and zinc chloride (2.12 g, 15.6 mmol, 2.4 eq) in water (60 mL) was stirred under reflux at 100 °C for 1 d. Subsequently, 2 M aqueous hydrochloric acid solution (25 mL) was added to the suspension. The residual solid was filtered off and washed with water to yield compound **9** as colorless solid (0.94 g, 3.76 mmol, 58 %).

^{1}H NMR (400 MHz, DMSO d_6): δ = - ppm; **^{13}C NMR** (101 MHz, DMSO d_6): δ = 147.9, 142.7, 131.7 ppm; **IR** (ATR, rel. int.): ν (cm^{-1}) = 3080 (m), 1610 (m), 1580 (m), 1529 (s), 1395 (s), 1312 (m), 1179 (m),

1098 (m), 1042 (m), 973 (s), 779 (s), 755 (s); **Elemental analysis:** calcd. (%) for $C_5H_5N_{11}O_3$ (M = 267.17 g mol^{-1}): C 22.48, H 1.89, N 57.67; found: C 22.02, H 2.08, N 56.94; **DTA** (5 °C min^{-1}): 119 °C (melt.), 246 °C (dec.); **Mass spectrometry**: m/z (FAB$^-$) = 248.2 $[C_5H_3N_{11}O_2]^-$.

6.5.4 References

[S1] *CrysAlisPro*, Oxford Diffraction Ltd., version 171.33.41, **2009**.

[S2] *SIR-92*, *A program for crystal structure solution*: A. Altomare, G. Cascarano, C. Giacovazzo, A. Guagliardi, *J. Appl. Crystallogr.* **1993**, *26*, 343.

[S3] a) A. Altomare, G. Cascarano, C. Giacovazzo, A. Guagliardi, A. G. G. Moliterni, M. C. Burla, G. Polidori, M. Camalli, R. Spagna, *SIR97*, **1997**; b) A. Altomare, M. C. Burla, M. Camalli, G. L. Cascarano, C. Giacovazzo, A. Guagliardi, A. G. G. Moliterni, G. Polidori, R. Spagna, *J. Appl. Crystallogr.* **1999**, *32*, 115–119.

[S4] a) G. M. Sheldrick, *SHELX-97*, University of Göttingen, Göttingen, Germany, **1997**; b) G. M. Sheldrick, *Acta Crystallogr., Sect. A* **2008**, *64*, 112–122.

[S5] A. L. Spek, *PLATON*, *A Multipurpose Crystallographic Tool*, Utrecht University, The Netherlands, **1999**.

[S6] *SCALE3 ABSPACK – An Oxford Diffraction program* (1.0.4, gui: 1.0.3), Oxford Diffraction Ltd., **2005**.

[S7] *APEX3*. Bruker AXS Inc., Madison, Wisconsin, USA.

[S8] M. J. Frisch, G. W. Trucks, H. B. Schlegel, G. E. Scuseria, M. A. Robb, J. R. Cheeseman, G. Scalmani, V. Barone, B. Mennucci, G. A. Petersson, H. Nakatsuji, M. Caricato, X. Li, H.P. Hratchian, A. F. Izmaylov, J. Bloino, G. Zheng, J. L. Sonnenberg, M. Hada, M. Ehara, K. Toyota, R. Fukuda, J. Hasegawa, M. Ishida, T. Nakajima, Y. Honda, O. Kitao, H. Nakai, T. Vreven, J. A. Montgomery, Jr., J. E. Peralta, F. Ogliaro, M. Bearpark, J. J. Heyd, E. Brothers, K. N. Kudin, V. N. Staroverov, R. Kobayashi, J. Normand, K. Raghavachari, A. Rendell, J. C. Burant, S. S. Iyengar, J. Tomasi, M. Cossi, N. Rega, J. M. Millam, M. Klene, J. E. Knox, J. B. Cross, V. Bakken, C. Adamo, J. Jaramillo, R. Gomperts, R. E. Stratmann, O. Yazyev, A. J. Austin, R. Cammi, C. Pomelli, J. W. Ochterski, R. L. Martin, K. Morokuma, V. G. Zakrzewski, G. A. Voth, P. Salvador, J. J.

Dannenberg, S. Dapprich, A. D. Daniels, O. Farkas, J.B. Foresman, J. V. Ortiz, J. Cioslowski, D. J. Fox, Gaussian 09 A.02, Gaussian, Inc., Wallingford, CT, USA, **2009**.

[S9] a) J. W. Ochterski, G. A. Petersson, and J. A. Montgomery Jr., *J. Chem. Phys.* **1996**, *104*, 2598–2619; b) J. A. Montgomery Jr., M. J. Frisch, J. W. Ochterski G. A. Petersson, *J. Chem. Phys.* **2000**, *112*, 6532–6542.

[S10] a) L. A. Curtiss, K. Raghavachari, P. C. Redfern, J. A. Pople, *J. Chem. Phys.* **1997**, *106*, 1063–1079; b) E. F. C. Byrd, B. M. Rice, *J. Phys. Chem*. A **2006**, *110*, 1005–1013; c) B. M. Rice, S. V. Pai, J. Hare, *Comb. Flame* **1999**, *118*, 445–458.

[S11] P. J. Lindstrom, W. G. Mallard (Editors), NIST Standard Reference Database Number 69, http://webbook.nist.gov/chemistry/ (accessed June **2011**).

[S12] M. S. Westwell, M. S. Searle, D. J. Wales, D. H. Williams, *J. Am. Chem. Soc*. **1995**, *117*, 5013–5015; b) F. Trouton, *Philos. Mag*. **1884**, *18*, 54–57.

[S13] a) H. D. B. Jenkins, H. K. Roobottom, J. Passmore, L. Glasser, *Inorg. Chem.* **1999,** *38,* 3609–3620; b) H. D. B. Jenkins, D. Tudela, L. Glasser, *Inorg. Chem.* **2002**, *41*, 2364–2367.

[S14] NATO standardization agreement (STANAG) on explosives, *impact sensitivity tests*, no. 4489, 1st ed., Sept. 17, **1999**.

[S15] WIWEB-Standardarbeitsanweisung 4-5.1.02, Ermittlung der Explosionsgefährlichkeit, hier der Schlagempfindlichkeit mit dem Fallhammer, Nov. 8, **2002**.

[S16] http://www.bam.de

[S17] NATO standardization agreement (STANAG) on explosive, *friction sensitivity tests*, no. 4487, 1st ed., Aug. 22, **2002**.

[S18] WIWEB-Standardarbeitsanweisung 4-5.1.03, Ermittlung der Explosionsgefährlichkeit oder der Reibeempfindlichkeit mit dem Reibeapparat, Nov. 8, **2002**.

[S19] Impact: insensitive > 40 J, less sensitive ≥ 35 J, sensitive ≥ 4 J, very sensitive ≤ 3 J; Friction: insensitive > 360 N, less sensitive = 360 N, sensitive < 360 N and > 80 N, very sensitive ≤ 80 N, extremely sensitive ≤ 10 N, According to: *Recommendations on the Transport of Dangerous Goods, Manual of Tests and Criteria*, 4th edition, United Nations, New York-Geneva, **1999**.

[S20] http://www.ozm.cz

[S21] J. Bao, Z. Zhang, R. Tang, H. Han, Z. Yang, *Journal of Luminescence* **2013**, *136*, 68–74.

[S22] M. Mochizuki, S. Miura, (Takeda Pharmaceutical Company Limited, Japan), CA2718727A1, **2009**.

[S23] A. A. Trabanco-Suárez, H. J. M. Gijsen, M. L. M. v. Gool, J. A. V. Ramiro, F. Delgado-Jiménez, (Janssen Pharmaceutica NV), WO 2012/117027 A1, **2012**.

[S24] M. E. Bunnage, G. Maw, D. Rawson, A. Wood, J. P. Mathias, Pfizer Ltd., *WO0024745 (A1)* **2000**.

[S25] I. A. Korbukh, S. V. Kitaev, M. N. Probrazhenskaya, *Zh. Org. Khim.* **1976**, *12*, 682–683.

7 Metal Salts and Complexes of 1,1’-Dinitramino-5,5’-bitetrazole

Norbert Szimhardt, Marc F. Bölter, Maximilian Born, Thomas M. Klapötke, and Jörg Stierstorfer

as published in

Dalton Trans. **2017**, *46*, 5033–5040 (DOI: 10.1039/C7DT00536A)

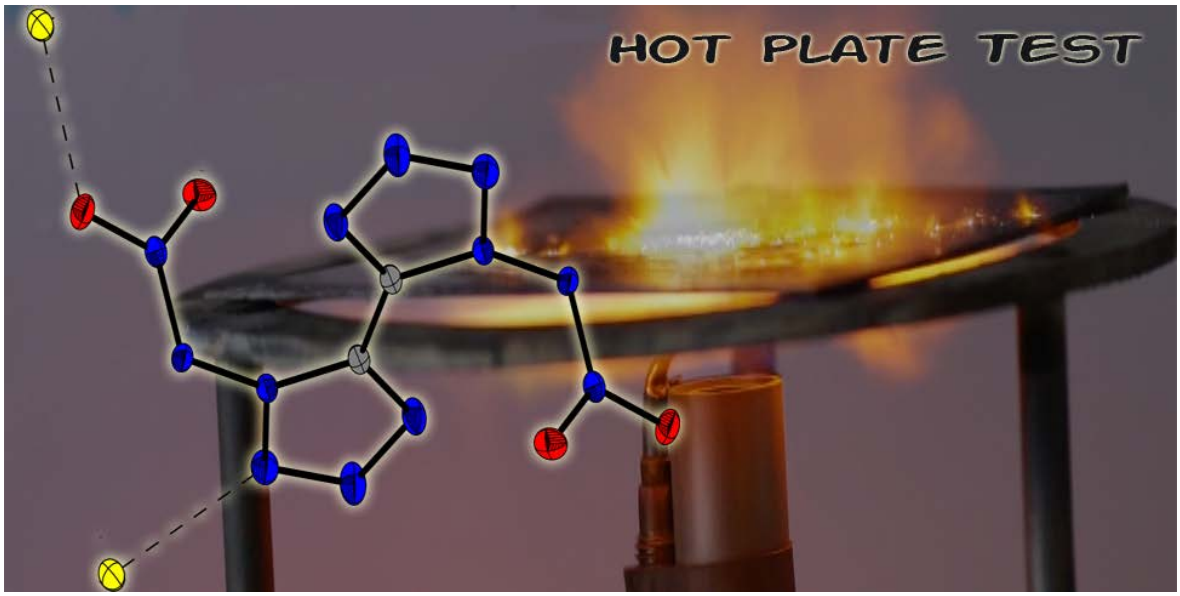

Abstract: Potassium 1,1'-dinitramino-5,5'-bitetrazolate is one of the most promising primary explosives which is currently under investigation for different applications. This is due to its high initiation power and the exclusion of heavy metals. To close the gap, the remaining alkali metal salts such as the lithium **6**, sodium **7**, rubidium **8** and cesium **9** salts were synthesized by reaction of the highly soluble ammonium salt **5** with corresponding metal hydroxide solutions. In addition, the highly explosive silver salt **10** as well as several other transition metal(II) amine complexes with nickel(II) **11**, copper(II) **12** and zinc(II) **13** were prepared in a similar manner. The structure of all compounds was determined by X-ray diffraction. The sensitivities toward impact, friction, heat and electrostatic discharge as well as their behavior on laser irradiation of the transition metal complexes was explored.

7.1 Introduction

The research on green energetic materials is still an ongoing project in many research groups world-wide.[1–5] All classes of energetic materials such as explosives, propellants, pyrotechnics contain ingredients or at least decomposition products which are not environmentally benign. Nitrogen-rich derivatives are promising alternatives as energetic materials due to their high heat of formation and the formation of molecular nitrogen as an end product of propulsion or explosion. The most applied primary explosives e.g. in blasting caps still are lead azide and lead styphnate.[6] Lead azide is reliable, cheap, easy to manufacture and shows perfect thermal stability. However they are listed by REACH regulations as "substances of very high concern" and are banned for future's applications.[7] Alternatives are strongly needed. In 2015, the dipotassium salt of 1,1'-dinitramino-5,5'-tetrazole (K_2DNABT) gained worldwide interest as a new and promising primary explosive.[8] It showed an extremely short DDT (deflagration to detonation) behavior[6] and also high sensitivities toward stimuli such as friction, impact and electrostatic discharge which is desirable for compounds used in initiators. In preliminary tests it showed almost no toxicity in aquatic media (toward the bacteria vibrio fischeri) which makes it an outstanding candidate for replacement of toxic lead azide. The search for alternatives for lead azide is an ongoing topic in many research groups or companies worldwide.[9] Mostly metal salts of acidic energetic organic molecules were described since they often show higher decomposition temperatures than pure organic salts or the corresponding organic acid. Examples are KDNP (potassium 4,6-dinitro-7-hydroxybenzofuroxan)[10] or DBX-1 (copper(I) 5-nitrotetrazolate).[11]

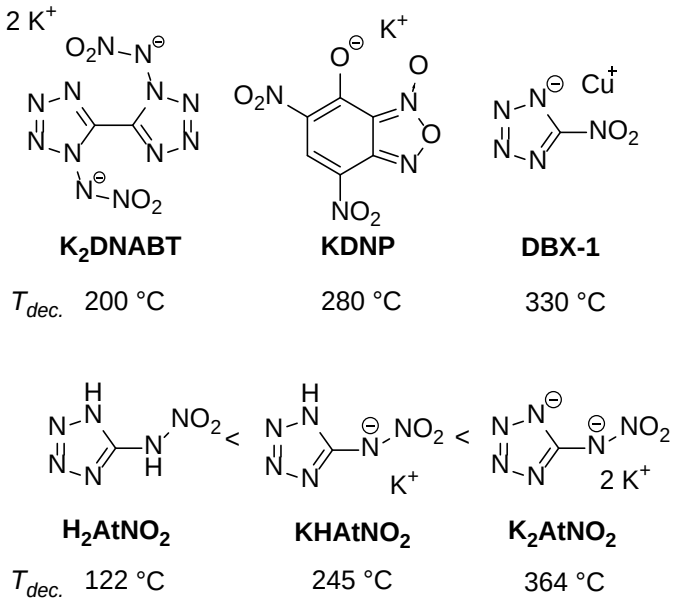

Figure 7.1. Structural formula of K_2DNABT, KDNP, DBX-1, 5-nitriminotetrazole (H_2AtNO2) and its mono- ($KHAtNO_2$) and di-potassium (K_2AtNO2) salts. Temperatures of decomposition were taken from different references and measured at variable heating rates and methods.

The same trend can be observed for metal free salts of 1,1'-dinitramino-5,5'-tetrazole such as the ammonium or hydrazinium salts.[12] They are extremely powerful energetic materials with outstanding detonation velocities, however their high sensitivities and low thermal stabilities will probably prevent any application as secondary explosives.[12] An exceptional high thermal resistance of 223 °C was only found for 4,4',5,5'-tetraamino-3,3'-bi-1,2,4-triazolium 1,1'-dinitramino-5,5'-tetrazolate.[13] Low thermal stabilities were observed for a huge number of metal-free 1- and 5-nitraminotetrazoles.[1c] The trend of increasing thermal stability by deprotonation and introduction of metal cations can impressively been on the following examples: 5-nitrimino-*1,4-H*-tetrazole (H_2AtNO_2, $T_{dec.}$: 122 °C)[14] < potassium 5-nitrimino-*1H*-tetrazolate ($KHAtNO_2$, $T_{dec.}$: 245 °C)[14] < dipotassium 5-nitriminotetrazolate (K_2AtNO_2, $T_{dec.}$: 364 °C)[15]. Consequently in this paper the synthesis and characterization of a large variety of highly energetic (alkaline, alkaline earth and transition) metal 1,1'-dinitramino-5,5'-tetrazolates is presented.

7.2 Results and Discussion

7.2.1 Synthesis

Warning (!): Synthesized compounds **5**–**13** (especially **8**–**10**) are extremely powerful and sensitive compounds. Unintentionally explosions of **8** and **10** happened during handling. Protective measures are mandatory.

All metal salts were synthesized starting from diammonium 1,1'-dinitramino-5,5'-tetrazolate (**5**) as precursor.[12] Compound **5** was prepared slightly different in comparison to our previous method illustrated in Scheme 7.1. During the synthesis of the 1,1'-dinitramino-5,5'-tetrazolate dianion the diazido compound **3** could be crystallized and the structure determined. Also the nitrated bitetrazole **4**, which is highly energetic but rather unstable, could be isolated and characterized.

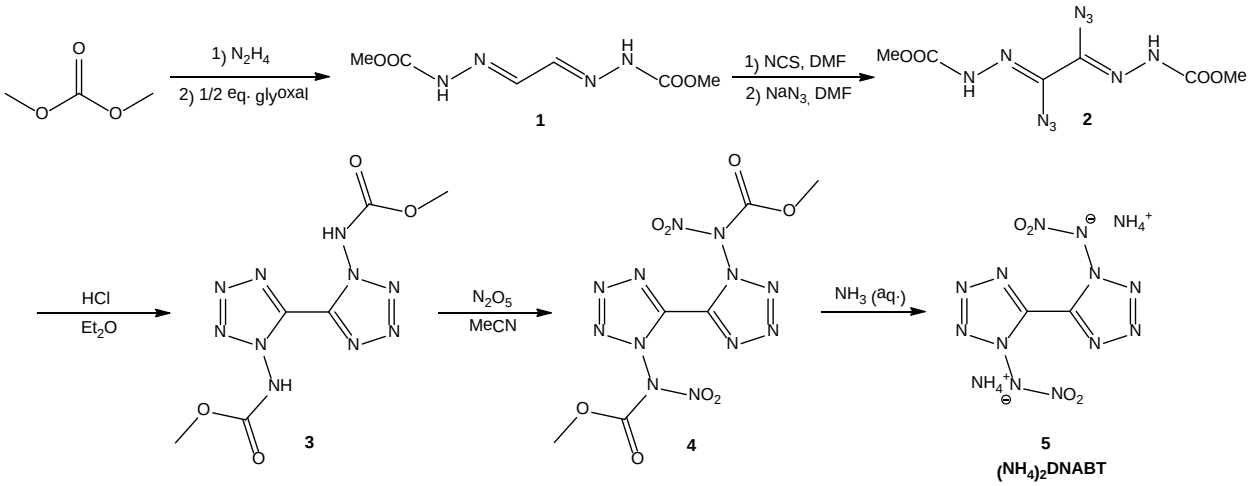

Scheme 7.1. New synthetic route to compound **5**.

The ammonium salt **5** shows a high solubility in water or concentrated ammonia and was therefore very well suited as starting material. The metal salts/complexes were prepared in straightforward ionic metathesis reactions by combining solutions of compound **5** and metal salts in the corresponding solvent (Scheme 7.2). Very careful heating of the reaction mixture is required to ensure a complete acid-base reaction. The alkaline earth metal salts **14**–**16** could only be synthesized insufficiently. In contrast to expectations compounds **14**–**16** are highly soluble in water. These solutions could not be stored by exposure to air because of the intake of carbon dioxide which led to the precipitation of Ca-, Sr- and $BaCO_3$ again. Therefore **14**–**16** could not be purified in larger quantities. Solely the crystal structures of **15** as tetrahydrate and **16** as hexahydrate could be determined which are shown in the SI. A practical elemental analysis of **14** confirmed the inclusion

of four crystal water molecules. In contrast the water-free alkaline salts K_2DNABT, **8** and **9** as well as the silver salt are hardly soluble in water. The rubidium **8** and cesium salt **9** started to precipitate right after addition of the metal(I) hydroxide solution. In case of **9** a very fast precipitation led to a violent detonation of the reaction mixture and should be avoided. Recrystallization from hot water afforded single crystals suitable for X-ray diffraction. Single crystals of **6**–**9** and **11**–**13** were grown directly from the corresponding reaction media. Two drops of concentrated ammonia were added in order to better the solubility of the silver salt **10**. Single crystals could be isolated from the mother liquor and transferred into perfluorinated oil for XRD. All attempts to dry the silver salt for further characterization failed and led to detonation of the compound! The sodium salt was obtained in two different polymorphs (**7a** and **7b**) with varying physicochemical properties depending on the solvent. H_2O afforded monoclinic **7a**, recrystallization of the compound from EtOH yielded orthorhombic **7b**.

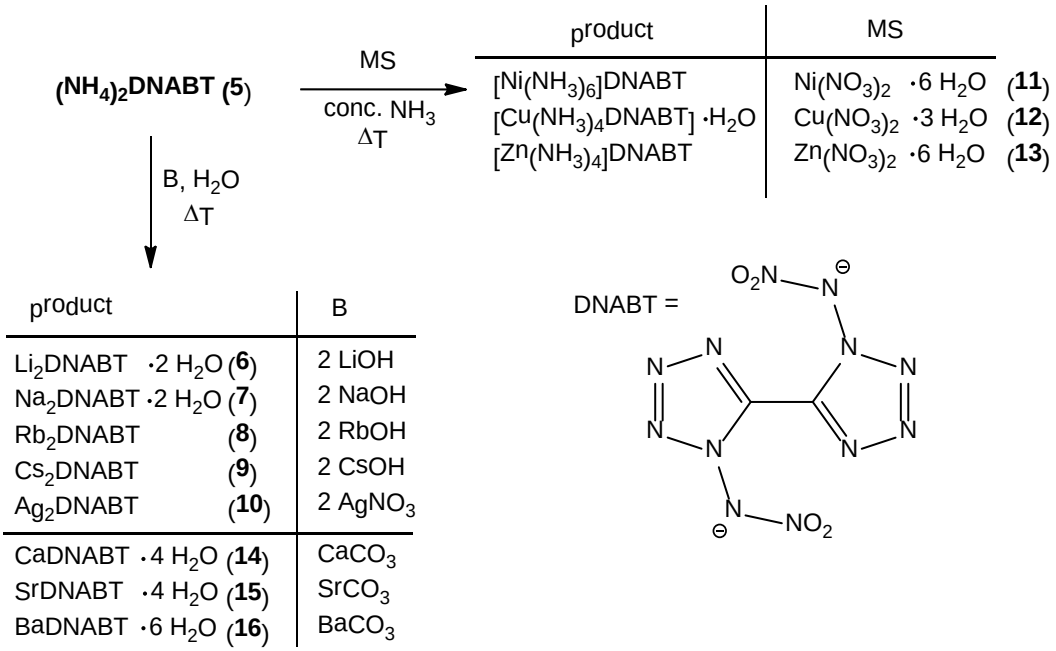

Scheme 7.2. Synthesis of **6**–**16** based on ionic metathesis reactions.

7.2.2 Crystal structures

The structures of **2**, **6**–**13** as well as **15** and **16** were determined by low temperature crystal X-ray diffraction. Details on the measurements and refinements are given in the SI. The crystal structures were deposited in the CSD database [16] and can be obtained free of charge with the CCDC Nos. 1502966 (**2**), 1500005 (**6**), 1500002 (**7a**), 1500003 (**7b**), 1500001 (**8**), 1500004 (**9**), 1502967 (**10**), 1510458 (**11**), 1502968 (**12**), 1510459 (**13**), 1524647 (**15**) and 1524646 (**16**).

Azide **2** crystallizes in the form of red rods in the triclinic space group *P*–1 with one formula unit per unit cell and a calculated density of 1.584 g cm^{-3} at 173 K. The molecular unit consists of two asymmetric moieties with a centre of inversion on the C1–C1^{i} bond and is illustrated in Figure 7.2. The molecule shows an obvious conjugation of the π-electrons and is almost planar. Only the azide chains are marginally twisted out of the plane. All bond lengths in the chain from oxygen atom O2 to O2^{i} are between typical single and double bonds.

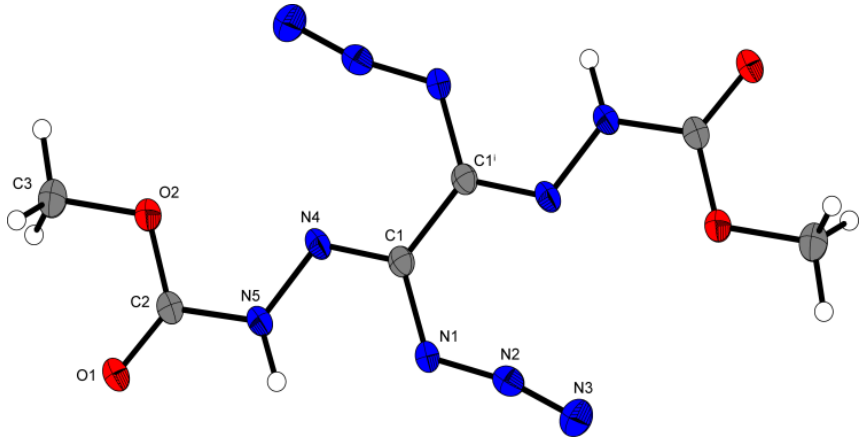

Figure 7.2. Molecular structure of **2** showing the atom-labelling scheme. Selected bond lengths [Å]: C1–C1^{i} 1.468(4), N1–C1 1.399(3), N1–N2 1.242(2), N2–N3 1.126(3), N4–C1 1.282(3), N4–N5 1.364(2), N5–C2 1.356(3), C2–O1 1.215(3), C2–O2 1.334(2), O2–C3 1.439(3). Selected bond angles [°]: N1–N2–N3 168.7(2), C1–N1–N2 122.5(2). Thermal ellipsoids in all structures represent the 50 % probability level. Hydrogen atoms are shown as small spheres of arbitrary radii Symmetry code (i) 2–x, 1–y, 1–z.

The bond lengths, bond angles, and torsion angles for the 1,1'-dinitramino-5,5'-tetrazolate dianion in all metal salts **6**–**13** are in the range of the literature reported neutral parent compound and its potassium salt.[12,8] All four alkaline metal salts crystallize in common space groups (**8**: *P*–1; **6**, **7a**, **9**: $P2_1/c$; **7b**: *Pbca*) with almost increasing densities (**7a**: 1.927 g cm^{-3} (173 K) < **7b**: 1.940 g cm^{-3} (123 K); **6**: 1.949 g cm^{-3} (123 K); **8**: 2.551 g cm^{-3} (173 K) < **9**: 2.829 g cm^{-3} (173 K)) in different coordination spheres (**6**: fivefold; **7a/b**: sixfold; **8**: ninefold; **9**: eightfold). The lithium and sodium salts were the only two alkaline metals, which crystallized as dihydrates. Their molecular units are shown in Figure 7.3 and 7.4.

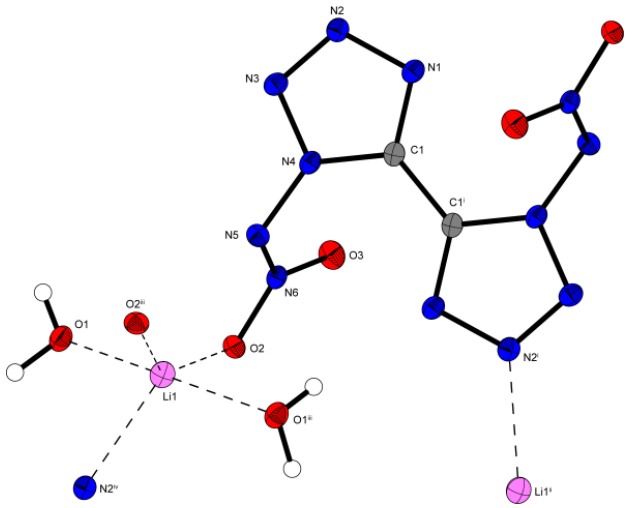

Figure 7.3. Extended molecular structure of **6** showing the atom-labelling scheme. Selected bond lengths [Å]: O1–Li1 2.047(3), $O1^{iii}$–Li1 2.114(3), O2–Li1 2.097(3), $O2^{iii}$–Li1 2.051(3), $N2^{iii}$–Li1 2.208(4). Symmetry codes (i) 1−x, −y, 1−z); (ii) −x, 0.5+y, 0.5−z; (iii) x, −0.5−y, −0.5+z; (iv) x, −0.5−y, −0.5+z.

The sodium salt 7 crystallizes in two varying polymorphs (Figure 7.3) depending on the solvent used. Each compound exhibits a different hydrogen bond network that affects their packing. Therefore both compounds can be clearly distinguished through infrared spectroscopy (Figure 7.S3).

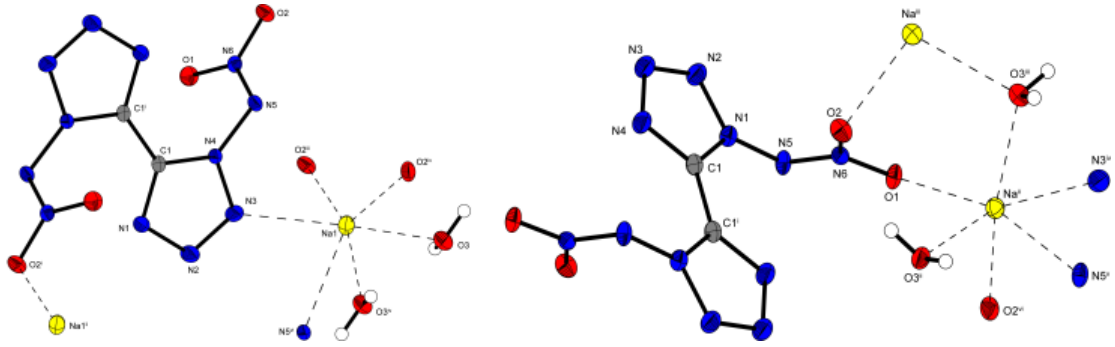

Figure 7.4. Extended molecular structures of **7a** (left) and **7b** (right) showing the atom-labelling scheme. Selected coordination distances [Å] **7a**: Na1–O3 2.368(2), Na–$O3^{v}$ 2.391(2), Na–N3 2.491(2), Na–$N5^{vi}$ 2.594(2), Na–$O2^{iv}$ 2.454(2), Na–$O2^{iii}$ 2.433(2); **7b**: Na^{ii}–O1 2.378(1), Na^{ii}–$O3^{iii}$ 2.336(1), Na^{ii}–$N3^{iv}$ 2.602(1), Na^{ii}–$O2^{vi}$ 2.377(2), Na^{ii}–$N5^{v}$ 2.543(1), Na^{ii}–$O3^{ii}$ 2.392(1). Symmetry codes **7a**: (i) −x, 1−y, 1−z; (ii) −1+x, y, z; (iii) 1−x, 1−y, 1−z; (iv); 1−x, −0.5+y, 1.5−z; (v) 1−x, −y, 1−z; (vi) x, 0.5−y, −0.5+z. **7b**: (i) −1−x, 1−y, −z; (ii) −0.5−x, 0.5+y, z; (iii) −x, 0.5+y, 0.5−z; (iv) −0.5−x, 1−y, 0.5+z; (v) −1−x, 0.5+y, 0.5−z; (vi) −1.5+x, y, 0.5−z.

The very sensitive heavy metal rubidium **8** and cesium **9** salts crystallize without inclusion of crystal water and are illustrated in Figure 7.5.

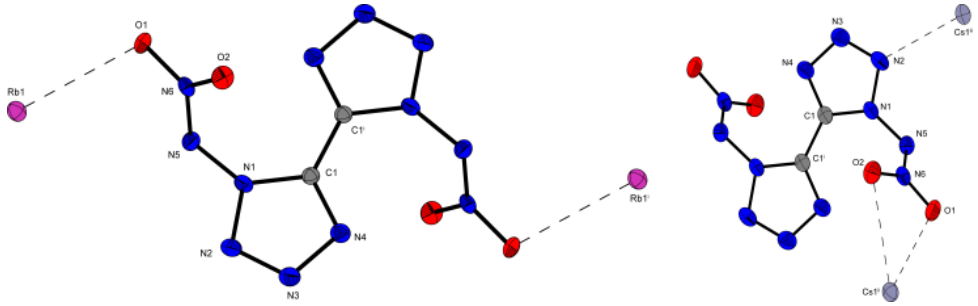

Figure 7.5. Molecular structures of **8** (left) and **9** (right) showing the atom-labelling scheme. Selected coordination distances lengths [Å] **8**: Rb1–O1 2.872(2); **9**: $Cs1^{iii}$–N2 3.334(3), $Cs1^{ii}$–O2 3.335(3), $Cs1^{ii}$–O1 3.043(2). Symmetry codes **8**: (i) −x, 1−y, 1−z; **9**: (i) x, 0.5−y, 0.5+z; (ii) 1+x, 0.5−y, 0.5+z; (iii) 1−x, −0.5+y, 0.5−z.

The silver salt **10** crystallizes in the form of colorless needles in the monoclinic space group *P*2/*c* with four formula units per unit cell and a calculated density of 3.240 g cm^{-3} at 173 K. Figure 7.6 displays the extended molecular structure of compound **10** and its labeling scheme. Both silver cations show different surroundings. Silver atom Ag2 is positioned on the crystallographic origin (0,0,0), while atom Ag1 is on (0,0.0140(1),1/4) bearing a rotation axis. Both are strongly linear coordinated (Ag1–N4/$N4^{iv}$ 2.267(7) Å, Ag2–N3/$N3^{ii}$ 2.250(7) Å). Taking into account also weaker coordination distances up to 3 Å, atom Ag1 is coordinated by eight donor atoms, while atom Ag2 is octahedrally coordinated by six donors. The coordination distances are in agreement with values reported for silver 1-methyl-5-nitriminotetrazolate in literature.[17]

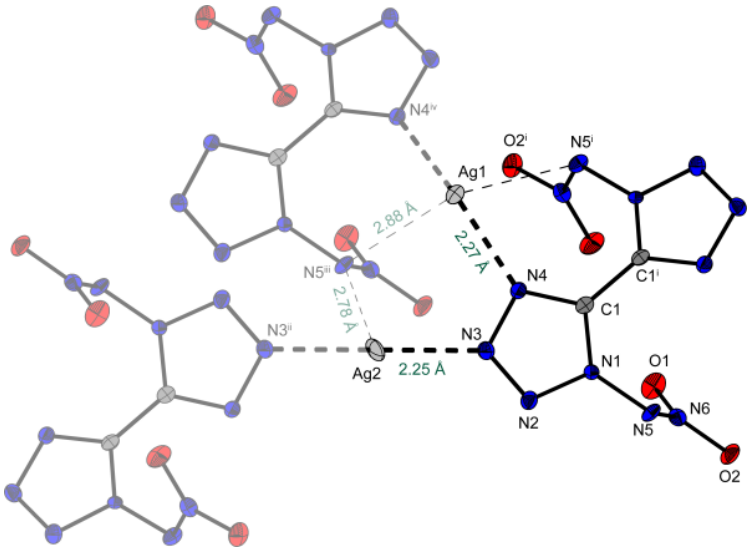

Figure 7.6. Extended molecular structure of **10**, indicating a strong linear coordination of the silver cations by the nitrogen atoms N4 and N3. Selected bond lengths [Å]: Ag2–N3 2.250(7), Ag2–N5^{ii} 2.776(7), Ag2–O2^{v} 2.680(4), Ag1–N4 2.267(7), Ag1–N5^{iii} 2.883(8), Ag1–O2^{vi} 2.594(4), Ag1–O1^{vi} 2.881(6). Symmetry codes (i): 1–x, y, 0.5–z; (ii) –x, –y, –z; (iii) –1+x, y, z; (iv) –x, y, 0.5–z; (v) 1–x, 1–y, –z; (vi) 1–x, –1+y, 0.5–z.

Compound **11** is, to the best of our knowledge, the first energetic hexamminenickel(II) complex in literature. It crystallizes in the form of clear light purple cylinders in the monoclinic space group $P2_1/c$ with four formula units per unit cell and a calculated density of 1.708 g cm^{-3} at 173 K. The nickel(II) centers are octahedrally coordinated (Figure 7.7) by six ammine ligands. The DNABT counterion is (in contrast to the other already discussed metal salts) not involved in coordination. All bond lengths between the d^8-metal(II) center and the ligands lie in the same range between 2.09 and 2.16 Å and are in good agreement with values reported in the literature.[18]

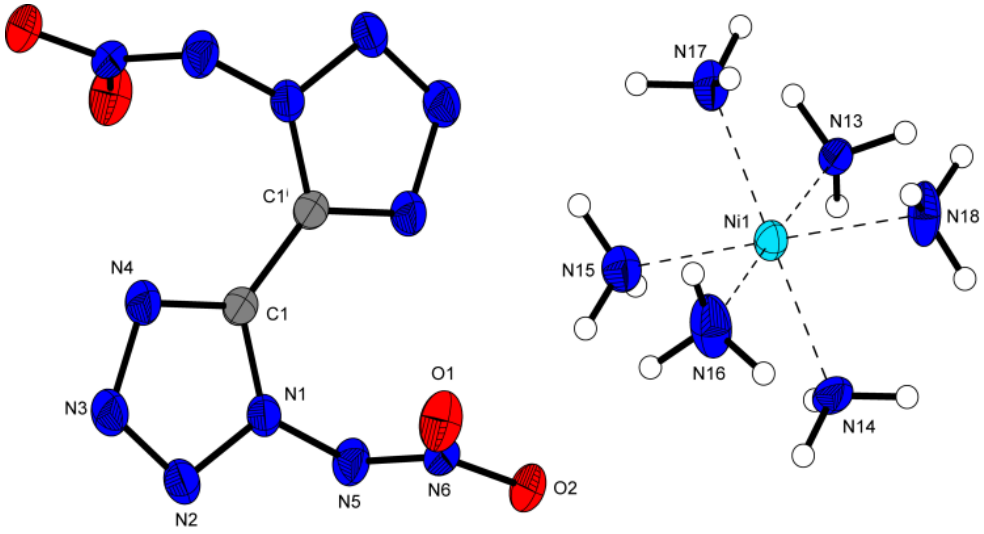

Figure 7.7. Molecular structure of **11** showing the atom-labelling scheme. Selected bond lengths [Å]: Ni1–N17 2.098(4), Ni1–N13 2.116(3), Ni1–N15 2.119(3), Ni1–N16 2.124(4), Ni1–N14 2.128(4), Ni1–N18 2.154(4). Symmetry code (i): 1−x, 1−y, −z.

Complex **12** crystallizes in the form of blue blocks in the monoclinic space group $C2/c$ with four formula units per unit cell and a calculated density of 1.860 g cm^{-3} at 123 K. The extended molecular structure is illustrated in Figure 7.8 and shows an Jahn-Teller distorted octahedral coordination sphere of the copper(II) cation. The metal centers are coordinated by four ammine ligands in a plane (Cu1–N7 2.022(7) Å, Cu1–N8 2.008(7) Å) and two longer coordinated nitramine nitrogen atoms N5 of the DNABT in axial positions (Cu1–N5 2.573(2) Å). The coordination octahedron is slightly distorted and deviates partly from 90° (< N5^{i}–Cu1–N8 = 94.83(8)° and < N5^{i}–Cu1–N8^{i} = 85.17(8)°) which might be the sterical influence of the DNABT dianion. The structure (bond lengths and angles) of the complex is comparable to a similar copper(II)-ammine-tetrazolate described in literature.[19] Both compounds crystallize with one crystal water. In the case of **8** a hydrogen bond to the tetrazole nitrogen atom N3 and the nitrogen atom N7 of one of the ammine ligands is formed. The bidentate DNABT ligand bridges the copper atoms to linear one-dimensional polymeric chains along the *c* axis. The closest Cu-Cu distance is 6.82 Å along *a/b*. Hydrogen bonds between the ammine and tetrazole ligands stabilize the polymeric chains to each other.

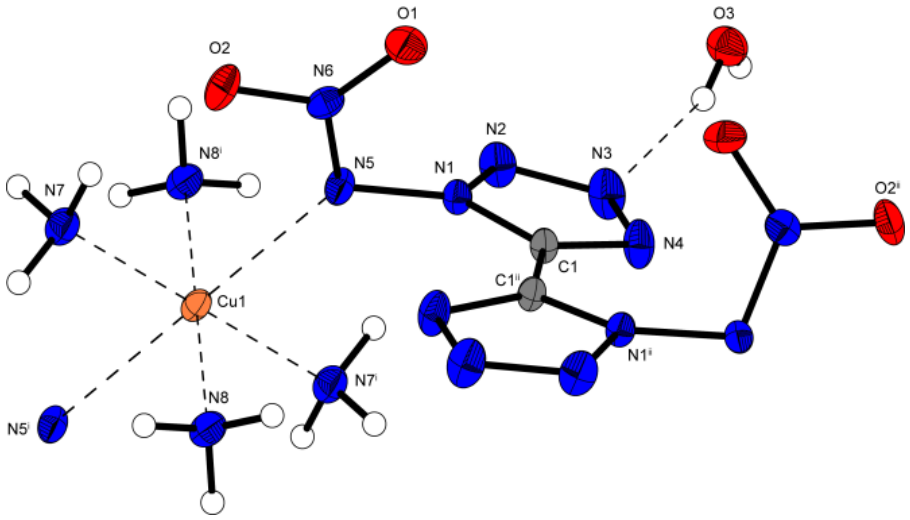

Figure7.8. Extended molecular structure of **12** showing the distorted octahedral coordination sphere of the copper cation. Selected bond lengths [Å]: Cu1–N5 2.573(2), Cu1–N7 2.022(2), Cu1–N8 2.008(2). Selected bond angles [°]: $N5^{i}$–Cu1–N8 94.83(8), $N5^{i}$–Cu1–$N8^{i}$ 85.17(8). Symmetry codes (i) −x, −y, −z; (ii) −x, y, 0.5−z.

To the best of our knowledge, tetramminezinc(II) complexes with energetic counter anions have not been reported in literature so far. The zinc(II) DNABT complex **13** crystallizes in the form of colorless rods in the monoclinic space group $P2_1/n$ with four formula units per unit cell and a calculated density of 1.812 g cm^{-3}. In contrast to **9** and **10** the coordination sphere of the zinc(II) metal center (Figure 7.9) is tetrahedral and consists of four ammine ligands with similar bond distances (Zn–N15 1.995(2) Å, Zn–N16 2.009(2) Å, Zn–N13 2.019(2) Å and Zn–N14 2.016(2) Å). The observed zinc ammine distance values are consistent with the literature data.[21] The tetrahedral coordination sphere only show small divergences (Figure 9 caption) to the perfect angle of 109.4°. This may be due to the large set of hydrogen bonds of the NH_3 ligands formed.

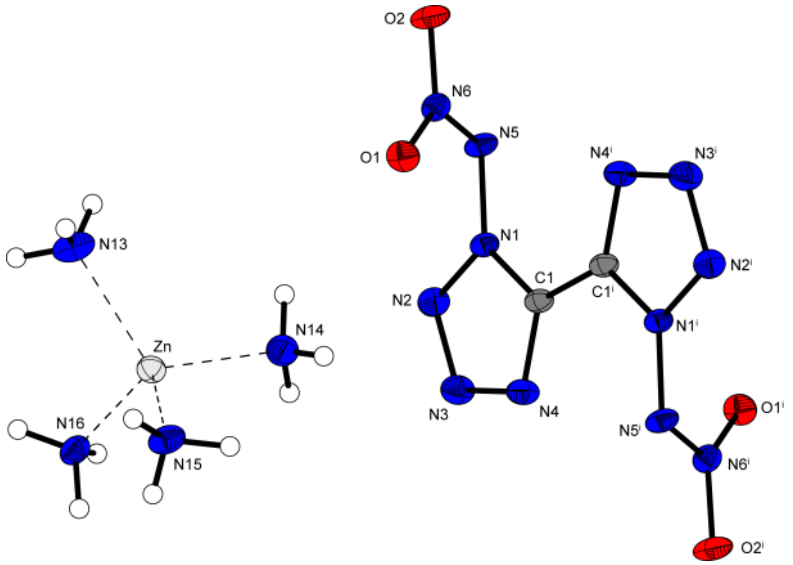

Figure 7.9. Molecular structure of **13**. Selected bond lengths [Å]: Zn–N15 1.995(2), Zn–N16 2.009(2), Zn–N13 2.019(2), Zn–N14 2.016(2). Selected bond angles [°]: N15–Zn–N16 109.86(9), N14–Zn–N16 106.74(9), N13–Zn–N16 103.44(9). Symmetry code (i) 1−x, −y, −z.

7.2.3 Energetic Properties and Laser Initiation

The sensitivities toward friction, impact and electrostatic discharge for **4** and **6**–**13** were determined according to BAM standards. The compounds have been classified in accordance to the *UN recommendations on the transport of dangerous goods* using the obtained values.[22] In addition, the thermal stabilities were determined by various methods. An overview of the physicochemical properties of **4** and **6**–**13** is given in Table 1.

7.2.4 Thermal behavior

The thermal stabilities of **4** and **6**–**13** were determined either by DSC, DTA or TGA scans at a heating rate of 5 °C min^{-1}. All of the compounds **6**–**13** have the ability to strongly damage the thermal analytical device during their violent decomposition or detonation, respectively. All synthesized DNABT salts and complexes showed a higher thermal stability than the neutral parent compound H_2DNABT of 107 °C.[2] The decomposition temperatures of the investigated metal compounds, given as the extrapolated onset temperatures, range from 186 °C (**8**) up to a 247 °C (**7b** dehydrated) for the metal salts and from 155 °C (**12**, Figure 10) to 182 °C (**13**) for the metal complexes. Compound **4**

shows an even lower thermal stability than H_2DNABT (**4**: 102 °C, H_2DNABT: 107 °C). The quite disappointing low thermal stabilities of the complexes **11**–**13** can be explained by the loss of the coordinated ammine ligands, which leads to decomposition of the compound (Cu < Ni < Zn). The thermo plots of compound **6** and **12** show endothermic signals (**6**: 50–70 °C, **12**: 123 °C), which indicates the loss of crystal water. This loss could also be observed in the TGA scans of the sodium salts **7a** and **7b**. Interestingly the two sodium salts show different decomposition temperatures, which can be explained by the different hydrogen bond networks. With 220 °C cesium salt **9** is the most temperature stable of all investigated water-free compounds although being one of the most sensitive.

7.2.5 Sensitivities

All investigated compounds show sensitivities in the range of primary explosives such as lead or silver azide. They are very sensitive toward impact with sensitivities of 1 J (or less) (**2**, **6**–**9**) up to 3 J for the nickel ammine complex (**11**). The friction sensitivities are comparable with values from less than 5 N (**2**, **6**–**9**) up to 80 N for compound **11**. A possible explanation for the low sensitivity of **11** could be the high number of non-energetic ammine ligands. As expected, the silver salt (**10**) is the most sensitive compound, which can even detonate without any external manipulation! The range of sensitivities toward electrostatic discharge range from 0.003 to 0.150 J. Interestingly, polymorph **7b** is significantly less sensitive toward electrostatic discharge than **7a**.

7.2.6 Hot plate and hot needle test

The ignitibility of metal compounds **6**–**9** and **11**–**13** was further tested through hot needle and hot plate tests. The hot needle test was performed by securing a small amount of sample underneath adhesive tape, followed by penetration with a red heated needle. Except for the rubidium (**8**) and cesium (**9**) salts, which detonated to the extent desired, all tested compounds only decomposed or deflagrated. Detonation of the compound indicates a primary explosive. The practicable hot plate test instead, only shows the behavior of the unconfined sample toward fast heating on a hot copper plate. It does not necessarily allows to draw conclusions on its capability as a primary explosive. All compounds except the copper complex **12** which deflagrated sharply, detonated when reaching their respective ignition temperatures.

7.2.7 Laser initiation

Approximately 15 mg of **11** and **12** (which are the only colored compounds in this work) were filled into a plastic cap, pressed with 1 kN and sealed by an UV-curing adhesive. The confined samples were then irradiated through an optical lens connected to an optical fibre with a monopulsed diode laser at a wavelength of 915 nm, a pulse length of 15 ms and a current of 7 A. Both investigated complexes **11** and **12** detonated after initiation by laser irradiation and could therefore be used as photosensitive primary explosives in suitable detonation systems.

Table 7.1. Energetic properties and laser initiation tests of **2**, **6–13**.

	2	**6**	**7a**	**7b**	**8**	**9**	**10**	**11**	**12**	**13**
formula	$C_6H_6N_{12}O_8$	$C_2H_4Li_2N_{12}O_6$	$C_2H_4Na_2N_{12}O_6$	$C_2H_4Na_2N_{12}O_6$	$C_2Rb_2N_{12}O_4$	$C_2Cs_2N_{12}O_4$	$C_2Ag_2N_{12}O_4$	$C_2H_{18}NiN_{18}O_4$	$C_2H_{14}CuN_{16}O_5$	$C_2H_{12}ZnN_{16}O_4$
FW [g mol^{-1}]	374.2	306.0	338.1	338.1	427.0	512.9	471.8	417.0	405.8	389.7
IS [J] [a]	< 1	< 1	< 1	< 1	< 1	< 1	n.d.	3	2	1.5
FS [N] [b]	< 5	< 5	< 5	< 5	< 5	< 5	n.d.	80	10	6
ESD [J] [c]	0.003	0.020	0.030	0.150	0.020	< 0.020	n.d.	0.130	0.150	0.100
grain size [µm]	< 100	< 100	500–1000	500–1000	100–500	100–500	n.d.	100–500	100–500	100–500
N [%] [d]	44.9	54.9	49.7	49.7	39.4	32.2	35.6	60.5	55.2	57.5
$T_{dec.}$ [°C] [e]	102	239	241	247	186	220	n.d.	167	155	182
ρ [g cm^{-3}] [f]	1.538	1.911	1.889	1.887	2.501	2.774	3.177	1.675	1.809	1.777
hot needle	n.d.	dec. [i]	dec. [i]	dec. [i]	det. [k]	det. [k]	n.d.	defl. [j]	dec. [i]	defl. [j]
hot plate	n.d.	det. [k]	det. [k]	det. [k]	det. [k]	det. [k]	n.d.	det. [k]	defl. [j]	det. [k]
laser init. [g]	n.d.	n.d.	n.d.	n.d.	n.d.	n.d.	n.d.	det. [k]	det. [k]	n.d.

[a] Impact sensitivity according to the BAM drophammer (method 1 of 6); [b] Friction sensitivity according to the BAM friction tester (method 1 of 6); [c] electrostatic discharge sensitivity (OZM ESD tester); [d] Nitrogen content; [e] Temperature of decomposition according to DSC, DTA or TGA (onset temperatures at a heating rate of 5 ° min^{-1}); [f] X-ray density converted to RT ($(\rho_{298K} = \rho_T / (1 + \alpha_V(298 - T_0)$; $\alpha_V = 10^{-4}$ K^{-1}); [h] Laser initiation (λ = 915 nm, τ = 15 ms); [i] Decomposition; [j] Deflagration; [k] Detonation; n.d. = not determined (either not possible or meaningful)

7.3 Conclusion

The synthesis and characterization of several new metal salts and complexes of 1,1'-dinitramino-5,5'-bitetrazole (H_2DNABT) is described. Since the potassium salt K_2DNABT is a very promising environmentally benign primary explosive the remaining alkaline salts as well as selected alkaline earth and transition metal complexes should be investigated toward their energetic behavior. Within the group of alkali metal salts (Li (**6**), Na (**7**), K_2DNABT, Rb (**8**), Cs (**9**)) the lithium and sodium salts form dihydrates which can reversibly be dehydrated. Two polymorphs of latter one were explored formed by recrystallization from water (**7a**) and ethanol (**7b**), respectively. The rubidium, cesium and silver (**10**) salts are poorly soluble in water. All are highly sensitive showing a super fast "deflagration to detonation" behavior on contact with flame or hot surfaces. The silver salt usually explodes during drying, latest on lightest touch when dry. The alkaline earth metal salts (Ca (**14**), Sr (**15**), Ba (**16**)) are highly soluble in water and could not be purified sufficiently. They are forming tetra- (**14**, **15**) and hexahydrates (**16**) in the solid state. Neat transition metal complexes could only be synthesized with Ni(II) (**11**), Cu(II) (**12**) and Zn(II) (**13**) under addition and coordination of ammonia. The nickel and copper salts could be successfully initiated by laser irradiation. For the first time the cations hexaamminenickel(II) and tetraamminezinc(II) were combined with energetic counterions. The crystal structure of all compounds except for **14** could be determined by low temperature X-ray diffraction, which gave insight in the coordination of the metal centers and hydrogen bond interactions. Sensitivities of the alkaline and transition metal salts were measured showing extremely high values partly much more susceptible. The lowest thermal stability of 155 °C was observed for the tetrammine-copper(II) complex which might be caused by the loss of ammonia. The highest value (247 °C) was observed for the dehydrated sodium salt **7b**. With respect to potential application in priming charges the potassium salt is still the most promising due to its manageable sensitivities in combination with a thermal stability of 200 °C.

7.4 Experimental Section

General methods:

All chemicals and solvents were employed as received (Sigma-Aldrich, Fluka, Acros). The synthesis of compounds **1**–**5** can be found in the Supporting Information. ^{1}H, ^{13}C and ^{14}N spectra were recorded with neat solids as samples at ambient temperature using a JEOL Eclipse 270, JEOL EX 400 or a JEOL Eclipse 400 instrument. The chemical shifts quoted in ppm in the text refer to typical

standard tetramethylsilane (^{1}H, ^{13}C) and nitromethane (^{14}N) in d_6-DMSO as the solvent. Decomposition temperatures were measured through differential thermal analysis (DTA) with an OZM Research DTA 552-Ex instrument, through differential scanning calorimetry (DSC) with a LINSEIS DSC PT10 or by thermogravimetric analysis (TGA) with a Perkin Elmer TGA4000 instrument. The samples were measured in a range of 25–400 °C at a heating rate of 5 °C min^{-1}. Infrared spectra were measured with a Perkin–Elmer FT-IR Spectrum BXII instrument equipped with a Smith Dura Sampl*IR* II ATR unit. Mass spectra of the described compounds were measured at a JEOL MStation JMS 700 using FAB technique. Determination of the carbon, hydrogen and nitrogen contents were carried out by combustion analysis using an Elementar Vario El (nitrogen values determined are often lower than the calculated ones due to their explosive behavior. Sensitivity tests are described in the SI.

CAUTION! *All investigated compounds are potentially explosive energetic materials, which show increased sensitivities toward various stimuli (e.g. elevated temperatures, impact, friction or electrostatic discharge). Therefore, proper security precautions (safety glass, face shield, earthed equipment and shoes, leather coat, Kevlar gloves, Kevlar sleeves and ear plugs) have to be applied while synthesizing and handling the described compounds.*

General procedure for the preparation of the DNABT alkali salts (**6, 7a, 8–9**): An aqueous solution of the ammonium salt **5** (**6/7a**: 100 mg, 0.34 mmol; **8/9**: 29.0 mg, 0.10 mmol) was treated with the corresponding aqueous metal hydroxide solution (**6**: lithium hydroxide (8.14 mg, 0.34 mmol); **7a**: sodium hydroxide (13.6 mg, 0.34 mmol); **8**; 50 wt.% rubidium hydroxide (20.5 mg, 0.10 mmol); **9**; 50 wt.% cesium hydroxide (30.0 mg, 0.10 mmol)) and stirred mechanically for 10 min at 70 °C. The clear solutions were left to crystallize until a crystalline solid appeared. The products were filtered off, washed with ethanol and dried in air.

Li_2DNABT · 2 H_2O (**6**): Colorless crystals of compound **6**, which were suitable for X-ray, started to crystallize within several days. Yield: 84.1 mg (0.27 mmol, 80 %). **DSC** (5 °C min^{-1}): 50–70 °C (dehydration), 239 °C (dec.); **IR** (atr, cm^{-1}): $\tilde{\nu}$ = 3441 (m), 3293 (m), 3210 (m), 3083 (w), 1652 (m), 1432 (s), 1401 (s), 1373 (s), 1288 (vs), 1271 (vs), 1184 (s), 1129 (s), 1048 (m), 1042 (m), 1020 (m), 1002 (m), 876 (s), 778 (s), 731 (w), 714 (m), 672 (w), 622 (m), 488 (w), 467 (w); **EA** ($C_2H_4Li_2N_{12}O_6$, 306.01): calc.: C 7.85, H 1.32, N 54.93 %; found: C 8.36, H 1.75, N 55.34 %; **BAM drophammer**: < 1 J; **friction tester**: < 5 N; **ESD**: 25 mJ.

Na_2DNABT · 2 H_2O (**7a**): Compound **7a** was isolated within several days in the form of colorless blocks suitable for X-ray determination. Yield: 95.4 mg (0.28 mmol, 83 %). **TGA** (5 °C min^{-1}): 95–105 °C (dehydration), 241 °C (dec.); **IR** (atr, cm^{-1}): $\tilde{\nu}$ = 3568 (m), 3469 (w), 1616 (w), 1430 (m), 1370 (s), 1325 (s), 1299 (vs), 1268 (s), 1177 (m), 1168 (m), 1129 (m), 1037 (m), 1004 (m), 881 (m), 835 (m), 774 (m), 733 (w), 713 (w), 676 (w), 463 (s), 457 (s); **EA** ($C_2H_4Na_2N_{12}O_6$, 338.11): calc.: C 7.10, H 1.19, N 49.71 %; found: C 7.39, H 1.39, N 49.78 %; **BAM drophammer**: < 1 J; **friction tester**: < 5 N; **ESD**: 30 mJ.

Na_2DNABT · 2 H_2O (**7b**): Colorless blocks of polymorph **7b** were obtained by recrystallization of compound **7a** (42.3 mg, 0.13 mmol) out of ethanol within one day suitable for X-ray determination. Yield: 38.8 mg (0.11 mmol, 92 %). **TGA** (5 °C min^{-1}): 112–126 °C (dehydration), 247 °C (dec.); **IR** (atr, cm^{-1}): $\tilde{\nu}$ = 3574 (s), 3399 (m), 1622 (m), 1428 (vs), 1369 (s), 1299 (vs), 1265 (vs), 1166 (m), 1122 (s), 1035 (m), 1018 (m), 995 (m), 883 (s), 776 (m), 733 (w), 714 (w), 675 (w), 614 (w), 531 (m), 492 (m), 457 (m); **EA** ($C_2H_4Na_2N_{12}O_6$, 338.11): calc.: C 7.10, H 1.19, N 49.71 %; found: C 7.37, H 1.23, N 49.45 %; **BAM drophammer**: < 1 J; **friction tester**: < 5 N; **ESD**: 1.50 J.

Rb_2DNABT (**8**): Suitable crystals for X-ray determination were obtained of compound **8** in a quantitative yield within one day. **DTA** (5 °C min^{-1}): 186 °C (dec.); **IR** (atr, cm^{-1}): $\tilde{\nu}$ = 1424 (s), 1394 (m), 1359 (m), 1283 (vs), 1253 (vs), 1170 (m), 1161 (s), 1121 (s), 1031 (s), 1005 (m), 998 (s), 870 (s), 828 (m), 809 (m), 803 (m), 772 (vs), 726 (s), 714 (s), 698 (m), 691 (m), 680 (m), 671 (m), 658 (m); **BAM drophammer**: < 1 J; **friction tester**: < 5 N; **ESD**: 20 mJ.

Cs_2DNABT (**9**): Compound **9** was isolated in a quantitative yield in form of colorless needles suitable for X-ray determination within a few hours. **DTA** (5 °C min^{-1}): 220 °C (dec.); **IR** (atr, cm^{-1}): $\tilde{\nu}$ = 1410 (s), 1360 (m), 1281 (vs), 1254 (s), 1171 (m), 1161 (m), 1128 (s), 1124 (s), 1034 (m), 1000 (m), 868 (s), 774 (m), 723 (w), 715 (m), 672 (w); **BAM drophammer**: < 1 J; **friction tester**: < 5 N; **ESD**: < 20 mJ.

Ag_2DNABT (**10**): An aqueous solution of compound **5** (50.0 mg, 0.17 mmol) was reacted with an aqueous solution of silver nitrate (28.9 mg, 0.17 mmol). The precipitating colorless silver salt **10** was dissolved in 2 drops of concentrated ammonia. Colorless crystals suitable for X-ray determination were isolated overnight.

General procedure for the synthesis of metal(II) DNABT amine complexes (11–13):

Compound **5** (**11**: 182 mg, 0.62 mmol; **12**: 35.0 mg, 0.12 mmol; **13**: 189 mg, 0.65 mmol) was dissolved in the least necessary amount of concentrated ammonia and added to a solution of the corresponding metal(II) nitrate (**11**: nickel(II) nitrate hexahydrate (180 mg, 0.62 mmol); **12**: copper(II) nitrate trihydrate (29.0 mg, 0.12 mmol); **13**; zinc(II) nitrate hexahydrate (193 mg, 0.65 mmol)) in concentrated ammonia and stirred mechanically for 1 min at room temperature. The reaction mixtures were left to crystallize until a solid appeared. The products were filtered off and dried at 50 °C overnight.

[Ni(NH$_3$)$_6$]DNABT (**11**): Complex **11** was obtained within 30 min in the form of purple cylinders suitable for X-ray determination. Yield: 133 mg (0.32 mmol, 51 %). **DTA** (5 °C min^{-1}): 167 °C (dec.); **IR** (atr, cm^{-1}): $\tilde{\nu}$ = 3354 (m), 3282 (m), 1615 (m), 1478 (m), 1415 (s), 1365 (m), 1285 (vs), 1245 (vs), 1161 (s), 1124 (s), 1034 (m), 996 (m), 874 (m), 777 (m), 629 (s); **EA** ($C_2H_{18}NiN_{18}O_4$, 416.98): calc.: C 5.76, H 4.35, N 60.46 %; found: C 6.27, H 4.24, N 57.05 %; **BAM drophammer**: 3 J; **friction tester**: 80 N; **ESD**: 0.13 J.

[Cu(NH$_3$)$_4$DNABT] · H$_2$O (**12**): Compound **12** was isolated within 20 min in the form of blue crystals suitable for X-ray determination. Yield: 32.9 mg (0.08 mmol, 68 %). **DSC** (5 °C min^{-1}): 123 °C (dehydration), 155 °C (dec.); **IR** (atr, cm^{-1}): $\tilde{\nu}$ = 3543 (w), 3361 (m), 3342 (m), 3269 (m), 3194 (w), 1618 (m), 1414 (s), 1368 (m), 1290 (s), 1264 (vs), 1247 (vs), 1166 (m), 1151 (m), 1123 (m), 1013 (w), 994 (w), 877 (m), 770 (m), 678 (s), 558 (w), 544 (w); **EA** ($C_2H_{14}CuN_{16}O_5$, 405.79): calc.: C 5.92, H 3.48, N 55.23 %; found: C 6.45, H 3.44, N 54.63 %; **BAM drophammer**: 2 J; **friction tester**: 10 N; **ESD**: 0.15 J.

[Zn(NH$_3$)$_4$]DNABT (**13**): The tetrammine zinc(II) complex 13 was obtained within several hours in the form of colorless rods suitable for X-ray determination. Yield: 105 mg (0.27 mmol, 41 %). DTA (5 °C min^{-1}): 182 °C (dec.); IR (atr, cm^{-1}): $\tilde{\nu}$ = 3309 (m), 3263 (m), 3252 (m), 3224 (m), 3183 (m), 1620 (w), 1408 (s), 1367 (m), 1280 (vs), 1268 (vs), 1249 (vs), 1160 (m), 1127 (s), 1117 (s), 1032 (w), 999 (w), 872 (m), 773 (m), 692 (s), 674 (s); EA ($C_2H_{12}ZnN_{16}O_4$, 389.61): calc.: C 6.17, H 3.10, N 57.52 %; found: C 6.68, H 3.06, N 56.13 %; BAM drophammer: 1.5 J; friction tester: 6 N; ESD: 0.10 J.

7.5 References

[1] a) J. Zhang, S. Dharavath, L. A. Mitchell, D. A. Parrish and J. M. Shreeve, *J. Am. Chem. Soc.* 2016, **138**, 7500; b) P. Yin, D. A. Parrish and J. M. Shreeve, J. *Am. Chem. Soc.*, 2015, **137**, 4778; c) H. Gao and J. M. Shreeve, *Chem. Rev.* 2011, **111**, 7377.

[2] a) K. B. Landenberger, O. Bolton and A. J. Matzger, *J. Am. Chem. Soc.*, 2015, **137**, 5074; b) S. Seth and A. J. Matzger, *Inorg. Chem.*, Article ASAP, **DOI:** 10.1021/acs.inorgchem.6b02383.

[3] a) D. E. Chavez, D. A. Parrish and L. Mitchell, *Angew. Chem. Int. Ed.* 2016, **55**, 8666; b) D. G. Piercey, D. E. Chavez, B. L. Scott, G. H. Imler and D. A. Parrish, *Angew. Chem. Int. Ed.* 2016, **55**, 15315; c) T. W. Myers, C. J. Snyder, D. E. Chavez, R J. Scharff and J. M. Veauthier, *Chem. Eur. J.* 2016, **22**, 10590; d) D. E. Chavez, J. C. Bottaro, M. Petrie and D. A. Parrish, *Angew. Chem. Int. Ed.* 2015, **54**, 12973.

[4] a) X. X. Zhao, S. H. Li, Y. C. Li, F. Q. Zhao and S. P. Pang, *J. Mater. Chem.* A**,** 2016, **4,** 5495; b) Y.-C. Li, C. Qi, S.-H. Li, H.-J. Zhang, C.-H. Sun, Y.-Z. Yu and S.-P. Pang, *J. Am. Chem. Soc.*, 2010, **132**, 12172.

[5] a) D. Fischer, J. L. Gottfried, K. Karaghiosoff, T. M. Klapötke, J. Stierstorfer and T. Witkowski, *Angew. Chem*. *Int. Ed.* 2016, **55**, 16132; b) N.-D. H. Gamage, B. Stiasny, J. Stierstorfer, P. D. Martin, T. M. Klapötke and C. H. Winter, *Chem. Eur. J.* 2016, **22**, 2582; c) D. Fischer, T. M. Klapötke and J. Stierstorfer, *Chem. Commun.* 2016, **52**, 916.

[6] R. Matyas, J. Pachman, Primary Explosives, Springer, 2013.

[7] http://www.speciation.net/News/REACH-Update-List-of-300-chemicals-of-very-high-concern-;~/2008/09/18/3831.html (accessed on 27.12.2016)

[8] D. Fischer, T. M. Klapötke, J. Stierstorfer, *Angew. Chem. Int. Ed.* 2014, **53**, 8172. b) a) D. Fischer, T. M. Klapötke and J. Stierstorfer, *Angew. Chem.* 2014, **126**, 8311.

[9] S. R. Ahmad and M. Cartwright, Laser Ignition of Energetic Materials, Wiley, 2014, chapter 8, 193.

[10] J. W. Fronabarger, M. D. Williams, W. B. Sanborn, J. G. Bragg, D. A. Parrish and M. Bichay, *Propellants Explos. Pyrotech*. 2011, **36**, 541.

[11] a) J. W. Fronabarger, M. D. Williams, W. B. Sanborn and D. A. Parrish, Magdy Bichay, *Propellants Explos. Pyrotech.* 2011, 36, 459. b) Frohnabarger, M. Williams and M. Bichay, Joint Armaments Conference, Dallas, TX, 2010 http://www.dtic.mil/ndia/2010armament/Thursday ReunionMichael Williams.pdf (accessed on 27.12.2016)

[12] D. Fischer, T. M. Klapötke and J. Stierstorfer, N. Szimhardt, *Chem. Eur. J.* 2016, **22**, 4966.

[13] T. M. Klapötke, P. C. Schmid and J. Stierstorfer, *J. Mater. Chem. A*, 2015, **3**, 2658.

[14] T. M. Klapötke and J. Stierstorfer, *Helv. Chim. Acta* 2007, **90**, 2132.

[15] S. N. Semenov, A. Yu. Rogachev, S. V. Eliseeva, Y. A. Belousov, A. A. Drozdov and S. I. Troyanov, *Polyhedron*, 2007, **26**, 4899.

[16] J. Stierstorfer, dissertation, Ludwig-Maximilians Universität München, 2009, p. 311.

[17] Crystallographic data for the structure(s) have been deposited with the Cambridge Crystallographic Data Centre. Copies of the data can be obtained free of charge on application to The Director, CCDC, 12 Union Road, Cambridge CB2 1EZ, UK (Fax: int.code_(1223)336-033; e-mail for inquiry: fileserv@ccdc.cam.ac.uk; e-mail for deposition: (deposit@ccdc.cam.ac.uk).

[18] T. M. Klapötke, J. Stierstorfer and A. U. Wallek, *Chem. Mat.* 2008, **20**, 4519.

[19] P. Schwendt, D. Dudasova, J. Chrappova, M. Drabik and J. Marek, *J. Therm. Anal. Calorim.* 2008, **91**, 293.

[20] T. M. Klapötke, J. Stierstorfer and B. Weber, *Inorg. Chim. Acta,* 2009, **362**, 2311.

[21] Y. Qu, Z.-D. Liu, M.-Y. Tan and H.-L. Zhu, *Acta Crystallogr.* 2004, ***E60***, m1343.

[22] Impact: insensitive > 40 J, less sensitive ≥ 35 J, sensitive ≥ 4 J, very sensitive ≤ 3 J; Friction: insensitive > 360 N, less sensitive = 360 N, sensitive < 360 N and > 80 N, very sensitive ≤ 80 N, extremely sensitive ≤ 10 N, According to: *Recommendations on the Transport of Dangerous Goods, Manual of Tests and Criteria*, 4th edition, United Nations, New York-Geneva, **1999**.

7.6 Supplementary Information

7.6.1 X-ray Diffraction

For all compounds (except for **4**, **15** and **16**), an Oxford Xcalibur3 diffractometer with a CCD area detector was employed for data collection using Mo-*K*α radiation (λ = 0.71073 Å). By using the CRYSALISPRO software[S1] the data collection and reduction were performed. The structures were solved by direct methods (SIR-92, [S3] SIR-97[S3] or SHELXS-97[S4]) and refined by full-matrix least-squares on *F*2 (SHELXL [S4]) and finally checked using the PLATON software [S5] integrated in the WinGX software suite. The non-hydrogen atoms were refined anisotropically and the hydrogen atoms were located and freely refined. The absorptions were corrected by a SCALE3 ABSPACK multiscan method.[S6]. All DIAMOND2 plots are shown with thermal ellipsoids at the 50% probability level and hydrogen atoms are shown as small spheres of arbitrary radii. The crystal structures of compounds **4**, **15** and **16** were determined at 100 K on a Bruker D8 Venture TXS diffractometer equipped with a multilayer monochromator, a Photon 2 detector, and a rotating-anode generator (MoKα radiation). The SADABS program embedded in the Bruker APEX3 software has been used for multi-scan absorption corrections in all structures.[S7]

Table 7.S1. Crystallographic data and refinement parameters of compound **2**, **6**, **7a** and**7b**.

	2	**6**	**7a**	**7b**
Formula	$C_6H_8N_{10}O_4$	$CH_2LiN_4O_4$	$C_2H_4N_{12}Na_2O_6$	$C_2H_4N_{12}Na_2O_6$
FW [g mol^{-1}]	284.22	306.06	338.08	338.08
Crystal system	Triclinic	Monoclinic	Monoclinic	Orthorhombic
Space Group	*P*–1 (No. 2)	$P2_1/c$ (No. 14)	$P2_1/c$ (No. 14)	*Pbca* (No. 61)
Color / Habit	Colorless block	Colorless block	Colorless block	Colorless block
Size [mm]	0.01 x 0.03 x 0.10	0.15 x 0.34 x 0.39	0.08 x 0.15 x 0.28	0.29 x 0.45 x 0.56
a [Å]	4.1866(7)	8.2760(9)	8.8347(5)	6.2136(3)
b [Å]	7.2348(10)	10.8140(8)	9.4711(5)	10.9858(6)
c [Å]	10.3368(13)	6.0650(4)	7.2402(4)	16.9609(8)
α [°]	81.092(5)	90	90	90
β [°]	83.309(6)	106.073(10)	105.804(5)	90
γ [°]	75.044(6)	90	90	90
V [Å^3]	297.88(8)	521.58(8)	582.92(6)	1157.77(10)
Z	1	2	2	4
$\rho_{calc.}$ [g cm^{-3}]	1.584	1.949	1.927	1.940
μ [mm^{-1}]	0.134	0.176	0.236	0.238
F(000)	146	308	340	680
$\lambda_{MoK\alpha}$[Å]	0.71073	0.71073	0.71073	0.71073
T [K]	173	173	173	123
ϑ min-max [°]	3.3, 26.0	4.2, 26.7	4.3, 26.0	4.4, 26.0
Dataset h; k; l	−5:4; −8:8; −12:12	−5:10; −13:13; −7:7	−10:10; −11:11; −6:8	−7:6; −13:13; −20:20
Reflect. coll.	3156	3905	2933	8554
Independ. refl.	1159	1105	1136	1132
R_{int}	0.039	0.032	0.027	0.022
Reflection obs.	880	893	956	1059
No. parameters	96	108	108	108
R_1 (obs)	0.0481	0.0334	0.0305	0.0277
wR_2 (all data)	0.1184	0.0805	0.0812	0.0791
S	1.08	1.08	1.11	1.09
Resd. Dens.[e Å^{-3}]	−0.22, 0.22	−0.28, 0.26	−0.26, 0.26	−0.21, 0.37
Device type	Bruker D8 Venture rotating anode	Oxford XCalibur3 CCD	Oxford XCalibur3 CCD	Oxford XCalibur3 CCD
Solution	SIR-92	SIR-92	SIR-92	SHELXS-97
Refinement	SHELXL-97	SHELXL-97	SHELXL-97	SHELXL-97
Absorpt. corr.	multi-scan	multi-scan	multi-scan	multi-scan
CCDC	1502966	1500005	1500002	1500003

Table 7.S2. Crystallographic data and refinement parameters of compound **8–11**.

	8	**9**	**10**	**11**
Formula	$C_2N_{12}O_4Rb_2$	$C_2N_{12}O_4Cs_2$	$C_2Ag_2N_{12}O_4$	$C_2H_{18}N_{18}O_4Ni$
FW [g mol^{-1}]	427.08	521.96	471.88	417.05
Crystal system	Triclinic	Monoclinic	Monoclinic	Monoclinic
Space Group	*P–1* (No. 2)	$P2_1/c$ (No. 14)	$P2/c$ (No. 13)	$P2_1/c$ (No. 14)
Color / Habit	Colorless needle	Colorless needle	Colorless plate	Purple cylinder
Size [mm]	0.03 x 0.05 x 0.44	0.04 x 0.09 x 0.37	0.02 x 0.10 x 0.12	0.09 x 0.13 x 0.26
a [Å]	5.3034(5)	5.5885(2)	6.7520(4)	13.5062(12)
b [Å]	7.0632(6)	12.4847(4)	5.0649(4)	11.5426(8)
c [Å]	8.5675(7)	8.7893(3)	14.1529(9)	10.4455(7)
α [°]	66.821(8)	90	90	90
β [°]	86.667(7)	92.250(3)	92.180(6)	95.176(7)
γ [°]	70.964(8)	90	90	90
V [Å^3]	277.98(5)	612.76(4)	483.65(6)	1621.8(2)
Z	1	2	2	4
$\rho_{calc.}$ [g cm^{-3}]	2.551	2.829	3.240	1.708
μ [mm^{-1}]	8.845	5.989	4.097	1.255
F(000)	202	476	444	864
$\lambda_{MoK\alpha}$[Å]	0.71073	0.71073	0.71073	0.71073
T [K]	173	173	173	173
ϑ min-max [°]	4.3, 26.0	4.6, 26.0	4.3, 26.0	4.1, 25.0
Dataset h; k; l	−6:6; −8:8; −10:10	−6:6; −15:15; −10:10	−7:8; −5:6; −17:17	−10:16; −13:13; −12: 12
Reflect. coll.	3969	8446	2377	7466
Independ. refl.	1096	1195	955	2837
R_{int}	0.041	0.034	0.029	0.063
Reflection obs.	1000	1061	761	1838
No. parameters	91	91	93	232
R_1 (obs)	0.0242	0.0172	0.0333	0.0503
wR_2 (all data)	0.0509	0.0386	0.0779	0.0992
S	1.04	1.08	1.05	0.97
Resd. Dens.[e Å^{-3}]	−0.47, 0.49	−0.37, 0.77	−1.43, 0.85	−0.53, 0.81
Device type	Oxford XCalibur3 CCD	Oxford XCalibur3 CCD	Oxford XCalibur3 CCD	Bruker D8 Venture rotating anode
Solution	SIR-92	SIR-92	SHELXS-97	SHELXS-97
Refinement	SHELXL-97	SHELXL-97	SHELXL-97	SHELXL-97
Absorpt. corr.	multi-scan	multi-scan	multi-scan	multi-scan
CCDC	1500001	1500004	1524647	1524646

Table 7.S3. Crystallographic data and refinement parameters of compound **12**, **13**, **15** and **16**.

	12	**13**	**15**	**16**
Formula	$C_2H_{14}CuN_{16}O_5$	$C_2H_{12}N_{16}O_4Zn$	$C_2H_8N_{12}O_8Ba$	$C_2H_{12}N_{12}O_{10}Ba$
FW [g mol^{-1}]	405.83	389.65	415.82	501.58
Crystal system	Monoclinic	Monoclinic	Monoclinic	Monoclinic
Space Group	*C*2/*c* (No. 15)	*P*2$_1$/*n* (No. 14)	*P*2$_1$/*c* (No. 14)	*P*2$_1$/*n* (No. 14)
Color / Habit	Blue block	Colorless block	Colorless block	Colorless block
Size [mm]	0.05 x 0.11 x 0.23	0.10 x 0.13 x 0.20	0.03 x 0.07 x 0.10	0.03 x 0.06 x 0.09
a [Å]	11.4131(5)	10.2414(3)	10.7948(3)	8.9593(3)
b [Å]	7.4648(3)	10.6483(3)	15.0619(4)	9.5952(3)
c [Å]	17.2079(8)	13.1297(4)	9.3539(2)	17.9981(6)
α [°]	90	90	90	90
β [°]	98.739(5)	94.149(3)	110.333(1)	92.798(1)
γ [°]	90	90	90	90
V [Å^3]	1449.03(11)	1428.09(7)	1426.09(6)	1545.39(9)
Z	4	4	4	4
$\rho_{calc.}$ [g cm^{-3}]	1.860	1.812	1.937	2.156
μ [mm^{-1}]	1.570	1.774	3.849	2.651
F(000)	828	792	824	976
$\lambda_{MoK\alpha}$[Å]	0.71073	0.71073	0.71073	0.71073
T [K]	123	173	100	173
ϑ min-max [°]	4.2, 26.0	4.1, 26.0	2.8, 27.5	2.3, 26.0
Dataset h; k; l	−13:14; −9:9; −21:21	−12:12; −13:8; −16:14	−14:14; −19:19; −12:12	−11:11; −11:11; −22:22
Reflect. coll.	5250	10947	23112	49826
Independ. refl.	1422	2785	3271	3024
R_{int}	0.040	0.030	0.029	0.030
Reflection obs.	1205	2310	2910	2875
No. parameters	117	256	240	246
R_1 (obs)	0.0300	0.0257	0.0202	0.0162
wR_2 (all data)	0.0695	0.0675	0.0501	0.0868
S	1.08	1.03	1.07	1.43
Resd. Dens.[e Å^{-3}]	−0.31, 0.27	−0.37, 0.58	−0.29, 0.86	−1.12, 0.80
Device type	Oxford XCalibur3 CCD	Oxford XCalibur3 CCD	Oxford XCalibur3 CCD	Oxford XCalibur3 CCD
Solution	SHELXS-97	SHELXS-97	SHELXS-97	SHELXS-97
Refinement	SHELXL-97	SHELXL-97	SHELXL-97	SHELXL-97
Absorpt. corr.	multi-scan	multi-scan	multi-scan	multi-scan
CCDC	1502968	1510459	1510459	1510459

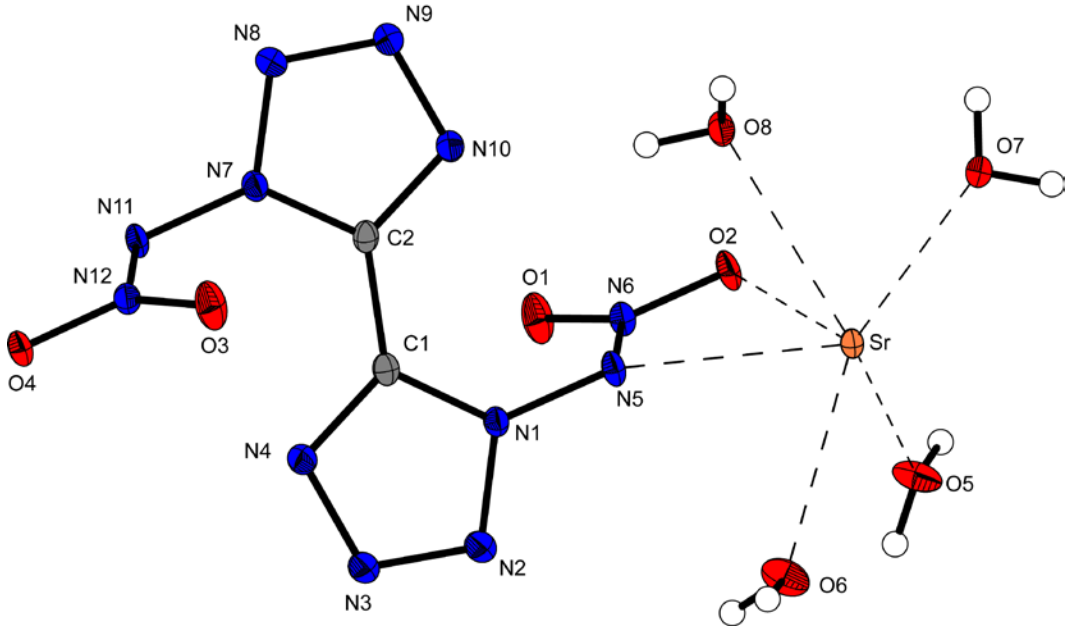

Figure 7.S1. Molecular structure of **15** showing the atom-labelling scheme. Thermal ellipsoids represent the 50% probability level.

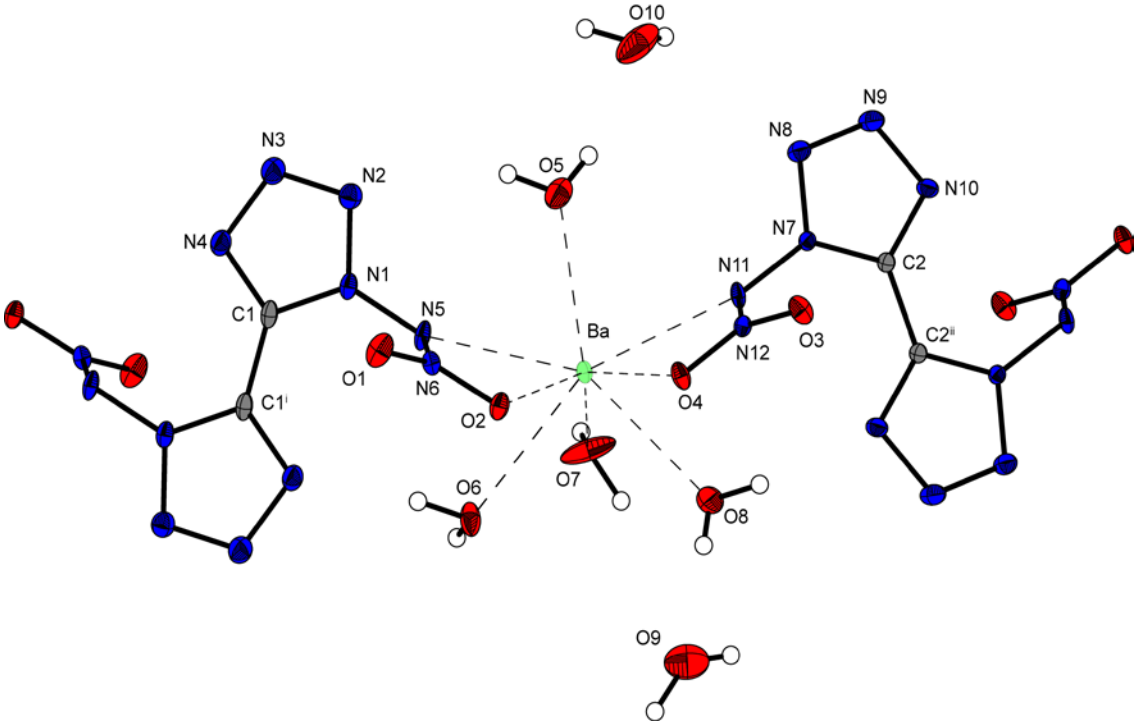

Figure 7.S2. Extended molecular structure of **16** showing the atom-labelling scheme. Thermal ellipsoids represent the 50% probability level. Symmetry codes: (i) −x, −y, 2−z; (ii) 1−x, −y, 1−z.

7.6.2 Experimental Part

General Procedures

Differential Scanning Calorimetry (DSC) was performed on a LINSEIS DSC PT10 with about 1 mg substance in a perforated aluminum vessel with a heating rate of 5 K·min^{-1} and a nitrogen flow of 5 dm^3·h^{-1}. Differential Thermal Analysis (DTA) measurements were carried out in glass tubes on an OZM *DTA* 552-Ex device with a heating rate of 5 K·min^{-1}. Thermal gravimetric analysis (TGA) measurements were performed on a Perkin Elmer TGA4000 with a heating rate of 5 K min^{-1} in Al_2O_3 crucibles. The NMR spectra were recorded with a 400 MHz instrument (^{1}H 399.8 MHz, ^{13}C 100.5 MHz, ^{14}N 28.9 MHz, and ^{15}N 40.6 MHz). Chemical shifts are given in parts per million relative to tetramethylsilane (^{1}H, ^{13}C) and nitromethane (^{14}N, ^{15}N). Infrared spectra were measured with a Perkin-Elmer Spectrum BX-FTIR spectrometer equipped with a Smiths DuraSamplIR II ATR device. Transmittance values are qualitatively described as "very strong" (vs), "strong" (s), "medium" (m), and "weak" (w). Raman spectra were recorded using a Bruker MultiRAM FT-Raman instrument fitted with a liquid-nitrogen cooled germanium detector and a Nd:YAG laser (λ = 1064 nm). The intensities are quoted as percentages of the most intense peak and are given in parentheses. Low-resolution mass spectra were recorded with a JEOL MStation JMS 700 (DEI+ / FAB+/−). Elemental analysis was carried out using a Vario Micro from the Elementar Company.

The impact sensitivity tests were carried out according to STANAG 4489[S8] modified instruction[S9] using a Bundesanstalt für Materialforschung (BAM) drophammer.[S10] The friction sensitivity tests were carried out according to STANAG 4487[S11] modified instruction[S12] using the BAM friction tester. The classification of the tested compounds results from the "UN Recommendations on the Transport of Dangerous Goods".[S13] All compounds were tested upon the sensitivity toward electrical discharge using the Electric Spark Tester ESD 2010 EN.[S14]

***1N,1N'*-Dimethylnitrocarbamate-*5,5'*-bitetrazole (4)**

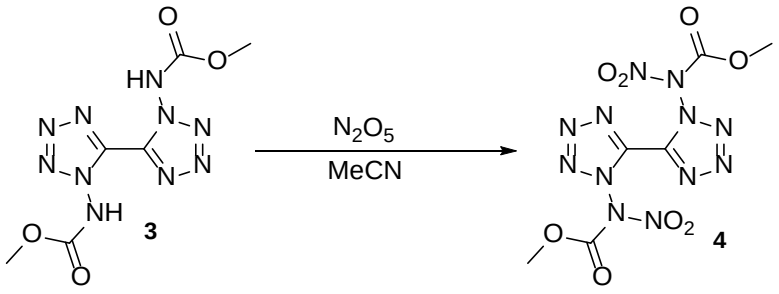

0.45 g (4.17 mmol) N_2O_5 was dissolved in 50 mL MeCN at −5°C and 0.3 g **3** (1.05 mmol) was added portion wise. The mixture was stirred for 2.5 h at −5 °C and finally quenched by adding the mixture to 50 g of ice-water. The precipitate was filtered off giving **4** (355 mg, 0.95 mmol, 90 %). **DTA** (5 °C min^{-1}): 102 °C (dec.); **IR** (atr, cm^{-1}) $\tilde{\nu}$ = 3223 (w), 2969 (w), 1794 (m), 1658 (m), 1438 (w), 1408 (w), 1322 (m), 1220 (s), 1180 (m), 1103 (w), 1041 (w), 990 (w), 936 (w), 864 (w), 818 (m), 769 (s), 732 (m), 666 (m), 590 (w); **^{1}H NMR** (dmso-d_6, 25 °C, ppm): δ: 3.85 (s, 6H, CH_3); **^{13}C{^{1}H} NMR** (dmso-d_6, 25 °C, ppm) δ: 48.7 (CH_3), 124.3 (C_Q), 141.0 (C=O); **^{14}N NMR** (dmso-d_6, 25 °C, ppm): δ = −66; **MS** *m/z* (FAB$^+$): 375.4 ($C_6H_7N_{12}O_8^+$); **EA** ($C_6H_6N_{12}O_8$, 374.19): calc.: C 19.26, H 1.62; N 44.92; found: C 20.31, H 1.90, N 44.73 %; **BAM drophammer**: 1 J, **friction tester**: <5 N, **ESD**: 3 mJ.

Diammonium 1,1'-dinitramino-5,5'-bitetrazolate (5)

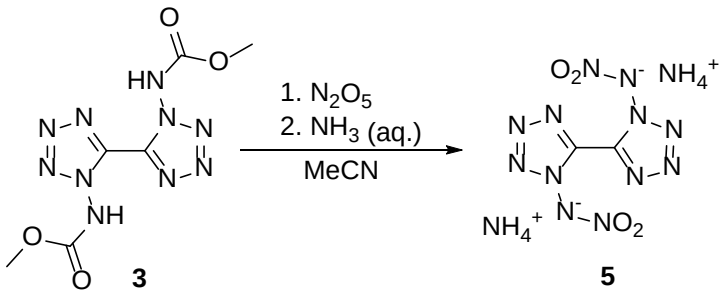

1.00 g (3.52 mmol) of **3** was suspended in 50 mL dry acetonitrile and cooled to −10°C. 1.5 g of dinitrogen pentoxide (13.9 mmol) was added all at once and the reaction mixture was stirred for 2 h at the initial temperature. An excess of concentrated ammonia solution (3 mL) was added to the obtained solution and the suspension was stirred for 20 minutes. The pH-value was checked to be above 9 and the colorless precipitate was collected by suction filtration and washed with ice-cold water (1 mL) and ethanol to give **5** (0.89 g, 3.06 mmol, 87 %). **IR** (atr, cm^{-1}) $\tilde{\nu}$ = 3177 (w), 3050 (w), 1395 (s), 1368 (s), 1280 (s), 1259 (s), 1179 (w), 1126 (m), 1036 (w), 1009 (w), 995 (w), 875 (s), 778 (m), 772 (w); **^{1}H NMR** (dmso-d_6, 25 °C, ppm): δ: 7.07 (s, 8H, NH_4^+); **^{13}C{^{1}H} NMR** (dmso-d_6, 25 °C, ppm) δ: 140.4 (C_Q); **^{14}N NMR** (dmso-d_6, 25 °C, ppm): δ = −359.

7.6.3 IR spectroscopy of 7a and 7b

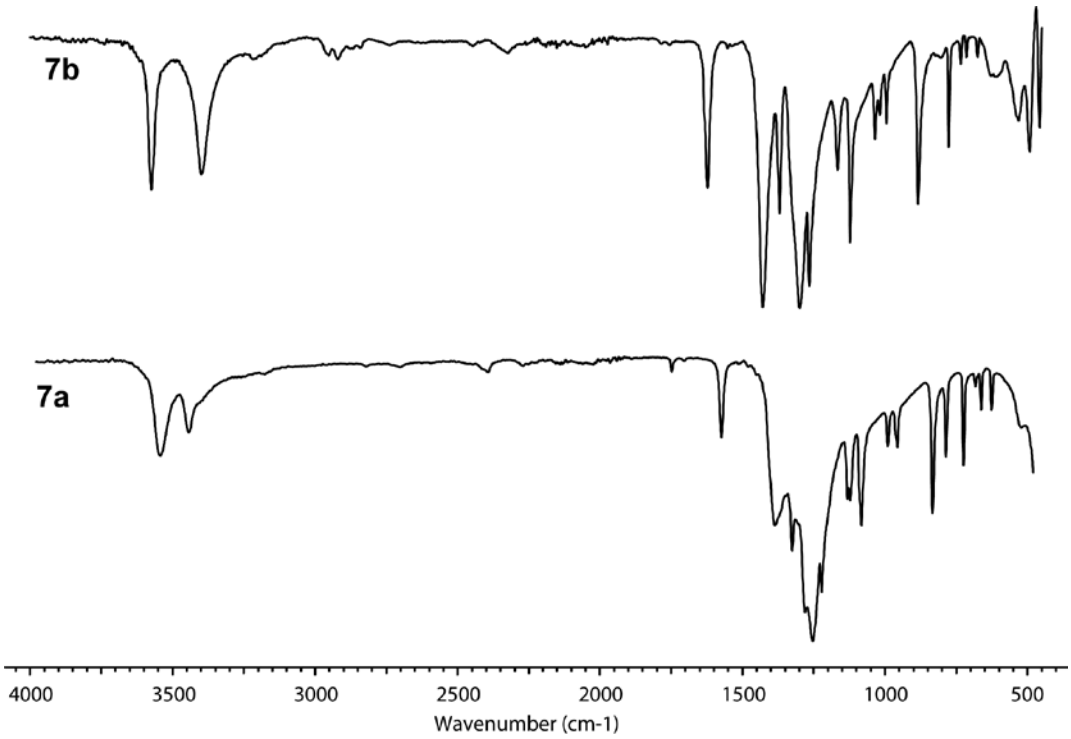

7.6.4 References

[S1] *CrysAlisPro*, Oxford Diffraction Ltd., version 171.33.41, **2009**.

[S2] *SIR-92*, *A program for crystal structure solution*: A. Altomare, G. Cascarano, C. Giacovazzo, A. Guagliardi, *J. Appl. Crystallogr.* **1993**, *26*, 343.

[S3] a) A. Altomare, G. Cascarano, C. Giacovazzo, A. Guagliardi, A. G. G. Moliterni, M. C. Burla, G. Polidori, M. Camalli and R. Spagna, *SIR97*, 1997; b) A. Altomare, M. C. Burla, M. Camalli, G. L. Cascarano, C. Giacovazzo, A. Guagliardi, A. G. G. Moliterni, G. Polidori and R. Spagna, *J. Appl. Crystallogr.* 1999, **32**, 115.

[S4] a) G. M. Sheldrick, *SHELX-97*, University of Göttingen, Göttingen, Germany, **1997**; b) G. M. Sheldrick, *Acta Crystallogr., Sect. A* 2008, **64**, 112.

[S5] A. L. Spek, *PLATON*, *A Multipurpose Crystallographic Tool*, Utrecht University, The Netherlands, 1999.

[S6] *SCALE3 ABSPACK – An Oxford Diffraction program* (1.0.4, gui: 1.0.3), Oxford Diffraction Ltd., 2005.

[S7] *APEX3*. Bruker AXS Inc., Madison, Wisconsin, USA.

[S8] NATO standardization agreement (STANAG) on explosives, *impact sensitivity tests*, no. 4489, 1st ed., Sept. 17, 1999.

[S9] WIWEB-Standardarbeitsanweisung 4-5.1.02, Ermittlung der Explosionsgefährlichkeit, hier der Schlagempfindlichkeit mit dem Fallhammer, Nov. 8, 2002.

[S10] http://www.bam.de

[S11] NATO standardization agreement (STANAG) on explosive, *friction sensitivity tests*, no. 4487, 1st ed., Aug. 22, 2002.

[S12] WIWEB-Standardarbeitsanweisung 4-5.1.03, Ermittlung der Explosionsgefährlichkeit oder der Reibeempfindlichkeit mit dem Reibeapparat, Nov. 8, 2002.

[S13] Impact: insensitive > 40 J, less sensitive ≥ 35 J, sensitive ≥ 4 J, very sensitive ≤ 3 J; Friction: insensitive > 360 N, less sensitive = 360 N, sensitive < 360 N and > 80 N, very sensitive ≤ 80 N, extremely sensitive ≤ 10 N, According to: *Recommendations on the Transport of Dangerous Goods, Manual of Tests and Criteria*, 4th edition, United Nations, New York-Geneva, 1999.

[S14] http://www.ozm.cz

10 Appendix

10.1 General Analytical Information

All solvents and chemicals were purchased (Sigma-Aldrich, Acros, Fluka, Grüssing) and used without any further purification.

The NMR spectra were carried out using a JEOL Eclipse 270, JEOL EX 400 or a JEOL Eclipse 400 (^{1}H 399.8 MHz, ^{13}C 100.5 MHz, ^{14}N 28.9 MHz, and ^{15}N 40.6 MHz). Chemical shifts are given in parts per million (ppm) relative to the reference tetramethylsilane (^{1}H, ^{13}C) or nitromethane (^{14}N, ^{15}N).

Infrared spectra were measured with a Perkin-Elmer Spectrum BX-FTIR spectrometer equipped with a Smiths DuraSamplIR II ATR device. Transmittance values are qualitatively described as "strong" (s), "medium" (m), and "weak" (w). Raman spectra were recorded using a Bruker MultiRAM FT-Raman instrument fitted with a liquid-nitrogen cooled germanium detector and a Nd:YAG laser (λ = 1064 nm). The intensities are quoted as percentages of the most intense peak and are given in parentheses.

Differential Scanning Calorimetry (DSC) was recorded on a LINSEIS DSC PT10 with about 1–2 mg substance in a perforated aluminum vessel with a heating rate of 5 K·min^{-1} and a nitrogen flow of 5 dm^{3}·h^{-1}. DTA spectra were carried out using a OZM DTA 551-EX with a heating rate of 5 K·min^{-1}. TGA spectra were recorded on a Perkin Elmer TGA 4000 with a heating rate of 5 K min^{-1}.

Low-resolution mass spectra were recorded with a JEOL MStation JMS 700 (DEI+ / FAB+/−). Elemental analysis (C/H/N) were carried out using a Vario Micro from the Elementar Company.

Pynometer measurements were performed on a Quantachrome gas pycnometer Ultrapyc 1200e using helium as inert gas.

HPLC measurements were carried out on a Shimadzu HPLC Prominence equipped with a Shimadzu SPD-M30A UV detector and a reversed phase column (Kinetex 2.6 µm Biphenyl 100 Å, LC Column 150 x 4.6 mm, Ea).

Single crystals were picked and measured on an Oxford Xcalibur3 diffractometer with a Spellman generator (voltage 50 kV, current 40 mA) and a CCD area detector for data collection using Mo-*K*α radiation (λ = 0.71073 Å). The crystal structures of compound **5** was determined on a Bruker D8 Venture TXS diffractometer equipped with a multilayer monochromator, a Photon 2 detector, and a rotating-anode generator (MoKα radiation). The data collection was carried out using CRYSALISPRO software[S1] and the reduction were performed. The structures were solved using direct methods

(SIR-92,[S2] SIR-97[S3] or SHELXS-97[S4]) and refined by full-matrix least-squares on *F*2 (SHELXL[S4]): The final check was done with the PLATON software[S5] integrated in the WinGX software suite. The non-hydrogen atoms were refined anisotropically and the hydrogen atoms were located and freely refined. The absorptions were corrected by a SCALE3 ABSPACK multiscan method.[S6] The DIAMOND2 plots are shown with thermal ellipsoids at the 50% probability level and hydrogen atoms are shown as small spheres of arbitrary radii. The SADABS program embedded in the Bruker APEX3 software has been used for multi-scan absorption corrections in all structures.[S7]

Impact sensitivity tests were performed according to STANAG 4489[S14] modified instruction[S15] using a Bundesanstalt für Materialforschung (BAM) drophammer.[S16] Friction sensitivity tests were carried out according to STANAG 4487[S17] modified instruction[S18] using a BAM friction tester. The grading of the tested compounds results from the "UN Recommendations on the Transport of Dangerous Goods".[S19] ESD values were carried out using the Electric Spark Tester ESD 2010 EN.[S20]

10.2 References

[S1] *CrysAlisPro*, Oxford Diffraction Ltd., version 171.33.41, **2009**.

[S2] *SIR-92*, *A program for crystal structure solution*: A. Altomare, G. Cascarano, C. Giacovazzo, A. Guagliardi, *J. Appl. Crystallogr.* **1993**, *26*, 343.

[S3] a) A. Altomare, G. Cascarano, C. Giacovazzo, A. Guagliardi, A. G. G. Moliterni, M. C. Burla, G. Polidori, M. Camalli, R. Spagna, *SIR97*, **1997**; b) A. Altomare, M. C. Burla, M. Camalli, G. L. Cascarano, C. Giacovazzo, A. Guagliardi, A. G. G. Moliterni, G. Polidori, R. Spagna, *J. Appl. Crystallogr.* **1999**, *32*, 115–119.

[S4] a) G. M. Sheldrick, *SHELX-97*, University of Göttingen, Göttingen, Germany, **1997**; b) G. M. Sheldrick, *Acta Crystallogr., Sect. A* **2008**, *64*, 112–122.

[S5] A. L. Spek, *PLATON*, *A Multipurpose Crystallographic Tool*, Utrecht University, The Netherlands, **1999**.

[S6] *SCALE3 ABSPACK – An Oxford Diffraction program* (1.0.4, gui: 1.0.3), Oxford Diffraction Ltd., **2005**.

[S7] *APEX3*. Bruker AXS Inc., Madison, Wisconsin, USA.

[S8] M. J. Frisch, G. W. Trucks, H. B. Schlegel, G. E. Scuseria, M. A. Robb, J. R. Cheeseman, G. Scalmani, V. Barone, B. Mennucci, G. A. Petersson, H. Nakatsuji, M. Caricato, X. Li, H.P.

Hratchian, A. F. Izmaylov, J. Bloino, G. Zheng, J. L. Sonnenberg, M. Hada, M. Ehara, K. Toyota, R. Fukuda, J. Hasegawa, M. Ishida, T. Nakajima, Y. Honda, O. Kitao, H. Nakai, T. Vreven, J. A. Montgomery, Jr., J. E. Peralta, F. Ogliaro, M. Bearpark, J. J. Heyd, E. Brothers, K. N. Kudin, V. N. Staroverov, R. Kobayashi, J. Normand, K. Raghavachari, A. Rendell, J. C. Burant, S. S. Iyengar, J. Tomasi, M. Cossi, N. Rega, J. M. Millam, M. Klene, J. E. Knox, J. B. Cross, V. Bakken, C. Adamo, J. Jaramillo, R. Gomperts, R. E. Stratmann, O. Yazyev, A. J. Austin, R. Cammi, C. Pomelli, J. W. Ochterski, R. L. Martin, K. Morokuma, V. G. Zakrzewski, G. A. Voth, P. Salvador, J. J. Dannenberg, S. Dapprich, A. D. Daniels, O. Farkas, J.B. Foresman, J. V. Ortiz, J. Cioslowski, D. J. Fox, Gaussian 09 A.02, Gaussian, Inc., Wallingford, CT, USA, **2009**.

[S9] a) J. W. Ochterski, G. A. Petersson, and J. A. Montgomery Jr., *J. Chem. Phys.* **1996**, *104*, 2598–2619; b) J. A. Montgomery Jr., M. J. Frisch, J. W. Ochterski G. A. Petersson, *J. Chem. Phys.* **2000**, *112*, 6532–6542.

[S10] a) L. A. Curtiss, K. Raghavachari, P. C. Redfern, J. A. Pople, *J. Chem. Phys.* **1997**, *106*, 1063–1079; b) E. F. C. Byrd, B. M. Rice, *J. Phys. Chem*. A **2006**, *110*, 1005–1013; c) B. M. Rice, S. V. Pai, J. Hare, *Comb. Flame* **1999**, *118*, 445–458.

[S11] P. J. Lindstrom, W. G. Mallard (Editors), NIST Standard Reference Database Number 69, http://webbook.nist.gov/chemistry/ (accessed June **2011**).

[S12] M. S. Westwell, M. S. Searle, D. J. Wales, D. H. Williams, *J. Am. Chem. Soc*. **1995**, *117*, 5013–5015; b) F. Trouton, *Philos. Mag*. **1884**, *18*, 54–57.

[S13] a) H. D. B. Jenkins, H. K. Roobottom, J. Passmore, L. Glasser, *Inorg. Chem.* **1999,** *38,* 3609–3620; b) H. D. B. Jenkins, D. Tudela, L. Glasser, *Inorg. Chem.* **2002**, *41*, 2364–2367.

[S14] NATO standardization agreement (STANAG) on explosives, *impact sensitivity tests*, no. 4489, 1st ed., Sept. 17, **1999**.

[S15] WIWEB-Standardarbeitsanweisung 4-5.1.02, Ermittlung der Explosionsgefährlichkeit, hier der Schlagempfindlichkeit mit dem Fallhammer, Nov. 8, **2002**.

[S16] http://www.bam.de

[S17] NATO standardization agreement (STANAG) on explosive, *friction sensitivity tests*, no. 4487, 1st ed., Aug. 22, **2002**.

[S18] WIWEB-Standardarbeitsanweisung 4-5.1.03, Ermittlung der Explosionsgefährlichkeit oder der Reibeempfindlichkeit mit dem Reibeapparat, Nov. 8, **2002**.

[S19] Impact: insensitive > 40 J, less sensitive ≥ 35 J, sensitive ≥ 4 J, very sensitive ≤ 3 J; Friction: insensitive > 360 N, less sensitive = 360 N, sensitive < 360 N and > 80 N, very sensitive ≤ 80 N, extremely sensitive ≤ 10 N, According to: *Recommendations on the Transport of Dangerous Goods, Manual of Tests and Criteria*, 4th edition, United Nations, New York-Geneva, **1999**.

[S20] http://www.ozm.cz

10.3 List of Publications

Publications

[1] S. Aroua, M. Garcia-Borràs, **M. F. Bölter,** S. Osuna, Y. Yamakoshi, Endohedral Metal-Induced Regioselective Formation of Bis-Prato Adduct of $Y_3N@I_h$-C_{80} and $Gd_3N@I_h$-C_{80}, *J. Am. Chem. Soc.* **2015**, *137*, 58–61. (DOI: 10.1021/ja511008)

[2] N. Szimhardt, **M. F. Bölter**, M. Born, T. M. Klapötke, J. Stierstorfer, Metal Salts and Complexes of 1,1'-Dinitramino-5,5'-bitetrazole, *Dalton Trans.* **2017**, *46*, 5033–5040 (DOI: 10.1039/C7DT00536A)

[3] **M. F. Bölter**, A. Harter, T. M. Klapötke, J. Stierstorfer, Isomers of Dinitropyrazoles: Synthesis, Comparison and Tuning of their Physicochemical Properties, *ChemPlusChem* **2018**, accepted. (DOI: 10.1002/cplu.201800318R1)

[4] **M. F. Bölter**, T. M. Klapötke, T. Kustermann, T. Lenz, J. Stierstorfer, Utilization of Current Concepts on Improving the Energetic Properties of Dinitropyrazoles, *Eur. J. Inorg. Chem.* **2018**, accepted. (DOI: 10.1002/ejic.201800781)